



Universiteit
Leiden
The Netherlands

Design and development of polynuclear ruthenium and platinum polypyridyl complexes in search of new anticancer agents

Schilden, Karlijn van der

Citation

Schilden, K. van der. (2006, January 26). *Design and development of polynuclear ruthenium and platinum polypyridyl complexes in search of new anticancer agents*. Retrieved from <https://hdl.handle.net/1887/4377>

Version: Corrected Publisher's Version

License: [Licence agreement concerning inclusion of doctoral thesis in the Institutional Repository of the University of Leiden](#)

Downloaded from: <https://hdl.handle.net/1887/4377>

Note: To cite this publication please use the final published version (if applicable).

Design and Development of
**Polynuclear Ruthenium and Platinum
Polypyridyl Complexes**
in Search of New Anticancer Agents

PROEFSCHRIFT

ter verkrijging van
de graad van Doctor aan de Universiteit Leiden,
op gezag van Rector Magnificus Dr. D. D. Breimer,
hoogleraar in de faculteit der Wiskunde
en Natuurwetenschappen en die der Geneeskunde,
volgens besluit van het College voor Promoties
te verdedigen op donderdag 26 januari 2006
klokke 15.15 uur

door

Karlijn van der Schilden

geboren te Haarlem in 1974

Promotiecommissie

Promotor : Prof. Dr. J. Reedijk

Co-promotor : Dr. J. G. Haasnoot

Referent : Prof. Dr. E. Alessio (Università di Trieste)

Overige leden : Prof. Dr. J. Brouwer
Prof. Dr. H. S. Overkleeft
Prof. Dr. G. Sava (Università di Trieste)
Dr. M. Ubbink

The research described in this thesis was financially supported by the Council for Chemical Sciences of the Netherlands Organization for Scientific Research (CW-NWO). Financial support of COST Chemistry D20 for the stay in Brno is gratefully acknowledged.

Cover: Picture of the crystal structure of the dinuclear complex $[(\text{tpy})\text{Ru}(\text{dtdeg})\text{PtCl}]^{3+}$ and microscopic image of cisplatin-sensitive human ovarian carcinoma cells after three days of incubation with 20 μM of the tetranuclear complex $[\text{Cl}_3\text{Ru}(\text{dtdeg})\text{Ru}(\text{dtdeg})\text{Ru}(\text{dtdeg})\text{RuCl}_3]\text{Cl}_4$.

Printed by Optima Grafische Communicatie, Rotterdam, 2005

Table of contents

List of abbreviations	6
Chapter 1 General introduction	9
Chapter 2 A paramagnetic dinuclear ruthenium(II)-ruthenium(III) complex: synthesis and strategy for ^1H NMR studies	47
Chapter 3 Dinuclear ruthenium(II) complexes with long and flexible linkers: rotational behavior of coordinated 9-ethylguanine and biological properties	65
Chapter 4 Heterodinuclear ruthenium-platinum complexes with long and flexible linkers: crystal structure and cytotoxicity	87
Chapter 5 Trinuclear and tetranuclear ruthenium and platinum complexes with long and flexible linkers: syntheses, characterization and biological properties	109
Chapter 6 Heteropolynuclear ruthenium(II)-platinum(II) complexes with short and semi-rigid linkers: syntheses, characterization and DNA-model base studies	133

Chapter 7	151
Summary, general discussion and future prospects	
Samenvatting	159
Ontwerp en ontwikkeling van polynucleaire rutheniumcomplexen en ruthenium-platinacomplexen	
Op zoek naar nieuwe medicijnen tegen kanker	
Curriculum vitae	163
List of Publications	164
Nawoord	167

List of abbreviations

A2780cis	cisplatin-sensitive human ovarian carcinoma cell line
A2780R	cisplatin-resistant human ovarian carcinoma cell line
A549	lung cancer cell line
bpy	2,2'-bipyridine
cod	cyclooctadiene
COSY	Correlation Spectroscopy
d	doublet
DMF	dimethylformamide
DMSO	dimethylsulfoxide
DNA	deoxyribonucleic acid
dtdeg	bis[4'-(2,2':6',2''-terpyridyl)]-diethyleneglycolether
H ₄ edta	ethylene diamine tetraacetic acid
en	ethylene diamine
EPR	electron paramagnetic resonance spectroscopy
ESI-MS	electrospray ionization mass spectroscopy
EtOH	ethanol
9egua	9-ethylguanine
FAAS	flameless atomic absorption spectroscopy
FBS	fetal bovine serum
GSH	glutathione
HBL-100	non tumorigenic epithelial cell line
HCT-15	colorectal cancer cell line
hr	hour
Hs683	glioblastoma cell line
IC ₅₀	concentration of a compound that induces 50 % of growth inhibition of cells compared to untreated cells
J	couplin constant in NMR
KB	carcinoma cell line

L1210/0	cisplatin-sensitive mouse leukemia cell line
L1210/2	cisplatin-resistant mouse leukemia cell line
LoVo	colorectal cancer cell line
M	molar
MCF-7	breast cancer cell line
MeOH	methanol
MTT	3-(4,5-dimethylthiazol-2-yl)-2,5-diphenyl-2H-tetrazolium bromide
<i>m/z</i>	mass to charge ratio
NMR	nuclear magnetic resonance
NOE	nuclear Overhauser effect
NOESY	nuclear Overhauser effect spectroscopy
OD	optical density
PBS	phosphate buffered saline
ppm	parts per million
q	quartet
qpy	4'-pyridyl-2,2':6',2''-terpyridine
RT	room temperature
s	singlet, or second
SAR	structure-activity relationships
t	triplet
T ₁	nuclear longitudinal relaxation time
T ₂	nuclear transverse relaxation time
tpy	2,2:6',2''-terpyridine
U-373MG	glioblastoma cell line
UV-VIS	ultraviolet visible
VT	variable temperature

Chapter 1

General introduction

1.1 Introduction

Metals are often considered to be toxic for living systems. However, many metal ions are vital for the human body, since they play a diversity of important roles in biological processes. As already stated by Paracelsus (1493-1541): “*Dosis sola facit venenum*” (“Only the dose makes the poison”), any toxicity of metal ions depends on the actual concentration present. This knowledge has opened the way for medicinal application of metal ions. Metals in medicine hold great promise, since positively charged metal centers can interact with negatively charged biomolecules, and the constituents of proteins and nucleic acids supply good ligands for binding to metal ions. Especially complexes of the second- and third-row transition metals offer excellent perspectives for use as drugs, because of their slow ligand exchange, which usually provides reactivity only after hydrolysis. Because of the success of the anticancer drug cisplatin, which is introduced in the next section, a large variety of platinum and ruthenium compounds have been produced in search for new anticancer agents. The main achievements within this field of inorganic medicinal chemistry are summarized in this chapter. The research described in this thesis has been dealing with the development of homo- and heteropolynuclear platinum and ruthenium complexes, the potential of which as anticancer agents will be outlined here as well.

1.2 Development of metal-based anticancer drugs

Cancer, one of the major causes of death in the western world, is treated by conventional therapies such as surgical excision, chemotherapy and radiation, and more recently also by immunotherapy.^[1] In chemotherapy, cisplatin, *cis*-[Pt(NH₃)₂Cl₂] or *cis*-diamminedichloroplatinum(II) (**1**, Figure 1.1), is frequently used in combination with other anticancer drugs. It is one of the most used anticancer drugs, and is especially effective against testicular and ovarian carcinomas, bladder tumors and tumors of the head and neck. For testicular cancer, cure rates have been reported to be greater than 90 %.^[2] It is generally believed that the ultimate target of the drug is DNA.^[3] The DNA adducts formed interfere with DNA transcription and replication, eventually leading to cell death.^[4]

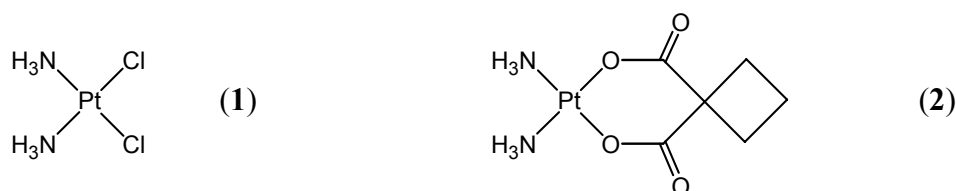


Figure 1.1 Cisplatin (**1**) and carboplatin (**2**).

The serendipitous discovery of cisplatin,^[5] and its clinical success have been a tremendous impetus for the design of metal-based anticancer drugs.^[6-9] Over the years, much attention has been focused on developing direct cisplatin analogues (section 1.3.4) to limit the serious side effects (*vide infra*) that result from reaction of cisplatin with cellular components of healthy tissues. However, so far only *cis*-[diammine(1,1-cyclobutane-dicarboxylato)platinum(II)], carboplatin (**2**, Figure 1.1), has received worldwide approval, thanks to its reduced toxicity to kidney cells and the nervous system (nephrotoxicity and neurotoxicity, respectively). Unfortunately, no significant improvement was achieved in the spectrum of activity compared to cisplatin, apparently owing to the similar type of DNA adducts formed by this cisplatin analogue.

To achieve anticancer activity in a broader range of tumors, alternative platinum complexes that can bind to DNA in a fundamentally different manner, have been developed. These include *trans*-platinum(II) complexes,^[10] sterically hindered *cis*-diamine platinum(II) complexes^[11] and platinum(IV) complexes (section 1.3.5).^[12] Metals other than platinum have also been used for the design of anticancer agents.^[13, 14] Among these are the ruthenium(II) and ruthenium(III) complexes (section 1.4), which probably function differently due to their octahedral structure as opposed to the square-planar geometry of cisplatin.^[15] A completely new class of “non-classical” platinum complexes comprises the polynuclear platinum

complexes^[16] (section 1.5), which have been shown to form long-range DNA adducts. The concept of polynuclear anticancer agents has also been applied to ruthenium complexes, although to a lesser extent (section 1.6). A challenging extension of the polynuclear concept has been the syntheses of heteropolynuclear complexes to achieve selective specificity and reactivity at each metal center (section 1.7).

1.3 “Classical” and “non-classical” mononuclear platinum complexes

1.3.1 Cisplatin and its mechanism of action

Cisplatin is administered by intravenous injection or infusion.^[4, 8, 17] In the bloodstream, cisplatin remains intact owing to the relatively high chloride ion concentration of 100 mM, which suppresses hydrolysis of the drug. It enters cells by passive diffusion although some evidence indicates the involvement of active transport mechanisms.^[18] Very recently, it was proposed that cisplatin uptake is mediated by the copper transporter Ctr1 in yeast and mammals.^[19] Inside the cell, the low chloride ion concentration of 4 mM is known to promote hydrolysis of the drug.^[4, 8, 17] The resulting activated hydrolysis products of cisplatin^[20] can react rapidly with a wide variety of cellular molecules,^[3, 21] but it is widely accepted that DNA damage is the decisive effect by which cisplatin exerts its antitumor activity. The major DNA adducts formed are intrastrand crosslinks to adjacent purines, which causes significant bending and unwinding of the helical structure of DNA.^[4] Subsequently, DNA replication and transcription are inhibited, which eventually result in programmed cell death, *i.e.* apoptosis.^[4] The 1,2-d(GpG) crosslink is thought to be primarily responsible for cell death, as it is not effectively repaired by the nucleotide excision repair (NER) system.^[22] It has been suggested^[4] that the specific adduct is being shielded from repair enzymes by binding of high-mobility group (HMG) domain proteins. Another hypothesis states^[4] that the specific adduct hijacks the HMG domain proteins away from their normal binding sites, thereby disrupting DNA transcription. These two mechanisms are not mutually exclusive and could work in concert to affect cisplatin cytotoxicity.

1.3.2 Cisplatin’s side effects

Several toxic side effects may occur during treatment with cisplatin in anticancer chemotherapy.^[8] Patients treated with cisplatin have shown serious signs of nephrotoxicity, neurotoxicity and ototoxicity (loss of hear). Other side effects are severe nausea and vomiting, diarrhea and an elevated blood pressure. Intravenous hydration and diuresis can reduce the

level of nephrotoxicity,^[23] and 5-HT₃-receptor blockers control nausea and vomiting.^[24] The recently approved^[8] chemoprotective agent amifostine (WR-2721), which is co-administered with cisplatin, alleviates nephro- and neurotoxicity by reducing the effects on normal tissues without compromising antitumor efficacy.

1.3.3 Cisplatin resistance

The major clinical problem of cisplatin, which limits its applicability to a narrow range of tumors, is the cellular resistance to the drug. Drug resistance can be either intrinsic or acquired, which develops after exposure to the drug. In general, the mechanism of resistance consists of mechanisms restricting the formation of DNA adducts, and of mechanisms operating downstream of the DNA adduct to promote cell survival.^[4, 25] The first include reduced uptake and enhanced efflux of the drug resulting in reduced accumulation inside the cell, and inactivation of cisplatin by reaction with intracellular thiols such as glutathione (GSH). Interestingly, regulation of the intracellular GSH level appears to be a promising strategy to circumvent cisplatin resistance.^[26] Increased capability of cells to repair cisplatin-damaged DNA, and increased tolerance of the DNA damage are involved in the second group of mechanisms. The tumor suppressor protein p53 has been hypothesized to influence sensitivity or resistance of tumor cells to cisplatin through its regulation of other proteins involved in cell cycle control, DNA repair and apoptosis.^[27]

1.3.4 Direct cisplatin analogues

Since the introduction of cisplatin in 1971, thousands of platinum compounds have been synthesized and evaluated as potential antitumor active agents. The majority of them adhered to the set of structure-activity relationships originally stated for platinum complexes to display antitumor activity.^[28] Platinum(II) and platinum(IV) complexes should have *cis* geometries with the general formula of *cis*-[PtX₂(Am)₂] or *cis,trans*-[PtX₂Y₂(Am)₂], where X is the leaving group and Am is an inert amine with at least one N-H moiety. The leaving group X should be an anion with intermediate binding strength to platinum and have a weak trans-effect to avoid labilizing the amine. Complexes with labile leaving groups such as ClO₄⁻ or NO₃⁻ are highly toxic, while complexes with inert leaving groups are generally inactive. The N-H moiety should be present to afford hydrogen bonding upon binding of the drug to DNA, and to stabilize the DNA adduct.

The development of direct cisplatin analogues has resulted in only a few clinically useful complexes, one of which is carboplatin (**2**, Figure 1.1). It displays the same spectrum of

activity against cancer cell lines as cisplatin, but displays a more tolerable toxicological profile. Bone marrow toxicity is the dose-limiting factor in carboplatin treatment.^[29] The lower toxicity is attributed to its higher stability and lower reactivity due to the relative inertness of the didentate carboxylate ligand. Because of the milder toxicity, but equivalent efficacy, it has largely replaced cisplatin in therapies of ovarian, non-small cell and small cell lung cancers.^[6, 8]

Nedaplatin (**3**, Figure 1.2) is only clinically used in Japan.^[6] It is cross-resistant to cisplatin, but shows improved toxicological properties.^[30] As no studies directly compared nedaplatin with carboplatin yet, no clear evidence is available for any distinct advantage of the former over the latter.

Oxaliplatin (**4**, Figure 1.2) was the first platinum drug to show clinical activity in a tumor with primary resistance to cisplatin.^[31] Oxaliplatin forms adducts at DNA sites that are nearly identical to cisplatin DNA adducts.^[32] However, the conformation of the major DNA adduct formed (the 1,2-GG intrastrand crosslink) shows some distinct features,^[33] and these have been suggested to influence further processing of the crosslink in the cell.^[34] Oxaliplatin has been approved for clinical use in Europe, Asia and Latin America for the first-line treatment and in the United States for the secondary treatment of metastatic colorectal cancers in combination with 5-fluorouracil.^[35] It lacks nephrotoxicity,^[36] but neurotoxicity is limiting dose escalation.^[37]

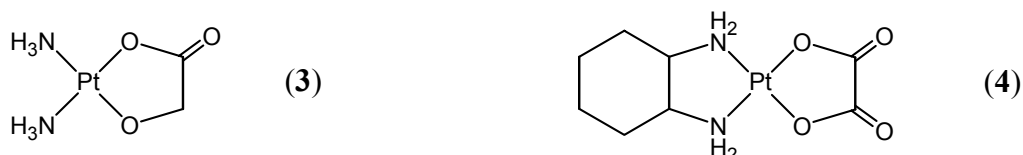


Figure 1.2 The direct cisplatin analogues nedaplatin (**3**) and oxaliplatin (**4**).

1.3.5 New approaches

More recently, new concepts in designing platinum-based antitumor drugs with a broader spectrum of activity and less side effects have been introduced. Platinum prodrugs have been designed, which are only activated in solid tumors with low pH.^[38] Targeted platinum drugs have been developed to accumulate in certain tissues.^[8] Kinetically inert octahedral platinum(IV) complexes, for which reduction by extracellular and intracellular agents to platinum(II) is necessary for activation, have been receiving increased interest.^[8, 12] Satraplatin (JM216, *cis,trans*-[PtCl₂(OAc)₂(NH₃)(cyclohexylamine)]), **5**, Figure 1.3) showed

great promise in Phase I and II clinical trials.^[39] It represented the first platinum drug, which was suitable for oral administration because of favorable physicochemical properties. However, it was abandoned from Phase III trials due to variability in drug uptake.^[12] The drug is supposedly too readily reduced to platinum(II) in the blood stream. It has been suggested that the consequent loss of its lipophilicity accounts for the disparity in activity between in vitro and in vivo systems.^[40]

Cis-platinum complexes with bulky ligands have been designed to broaden the spectrum of anticancer activity, as it is believed that cisplatin resistance can be circumvented by sterically hindering inactivating reactions with glutathione and other cellular thiols.^[11] A lead compound within this series of complexes is ZD0473 (*cis*-amminedichloro(2-methylpyridine)platinum(II), **6**, Figure 1.3). Its crystal structure has confirmed that the methyl group is imposing steric hindrance for associative substitution reactions on the square-planar platinum(II), as the 2-methylpyridine ring is tilted nearly perpendicular with respect to the PtN₂Cl₂ plane.^[41] The complex shows a unique pattern of response, and has shown lower resistance factors than cisplatin in cell lines, which represent different mechanisms of resistance.^[42] Initiation of phase-III clinical trials in patients with ovarian cancer has been announced recently.^[8] ZD0473 also demonstrates good oral availability and activity.^[43]

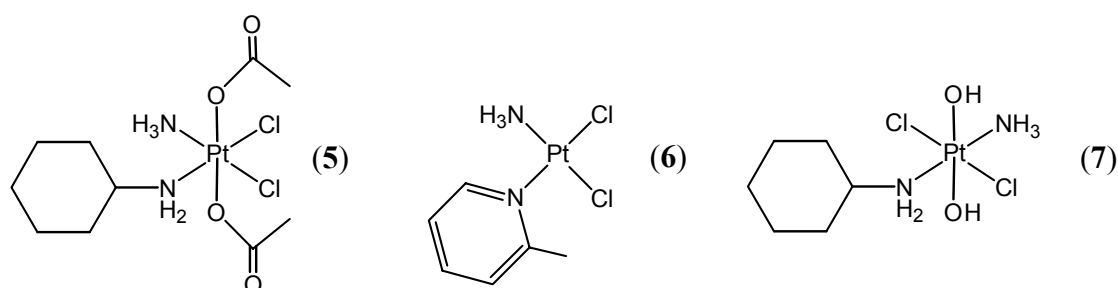


Figure 1.3 The non-classical mononuclear platinum complexes satraplatin (**5**), ZD0473 (**6**) and JM335 (**7**).

Trans-platinum complexes have also been developed using bulky ligands to reduce kinetic reactivity inherent to the inactive complex transplatin, *trans*-[Pt(NH₃)₂Cl₂], thereby decreasing susceptibility to deactivating side reactions on route to the DNA.^[8, 10] It is believed that trans-platinum complexes can overcome cisplatin resistance, as they form DNA adducts which are different from those formed by cisplatin. The three main series of trans-platinum complexes can be classified in those using planar aromatic amines, iminoethers or aliphatic amines, the latter being used in designing trans-platinum(IV) as well as trans-platinum(II) compounds. The first type of complexes form a high portion of interstrand adducts^[44] and show the formation of bifunctional DNA adducts and DNA-protein crosslinks.^[45] This may

account for the higher activity compared to the cis analogues, and for the lack of cross-resistance with cisplatin.^[46] Stable monofunctional DNA adducts are most likely responsible for the cytotoxic activity of the iminoether class of complexes.^[47] The specific activity of the most promising trans-platinum(IV) complex^[48], JM335 or *trans*-amine(dichlorocyclohexylamine)dihydroxoplatinum(IV) (7, Figure 1.3), has been found to correlate with the inability of gene-specific repair^[49] of its DNA interstrand adducts.^[50]

1.4 Anticancer mononuclear ruthenium complexes

1.4.1 Introduction

Many ruthenium complexes have been evaluated for the treatment of cancer,^[15] in part because ruthenium(II) and ruthenium(III) complexes exhibit relatively low ligand exchange rates, which are comparable to those of platinum(II) complexes.^[51] Slow ligand exchange may ensure that the drug reaches its biological target without being modified. Moreover, the various oxidation states (II, III and IV) of ruthenium are all accessible under physiological conditions.^[52] In these oxidation states the ruthenium center is predominantly hexacoordinated with octahedral geometry in contrast to the square-planar geometry of platinum(II). The octahedral geometry of ruthenium compounds imposes different steric effects upon interaction with biomolecules, which in turn may cause a different anticancer profile from cisplatin.

1.4.2 Hypotheses on the mechanism of action

In the blood, ruthenium mimics iron in binding to certain biomolecules, such as albumin and transferrin.^[52] Specific intake of ruthenium(III) and ruthenium(II) ions might be mediated by the transferrin-based iron transport system.^[53, 54] The serum transferrin system specifically recognizes iron(III) (and not iron(II)) along with a synergistic anion (usually carbonate).^[54] Transferrin binds strongly to its receptor when it is loaded with two iron(III) ions, after which it is internalized by cells. Release of iron(III) from transferrin is induced at low pH. The protein is then recirculated into the blood. There is potential for use of this transport mechanism in cancer therapy, as high levels of transferrin receptors are expressed by many solid tumor cells, due to their higher iron requirement than normal cells. Moreover, the relatively low pH of tumor cells facilitates readily the release of transferrin-bound metal ions. Selective tumor toxicity may also be reached by what is known as the “activation by reduction” mechanism. It has been suggested that ruthenium(III) complexes may serve as

prodrugs, which are activated by reduction *in vivo* to coordinate more rapidly to biomolecules, since ruthenium(II) species are usually less inert than the corresponding ruthenium(III) complexes.^[14, 15, 55] The low oxygen content and low pH in tumor cells cause a relatively low electrochemical potential inside tumors. Therefore, the reduction of ruthenium(III) to ruthenium(II) is favored in tumors relative to normal tissue. *In vivo*, reduction of ruthenium(III) species can occur by glutathione and redox proteins available in the cell.

Glutathione, which appears to contribute to cisplatin resistance in tumor cells (section 1.3.3), may also be involved in the metabolism of many types of ruthenium pharmaceuticals. GSH has been shown to bind to ammineruthenium(III) complexes, and depending on its concentration it either facilitates or inhibits ruthenium coordination to DNA.^[56] In general, cytotoxicity of ruthenium complexes correlates with their ability to coordinate to DNA.^[15]

1.4.3 Ruthenium anticancer compounds: state of the art

A number of ammine and amine ruthenium complexes, as well as complexes with monodentate and chelating heterocyclic ligands have been synthesized for anticancer purposes.^[9, 14, 15] The tetrachlororuthenium(III) complexes of the type (HL)[RuCl₄L₂] (where L is imidazole (im) or indazole (ind)) have emerged as promising compounds as they display activity against a number of cancer cell lines,^[57] and in particular against colorectal tumors.^[58-61] Human colon cancer is the second highest occurring cancer after bronchial carcinomas.^[62] The complex (Hind)[RuCl₄(ind)₂] (KP1019 (**8**), Figure 1.4) is highly active against a model of colorectal cancer,^[63] which has been used as sometimes only weak activity is observed against colorectal tumors using conventional treatments.^[59] KP1019 is completely devoid of side effects and drug induced lethality at active dosages, and it has shown a better therapeutic index than the imidazole derivative.^[60] The complex has been announced^[38] to enter phase I clinical trials. Results have demonstrated that the transferrin-bound species of both KP1019 and its imidazole analogue, as well as the apotransferrin form of (Him)[RuCl₄(im)₂] exhibit anticancer activity superior to that of the protein-free complexes.^[64] Therefore, the low toxicity of **8** presumably stems from a transferrin-mediated accumulation in tumor cells.^[65] An “activation by reduction mechanism”, and a different DNA binding mode compared to cisplatin have been proposed to account for the unique cytotoxicity in tumor cells.^[61, 66]

The first ruthenium complex, *i.e.* NAMI-A (*trans*-(H₂im)[RuCl₄(dmsO)(Him)] (**9**), Figure 1.4), has recently accomplished phase I clinical trials.^[67, 68] The complex belongs to the class of ruthenium dimethylsulfoxide complexes. It is relatively nontoxic *in vitro* against tumor cells,^[69] and shows a remarkable high efficiency *in vivo* against lung metastasis,^[70] a common feature of many human tumors. Because of the S-bonded dmsO ligand, NAMI-A is easily

reduced to the corresponding ruthenium(II) species by biological reducing agents under physiological conditions.^[71, 72] It has been proven that these reduced species maintain their anticancer activities. Interestingly, the antimetastatic activity appears not to be related to DNA binding,^[73] even though the complex interacts with DNA *in vitro*.^[71] Instead, NAMI-A interferes with fibrous collagen of the lung and with basement membrane collagen type IV.^[67] It significantly increases the thickness of connective tissue around the tumor capsule and around tumor blood vessels, thereby probably hindering blood flow to the tumor.^[74] The inhibition of angiogenesis has been attributed to induction of apoptosis, as has recently been shown in ECV304 cells.^[75] Since angiogenesis is crucial for metastasis formation, and in particular for metastases growth, it is likely that the inhibition of this process is relevant for the activity of NAMI-A against metastasis.

Organometallic ruthenium(II) complexes with arene ligands represent a relatively new group of water-soluble ruthenium compounds with antitumor activity displayed *in vitro* and *in vivo*.^[76] No cross-resistance has been observed in cisplatin-resistant cells, but did occur in the multi-drug-resistant cell line 2780^{AD}. The most hydrophobic arene species $[(\eta^6\text{-C}_6\text{H}_5\text{C}_6\text{H}_5)\text{RuCl}(\text{en})](\text{PF}_6)$ (**10**, Figure 1.4) and $[(\eta^6\text{-C}_6\text{H}_5\text{C}_6\text{H}_5)\text{RuCl}(\text{en-Et})]\text{PF}_6$ (en = ethylenediamine, and en-Et = *N*-ethylethylenediamine), in which a phenyl is substituent at the arene ligand, showed the highest tumor-inhibiting activity. It has been suggested that the presence of the hydrophobic planar arene ligand facilitates recognition and transport of these complexes through cell membranes. The relative conformational flexibility of the arene ligand makes simultaneous intercalation and coordination of ruthenium to DNA possible.

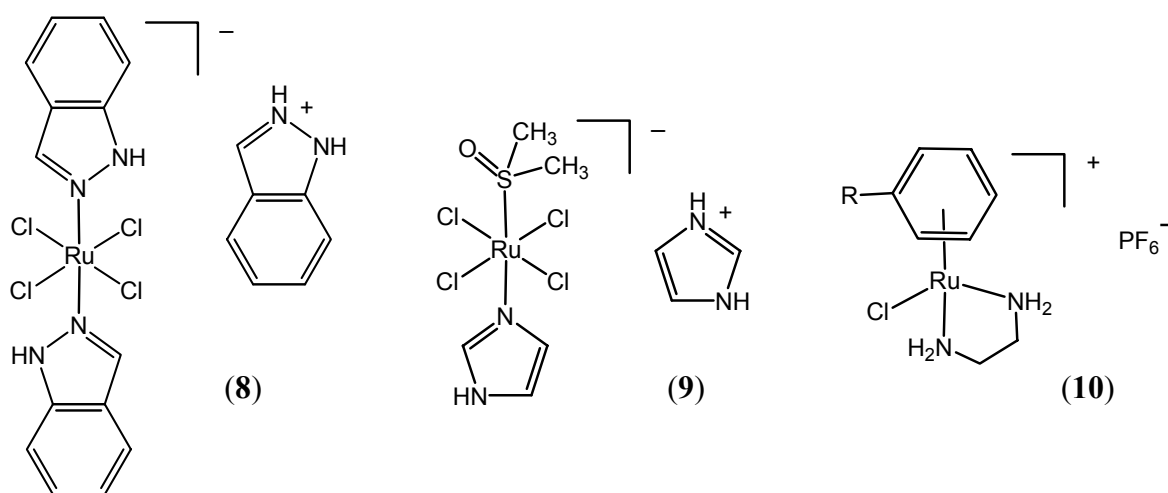


Figure 1.4 The ruthenium(III) pharmaceuticals KP1019 (**8**) and NAMI-A (**9**), and the ruthenium(II) complex $[(\eta^6\text{-C}_6\text{H}_5\text{C}_6\text{H}_5)\text{RuCl}(\text{en})]^+$ (**10**), in which the R represents a phenyl group.

1.5 Polynuclear platinum complexes

1.5.1 A new paradigm

Polynuclear platinum complexes represent a completely new paradigm in the development of novel anticancer agents.^[9, 16, 77] They are probably the most distinctively different from cisplatin of all “third generation” platinum complexes developed. These polynuclear complexes consist of two or more linked platinum centers that can each interact with DNA. Consequently, they are capable of DNA interactions which are not possible for their mononuclear counterparts.

It is believed^[77] that polynuclear platinum complexes of long and flexible α,ω -diaminoalkane linkers can overcome both acquired and intrinsic resistance to the antitumor drug cisplatin by their ability to form long-range DNA adducts (*vide infra*). From studies with these complexes, chain length and flexibility, hydrogen-bonding capacity and charge of the linker, and finally the position of the leaving group (usually chloride) relative to the linker chain appear to be major factors in designing polynuclear platinum antitumor drugs. However, very short and rigid linked polynuclear platinum complexes have also shown promising biological activity (*vide infra*). It appears that the class of polynuclear platinum agents is too diverse to infer general structure-activity relationships for this new series of anticancer drugs. Therefore, it is of great importance to understand the mechanisms of action within a particular series of polynuclear complexes. Results reported so far are summarized below.

1.5.2 Polynuclear complexes with alkanediamine linkers

The first polynuclear platinum antitumor agents reported^[78] were dinuclear complexes based upon the linking of two cisplatin-like, or transplatin-like, centers by long and flexible α,ω -diaminoalkane linkers of variable length, *i.e.* [$\{cis\text{-PtCl}_2(\text{NH}_3)\}_2(\text{H}_2\text{N}(\text{CH}_2)_n\text{NH}_2)]\text{Cl}_2$, 2,2/c,c (**11**) and [$\{trans\text{-PtCl}_2(\text{NH}_3)\}_2(\text{H}_2\text{N}(\text{CH}_2)_n\text{NH}_2)]\text{Cl}_2$, 2,2/t,t, (**12**) (Figure 1.5), in which $n = 2$ to 6.

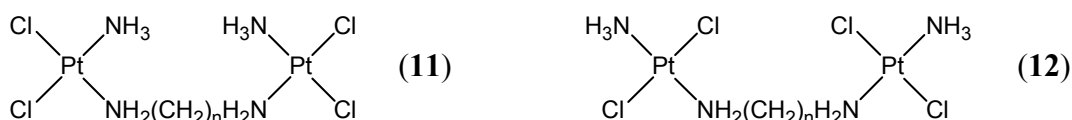


Figure 1.5 The tetrafunctional dinuclear *cis*- and *trans*-platinum complexes 2,2/c,c (**11**) and 2,2/t,t (**12**), for which $n = 2$ -6.

The tetrafunctional nature of the compounds (after chloride dissociation) allows for a complex array of inter- and intrastrand crosslinks upon reaction with DNA. The 2,2/c,c complexes have been shown to be particularly active in cells resistant to cisplatin, whereas the 2,2/t,t isomers did not show significantly improved cytotoxicity over their mononuclear analogue, transplatin.^[79, 80] Of specific interest was the fact that the complexes produce a large number of interstrand DNA crosslinks.^[81] The activity of the mixed *cis,trans* species 2,2/c,t in both cisplatin sensitive and resistant cell lines, indicated that only one cisplatin-like unit is necessary for activity. The nature of the second platinum coordination sphere appeared not to be critical, as long as interstrand crosslinks are formed.^[79]

DNA-binding studies of dinuclear complexes with monofunctional platinum centers of general formula [$\{\text{PtCl}(\text{NH}_3)_2\}_2(\text{H}_2\text{N}(\text{CH}_2)_n\text{NH}_2)\text{Cl}_2$] (1,1/c,c (**13**) and 1,1/t,t (**14**), Figure 1.6) showed that DNA interstrand crosslinking is more efficient for the 1,1/t,t complexes than for the 2,2/c,c isomers.^[82] Apparently, interstrand crosslinks are easily formed by bifunctional coordination of two independent monofunctional platinum moieties as in the 1,1/t,t isomers. The latter are deficient of many of the steric requirements faced when two nucleobases are bound to one platinum center. Studies using relatively bulky ligands, confirmed steric hindrance to affect relative tendencies to form inter- or intrastrand crosslinks or monoadducts.^[83, 84] The higher activity of the 1,1/t,t complexes compared to the 2,2/c,c complexes observed in cisplatin resistant cells^[82] stressed that the contribution of the interstrand crosslink to the biological effects is independent of any involvement from the cisplatin-like intrastrand crosslink.

As opposed to the dinuclear complexes with bifunctional coordination spheres, this series of dinuclear platinum complexes induces unique DNA conformational changes,^[82, 85] which include B \rightarrow Z conformational changes in poly(dG-dC)·poly(dG-dC).^[86] Ionic charges have been stated to be necessary to induce the B \rightarrow Z transition. Coordination appears to be of importance for locking DNA in the induced Z form.^[87] In contrast, cisplatin supports the B form of DNA,^[88] and does not attack alternating purine-pyrimidine sequences.^[82] Although the role of Z DNA *in vivo* has not yet been firmly established,^[89] these differences may have consequences for “downstream effects” upon transcription and protein recognition.

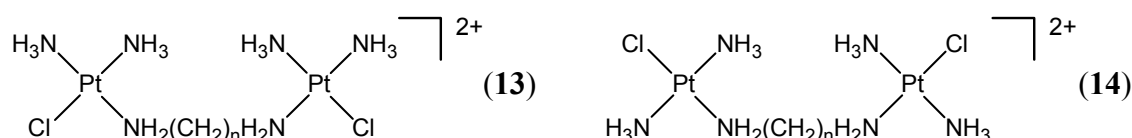


Figure 1.6 The bifunctional dinuclear cationic platinum complexes 1,1/c,c (**13**) and 1,1/t,t (**14**), with $n = 2$ to 8.

Within the series, the trans isomer is more active in cisplatin-resistant cell lines, the highest activity *in vitro* being observed for $n = 6$.^[77, 90] The high activity has been attributed to the fact that the trans isomer forms predominantly long-range interstrand adducts^[91] (~ 50 % *versus* ~ 5 % for cisplatin^[92]). Although the cis isomer is a more effective interstrand crosslinker (~ 80 %), it forms structurally more diverse adducts, also short-range cross links and even an interstrand cross link between a cytosine and guanine on the same base pair have been observed.^[77, 93] The sterically more constrained adducts of the cis isomer are more readily repaired in cisplatin resistant cells, thereby probably reducing the ability to circumvent cisplatin resistance.^[94]

The formation of the long-range 1,4-interstrand adduct of **14** with DNA has been studied.^[95] Initial electrostatic association of the intact 1,1/t,t ($n = 6$) isomer with the DNA duplex has been found to occur. Subsequently, the complex is mono-aquated to form the mono-aqua-monochloroplatinum(II) species. On the contrary, the mono-aquated cisplatin derivative pre-associates with DNA.^[96] Furthermore, monofunctional coordination of 1,1/t,t to the duplex was found, while the unbound platinum moiety remained electrostatically bound to the duplex. The electrostatic interaction probably ensures fast fixation of the crosslink, which finally results in two conformers of the 1,4-adduct. These results point out the importance of the positive charge of the complex. The charge is likely to cause the higher rate of bifunctional DNA binding in comparison with cisplatin. The 1,4-interstrand crosslink is not efficiently recognized by HMG proteins,^[97] which may be caused by the conformational flexibility of the crosslink and the consequent lack of a directed bend of DNA.

Concluding, results summarized for the dinuclear platinum complexes so far provide strong evidence for the hypothesis that platinum drugs, which bind to DNA in a fundamentally different way compared to cisplatin, have different pharmacological properties. This statement is being emphasized by recent studies of the two isomeric trifunctional dinuclear platinum complexes of formula $[\{\text{PtCl}(\text{NH}_3)_2\}(\mu\text{-H}_2\text{N}(\text{CH}_2)_6\text{NH}_2)\{\text{PtCl}_2(\text{NH}_3)\}]^+$ (1,2/c,c (**15**) and 1,2/t,c (**16**), Figure 1.7).

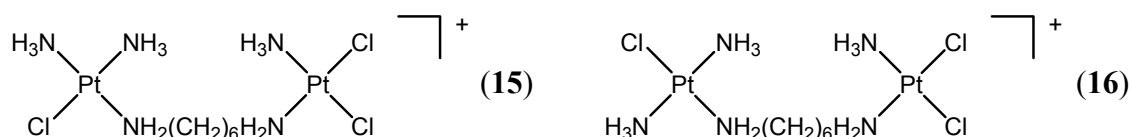


Figure 1.7 The trifunctional dinuclear cationic platinum complexes 1,2/c,c (**15**) and 1,2/t,c (**16**).

Protein binding to the complex might occur after formation of a long-range interstrand crosslink similar to that formed by the 1,1/t,t isomer.^[98] Results show that both isomers retain

activity in cisplatin resistant cell lines and exhibit a unique profile of activity compared to cisplatin, as well as within the class of polynuclear platinum complexes with α,ω -diaminoalkane linkers.^[99]

The most promising agent within this new structural class of polynuclear anticancer drugs, is the trinuclear complex $[\{trans\text{-PtCl}(\text{NH}_3)_2\}_2\{\mu\text{-trans-Pt}(\text{NH}_3)_2(\text{H}_2\text{N}(\text{CH}_2)_6\text{NH}_2)_2\}]^{4+}$ (1,0,1/t,t,t), or BBR3464 (**17**, Figure 1.8). The complex can bifunctionally bind to DNA with the two terminal monofunctional platinum units. The positively charged inert tetraamine platinum linker provides water solubility and high DNA affinity. BBR3464 was the first polynuclear platinum complex to enter clinical trials and has recently undergone Phase II clinical trials for treatment of a variety of cancers.^[7, 25] In Phase I clinical trials, short-lasting neutropenia and diarrhea appeared to be dose-limiting.^[100] Neither neurotoxicity nor renal toxic effects were observed, and nausea and vomiting were found to be rare. BBR3464 has been shown to be able to overcome acquired and intrinsic cisplatin resistance at remarkable low concentrations in a number of cancer cell lines,^[101, 102] including p53-mutant xenografts.^[103] It has been suggested that apoptosis induced in tumor cells by BBR3464 is not mediated by p53. “Bypassing” of the p53 pathway may have its origin in the specific DNA-binding mode of this trinuclear agent.^[104]

Interestingly, interstrand cross-linking efficiency for BBR3464 is only 20 % and intrastrand DNA adducts are equally being formed.^[105] Both inter- and intrastrand crosslinks of BBR3464 are not recognized by HMG proteins. However, only the major 1,4-interstrand crosslink is not effectively removed by the NER system, which suggests its relevance to the antitumor effects of the drug.^[106] It has been shown that the 1,4-interstrand adduct extends over the phosphate backbone by preassociation of the central tetraamine linker in the minor groove through electrostatic interactions, and subsequent coordination of the two outer platinum atoms in the major groove.^[107] This novel mode of DNA binding may account for the difference in antitumor activity between BBR3464 and the dinuclear analogues that lack the charged central linker. Conformational flexibility of the 1,4-interstrand adduct has also been observed for BBR3464, but the conformers are not interconvertable. This delocalization of the lesion can represent an extremely efficient block to excision repair.

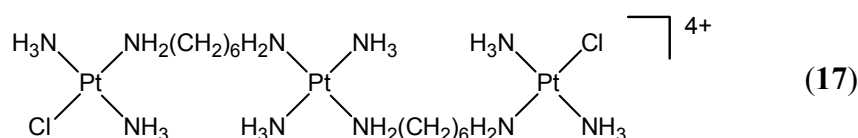


Figure 1.8 The bifunctional trinuclear cationic platinum complex 1,0,1/t,t,t (BBR3464, **17**).

1.5.3 Linkers exhibiting special features

The polyamines spermidine ($\text{H}_2\text{N}(\text{CH}_2)_3\text{NH}(\text{CH}_2)_4\text{NH}_2$) and spermine ($\text{H}_2\text{N}(\text{CH}_2)_3\text{NH}(\text{CH}_2)_4\text{NH}(\text{CH}_2)_3\text{NH}_2$) have been used as linkers for the syntheses of polynuclear platinum complexes, as they are known to play essential roles in normal cell growth and differentiation in eukaryotic cells.^[108] Since they are protonated at physiological pH, their polycationic character can provide electrostatic and hydrogen-bonding interactions with negatively charged nucleic acids.^[109] Moreover, these ligands can induce significant structural changes like B \rightarrow Z and B \rightarrow A transitions in DNA.^[110] The first polyamine complexes reported were the di- and trinuclear *cis*-dichloroplatinum(II) and platinum(IV) spermine and spermidine compounds, [*cis*-PtCl₂]₂(H₂N(CH₂)₃NH(CH₂)₄NH(CH₂)₃NH₂)] and [*cis*-PtCl₂](*cis*-PtCl₂(H₂N(CH₂)₃NH(CH₂)₄NH₂))₂], respectively. The central secondary amino groups of the polyamines were also involved in coordination to platinum, thereby forming chelates.^[111, 112] Cytotoxic activity has been demonstrated against breast carcinoma, leukemia cells^[112] and epithelial-type cells.^[113]

Very promising results have been revealed by bifunctional dinuclear *trans* platinum(II) complexes in which linear coordinated spermine and spermidine are incorporated, *i.e.* [*trans*-PtCl(NH₃)₂]₂(μ -spermine-*N*¹,*N*¹²)]Cl₄ (BBR3535) and [*trans*-PtCl(NH₃)₂]₂(μ -spermidine-*N*¹,*N*⁸)]Cl₃ (BBR3571, **18**, Figure 1.9), respectively. The flexibility of the linker and the distance between the metal centers is not reduced by the linear coordination of the polyamine linkers, thereby conserving the intrinsic advantages of the polyamines.

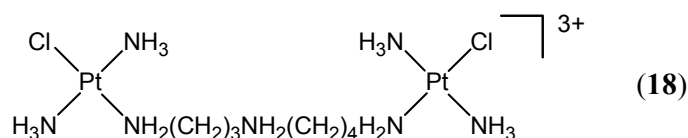


Figure 1.9 The spermidine dinuclear cationic platinum complex BBR3571 (**18**).

In particular, the spermidine complex **18** showed remarkable cytotoxicity against cisplatin resistant leukemia cells,^[114] which rather closely matched that of BBR3464 (**17**).^[101] Comparative studies suggested that the charge and hydrogen-bonding capabilities of the spermidine linker of **18**, and the tetraamineplatinum linker of BBR3464 (**17**), contribute significantly to the anticancer profiles of both complexes.^[101, 115] Moreover, cellular uptake, cytotoxicity, and antitumor activity are greatly enhanced in comparison to the 1,1/*t,t* derivative **14**, in which a “simple” diamine linker is utilized. Compared to **17**, DNA binding is more rapid for the polyamine complexes and significantly more interstrand crosslinks are formed by the latter (20 % *versus* 40 % and 57 % for **17**, BBR3535, and **18**, respectively).^[116]

It has been suggested that **17** is sterically more demanding in comparison with the polyamine complexes, which may hamper ready access to the minor groove and consequently decreases the DNA-binding rate. Moreover, the formation of a bifunctional interstrand crosslink from a monofunctional adduct may require larger conformational distortions for **17** than for the polyamine linked complexes.

Irreversible B \rightarrow Z conformational changes as well as B \rightarrow A transitions induced by the polyamine complexes at low doses^[117] have been proposed to contribute to the lack of repair observed in mouse leukemia cells.^[118] Preclinical investigations confirm the potency of the polyamine species, showing cytotoxicities in the nanomolar range.^[119] However, the remarkable potency has resulted in a relatively narrow therapeutic index. Therefore “prodrug” delivery of less toxic and better tolerated derivatives has been investigated by use of blocking carbamates with different structures and acid susceptibility.^[120]

A tetranuclear *trans* platinum complex **19** has been synthesized using a branched polyamine to link the platinum moieties (Figure 1.10). The polyamine ligand has, however, not been reported to display specific interactions with DNA. The complex showed low cytotoxicity against several cell lines.^[121] The highly charged and branched structure has been suggested to affect crossing of the molecule through the cell membrane.

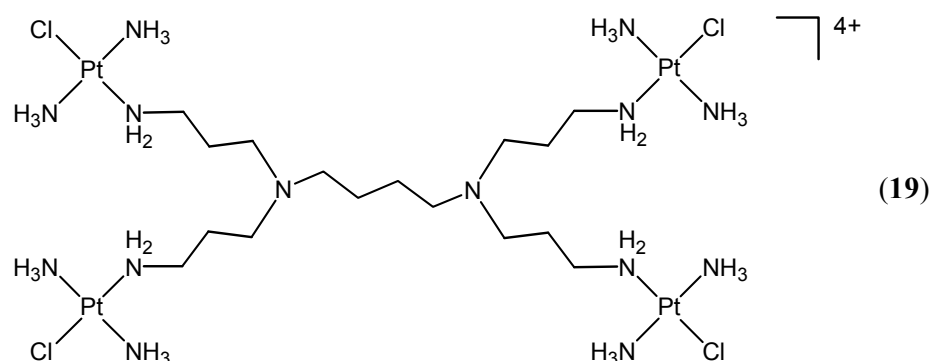


Figure 1.10 The dendritic tetranuclear cationic platinum complex **19**.

Chiral non-racemic bis(dichloro)platinum complexes have been prepared from *R* and/or *S* 1,2,4-triaminobutane units, in which the amino groups at position 1 and 2 are part of the chelate rings and are linked at position 4 as mono- or bisamides or ureides (**20**, **21** and **22**, respectively, Figure 1.11).^[122, 123] Only the dinuclear platinum complexes of the bisamide type exhibited activity close to that of cisplatin against cisplatin-sensitive mouse leukemia L1210 cells.^[123] This observation is consistent with the fact that they form a high amount of interstrand crosslinks,^[124] which may be related to the length and nature of the bisamide linker. The chirality of the different isomeric forms is, however, of no influence on the cytotoxicity or DNA binding properties of the bisamide complexes.^[123]

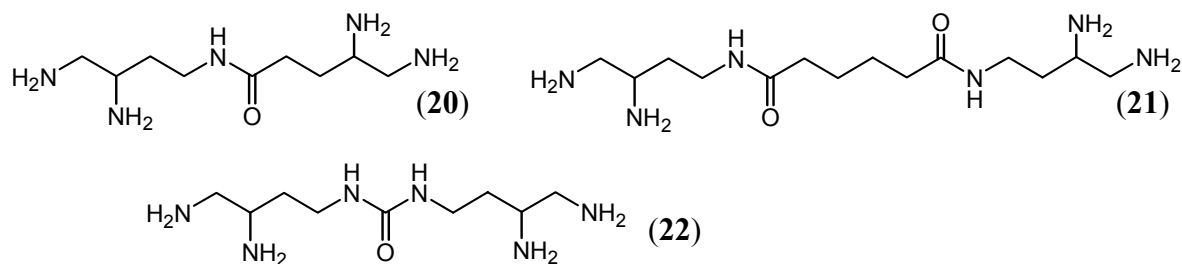


Figure 1.11 Mono- and bisamides (**20** and **21**, respectively) and ureide (**22**) linking two 1,2,4-triaminobutane- N^4 units.

Thiourea-bridged dinuclear platinum ethylenediamine (en) and *trans*-cyclohexane-1,2-diamine (dach) complexes, in which the *S*-donor ligand may alter the metabolism of the complex, were shown to display moderate to low activity in cisplatin-sensitive and -resistant leukemia cells, respectively.^[125]

Bisplatinum complexes in which two trans platinum moieties are linked using intercalating diaminoanthraquinone ligands (**23**, Figure 1.12) were found to be sensitive to the resistance mechanisms of cisplatin-resistant human ovarian cancer cells.^[126] It has been discovered that the platinum complexes accumulate in acidic vesicles in contrast to the free ligand by monitoring the fluorescent anthraquinones using fluorescence microscopy. The accumulation appears to be unrelated to the mechanism of deactivation of platinum compounds by glutathione.^[127] Dinuclear platinum complexes bridged by oxa-diaza crown ether ligands (one example is **24**, Figure 1.12) have been prepared to increase DNA interaction by the formation of cationic complexes with ions that are abundant in cells, such as sodium or potassium. However, the complexes lack cytotoxicity in human ovarian cancer cells.^[128]

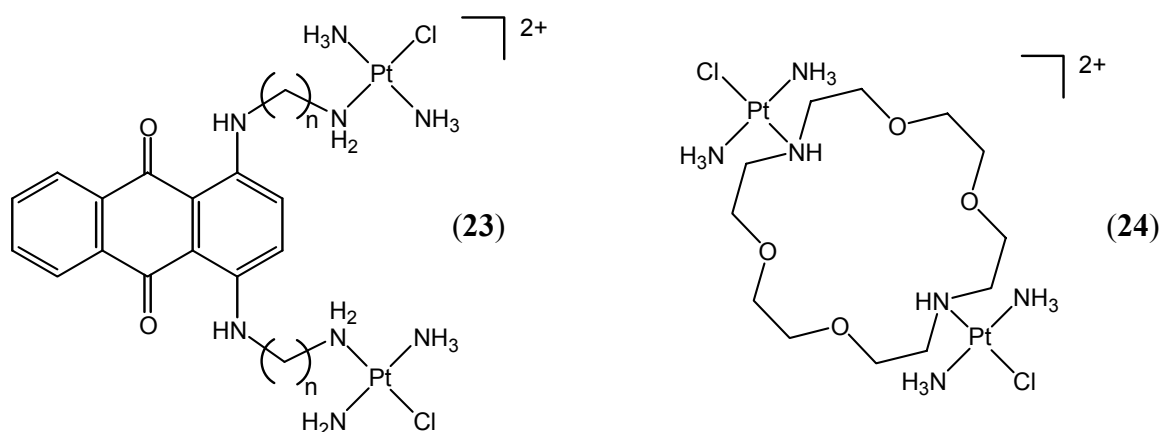


Figure 1.12 Dinuclear cationic platinum complexes of linking anthraquinones (**23**) and oxa-diaza crown ethers (**24**).

1.5.4 Short and (semi) rigid linkers

A series of highly rigid double-bridged dinuclear platinum chloride and mixed chloride/hydroxide complexes, with both square planar and octahedral geometries, have been synthesized by linking two cisplatin-like centers through the 4,4'-dipyrazolylmethane ligand dpzm (an example is **25**, Figure 1.13).^[129] From the more flexible single-bridged series with two chlorides *cis* or *trans* and either an amine or dmsoligand coordinated to platinum, the complex $[\{cis\text{-PtCl}_2(\text{NH}_3)\}_2(\mu\text{-dpzm})]$ exhibits higher cytotoxicity than the double-bridged complexes in three cancer cell lines.^[130] However, $[\{cis\text{-PtCl}_2(\text{NH}_3)\}_2(\mu\text{-dpzm})]$ did not show any advantage over cisplatin due to its poor water solubility.

Subsequently, the single-bridged dinuclear and trinuclear species $[\{trans\text{-Pt}(\text{NH}_3)_2\text{Cl}\}_2(\mu\text{-dpzm})]\text{Cl}_2$ (**26**, Figure 1.13) and $[\{trans\text{-Pt}(\text{NH}_3)_2\text{Cl}\}_2(\mu\text{-Pt}(\text{NH}_3)_2(\text{dpzm})_2)\text{Cl}_4]$, respectively, have been developed. The monofunctional trans-platinum centers provide an overall charge of 2+ and 4+, respectively.^[131, 132] The complexes form high levels of DNA interstrand crosslinks (50 %), which has been proposed to be due to the rigid nature of the dpzm ligand that prevents the complexes from forming short-range intrastrand adducts. The bifunctional dinuclear complex **26** was shown to bind preferentially at adenine residues,^[133] probably because of pre-association in the minor groove at A/T rich regions.^[134] Pre-association in the minor groove at G/C rich regions has been found to occur as well, but at a lower rate.^[135] The complexes do show cytotoxicity, but are not as active as their aliphatic equivalents, *i.e.* 1,1/t,t and BBR3464.^[131] The specific type of interstrand crosslink formed, and the preference for adenine binding may account for the difference in activity.

Recent studies of **26** encapsulated in cucurbit[7]uril (Q[7]) indicated that this molecular host Q[7] slowed down reactions rates by at least 3-fold, whereas only a small effect on cytotoxicity was observed.^[136]

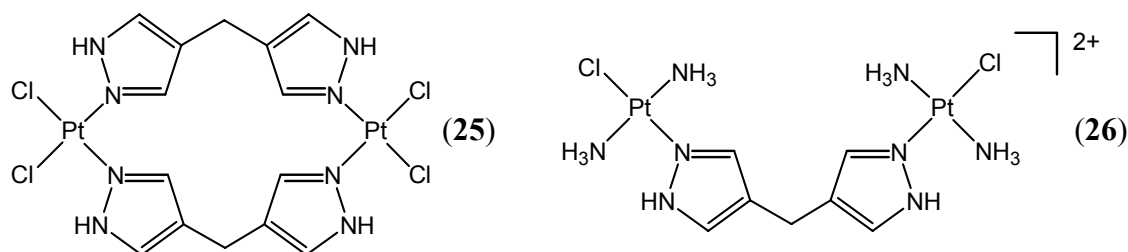


Figure 1.13 Double dpzm-linked dinuclear platinum complex **25**, and single dpzm-linked cationic platinum complex **26**.

Dinuclear platinum complexes bridged by 4,4'-dipyridylselenide or 4,4'-dipyridylsulfide (**27**, Figure 1.14) were prepared^[137] to diminish or antagonize the toxic side effects of anticancer

drugs, as selenium and sulfur containing compounds are known for their chemoprotective activity.^[138] The bifunctional *cis* derivatives have shown significant cytotoxicity, the complexes containing sulfur exhibiting an activity superior to their selenium analogues.^[139] DNA-binding studies indicated that the complex $[\{cis\text{-Pt}(\text{NH}_3)_2\text{Cl}\}_2(\mu\text{-}4,4'\text{-dipyridylsulfide})](\text{NO}_3)_2$ binds bifunctionally to DNA in a non-intercalative mode. The complex shows a lower interstrand crosslinking efficiency compared to the aliphatic analogue 1,1/*c,c* and is not able to induce the B \rightarrow Z transition in poly(dG-dC) \cdot poly(dG-dC).^[140] It has been suggested that the *trans* derivatives have different DNA-binding properties in comparison to the *cis* complexes.^[141] Dinuclear organoplatinum complexes with relatively “simple” 4,4'-dipyridyl and 1,2-bis(4'-pyridyl)ethane bridging ligands were also synthesized, but no biological data have been reported.^[84]

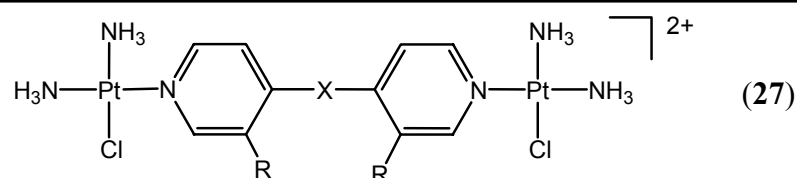


Figure 1.14 Dipyriddy-linked dinuclear cationic platinum complexes (**27**) with X = S or Se and R = H or CH₃.

A series of very short and rigid pyrazole- and hydroxo- bridged dinuclear platinum complexes, in which the hydroxide acts as a leaving group, were produced to mimic cisplatin binding.^[142, 143] They were anticipated to form 1,2-intrastrand adducts without major distortions of the DNA, thereby avoiding recognition and repair of the adduct. A crystal structure of the bis(9-ethylguanine) adduct of $[\{cis\text{-Pt}(\text{NH}_3)_2\}_2(\mu\text{-OH})(\mu\text{-pyrazolate})](\text{NO}_3)_2$ (**28**, Figure 1.15), illustrates that the platinum atoms are close enough to form a stable adduct to neighboring guanines on the DNA.^[142]

The rate of reaction of the azolato-bridged complexes with 9egua,^[144] GMP^[145] or DNA^[146] has been shown to be relatively slow. However, once the five-membered ring is opened via nucleophilic attack of the first base, the second platinum center reacts faster with a second base. After binding of one 9egua to the triazolato derivatives **29** (Figure 1.15), migration of the platinum atom from N2 to N3 occurs.^[144] The fact that a widely opened platinum coordination sphere results may explain why **29** not only serves as an intrastrand crosslinker, but also generates interstrand GC crosslinks,^[146] whereas complex **28** yields only the 1,2-intrastrand GG adduct on a hairpin stabilized double-stranded DNA. The significant cytotoxicity of **28** and **29** on several human tumor cell lines (compared to cisplatin),^[143] as well as of **29** against cisplatin-resistant mouse leukemia cells,^[144] have been postulated to be induced by minimal structural perturbations to DNA upon binding.^[147]

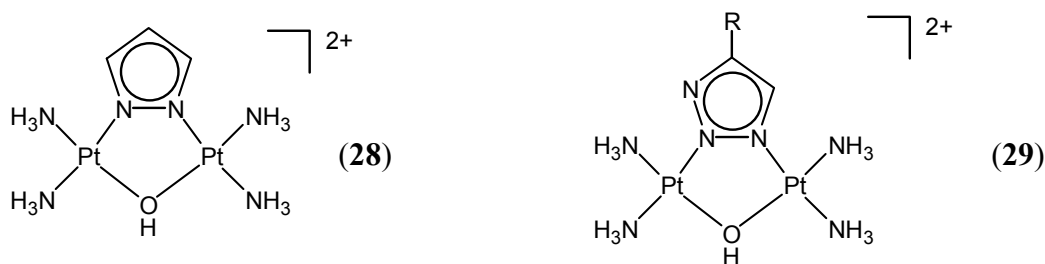


Figure 1.15 Pyrazole-bridged and triazolato-bridged dinuclear cationic platinum complexes **28** and **29**, respectively, with R = H or phenyl.

In general, azine-bridged dinuclear platinum(II) complexes^[148, 149] (**30**, **31** and **32**, Figure 1.16), and more bulky derivatives, show lower cytotoxicity than cisplatin in several human tumor cell lines. However, activity is comparable or higher against mouse leukemia cells sensitive or resistant to cisplatin.^[148] The complexes have been shown to undergo substitution of both chlorides by 9egua, except for complex **30**. Reaction of the latter with GMP results in cleavage of one of the Pt-N bonds to form N7,O6-platinated polymers.^[148]

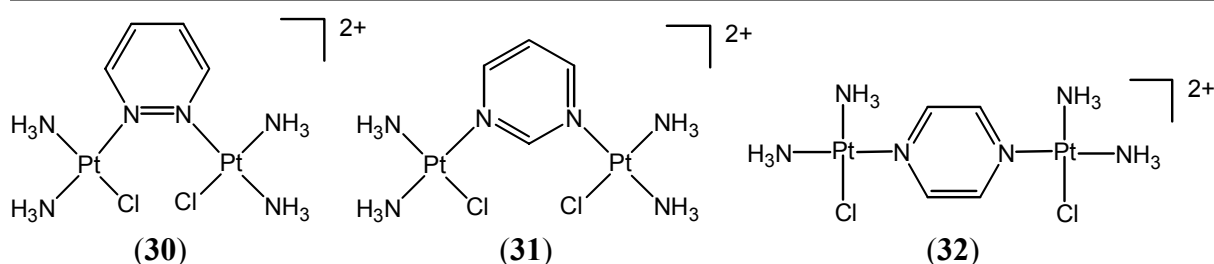


Figure 1.16 Azine-bridged dinuclear cationic platinum complexes **30**, **31** and **32**.

1.5.5 Heterocyclic coordinating ligands

Based upon the corresponding cytotoxic mononuclear complexes,^[150, 151] heterocyclic ligands capable of intercalation like 2,2'-bipyridine (bpy) and 2,2':6',2''-terpyridine (tpy) have also been used for the synthesis of dinuclear platinum complexes. Compounds capable of “stapling” DNA by intramolecular bis-intercalation are considered to have higher antitumor activity than the mononuclear analogues.^[152] For dinuclear bipyridine platinum(II) complexes different chelating bis(amino) acids were used as linkers to induce additional weak DNA interactions (an example is **33**, Figure 1.17).^[153] Short linkers resulted in low activity against P388 lymphocytic leukemia cells. Interestingly, binding to calf thymus DNA has been proposed not to occur by intercalation (or coordination), but rather by hydrogen bonding and electrostatic and Van der Waals interactions. Less flexible trinuclear chloride (**34**, Figure

1.17) and cyclobutane dicarboxylic acid (CBDCA) imine platinum complexes, were developed by linking three imine platinum centers through a central benzene group.^[154]

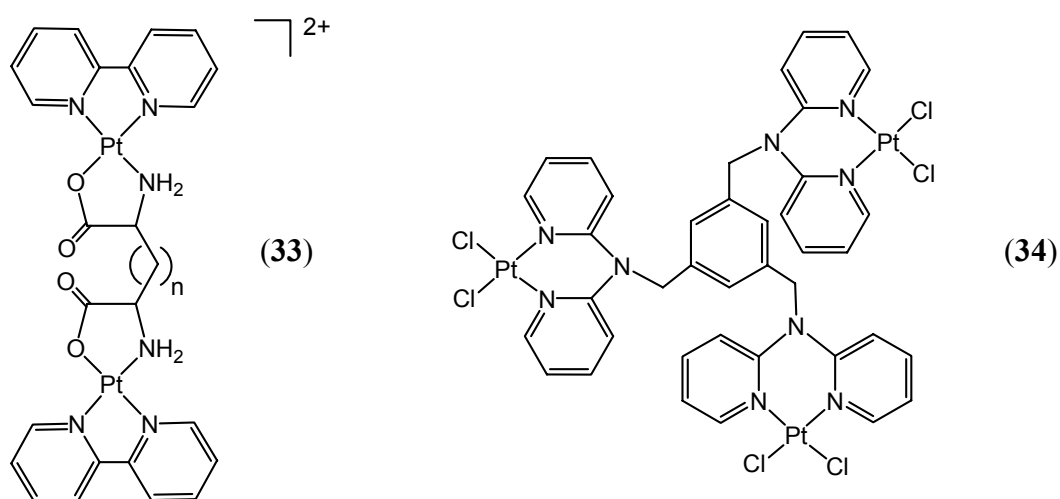


Figure 1.17 The dinuclear cationic platinum bipyridine complex **33** ($n = 2$ and 4) and the trinuclear imine complex **34**.

Dinuclear terpyridine platinum(II) complexes, in which the platinum centers are joined by a long and flexible linker attached at the 4' position of the tpy ligand, do not show high activity against several human ovarian carcinoma cell lines.^[150] Dinuclear 6-phenyl-2,2'-bipyridine organoplatinum(II) complexes, in which a long and flexible linker is attached at the 4 position of a fourth coordinating pyridine ligand, do not show activity either.^[155] The low activity of the latter is in agreement with the inactivity of the parental mononuclear complex.

Cytotoxicity is displayed by platinum terpyridine complexes that are bridged through more rigid coordinating dipyridyl linkers. The linkers contain ethynyl bonds of variable length with or without phenyl groups in between, or a charged dipyridyl diamine-platinum coordination center, or contain no substituent at all (**35**, Figure 1.18).^[156] Studies indicated that increasing the length of the linker does not improve antitumor activity. The complex with the shortest linker length is the most effective against several cancer cell lines showing no or little cross-resistance to cisplatin.^[150] However, high activity is displayed by a trinuclear platinum complex in which the linker contains a tetraamine-platinum center. Its cytotoxicity points out that the charge on each platinum center may be of importance for activity. Intercalation of these complexes has not been demonstrated.

A 1,3-substituted xyllythiolate-bridged dinuclear platinum terpyridine complex (**36**, Figure 1.18) has been reported to interact strongly with DNA by intercalation in comparison to the 1,4-substituted analogue.^[157] The latter has been suggested to be less flexible for bisintercalation into DNA.

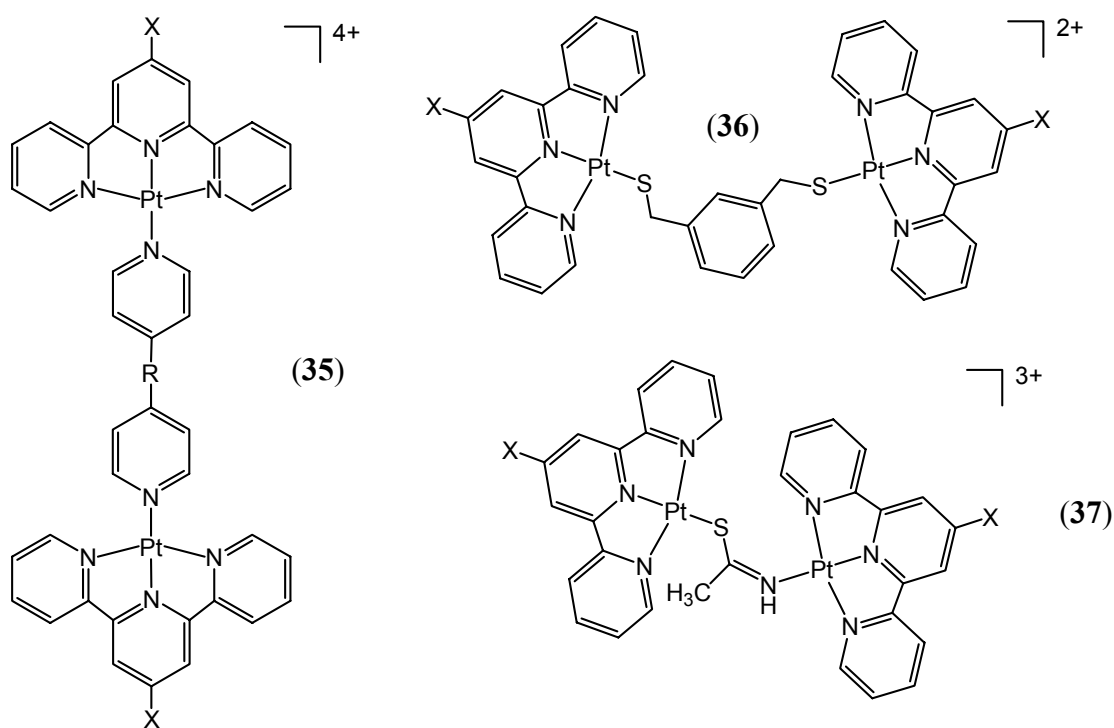


Figure 1.18 Polynuclear cationic platinum terpyridine complexes **35**, **36**, and **37**, in which X and R are different substituents and linkers (see text), respectively.

Bisintercalation of dinuclear dithiolatoalkane-linked terpyridine platinum complexes has been shown for complexes that are linked by α,ω -dithioalkanes with $n = 5, 6$, and 7 , whereas those with $n = 8$ and 10 form mono- and bisadducts by intercalation with either one or two platinum units.^[158] However, enhanced sequence specificity compared to the mononuclear derivative is not displayed.^[159] It has been suggested that the length and flexibility of the used linkers is not sufficient for bisintercalation at remote sites. Intercalation to two nearby binding sites may interrupt the geometry of DNA, thereby leading to a loss of specificity.

A new antitumor strategy has been implied for shorter thiolato-linked dinuclear platinum terpyridine complexes, which interact with two different intracellular targets, *i.e.* DNA and the selenoenzyme thioredoxin reductase (TrxR).^[160] Reduced thioredoxin provides reducing equivalents for a number of processes including the formation of deoxyribonucleotides by ribonucleotide reductase, one of the key steps in DNA synthesis. The complexes show very high specificity for human thioredoxin, which has been considered to be due to the high affinity of thiols for thiolato-platinum(II) complexes. Cytotoxic activity of complex **37** (Figure 1.18) has been shown against different glioblastoma, and head-and-neck squamous carcinoma cells.^[160] Only for a mononuclear derivative,^[160] reduced activity of TrxR was shown in glioblastoma cells.

1.6 Polynuclear ruthenium complexes

1.6.1 Introduction

In comparison to the field of anticancer polynuclear platinum complexes, the field of polynuclear ruthenium complexes has been relatively unexplored. Dinuclear analogues of the antimetastatic ruthenium complex NAMI-A, in which different bridging (poly)pyridyl ligands are used, have been studied in some detail.^[67] A few complexes bridged by rather short linkers have been investigated. Attention has been focused mostly on the extension of substitution-inert mononuclear ruthenium polypyridyl complexes, designed as photo-probes and photo-reagents of DNA, to dinuclear photoreactive complexes.

1.6.2 Substitution-labile polynuclear ruthenium complexes

A new series of anticancer ruthenium complexes structurally mimics the antimetastatic compound NAMI-A (**9**) by the linkage of two (NAMI-A)-type moieties through heterocyclic ligands, such as pyrazine (pyz), pyrimidine (pym) and 4,4'-bipyridine (bipy) and derivatives thereof.^[67, 161] The complexes $\text{NH}_4[\{\text{RuCl}_4(\text{dmsO-S})\}_2(\mu\text{-pyz})\{\text{RuCl}_3(\text{dmsO-S})(\text{dmsO-O})\}]$ and $\text{Na}_2[\{\text{RuCl}_4(\text{dmsO-S})\}_2(\mu\text{-bpy})]$ (**38** and **39**, respectively, Figure 1.19) have been shown to modify cell cycle distribution of human and murine carcinoma cells similarly to the parental mononuclear complex. An intracellular ruthenium concentration threshold, which imparted cell cycle arrest, was reached.^[162] The dinuclear complexes have been shown to form interstrand crosslinks with linearized plasmid DNA more actively than NAMI-A.^[163] They exhibit promising activity of inhibition of gelatinase MMP-9, an enzyme that degrades the extracellular matrix to promote metastasis, and reduce tumor cell invasion.

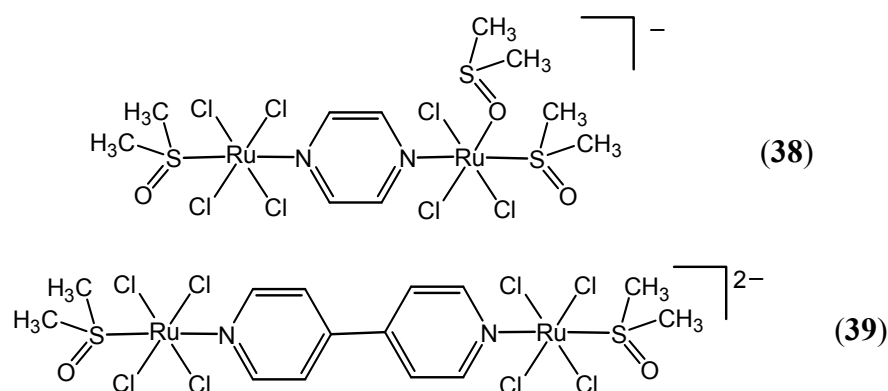


Figure 1.19 Dinuclear NAMI-A type anionic ruthenium(III) complexes, **38** and **39**.

Unfortunately, *in vivo* activity of the dinuclear complexes appeared not to be superior to that of NAMI-A.^[164] Moreover, higher liver and kidney toxicity contributes to a less favorable therapeutic index relative to NAMI-A.

The ruthenium atoms in the mixed-valent dinuclear complexes of the type $[\text{Ru}_2(\text{RCO}_2)_4\text{Cl}_2]^{2-}$ (R = CH₃ or CH₃CH₂) are linked by the four carboxylate ligands. The complexes have been demonstrated to bind to two 9-ethylguanine molecules in an unusual N⁷,O⁶-bridging mode with the bases in a head-to-tail fashion,^[165] and have shown good activity against P388 lymphocyte leukemia cells.^[166] The trinuclear μ -oxo bridged complex ruthenium red, $[(\text{NH}_3)_5\text{Ru}(\text{III})\text{ORu}(\text{IV})(\text{NH}_3)_4\text{ORu}(\text{III})(\text{NH}_3)_5]^{6+}$, has long been known to affect calcium metabolism, which has been linked to inhibition of tumor growth.^[167] However, it is the dinuclear impurity μ -O-[X(NH₃)₄Ru]₂³⁺ (X = Cl or OH) that has later been shown to be responsible for most of the inhibition of Ca²⁺ uptake in mitochondria.^[168] The dinuclear analogue μ -O-[(H₂O)(bpy)₂Ru(III)]₂⁴⁺ has been indicated to coordinate to DNA at relatively low levels with low stereoselectivity forming interstrand crosslinks.^[169]

1.6.3 Photoreactive polynuclear ruthenium(II) species

In photodynamic therapy (PDT) light is used to kill undesired cells in the body. The activity of PDT agents depends on their ability to associate with biopolymers or aggregates, such as cell membranes and DNA. DNA damage can occur by photoinduced electron transfer from the DNA to the excited state of the PDT molecule. Light absorption by a photosensitizing molecule can also lead to energy transfer to activate another molecule, such as O₂ to its excited singlet state. Ruthenium(II) complexes with polypyridine ligands have attracted considerable attention for studies aimed at photodynamic therapy, because of their rich photophysical repertoire.^[15] In contrast to mononuclear complexes, dinuclear ruthenium(II) complexes are greater in size, and charge, and vary more in shape. This may lead to increased DNA-binding affinity and specificity, which can be useful in the development of new photoprobes and stereochemical probes of nucleic acids.

Dinuclear systems, in which two $[\text{Ru}(\text{bpy})_3]^{2+}$ or $[\text{Ru}(\text{phen})_3]^{2+}$ (phen = 1,10-phenanthroline) moieties are linked by long and flexible alkane linkers, have been found to exhibit higher DNA binding affinity, more efficient photocleavage properties, and less sensitivity to ionic strength than their parental mononuclear analogues.^[170] DNA binding mainly occurs through electrostatic interactions. The linker length has been reported to be crucial for binding efficiency.

Dinuclear complexes based on $[\text{Ru}(\text{dpq})_2(\text{phen})]^{2+}$ (dpq = dipyrido[3,2-*d*:2',3'-*f*]-quinoxaline) (**40**, Figure 1.20), have been shown to bind to DNA with high affinity through intercalation of

the terminal dpq ligands.^[171] The position of attachment of the long and flexible mercaptoethyl ether linker to the phenanthroline ligands appears to have a profound effect on the binding size.

A dinuclear complex linked by 1,5-dipyridopentane, but with only one terminal ligand of extended aromaticity per moiety (*i.e.* dipyrido-[3,2-*a*:2',3'-*c*]-phenazine), does not show enhanced binding affinity with respect to the analogous monometallic complex.^[172]

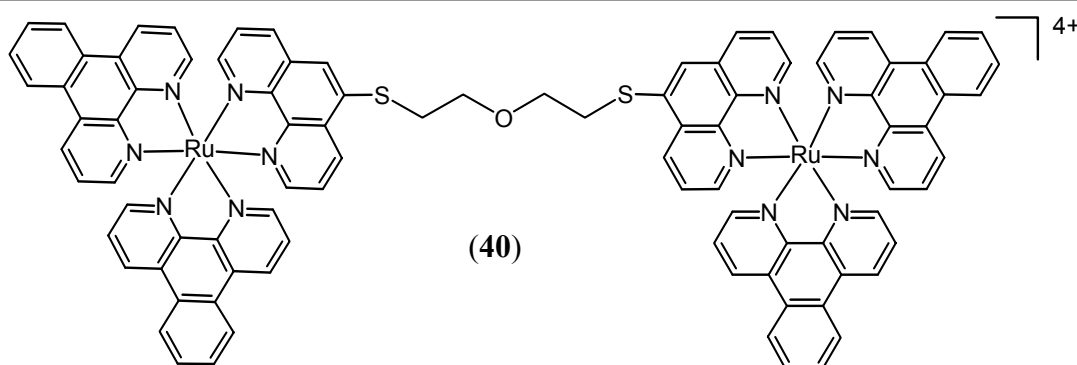


Figure 1.20 Dinuclear cationic ruthenium(II) dpq complex (40) linked by a long and flexible linker.

An interesting mode of DNA interaction has been suggested for the dinuclear ruthenium complex 41 (Figure 1.21), in which two $[\text{Ru}(\text{phen})_2\text{dppz}]^{2+}$ (dppz = dipyrido-[3,2-*a*:2',3'-*c*]-phenazine) moieties are joined through the phenazine ligand by a long and flexible alkane linker. The complex binds between base pairs of the DNA by bis-intercalation of the linked dppz moieties, thereby placing the ruthenium centers in the minor groove and the alkylamide linker in the major groove.^[173, 174] Kinetic results support a threading mechanism, in which the ruthenium moieties pass through the core of the DNA, rather than a mechanism in which the flexible linker is slinging itself around dissociated base pairs.^[173] The two enantiomers Δ - Δ and Λ - Λ both show high DNA affinities, but dissociation is markedly faster and also more dependent on the ionic strength for the Λ - Λ than for the Δ - Δ enantiomer. Each entity of the dinuclear complex binds to DNA almost identically to the monomer.^[174] The Δ - Δ enantiomer has been shown to be non-toxic for V79 Chinese hamster cells.^[175]

The semi-rigid dinuclear analogues (42, Figure 1.21) show even higher affinity for DNA.^[176] The initial binding of all three stereoisomers, including the *meso* form, is in the major groove.^[177] Subsequently, the isomers force one of their metal moieties through the DNA to slowly reach^[178] their final intercalative binding geometries. The final adducts have the bridging dppz ligand sandwiched between the DNA bases. The two metal centers are placed in opposite grooves.^[177] One is situated deeply in the minor groove. The enantiomeric forms (Δ - Δ and Λ - Λ) show distinct variations in their binding geometry. The *meso* stereoisomer

may provide a probe for stereoselectivity. The Λ part is deeply intercalated in the minor groove, probably as a result of a better fit of the Δ part in the major groove.

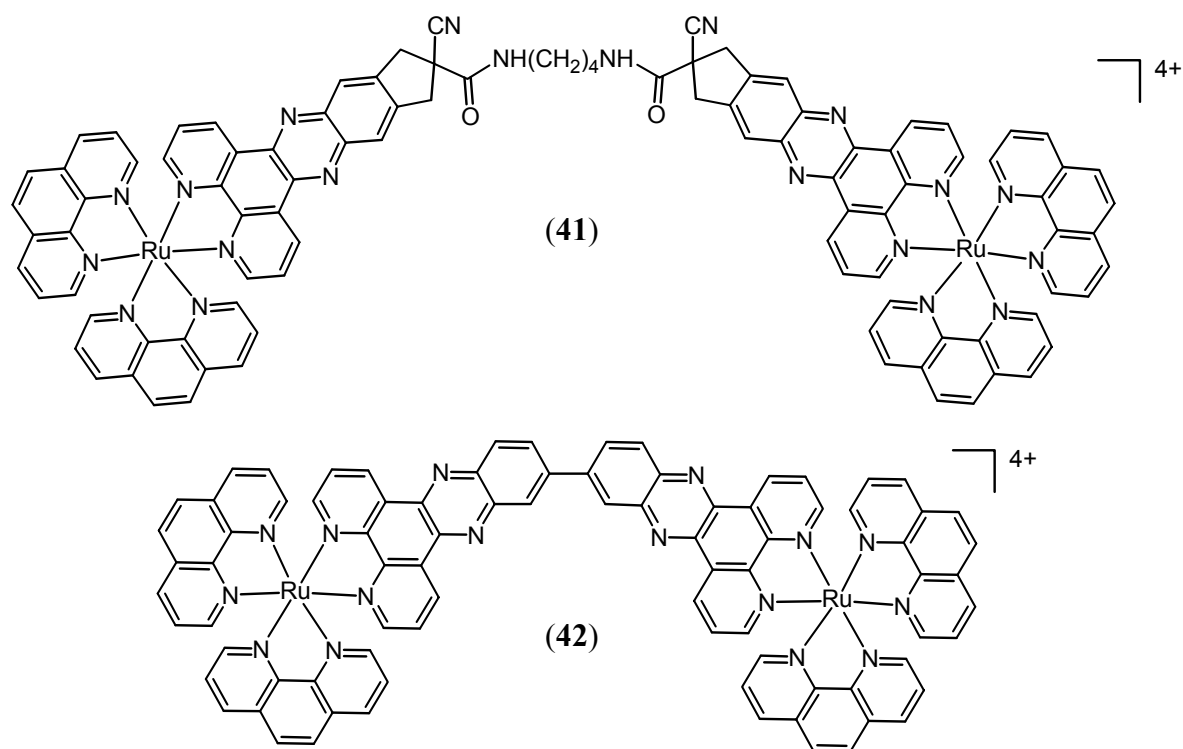


Figure 1.21 Long and flexible *versus* semi-rigid dinuclear cationic ruthenium(II) dppz complexes **41** and **42**, respectively.

DNA intercalation of the bridging ligand has also been suggested for dinuclear bipyridine complexes with semi-rigid phenanthroline linking ligands (*i.e.* bis([1,10]-phenanthroline[5,6-*f*]-imidazol-2-yl)).^[179] Dinuclear bipyridine complexes with an asymmetric phenanthroline linking ligand (*i.e.* 3-(pyrazin-2-yl)-*as*-triazino[5,6-*f*]1,10-phenanthroline) have been shown to bind to DNA only through electrostatic interactions.^[180] The dinuclear and trinuclear analogues, in which phenanthroline has been used for the terminal ligands, have also been reported.^[181] Groove-binding behavior has been demonstrated by dinuclear bipyridine complexes, which are linked by 4,4'-bipyridine-like ligands (*i.e.* 2,2'-bis(1,2,4-triazin-3-yl)-4,4'-bipyridine ligands with different substituents at the triazine).^[182-184] Some showed enantioselectivity.^[182, 183] Increasing the size of the plane of the bridging ligand, and thereby the hydrophobicity, resulted in stronger binding to DNA.^[183] Rigid dinuclear phenanthroline complexes, that share the short ligand HAT (HAT = 1,4,5,8,9,12-hezaazatriphenylene) (**43**, Figure 1.22) as the linking ligand, have been shown to bind weakly to DNA. Some preference for denatured or deformed segments along the DNA helix has been found.^[185, 186] The dinuclear HAT complexes exhibit the same photoreactivity

as the mononuclear parental complex.^[185] The interaction with purine mononucleotides and denatured CT-DNA appeared to be stereoselective and in favor of the *meso* form in both the excited and ground state.^[186] Stereoselectivity in DNA binding has also been seen for rigid dinuclear bipyridine complexes for which the short linking ligand 2,2'-bipyrimidine has been used.^[187, 188] These complexes have been shown to bind selectively to the minor groove^[187] at adenine bulge sites.^[188, 189] For dinuclear dpb complexes (2,3-bis(2-pyridyl)benzo[*g*]quinoxaline), the size of the spectator ligands has been shown to be of importance for the degree of binding.^[190]

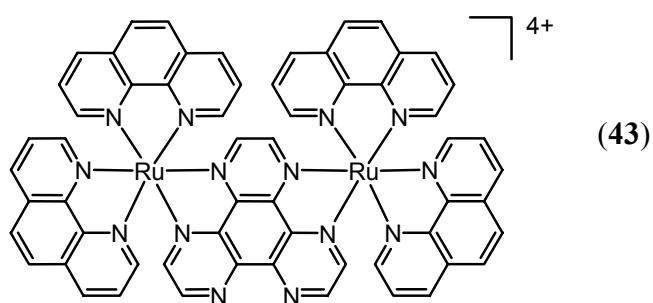


Figure 1.22 Short-bridged dinuclear cationic ruthenium HAT complex **43**.

1.7 Polynuclear ruthenium-platinum complexes

1.7.1 Introduction

Heteropolynuclear complexes of ruthenium and platinum have been developed to achieve selective reactivity at each metal center. Since ruthenium and platinum anticancer complexes display different mechanisms of action, the combination of the different metals may result in a unique profile of activity. The preparation of only a few ruthenium-platinum polynuclear complexes have been described, but biological activity has not been reported so far.

1.7.2 Heterodinuclear ruthenium platinum complexes

The complex [*cis*-RuCl₂(dms_o)₃](H₂N(CH₂)₄NH₂){*cis*-PtCl₂(NH₃)₂} (**44**, Figure 1.23), in which the two metal centers are linked by a long and flexible α,ω -diaminoalkane linker, was the first heterodinuclear ruthenium-platinum complex reported.^[191, 192] The complex has been found to form DNA crosslinks at which repair-proteins are associated. The DNA lesion responsible for efficient DNA-protein crosslinking is most probably a DNA-DNA interstrand crosslink in which each metal center is coordinated to one strand of the DNA helix. The DNA

crosslinks were suggested to act as potential suicide adducts by hijacking away critical proteins from their functions inside the cell. Unfortunately, the complex has been found to be too reactive for use as a probe, due to its light sensitivity and rapid hydrolysis.^[192]

Heterodinuclear ruthenium-platinum compounds have also been devised to photoreact with DNA. Systems, in which a ruthenium light-absorbing unit has been linked to a reactive platinum moiety, have been synthesized using short bridging heterocyclic ligands. The ruthenium unit provides water solubility and electrostatic interaction with DNA by its positive charge. The systems can be photoactivated through light absorption of the ruthenium unit, thereby imparting reactivity at the platinum unit. The latter may then coordinate to DNA.

The bridging ligand of the complex $[(bpy)_2Ru(dpbb)PtCl_2]Cl_2$ (**45**, Figure 1.23), affords an extra interaction with DNA by intercalation.^[193] Results have indicated that the complex primarily forms intrastrand crosslinks by coordination of the platinum unit, but a higher percentage of interstrand crosslinks than cisplatin has also been found. The system has been extended to complexes with 2,2':6',2''-terpyridine as the terminal ligand on ruthenium to eliminate enantiomeric forms, and with either chloride or PEt_2Ph as the sixth ligand.^[194] A variety of bridging ligands with different aromaticity, such as 2,2'-bipyrimidine, 2,3-bis(2-pyridyl)pyrazine and dpq, have been used to tune the spectroscopic and redox properties of the complexes. All have been shown to avidly bind to DNA, but photoreactivity has not been reported for these complexes.

Dinuclear dimethyltriaazolopyrimidine ruthenium-platinum complexes have been prepared by the use of the short linking ligands pyrazine and pyrimidine.^[195] Biological data have not been described.

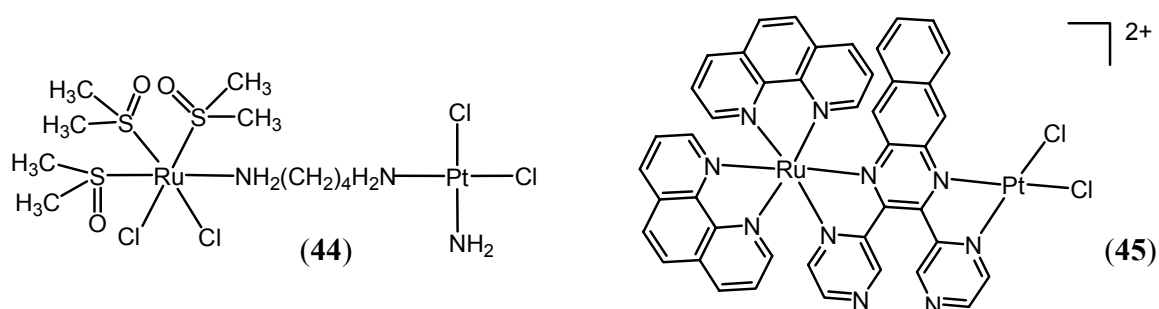


Figure 1.23 The long and flexible linked heterodinuclear ruthenium(II)-platinum(II) complex **44**, and the short and rigid linked heterodinuclear cationic ruthenium(II)-platinum(II) complex **45**.

1.8 Aim and contents of the thesis

The development of polynuclear platinum complexes in search for anticancer agents, which are effective against cisplatin resistant tumors, appears to be a productive field of research. Polynuclear ruthenium complexes on the other hand have not yet extensively been studied for their anticancer activities, and the synthesis of anticancer heteropolynuclear ruthenium-platinum complexes still presents a great challenge. The aim of the research described in this thesis has been the syntheses of polynuclear ruthenium polypyridyl complexes, as well as of heteropolynuclear ruthenium-platinum polypyridyl complexes as potential anticancer agents. These complexes have been designed to overcome cisplatin resistance. Their development has mainly been based upon the mononuclear complexes $[\text{Ru}(\text{tpy})\text{Cl}_3]$ and $[\text{Pt}(\text{tpy})\text{Cl}]\text{Cl}$ (tpy = 2,2':6',2''-terpyridine) (**46** and **47**, respectively, Figure 1.24).

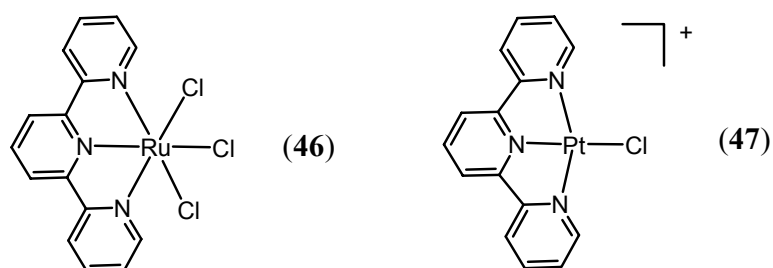


Figure 1.24 The mononuclear ruthenium(III) terpyridine complex **46**, and the mononuclear cationic platinum(II) terpyridine complex **47**.

The mononuclear ruthenium(III) complex $[\text{Ru}(\text{tpy})\text{Cl}_3]$ has been shown to display cytotoxicity and antitumor activity, which have been postulated to result from the interstrand binding to two guanines of the DNA in a *trans* position.^[196, 197] The mononuclear platinum(II) complex $[\text{Pt}(\text{tpy})\text{Cl}]\text{Cl}$ has been found^[150] to display cytotoxicity against a number of cancer cell lines, which has been ascribed to its ability to intercalate into DNA, as well as to coordinate to DNA.^[198]

The dinuclear ruthenium(III) complex $[\text{Cl}_3\text{Ru}(\text{dtdeg})\text{RuCl}_3]$ (**48**, Figure 1.25), in which the long and flexible ligand di[4'-(2,2':6',2''-terpyridyl)]-diethyleneglycolether links two trichlororuthenium(III) moieties, has previously been synthesized.^[195] However, the complex has been found to be poorly soluble in aqueous solutions. Poor water solubility is a major problem for the development of clinically active compounds, and is the main reason for the fact that the mononuclear complex $[\text{Ru}(\text{tpy})\text{Cl}_3]$ has not been developed any further.

Chapter 2 addresses the synthesis and characterization of a water-soluble dinuclear ruthenium dtdeg complex containing one trichloroterpyridylruthenium(III) moiety. The trifunctional moiety is linked to an inert bis(terpyridyl)-ruthenium(II) unit, which affords

water solubility and DNA affinity by its 2+ charge. Besides electrostatic DNA interactions, substitution-inert ruthenium polypyridyl complexes are also known to be capable of binding to DNA by surface binding, or partial intercalation.^[199] ¹H NMR resonances of the paramagnetic ruthenium(II)-ruthenium(III) complex are significantly broadened and shifted, due to the unpaired electron on the ruthenium(III) center. A unique approach to characterize the paramagnetic complex is presented.

In **Chapter 3** dinuclear ruthenium(II) polypyridyl complexes are described, in which the number of potential DNA coordination sites of each metal moiety has been varied by substitution of the relatively labile chloride ions with the inert ligands 2,2-bipyridine (bpy) or 2,2':6',2''terpyridine. The mononuclear analogue [Ru(tpy)(bpy)Cl]Cl has been reported^[197] to bind monofunctionally to DNA. The dinuclear complex [Cl(bpy)Ru(dtdeg)Ru(bpy)Cl]Cl₂ (**49**, Figure 1.25) has earlier been shown^[195] to bind bifunctionally to the small biomolecules methylimidazole and methylbenzimidazole. In this Chapter, the coordination of the DNA-model base 9-ethylguanine (9egua) to the dinuclear complex **49** is presented. The rotational behavior of coordinated 9egua is demonstrated by ¹H NMR techniques at variable temperatures. Biological experiments have been performed on these complexes, as well as on the dinuclear ruthenium complex reported in Chapter 2, to obtain structure-activity-relationships (SAR).

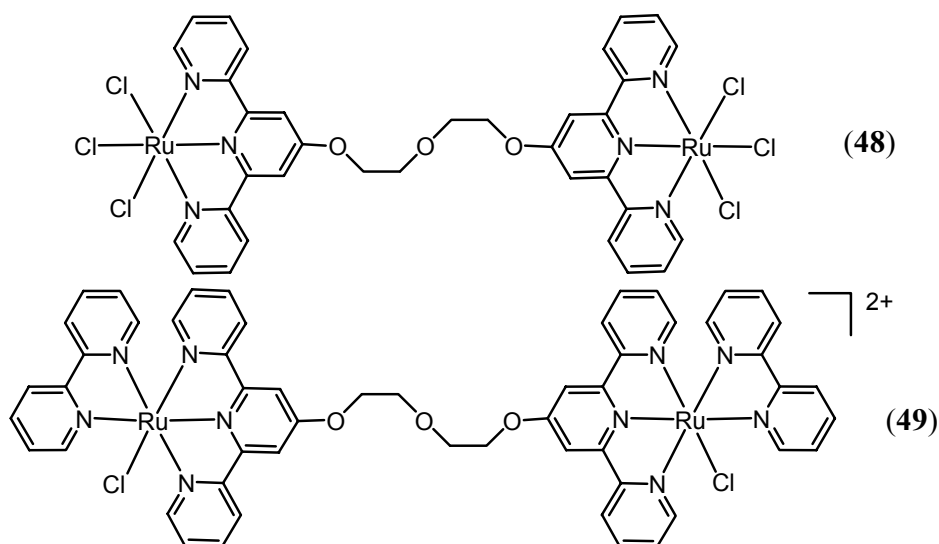


Figure 1.25 Dinuclear ruthenium polypyridyl complexes **48** and **49**.

The syntheses and characterization of heterodinuclear ruthenium(II)-platinum(II) dtdeg complexes are described in **Chapter 4**. The ruthenium moiety of these complexes has been modified by coordination of three labile chloride ligands, or the inert ligands bipyridine and terpyridine. The crystal structure of a prototype of this class of complexes shows the platinum

moiety not to be hindered for intercalation by the dangling ruthenium center. ¹H NMR data prove that coordination of platinum to 9-ethylguanine is feasible. The complexes have been tested for their cytotoxicity.

The syntheses and characterization of trinuclear and tetranuclear ruthenium(II)-ruthenium(III) and ruthenium(II)-platinum(II) dtdeg complexes, as well as their precursors, are illustrated in **Chapter 5**. These polynuclear complexes display appreciable cytotoxicity. Interestingly, cisplatin sensitive human ovarian cells adhere together and form clots upon incubation with the tetranuclear ruthenium compound. This behavior indicates that migration and metastasis of these cells may be hampered under influence of this complex in particular.

The short and semi-rigid bridging ligand 4'-pyridyl-2,2':6',2''-terpyridine (qpy) has been applied for the syntheses of the dinuclear and trinuclear ruthenium(II)-platinum(II) compounds presented in **Chapter 6**. According to ¹H NMR data, coordination of 9-ethylguanine to the ethylenediamine platinum unit occurs without hydrolysis. Inhibition of cell growth is substantially higher for the bifunctional trinuclear quaterpyridine complex than the monofunctional dinuclear derivative. However, the complexes do not show cytotoxicity.

The final chapter of this thesis summarizes the research described in this work. A general conclusion is given and future prospects for the development of polynuclear anticancer complexes are discussed.

Parts of this thesis have been published,^[200] or will be submitted for publication in the near future.^[201]

1.9 References

- [1] Blattman, J. N.; Greenberg, P. D., *Science* **2004**, *305*, 200-205. (b) Rosenberg, S. A., *Nature* **2001**, *411*, 380-384.
- [2] (a) Barnes, K. R.; Lippard, S. J., in *Metal Complexes in Tumor Diagnosis and as Anticancer Agents* (Ed.: Sigel, A.), FontisMedia S.A, Lausanne, **2004**, *42*, 143-177. (b) *Cisplatin. Chemistry and Biochemistry of a Leading Anticancer Drug* (Ed.: Lippert, B.), Verlag Helvetica Chimica Acta, Zurich, Wiley-VCH, Weinheim, **1999**.
- [3] Reedijk, J., *Chem. Rev.* **1999**, *99*, 2499-2510.
- [4] Jamieson, E. R.; Lippard, S. J., *Chem. Rev.* **1999**, *99*, 2467-2498.
- [5] (a) Rosenberg, B.; Vancamp, L.; Krigas, T., *Nature* **1965**, *205*, 698-699. (b) Rosenberg, B.; Vancamp, L.; Trosko, J. E.; Mansour, V. H., *Nature* **1969**, *222*, 385-386.
- [6] Lebwohl, D.; Canetta, R., *Eur. J. Cancer* **1998**, *34*, 1522-1534.
- [7] Boulikas, T.; Vougiouka, M., *Oncol. Rep.* **2003**, *10*, 1663-1682.
- [8] Jakupec, M. A.; Galanski, M.; Keppler, B. K., *Rev. Physiol. Biochem. Pharmacol.* **2003**, *146*, 1-53.
- [9] Reedijk, J., *Proc. Natl. Acad. Sci. U. S. A.* **2003**, *100*, 3611-3616.
- [10] (a) Perez, J. M.; Fuertes, M. A.; Alonso, C.; Navarro-Ranninger, C., *Crit. Rev. Oncol./Hematol.* **2000**, *35*, 109-120. (b) Natile, G.; Coluccia, M., *Coord. Chem. Rev.* **2001**, *216*, 383-410.
- [11] Wong, E.; Giandomenico, C. M., *Chem. Rev.* **1999**, *99*, 2451-2466.

- [12] Hall, M. D.; Hambley, T. W., *Coord. Chem. Rev.* **2002**, *232*, 49-67.
- [13] (a) Zhang, C. X.; Lippard, S. J., *Curr. Opin. Chem. Biol.* **2003**, *7*, 481-489. (b) Guo, Z. J.; Sadler, P. J., *Angew. Chem. Int. Ed.* **1999**, *38*, 1513-1531.
- [14] Clarke, M. J.; Zhu, F. C.; Frasca, D. R., *Chem. Rev.* **1999**, *99*, 2511-2533.
- [15] Clarke, M. J., *Coord. Chem. Rev.* **2003**, *236*, 209-233.
- [16] Wheate, N. J.; Collins, J. G., *Coord. Chem. Rev.* **2003**, *241*, 133-145.
- [17] Reedijk, J., *Chem. Commun.* **1996**, 801-806.
- [18] Gately, D. P.; Howell, S. B., *Br. J. Cancer* **1993**, *67*, 1171-1176.
- [19] (a) Ishida, S.; Lee, J.; Thiele, D. J.; Herskowitz, I., *Proc. Natl. Acad. Sci. U. S. A.* **2002**, *99*, 14298-14302. (b) Lin, X. J.; Okuda, T.; Holzer, A.; Howell, S. B., *Mol. Pharmacol.* **2002**, *62*, 1154-1159.
- [20] (a) Legendre, F.; Bas, V.; Kozelka, J.; Chottard, J. C., *Chem.-Eur. J.* **2000**, *6*, 2002-2010. (b) Kozelka, J.; Legendre, F.; Reeder, F.; Chottard, J. C., *Coord. Chem. Rev.* **1999**, *192*, 61-82. (c) Miller, S. E.; House, D. A., *Inorg. Chim. Acta* **1989**, *161*, 131-137.
- [21] Deubel, D. V., *J. Am. Chem. Soc.* **2004**, *126*, 5999-6004.
- [22] Whitehead, J. P.; Lippard, S. J., *Metal Ions in Biological Systems* **1996**, *32*, 687-726.
- [23] Hayes, D. M.; Cvitkovic, E.; Golbey, R. B.; Scheiner, E.; Helson, L.; Krakoff, I. H., *Cancer* **1977**, *39*, 1372-1381.
- [24] Navari, R. M.; Kaplan, H. G.; Gralla, R. J.; Grunberg, S. M.; Palmer, R.; Fitts, D., *J. Clin. Oncol.* **1994**, *12*, 2204-2210.
- [25] Brabec, V.; Kašpárková, J., *Drug Resist. Update* **2002**, *5*, 147-161.
- [26] Zhang, K.; Chew, M.; Yang, E. B.; Wong, K. P.; Mack, P., *Mol. Pharmacol.* **2001**, *59*, 837-843.
- [27] (a) Riva, C. M., *Anticancer Res.* **2000**, *20*, 4463-4471. (b) Jordan, P.; Carmo-Fonseca, M., *Cell. Mol. Life Sci.* **2000**, *57*, 1229-1235.
- [28] Cleare, M. J.; Hoeschele, J. D., *Bioinorg. Chem.* **1973**, *2*, 187-210. (b) Cleare, M. J.; Hoeschele, J. D., *Plat. Met. Rev.* **1973**, *17*, 2-13.
- [29] (a) O'Dwyer, P. J.; Stevenson, J. P.; Johnson, S. W., in *Cisplatin. Chemistry and Biochemistry of a Leading Anticancer Drug.* (Ed.: Lippert, B.), Verlag Helvetica Chimica Acta, Zurich, Wiley-VCH, Weinheim, **1999**, 31-69. (b) Go, R. S.; Adjei, A. A., *J. Clin. Oncol.* **1999**, *17*, 409-422. (c) Canetta, R.; Bragman, K.; Smaldone, L.; Rozenzweig, M., *Cancer Treat. Rev.* **1988**, *15*, 17-32.
- [30] Ota, K., *Cancer & Chemotherapy* **1996**, *23*, 379-387.
- [31] Lokich, J., *Cancer Invest.* **2001**, *19*, 756-760. (b) Wiseman, L. R.; Adkins, J. C.; Plosker, G. L.; Goa, K. L., *Drugs Aging* **1999**, *14*, 459-475.
- [32] (a) Jennerwein, M. M.; Eastman, A.; Khokhar, A., *Chem.-Biol. Interact.* **1989**, *70*, 39-49. (b) Woynarowski, J. M.; Chapman, W. G.; Napier, C.; Herzig, M. C. S.; Juniewicz, P., *Mol. Pharmacol.* **1998**, *54*, 770-777. (c) Saris, C. P.; Van deVaart, P. J. M.; Rietbroek, R. C.; Blommaert, F. A., *Carcinogenesis* **1996**, *17*, 2763-2769.
- [33] Spingler, B.; Whittington, D. A.; Lippard, S. J., *Inorg. Chem.* **2001**, *40*, 5596-5602.
- [34] Vaisman, A.; Lim, S. E.; Patrick, S. M.; Copeland, W. C.; Hinkle, D. C.; Turchi, J. J.; Chaney, S. G., *Biochemistry* **1999**, *38*, 11026-11039.
- [35] Misset, J. L., *Br. J. Cancer* **1998**, *77*, 4-7.
- [36] Mathe, G.; Kidani, Y.; Triana, K.; Brienza, S.; Ribaud, P.; Goldschmidt, E.; Ecstein, E.; Despax, R.; Musset, M.; Misset, J. L., *Biomed. Pharmacother.* **1986**, *40*, 372-376.
- [37] Extra, J. M.; Espie, M.; Calvo, F.; Ferme, C.; Mignot, L.; Marty, M., *Cancer Chemother. Pharmacol.* **1990**, *25*, 299-303.
- [38] Galanski, M.; Arion, V. B.; Jakupec, M. A.; Keppler, B. K., *Curr. Pharm. Design* **2003**, *9*, 2078-2089.

- [39] Kelland, L. R., in *Platinum-based Drugs in Cancer Therapy*. (Eds.: Kelland, L. R.; Farrell, N.), Humana Press Inc., Totowa N. J., **2000**, 299-319.
- [40] McKeage, M. J.; Raynaud, F.; Ward, J.; Berry, C.; Odell, D.; Kelland, L. R.; Murrer, B.; Santabarabara, P.; Harrap, K. R.; Judson, I. R., *J. Clin. Oncol.* **1997**, *15*, 2691-2700.
- [41] Chen, Y.; Guo, Z. J.; Parsons, S.; Sadler, P. J., *Chem.-Eur. J.* **1998**, *4*, 672-676.
- [42] Holford, J.; Sharp, S. Y.; Murrer, B. A.; Abrams, M.; Kelland, L. R., *Br. J. Cancer* **1998**, *77*, 366-373.
- [43] Raynaud, F. I.; Boxall, F. E.; Goddard, P. M.; Valenti, M.; Jones, M.; Murrer, B. A.; Abrams, M.; Kelland, L. R., *Clin. Cancer Res.* **1997**, *3*, 2063-2074.
- [44] (a) Brabec, V.; Nepelchová, K.; Kašpárková, J.; Farrell, N., *J. Biol. Inorg. Chem.* **2000**, *5*, 364-368. (b) Žakovská, A.; Nováková, O.; Balcarová, Z.; Bierbach, U.; Farrell, N.; Brabec, V., *Eur. J. Biochem.* **1998**, *254*, 547-557. (c) Zou, Y.; Van Houten, B.; Farrell, N., *Biochemistry* **1993**, *32*, 9632-9638.
- [45] Farrell, N., *Metal Ions in Biological Systems* **1996**, *32*, 603-639.
- [46] Farrell, N.; Kelland, L. R.; Roberts, J. D.; Van Beusichem, M., *Cancer Res.* **1992**, *52*, 5065-5072.
- [47] Natile, G.; Coluccia, M., *Top. Biol. Inorg. Chem.* **1999**, *1*, 73-98.
- [48] (a) Goddard, P. M.; Orr, R. M.; Valenti, M. R.; Barnard, C. F. J.; Murrer, B. A.; Kelland, L. R.; Harrap, K. R., *Anticancer Res.* **1996**, *16*, 33-38. (b) Kelland, L. R.; Barnard, C. F. J.; Evans, I. G.; Murrer, B. A.; Theobald, B. R. C.; Wyer, S. B.; Goddard, P. M.; Jones, M.; Valenti, M.; Bryant, A.; Rogers, P. M.; Harrap, K. R., *J. Med. Chem.* **1995**, *38*, 3016-3024.
- [49] O'Neill, C. F.; Hunakova, L.; Kelland, L. R., *Chem.-Biol. Interact.* **1999**, *123*, 11-29.
- [50] Mellish, K. J.; Barnard, C. F. J.; Murrer, B. A.; Kelland, L. R., *Int. J. Cancer* **1995**, *62*, 717-723.
- [51] *The Chemistry of Aqua Ions* (Ed.: Richens, D. T.), John Wiley and Sons Ltd., Chichester, **1997**.
- [52] Allardyce, C. S.; Dyson, P. J., *Plat. Met. Rev.* **2001**, *45*, 62-69.
- [53] Li, H. Y.; Qian, Z. M., *Med. Res. Rev.* **2002**, *22*, 225-250.
- [54] Sun, H. Z.; Li, H. Y.; Sadler, P. J., *Chem. Rev.* **1999**, *99*, 2817-2842.
- [55] Clarke, M. J.; Bitler, S.; Rennert, D.; Buchbinder, M.; Kelman, A. D., *J. Inorg. Biochem.* **1980**, *12*, 79-87.
- [56] Frasca, D. R.; Clarke, M. J., *J. Am. Chem. Soc.* **1999**, *121*, 8523-8532.
- [57] (a) Depenbrock, H.; Schmelcher, S.; Peter, R.; Keppler, B. K.; Weirich, G.; Block, T.; Rastetter, J.; Hanauske, A. R., *Eur. J. Cancer* **1997**, *33*, 2404-2410. (b) Galeano, A.; Berger, M. R.; Keppler, B. K., *Arzneimittelforschung* **1992**, *42-1*, 821-824. (c) Kreuser, E. D.; Keppler, B. K.; Berdel, W. E.; Piest, A.; Thiel, E., *Semin. Oncol.* **1992**, *19*, 73-81.
- [58] (a) Dhubhghaill, O. M. N.; Hagen, W. R.; Keppler, B. K.; Lipponer, K. G.; Sadler, P. J., *J. Chem. Soc.-Dalton Trans.* **1994**, 3305-3310. (b) Keppler, B. K.; Rupp, W.; Juhl, U. M.; Endres, H.; Niebl, R.; Balzer, W., *Inorg. Chem.* **1987**, *26*, 4366-4370. (c) Keppler, B. K.; Balzer, W.; Seifried, V., *Arzneimittelforschung* **1987**, *37-2*, 770-771. (d) Keppler, B. K.; Henn, M.; Juhl, U. M.; Berger, M. R.; Niebel, R.; E., W. F., in *Ruthenium and Other Non-Platinum Metal Complexes in Cancer Chemotherapy* (Ed.: Clarke, M. J.), Springer-Verlag, Heidelberg, **1989**, 41-70.
- [59] Seelig, M. H.; Berger, M. R.; Keppler, B. K., *J. Cancer Res. Clin. Oncol.* **1992**, *118*, 195-200.
- [60] Berger, M. R.; Garzon, F. T.; Keppler, B. K.; Schmahl, D., *Anticancer Res.* **1989**, *9*, 761-765.
- [61] Keppler, B. K.; Hartmann, M., *Metal-Based Drugs* **1994**, *1*, 145-149.
- [62] Keppler, B. K.; Dittrich, C., *Perspektiven* **1999**, *4-5*, 64.
- [63] Keppler, B. K.; Lipponer, K. G.; Stenzel, B.; Kratz, F., in *Metal Complexes in Cancer Chemotherapy* (Ed.: Keppler, B. K.), VCH, Weinheim, **1993**, 187-220.
- [64] Kratz, F.; Keppler, B. K.; Hartmann, M.; Messori, L.; Berger, M. R., *Metal-Based Drugs* **1996**, *3*, 15-24.

- [65] Keppler, B. K.; Eisenbrand, G.; Jakupec, M. A., in *Relevance of Tumor Models for Anticancer Drug Development* (Eds.: Fiebig, H. H.; Burger, A. M.), Karger, Basel, **1999**, *54*, 361-367.
- [66] (a) Hartmann, M.; Lipponer, K. G.; Keppler, B. K., *Inorg. Chim. Acta* **1998**, *267*, 137-141. (b) Malina, J.; Nováková, O.; Keppler, B. K.; Alessio, E.; Brabec, V., *J. Biol. Inorg. Chem.* **2001**, *6*, 435-445.
- [67] Alessio, E.; Mestroni, G.; Bergamo, A.; Sava, G., *Metal Ions in Biological Systems* **2004**, *42*, 323-351.
- [68] Redemaker-Lakhai, J. M.; Van den Bongard, D.; Pluim, D.; Beijnen, J. H.; Schellens, J. H. M., *Clin. Cancer Res.* **2004**, *10*, 3717-.
- [69] Bergamo, A.; Gagliardi, R.; Scarcia, V.; Furlani, A.; Alessio, E.; Mestroni, G.; Sava, G., *J. Pharmacol. Exp. Ther.* **1999**, *289*, 559-564.
- [70] Sava, G.; Zorzet, S.; Turrin, C.; Vita, F.; Soranzo, M.; Zabucchi, G.; Cocchietto, M.; Bergamo, A.; DiGiovine, S.; Pezzoni, G.; Sartor, L.; Garbisa, S., *Clin. Cancer Res.* **2003**, *9*, 1898-1905.
- [71] Sava, G.; Alessio, E.; Bergamo, A.; Mestroni, G., in *Top. Biol. Inorg. Chem.* (Eds.: Clarke, M. J.; Sadler, P. J.), Springer, Berlin, **1999**, *1*, 143-169.
- [72] Sava, G.; Bergamo, A.; Zorzet, S.; Gava, B.; Casarsa, C.; Cocchietto, M.; Furlani, A.; Scarcia, V.; Serli, B.; Iengo, E.; Alessio, E.; Mestroni, G., *Eur. J. Cancer* **2002**, *38*, 427-435.
- [73] Zorzet, S.; Bergamo, A.; Cocchietto, M.; Sorc, A.; Gava, B.; Alessio, E.; Iengo, E.; Sava, G., *J. Pharmacol. Exp. Ther.* **2000**, *295*, 927-933.
- [74] Vacca, A.; Bruno, M.; Boccarelli, A.; Coluccia, M.; Ribatti, D.; Bergamo, A.; Garbisa, S.; Sartor, L.; Sava, G., *Br. J. Cancer* **2002**, *86*, 993-998.
- [75] Sanna, B.; Debidda, M.; Pintus, G.; Tadolini, B.; Posadino, A. M.; Bennardini, F.; Sava, G.; Ventura, C., *Arch. Biochem. Biophys.* **2002**, *403*, 209-218.
- [76] (a) Aird, R. E.; Cummings, J.; Ritchie, A. A.; Muir, M.; Morris, R. E.; Chen, H.; Sadler, P. J.; Jodrell, D. I., *Br. J. Cancer* **2002**, *86*, 1652-1657. (b) Morris, R. E.; Aird, R. E.; Murdoch, P. D.; Chen, H. M.; Cummings, J.; Hughes, N. D.; Parsons, S.; Parkin, A.; Boyd, G.; Jodrell, D. I.; Sadler, P. J., *J. Med. Chem.* **2001**, *44*, 3616-3621.
- [77] Farrell, N.; Qu, Y.; Bierbach, U.; Valsecchi, M.; Menta, E., in *Cisplatin. Chemistry and Biochemistry of a Leading Anticancer Drug* (Ed.: Lippert, B.), Verlag Helvetica Chimica Acta, Zurich, Wiley-VCH, Weinheim, **1999**, 479-496.
- [78] Farrell, N. P.; De Almeida, S. G.; Skov, K. A., *J. Am. Chem. Soc.* **1988**, *110*, 5018-5019. (b) Farrell, N.; Qu, Y., *Inorg. Chem.* **1989**, *28*, 3416-3420.
- [79] Farrell, N.; Qu, Y.; Hacker, M. P., *J. Med. Chem.* **1990**, *33*, 2179-2184.
- [80] Kraker, A. J.; Hoeschele, J. D.; Elliott, W. L.; Showalter, H. D. H.; Sercel, A. D.; Farrell, N. P., *J. Med. Chem.* **1992**, *35*, 4526-4532.
- [81] Roberts, J. D.; Van Houten, B.; Qu, Y.; Farrell, N. P., *Nucleic Acids Res.* **1989**, *17*, 9719-9733.
- [82] Farrell, N.; Qu, Y.; Feng, L.; Van Houten, B., *Biochemistry* **1990**, *29*, 9522-9531.
- [83] (a) Fontes, A. P. S.; Zou, Y.; Farrell, N., *J. Inorg. Biochem.* **1994**, *55*, 79-85. (b) Marini, V.; Kašpárková; Nováková, O.; Scolaro, L. M.; Romeo, R.; Brabec, V., *J. Biol. Inorg. Chem.* **2002**, *7*, 725-734.
- [84] Cafeo, G.; Lo Passo, C.; Scolaro, L. M.; Pernice, I.; Romeo, R., *Inorg. Chim. Acta* **1998**, *276*, 141-149.
- [85] McGregor, T. D.; Balcarová, Z.; Qu, Y.; Tran, M. C.; Žaludová, R.; Brabec, V.; Farrell, N., *J. Inorg. Biochem.* **1999**, *77*, 43-46.
- [86] Johnson, A.; Qu, Y.; Van Houten, B.; Farrell, N., *Nucleic Acids Res.* **1992**, *20*, 1697-1703. (b) Wu, P. K.; Qu, Y.; Van Houten, B.; Farrell, N., *J. Inorg. Biochem.* **1994**, *54*, 207-220.
- [87] Wu, P. K.; Kharatishvili, M.; Qu, Y.; Farrell, N., *J. Inorg. Biochem.* **1996**, *63*, 9-18.
- [88] Malfoy, B.; Hartmann, B.; Leng, M., *Nucleic Acids Res.* **1981**, *9*, 5659-5669.
- [89] Herbert, A.; Rich, A., *Genetica* **1999**, *106*, 37-47.

- [90] Manzotti, C.; Pezzoni, G.; Giuliani, F.; Valsecchi, M.; Farrell, N.; Tognella, S., *Proc. Am. Assn. Cancer Res.* **1994**, *35*, 2628.
- [91] (a) Zou, Y.; Van Houten, B.; Farrell, N., *Biochemistry* **1994**, *33*, 5404-5410. (b) Žaludová, R.; Žakovská, A.; Kašpárková, J.; Balcarová, Z.; Kleinwachter, V.; Vrána, O.; Farrell, N.; Brabec, V., *Eur. J. Biochem.* **1997**, *246*, 508-517. (c) Farrell, N.; Appleton, T. G.; Qu, Y.; Roberts, J. D.; Soares Fontes, A. P.; Skov, K. A.; Wu, P. K.; Zou, Y., *Biochemistry* **1995**, *34*, 15480-15486.
- [92] Brabec, V.; Leng, M., *Proc. Natl. Acad. Sci. U. S. A.* **1993**, *90*, 5345-5349.
- [93] Kašpárková, J.; Nováková, O.; Vrána, O.; Farrell, N.; Brabec, V., *Biochemistry* **1999**, *38*, 10997-11005.
- [94] Lehnert, S.; Farrell, N., *Proc. Am. Assn. Cancer Res.* **1995**, *36*, 2376.
- [95] (a) Berners-Price, S. J.; Davies, M. S.; Cox, J. W.; Thomas, D. S.; Farrell, N., *Chem.-Eur. J.* **2003**, *9*, 713-725. (b) Cox, J. W.; Berners-Price, S.; Davies, M. S.; Qu, Y.; Farrell, N., *J. Am. Chem. Soc.* **2001**, *123*, 1316-1326.
- [96] Wang, Y. J.; Farrell, N.; Burgess, J. D., *J. Am. Chem. Soc.* **2001**, *123*, 5576-5577.
- [97] Kašpárková, J.; Farrell, N.; Brabec, V., *J. Biol. Chem.* **2000**, *275*, 15789-15798.
- [98] (a) Qu, Y.; Fitzgerald, J. A.; Rauter, H.; Farrell, N., *Inorg. Chem.* **2001**, *40*, 6324-6327. (b) Kloster, M.; Kostrhunová, H.; Žaludová, R.; Malina, J.; Kašpárková, J.; Brabec, V.; Farrell, N., *Biochemistry* **2004**, *43*, 7776-7786.
- [99] Qu, Y.; Rauter, H.; Fontes, A. P. S.; Bandarage, R.; Kelland, L. R.; Farrell, N., *J. Med. Chem.* **2000**, *43*, 3189-3192.
- [100] Sessa, C.; Capri, G.; Gianni, L.; Peccatori, F.; Grasselli, G.; Bauer, J.; Zucchetti, M.; Vigano, L.; Gatti, A.; Minoia, C.; Liati, P.; Van den Bosch, S.; Bernareggi, A.; Camboni, G.; Marsoni, S., *Ann. Oncol.* **2000**, *11*, 977-983.
- [101] Roberts, J. D.; Beggiolin, G.; Manzotti, C.; Piazzoni, L.; Farrell, N., *J. Inorg. Biochem.* **1999**, *77*, 47-50.
- [102] (a) Perego, P.; Caserini, C.; Gatti, L.; Carenini, N.; Romanelli, S.; Supino, R.; Colangelo, D.; Viano, I.; Leone, R.; Spinelli, S.; Pezzoni, G.; Manzotti, C.; Farrell, N.; Zunino, F., *Mol. Pharmacol.* **1999**, *55*, 1108-1108. (b) Perego, P.; Gatti, L.; Caserini, C.; Supino, R.; Colangelo, D.; Leone, R.; Spinelli, S.; Farrell, N.; Zunino, F., *J. Inorg. Biochem.* **1999**, *77*, 59-64.
- [103] Pratesi, G.; Perego, P.; Polizzi, D.; Righetti, S. C.; Supino, R.; Caserini, C.; Manzotti, C.; Giuliani, F. C.; Pezzoni, G.; Tognella, S.; Spinelli, S.; Farrell, N.; Zunino, F., *Br. J. Cancer* **1999**, *80*, 1912-1919.
- [104] Farrell, N., in *Platinum-Based Drugs in Cancer Therapy* (Eds.: Kelland, L. R.; Farrell, N. P.), Humana Press Inc., Totowa, N. J., **2000**, 321-338.
- [105] Brabec, V.; Kašpárková, J.; Vrána, O.; Nováková, O.; Cox, J. W.; Qu, Y.; Farrell, N., *Biochemistry* **1999**, *38*, 6781-6790.
- [106] Zehnulová, J.; Kašpárková, J.; Farrell, N.; Brabec, V., *J. Biol. Chem.* **2001**, *276*, 22191-22199. (b) Kašpárková, J.; Zehnulová, J.; Farrell, N.; Brabec, V., *J. Biol. Chem.* **2002**, *277*, 48076-48086.
- [107] (a) Qu, Y.; Scarsdale, N. J.; Tran, M. C.; Farrell, N. P., *J. Biol. Inorg. Chem.* **2003**, *8*, 19-28. (b) Hegmans, A.; Berners-Price, S. J.; Davies, M. S.; Thomas, D. S.; Humphreys, A. S.; Farrell, N., *J. Am. Chem. Soc.* **2004**, *126*, 2166-2180.
- [108] (a) Pegg, A. E., *Cancer Res.* **1988**, *48*, 759-774. (b) Pegg, A. E., *Biochem. J.* **1986**, *234*, 249-262. (b) Tabor, C. W.; Tabor, H., *Annu. Rev. Biochem.* **1984**, *53*, 749-790.
- [109] Hague, D. N.; Moreton, A. D., *J. Chem. Soc.-Perkin Trans. 2* **1994**, 265-270. (b) Feuerstein, B. G.; Williams, L. D.; Basu, H. S.; Marton, L. J., *J. Cell. Biochem.* **1991**, *46*, 37-47.
- [110] (a) Behe, M.; Felsenfeld, G., *Proc. Natl. Acad. Sci. U. S. A.* **1981**, *78*, 1619-1623. (b) Gosule, L. C.; Schellman, J. A., *J. Mol. Biol.* **1978**, *121*, 311-326. (c) Jain, S.; Zon, G.; Sundaralingam, M., *Biochemistry* **1989**, *28*, 2360-2364.

- [111] Amo-Ochoa, P.; González, V. M.; Pérez, J. M.; Masaguer, J. R.; Alonso, C.; Navarro-Ranninger, C., *J. Inorg. Biochem.* **1996**, *64*, 287-299.
- [112] Navarro-Ranninger, C.; Amo-Ochoa, P.; Pérez, J. M.; González, V. M.; Masaguer, J. R.; Alonso, C., *J. Inorg. Biochem.* **1994**, *53*, 177-190.
- [113] (a) Teixeira, L. J.; Seabra, M.; Reis, E.; da Cruz, M. T. G.; de Lima, M. C. P.; Pereira, E.; Miranda, M. A.; Marques, M. P. M., *J. Med. Chem.* **2004**, *47*, 2917-2925. (b) Marques, M. P. M.; Girao, T.; De Lima, M. C. P.; Gameiro, A.; Pereira, E.; Garcia, P., *Biochim. Biophys. Acta-Mol. Cell Res.* **2002**, *1589*, 63-70.
- [114] Rauter, H.; DiDomenico, R.; Menta, E.; Oliva, A.; Qu, Y.; Farrell, N., *Inorg. Chem.* **1997**, *36*, 3919-3927.
- [115] Qu, Y.; Harris, A.; Hegmans, A.; Petz, A.; Kabolizadeh, P.; Penazova, H.; Farrell, N., *J. Inorg. Biochem.* **2004**, *98*, 1591-1598.
- [116] McGregor, T. D.; Hegmans, A.; Kašpárková, J.; Nepelchová, K.; Nováková, O.; Penazova, H.; Vrána, O.; Brabec, V.; Farrell, N., *J. Biol. Inorg. Chem.* **2002**, *7*, 397-404.
- [117] McGregor, T. D.; Bousfield, W.; Qu, Y.; Farrell, N., *J. Inorg. Biochem.* **2002**, *91*, 212-219.
- [118] Roberts, J. D.; Peroutka, J.; Farrell, N., *J. Inorg. Biochem.* **1999**, *77*, 51-57.
- [119] Rauter, H.; DiDomenico, R.; Menta, E.; Da Re, G.; De Cillis, G.; Conti, M.; Lotto, A.; Pavesi, P.; Spinelli, S.; Manzotti, C.; Piazzoni, L.; Farrell, N., *Proc. Am. Assn. Cancer Res.* **1998**, *39*, 1096.
- [120] Hegmans, A.; Qu, Y.; Kelland, L. R.; Roberts, J. D.; Farrell, N., *Inorg. Chem.* **2001**, *40*, 6108-6114.
- [121] Jansen, B. A. J.; van der Zwan, J.; Reedijk, J.; den Dulk, H.; Brouwer, J., *Eur. J. Inorg. Chem.* **1999**, 1429-1433.
- [122] Schuhmann, E.; Altman, J.; Karaghiosoff, K.; Beck, W., *Inorg. Chem.* **1995**, *34*, 2316-2322.
- [123] Buning, H.; Altman, J.; Zorbas, H.; Beck, W., *J. Inorg. Biochem.* **1999**, *75*, 269-279.
- [124] Buning, H.; Altman, J.; Beck, W.; Zorbas, H., *Biochemistry* **1997**, *36*, 11408-11418.
- [125] (a) Bierbach, U.; Hambley, T. W.; Farrell, N., *Inorg. Chem.* **1998**, *37*, 708-716. (b) Bierbach, U.; Roberts, J. D.; Farrell, N., *Inorg. Chem.* **1998**, *37*, 717-723.
- [126] Jansen, B. A. J.; Wielaard, P.; Kalayda, G. V.; Ferrari, M.; Molenaar, C.; Tanke, H. J.; Brouwer, J.; Reedijk, J., *J. Biol. Inorg. Chem.* **2004**, *9*, 403-413.
- [127] Kalayda, G. V.; Jansen, B. A. J.; Molenaar, C.; Wielaard, P.; Tanke, H. J.; Reedijk, J., *J. Biol. Inorg. Chem.* **2004**, *9*, 414-422.
- [128] Jansen, B. A. J.; Wielaard, P.; den Dulk, H.; Brouwer, J.; Reedijk, J., *Eur. J. Inorg. Chem.* **2002**, 2375-2379.
- [129] (a) Broomhead, J. A.; Rendina, L. M.; Sterns, M., *Inorg. Chem.* **1992**, *31*, 1880-1889. (b) Broomhead, J. A.; Rendina, L. M.; Webster, L. K., *J. Inorg. Biochem.* **1993**, *49*, 221-234.
- [130] Broomhead, J. A.; Lynch, M. J., *Inorg. Chim. Acta* **1995**, *240*, 13-17.
- [131] Wheate, N. J.; Cullinane, C.; Webster, L. K.; Collins, J. G., *Anti-Cancer Drug Des.* **2001**, *16*, 91-98.
- [132] Collins, J. G.; Wheate, N. J., *J. Inorg. Biochem.* **2004**, *98*, 1578-1584.
- [133] Wheate, N. J.; Evison, B. J.; Herlt, A. J.; Phillips, D. R.; Collins, J. G., *Dalton Trans.* **2003**, 3486-3492.
- [134] (a) Wheate, N. J.; Webster, L. K.; Brodie, C. R.; Collins, J. G., *Anti-Cancer Drug Des.* **2000**, *15*, 313-322. (b) Wheate, N. J.; Collins, J. G., *J. Inorg. Biochem.* **2000**, *78*, 313-320.
- [135] Wheate, N. J.; Cutts, S. M.; Phillips, D. R.; Aldrich-Wright, J. R.; Collins, J. G., *J. Inorg. Biochem.* **2001**, *84*, 119-127.
- [136] Wheate, N. J.; Day, A. I.; Blanch, R. J.; Arnold, A. P.; Cullinane, C.; Collins, J. G., *Chem. Commun.* **2004**, 1424-1425.
- [137] Zhao, G. H.; Lin, H. K.; Zhu, S. R.; Sun, H. W.; Chen, Y. T., *J. Coord. Chem.* **1998**, *46*, 79-85.

- [138] (a) May, S. W., *Expert Opin. Investig. Drugs* **2002**, *11*, 1261-1269. (b) Links, M.; Lewis, C., *Drugs* **1999**, *57*, 293-308.
- [139] Zhao, G. H.; Lin, H. K.; Zhu, S. R.; Sun, H. W.; Chen, Y. Y., *Anti-Cancer Drug Des.* **1998**, *13*, 769-777.
- [140] Zhao, G. H.; Lin, H. K.; Yu, P.; Sun, H. W.; Zhu, S. R.; Chen, Y. T., *Chem.-Biol. Interact.* **1998**, *116*, 19-29.
- [141] Zhao, G. H.; Hu, X. S.; Yu, P.; Lin, H. K., *Transit. Met. Chem.* **2004**, *29*, 607-612.
- [142] Komeda, S.; Ohishi, H.; Yamane, H.; Harikawa, M.; Sakaguchi, K.; Chikuma, M., *J. Chem. Soc.-Dalton Trans.* **1999**, 2959-2962.
- [143] Komeda, S.; Lutz, M.; Spek, A. L.; Chikuma, M.; Reedijk, J., *Inorg. Chem.* **2000**, *39*, 4230-4236.
- [144] Komeda, S.; Lutz, M.; Spek, A. L.; Yamanaka, Y.; Sato, T.; Chikuma, M.; Reedijk, J., *J. Am. Chem. Soc.* **2002**, *124*, 4738-4746.
- [145] Komeda, S.; Yamane, H.; Chikuma, M.; Reedijk, J., *Eur. J. Inorg. Chem.* **2004**, 4828-4835.
- [146] Komeda, S.; Bombard, S.; Perrier, S.; Reedijk, J.; Kozelka, J. F., *J. Inorg. Biochem.* **2003**, *96*, 357-366.
- [147] Komeda, S., Ph.D. thesis, Leiden University (Leiden), **2002**.
- [148] (a) Kalayda, G. V.; Komeda, S.; Ikeda, K.; Sato, T.; Chikuma, M.; Reedijk, J., *Eur. J. Inorg. Chem.* **2003**, 4347-4355. (b) Komeda, S.; Kalayda, G. V.; Lutz, M.; Spek, A. L.; Yamanaka, Y.; Sato, T.; Chikuma, M.; Reedijk, J., *J. Med. Chem.* **2003**, *46*, 1210-1219.
- [149] Kas'yanenko, N. A.; Aia, E. E. F.; Bogdanov, A. A.; Kosmotynskaya, Y. V.; Yakovlev, K. I., *Mol. Biol.* **2002**, *36*, 594-599.
- [150] Lowe, G.; Droz, A. S.; Vilaivan, T.; Weaver, G. W.; Park, J. J.; Pratt, J. M.; Tweedale, L.; Kelland, L. R., *J. Med. Chem.* **1999**, *42*, 3167-3174.
- [151] (a) Canty, A. J.; Stevens, E. A., *Inorganica Chimica Acta-Bioinorganic Chemistry* **1981**, *55*, L57-L59. (b) Jain, N.; Mital, R.; Ray, K. S.; Srivastava, T. S.; Bhattacharya, R. K., *J. Inorg. Biochem.* **1987**, *31*, 57-64. (c) Kumar, L.; Kandasamy, N. R.; Srivastava, T. S.; Amonkar, A. J.; Adwankar, M. K.; Chitnis, M. P., *J. Inorg. Biochem.* **1985**, *23*, 1-11.
- [152] *Nucleic Acids in Chemistry and Biology* (Eds.: Blackburn, G. M.; Gait, M. J.), Oxford Univ. Press, Oxford, **1996**.
- [153] (a) Jain, N.; Mittal, R.; Srivastava, T. S.; Satyamoorthy, K.; Chitnis, M. P., *J. Inorg. Biochem.* **1994**, *53*, 79-94. (b) Mansuri-Torshizi, H.; Srivastava, T. S.; Parekh, H. K.; Chitnis, M. P., *J. Inorg. Biochem.* **1992**, *45*, 135-148.
- [154] Tu, C.; Lin, J.; Shao, Y.; Guo, Z., *Inorg. Chem.* **2003**, *42*, 5795-5797.
- [155] (a) Chan, H.-L.; Ma, D.-L.; Yang, M.; Che, C.-M., *J. Biol. Inorg. Chem.* **2003**, *8*, 761-769. (b) Chan, H.-L.; Ma, D.-L.; Yang, M.; Che, C.-M., *ChemBiochem* **2003**, *4*, 62-68.
- [156] Lowe, G.; Droz, A. S.; Park, J. J.; Weaver, G. W., *Bioorganic Chem.* **1999**, *27*, 477-486.
- [157] Kurosaki, H.; Yamakawa, N.; Sumimoto, M.; Kimura, K.; Goto, M., *Bioorg. Med. Chem. Lett.* **2003**, *13*, 825-828.
- [158] McFadyen, W. D.; Wakelin, L. P. G.; Roos, I. A. G.; Hillcoat, B. L., *Biochem. J.* **1986**, *238*, 757-763.
- [159] McFadyen, W. D.; Wakelin, L. P. G.; Roos, I. A. G.; Hillcoat, B. L., *Biochem. J.* **1987**, *242*, 177-183.
- [160] Becker, K.; Herold-Mende, C.; Park, J. J.; Lowe, G.; Schirmer, R. H., *J. Med. Chem.* **2001**, *44*, 2784-2792.
- [161] (a) Iengo, E.; Mestroni, G.; Geremia, S.; Calligaris, M.; Alessio, E., *J. Chem. Soc.-Dalton Trans.* **1999**, 3361-3371. (b) Serli, B.; Iengo, E.; Gianferrara, T.; Zangrando, E.; Alessio, E., *Metal-Based Drugs* **2001**, *8*, 9-18.
- [162] Bergamo, A.; Stocco, G.; Gava, B.; Cocchietto, M.; Alessio, E.; Serli, B.; Iengo, E.; Sava, G., *J. Pharmacol. Exp. Ther.* **2003**, *305*, 725-732.

- [163] Alessio, E.; Iengo, E.; Zorzet, S.; Bergamo, A.; Coluccia, M.; Boccarelli, A.; Sava, G., *J. Inorg. Biochem.* **2000**, *79*, 173-177.
- [164] Bergamo, A.; Stocco, G.; Casarsa, C.; Cocchietto, M.; Alessio, E.; Serli, B.; Zorzet, S.; Sava, G., *Int. J. Oncol.* **2004**, *24*, 373-379.
- [165] Crawford, C. A.; Day, E. F.; Saharan, V. P.; Folting, K.; Huffman, J. C.; Dunbar, K. R.; Christou, G., *Chem. Commun.* **1996**, 1113-1114.
- [166] Dunbar, K. R.; Matonic, J. H.; Saharan, V. P.; Crawford, C. A.; Christou, G., *J. Am. Chem. Soc.* **1994**, *116*, 2201-2202.
- [167] Anghileri, L. J.; Marchal, C.; Matrat, M.; Croneescanye, M. C.; Robert, J., *Neoplasma* **1986**, *33*, 603-608.
- [168] (a) Emerson, J.; Clarke, M. J.; Ying, W. L.; Sanadi, D. R., *J. Am. Chem. Soc.* **1993**, *115*, 11799-11805. (b) Reed, K. C.; Bygrave, F. L., *FEBS Lett.* **1974**, *46*, 109-114.
- [169] Grover, N.; Welch, T. W.; Fairley, T. A.; Cory, M.; Thorp, H. H., *Inorg. Chem.* **1994**, *33*, 3544-3548.
- [170] (a) O'Reilly, F. M.; Kelly, J.; Kirsch-De Mesmaeker, A., *Chem. Commun.* **1996**, 1013-1014. (b) O'Reilly, F. M.; Kelly, J. M., *J. Phys. Chem. B* **2000**, *104*, 7206-7213. (c) O'Reilly, F. M.; Kelly, J. M., *New J. Chem.* **1998**, *22*, 215-217.
- [171] Aldrich-Wright, J.; Brodie, C.; Glazer, E. C.; Luedtke, N. W.; Elson-Schwab, L.; Tor, Y., *Chem. Commun.* **2004**, 1018-1019.
- [172] Metcalfe, C.; Haq, I.; Thomas, J. A., *Inorg. Chem.* **2004**, *43*, 317-323.
- [173] Önfelt, B.; Lincoln, P.; Nordén, B., *J. Am. Chem. Soc.* **2001**, *123*, 3630-3637.
- [174] Önfelt, B.; Lincoln, P.; Nordén, B., *J. Am. Chem. Soc.* **1999**, *121*, 10846-10847.
- [175] Önfelt, B.; Gostring, L.; Lincoln, P.; Nordén, B.; Önfelt, A., *Mutagenesis* **2002**, *17*, 317-320.
- [176] Lincoln, P.; Nordén, B., *Chem. Commun.* **1996**, 2145-2146.
- [177] Wilhelmsson, L. M.; Esbjörner, E. K.; Westerlund, F.; Nordén, B.; Lincoln, P., *J. Phys. Chem. B* **2003**, *107*, 11784-11793.
- [178] Wilhelmsson, L. M.; Westerlund, F.; Lincoln, P.; Nordén, B., *J. Am. Chem. Soc.* **2002**, *124*, 12092-12093.
- [179] (a) Liu, F. R.; Wang, K. Z.; Bai, G. Y.; Zhang, Y. G.; Gao, L. H., *Inorg. Chem.* **2004**, *43*, 1799-1806. (b) Wu, J.-Z.; Yuan, L., *J. Inorg. Biochem.* **2004**, *98*, 41-45.
- [180] Zou, X.-H.; Ye, B.-H.; Li, H.; Lin, J.-G.; Xiong, Y.; Ji, L.-N., *J. Chem. Soc.-Dalton Trans.* **1999**, 1423-1428.
- [181] Chao, H.; Qiu, Z.-R.; Cai, L.-R.; Zhang, H.; Li, X.-Y.; Wong, K.-S.; Ji, L.-N., *Inorg. Chem.* **2003**, *42*, 8823-8830.
- [182] (a) Jiang, C.-W.; Chao, H.; Hong, X.-L.; Li, H.; Mei, W.-J.; Ji, L.-N., *Inorg. Chem. Commun.* **2003**, *6*, 773-775. (b) Jiang, C. W., *J. Inorg. Biochem.* **2004**, *98*, 497-501.
- [183] Jiang, C.-W., *Eur. J. Inorg. Chem.* **2004**, 2277-2282.
- [184] Jiang, C.-W., *Inorg. Chim. Acta* **2004**, *357*, 3403-3406.
- [185] Van Gijte, O.; Kirsch-De Mesmaeker, A., *J. Chem. Soc.-Dalton Trans.* **1999**, 951-956.
- [186] Brodkorb, A.; Kirsch-De Mesmaeker, A.; Rutherford, T. J.; Keene, F. R., *Eur. J. Inorg. Chem.* **2001**, 2151-2160.
- [187] Foley, F. M.; Keene, F. R.; Collins, J. G., *J. Chem. Soc.-Dalton Trans.* **2001**, 2968-2974.
- [188] Smith, J. A.; Collins, J. G.; Patterson, B. T.; Keene, F. R., *Dalton Trans.* **2004**, 1277-1283.
- [189] Patterson, B. T.; Collins, J. G.; Foley, F. M.; Keene, F. R., *J. Chem. Soc.-Dalton Trans.* **2002**, 4343-4350.
- [190] Carlson, D. L.; Huchital, D. H.; Mantilla, E. J.; Sheardy, R. D.; Murphy, W. R., *J. Am. Chem. Soc.* **1993**, *115*, 6424-6425.

- [191] Van Houten, B.; Illenye, S.; Qu, Y.; Farrell, N., *Biochemistry* **1993**, *32*, 11794-11801.
- [192] Qu, Y.; Farrell, N., *Inorg. Chem.* **1995**, *34*, 3573-3576.
- [193] (a) Milkevitch, M.; Shirley, B. W.; Brewer, K. J., *Inorg. Chim. Acta* **1997**, *264*, 249-256. (b) Milkevitch, M.; Storrie, H.; Brauns, E.; Brewer, K. J.; Shirley, B. W., *Inorg. Chem.* **1997**, *36*, 4534-4538.
- [194] (a) Swavey, S.; Fang, Z. L.; Brewer, K. J., *Inorg. Chem.* **2002**, *41*, 2598-2607. (b) Fang, Z. L.; Swavey, S.; Holder, A.; Winkel, B.; Brewer, K. J., *Inorg. Chem. Commun.* **2002**, *5*, 1078-1081. (c) Williams, R. L.; Toft, H. N.; Winkel, B.; Brewer, K. J., *Inorg. Chem.* **2003**, *42*, 4394-4400.
- [195] Velders, A. H., Ph.D. thesis, Leiden University (Leiden), **2000**.
- [196] Van Vliet, P. M.; Toekimin, S. M. S.; Haasnoot, J. G.; Reedijk, J.; Nováková, O.; Vrána, O.; Brabec, V., *Inorg. Chim. Acta* **1995**, *231*, 57-64.
- [197] Nováková, O.; Kašpárková, J.; Vrána, O.; Van Vliet, P. M.; Reedijk, J.; Brabec, V., *Biochemistry* **1995**, *34*, 12369-12378.
- [198] (a) Jennette, K. W.; Lippard, S. J.; Vassiliades, G. A.; Bauer, W. R., *Proc. Natl. Acad. Sci. U. S. A.* **1974**, *71*, 3839-3843. (b) Howe-Grant, M.; Wu, K. C.; Bauer, W. R.; Lippard, S. J., *Biochemistry* **1976**, *15*, 4339-4346.
- [199] (a) Barton, J. K., *Science* **1986**, *233*, 727-734. (b) Erkkila, K. E.; Odom, D. T.; Barton, J. K., *Chem. Rev.* **1999**, *99*, 2777-2795. (c) Pyle, A. M.; Rehmman, J. P.; Meshoyrer, R.; Kumar, C. V.; Turro, N. J.; Barton, J. K., *J. Am. Chem. Soc.* **1989**, *111*, 3051-3058. (d) Kelly, J. M.; Tossi, A. B.; McConnell, D. J.; Ohuigin, C., *Nucleic Acids Res.* **1985**, *13*, 6017-6034.
- [200] Van der Schilden, K.; Garcia, F.; Kooijman, H.; Spek, A. L.; Haasnoot, J. G.; Reedijk, J., *Angew. Chem. Int. Ed.* **2004**, *43*, 5668-5670.
- [201] Van der Schilden, K. et al., *Manuscripts in preparation*.

Chapter 2

A paramagnetic dinuclear ruthenium(II)-ruthenium(III) complex: synthesis and strategy for ^1H NMR studies

Abstract – The terpyridyl-ruthenium(II) complex $[(\text{tpy})\text{Ru}(\text{dtdeg})]\text{Cl}_2$ (**1**) (tpy = 2,2':6',2''-terpyridine, dtdeg = bis[4'-(2,2':6',2''-terpyridyl)]-diethyleneglycolether) has been produced for the synthesis of the dinuclear ruthenium(II)-ruthenium(III) complex $[(\text{tpy})\text{Ru}(\text{dtdeg})\text{RuCl}_3]\text{Cl}_2$ (**2**). A straightforward strategy to fully characterize the paramagnetic species **2** by 1D and 2D ^1H NMR is reported. Complex **2** represents the first example of a paramagnetic ruthenium complex, which has been fully characterized using 1D NOE difference experiments. Plots of the observed chemical shifts *versus* the reciprocal temperatures indicate Curie behavior. Both contact and dipolar interactions are suggested to contribute to the hyperfine shift and nuclear relaxation. Delocalization of unpaired-spin density into the central pyridine ring, which is coordinated to the paramagnetic ruthenium(III) center, probably occurs by a spin polarization mechanism. The chemical shifts of the protons of the diamagnetic ruthenium(II) moiety are also affected by the unpaired electron. The influence is the smallest for the protons of the terminal terpyridine ligand.

2.1 Introduction

Polynuclear platinum complexes represent a new class of anticancer agents.^[1] It is believed they can overcome resistance to the anticancer drug cisplatin, as they are capable of distinctive interactions with DNA, which is generally believed to be the ultimate target of platinum anticancer agents.^[2] Ruthenium complexes are also known for their anticancer activity, and polynuclear derivatives are under study.^[3] The synthesis of a series of dinuclear ruthenium complexes has been inspired by the mononuclear antimetastatic complex NAMI-A.^[4] Dinuclear photoreactive ruthenium complexes have been designed, as it is thought that the greater size, charge and variation in shape increase DNA-binding affinity and specificity relative to mononuclear complexes.^[5] The octahedral geometry of most ruthenium complexes is thought to impose unique interactions with biomolecules, which may cause a different anticancer profile from square-planar cisplatin.^[6] Moreover, ruthenium(III) complexes may serve as prodrugs, which are activated by reduction *in vivo* to coordinate more rapidly to biomolecules.^[3, 7] Selective tumor toxicity can be reached by the low oxygen content and the low pH in tumor cells, which are known to promote reduction.^[3]

A challenge in the investigation of ruthenium(III) complexes is their characterization by ¹H NMR, because of the presence of an unpaired electron in the t_{2g} orbital of the low-spin d^5 ruthenium(III) ions. Paramagnetism induces hyperfine shifts of ¹H NMR signals and shortening of nuclear longitudinal (T_1) and transverse (T_2) relaxation times, which exclude characterization by standard ¹H NMR techniques used for diamagnetic molecules. Proton NMR studies of paramagnetic compounds have become increasingly useful in applications such as probing metalloprotein active-site structure and mechanism.^[8, 9] However, for relatively small paramagnetic inorganic complexes, ¹H NMR has not been used intensively. It can be applied to small paramagnetic complexes in cases where the relaxation time of the unpaired electron is short enough, such that reasonably sharp ¹H NMR signals are observed. For low-spin ruthenium(III) complexes relatively short electronic relaxation rates of 10^{-11} s^{-1} have been reported,^[10] which might make characterization by ¹H NMR possible.

In this Chapter, the synthesis and characterization of the ruthenium(II) complex [(tpy)Ru(dtdeg)]Cl₂ (**1**) (tpy = 2,2':6',2''-terpyridine, dtdeg = bis[4'-(2,2':6',2''-terpyridyl)]-diethyleneglycolether) and of the paramagnetic dinuclear ruthenium(II)-ruthenium(III) complex [(tpy)Ru(dtdeg)RuCl₃]Cl₂ (**2**, Figure 2.1) are presented. The synthesis of **2** has been based upon the cytotoxic and antitumor active complex^[11] [Ru(tpy)Cl₃], and the dinuclear derivative^[12] [Cl₃Ru(dtdeg)RuCl₃]. These complexes have not been developed as possible anticancer drugs, because of their poor water solubility. The double positive charge of the bis(terpyridyl)-ruthenium(II) moiety of **2** is thought to increase water solubility. Moreover,

the positive charge of the ruthenium(II) moiety can direct **2** to the negatively charged DNA. Subsequently, the ruthenium(III) unit may coordinate to the DNA in a similar fashion^[11, 13] as the parental mononuclear complex [Ru(tpy)Cl₃].

The ruthenium(III) moiety of **2** is paramagnetic, as is its mononuclear derivative. ¹H NMR studies have already been performed^[12] on the latter and [Cl₃Ru(dtdeg)RuCl₃]. In this Chapter, a straightforward strategy is presented to fully characterize **2** by ¹H NMR experiments. It is shown for the first time that high-resolution ¹H 1D NOE NMR can be applied to low-spin ruthenium(III) complexes. To understand the relative weight of the different interactions between the unpaired electron and the nuclei on the hyperfine shift and nuclear relaxation, the ¹H NMR features displayed by **2** are discussed.

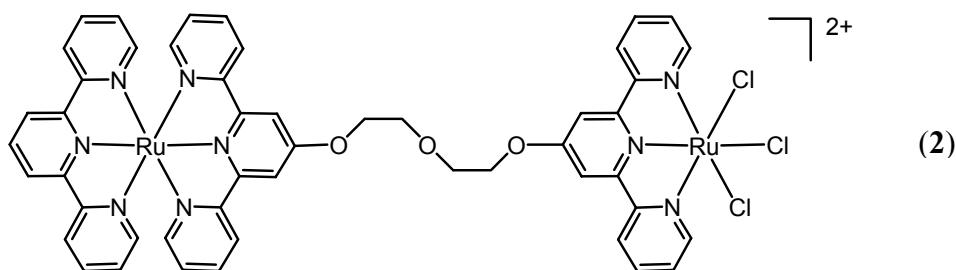


Figure 2.1 The dinuclear cationic ruthenium(II)-ruthenium(III) complex **2**.

2.2 Experimental section

2.2.1 General methods and starting materials

Elemental analyses on C, H and N were performed on a Perkin Elmer series II CHNS/O Analyzer 2400. Electrospray mass spectra were recorded on a Finnigan TSQ-quantum instrument with an electrospray interface (ESI). Hydrated RuCl₃·xH₂O (x ~ 3) was used as received from Johnson & Matthey. The ligand tpy was obtained from Sigma. The ligand 4'-chloro-2,2':6',2''-terpyridine and the complex [Ru(tpy)Cl₃] have been synthesized according to known procedures.^[14] The complex [(tpy)Ru(dtdeg)]Cl₂ has been synthesized according to a modified procedure for cationic [Ru(L₁)(L₂)]²⁺ complexes in which L represents different tridentate heterocyclic ligands.^[15] The acidic ruthenium(III) chloride solution and the ligand dtdeg have been synthesized^[12] previously, but their synthesis will also be reported here for convenience (*vide infra*).

2.2.2 ¹H NMR measurements

¹H NMR spectra were mainly acquired on a Bruker DPX 300 spectrometer. 1D ¹H NOE difference spectra were measured on a Bruker DMX 600 spectrometer. Spectra were recorded in deuterated DMSO, and calibrated on the residual solvent peak at δ 2.49 ppm. 1D ¹H spectra of **2** were obtained using a 100 ppm spectral width. Longitudinal relaxation times were measured by the standard inversion-recovery method, with 7 s relaxation delay and a spectral width of 100 ppm. Variable delays ranged from 50 μ s to 500 ms to define the T1 values for the proton signals of the paramagnetic ruthenium(III) moiety, and from 100 ms to 5000 ms to define the T1 values for the proton signals of the diamagnetic ruthenium(II) moiety. Magnetization recovery was exponential within experimental error. T₂ values were estimated from the peak half-widths. The COSY spectrum was obtained by collecting 1024 F₂ x 1024 F₁ data points with a relaxation delay of 20 ms. 1D NOE experiments were carried out according to published procedures.^[16] These procedures include a WEFT pulse sequence, which was not applied here. The irradiation time used for the 1D NOE experiment was 500 ms, and the number of scans 16384.

2.2.3 Syntheses

0.1 M ruthenium(III) solution:^[12] RuCl₃·xH₂O (1.20 g; ~ 5.0 mmol) was refluxed for 3 hours in 50 mL of a mixture of a 1 M HCl aqueous solution and EtOH (v:v = 1:1). The mixture was filtered and the filtrate was reduced *in vacuo* to 10 mL. A 1 M HCl aqueous solution (40 mL) was added to result in 50 mL of the required acidified ~ 0.1 M ruthenium(III) solution.

Dtdeg.^[12] A mixture of 4'-chloro-2,2':6',2''-terpyridine (2.05 g; 7.6 mmol), diethyleneglycol (0.45 g; 4.2 mmol) and KOH (1.22 g; 21.7 mmol) was stirred in 185 mL of DMSO for 24 hours at 338 K, under a moisture-free atmosphere. 160 mL of water was added to the mixture at RT, which resulted in a white precipitate. The mixture was filtered and the residue was dried on air. The residue was dissolved in 350 mL of EtOH 98 % by reflux for ~ 1 hour. The desired product was precipitated upon cooling of the solution in an ice bath for 0.5 hour. The mixture was filtered and the residue was washed twice with a small amount (~ 5 mL) of ice cold EtOH 98 %. The product was dried on air. Yield: 1.75 g (80 %).

[(tpy)Ru(dtdeg)]Cl₂, (1): An excess of AgBF₄ (4.5 g; 23.1 mmol) was dissolved in 200 mL of acetone and filtered. [Ru(tpy)Cl₃] (0.800 g; 1.815 mmol) was added to the filtrate and the mixture was refluxed in the dark for 16 hours to remove the chloride ions from ruthenium. After filtration to remove precipitated AgCl, the filtrate was evaporated *in vacuo*, which

resulted in a green oil (~ 6 mL). The ligand dtdeg (1.700 g; 2.993 mmol) was added and the mixture was refluxed for 1.5 hours in 200 mL of DMF, which acted as the reducing agent. The reaction mixture was filtered and the red filtrate was evaporated *in vacuo*, which resulted in ~ 6 mL of an oil. To synthesize the chloride salt of the product, 75 mL of a saturated LiCl solution in EtOH was added to the oil. The desired product was obtained by precipitation with a large amount of acetone (~ 2 L). Complex **1** was separated from [(tpy)Ru(dtdeg)Ru(tpy)]Cl₄ by column chromatography on neutral alumina with acetone/MeOH/EtOH (v:v:v = 8:1:1). The first orange band contained pure product. Yield: 0.899 g (51 %). Elemental analysis (%) calculated for C₄₉H₃₉Cl₂N₉O₃Ru·6H₂O (water, originating from the used solvents, was used to fit the elemental analysis as the C/N ratio of the analysis corresponds to the structural formula of the complex): C 54.40, N 11.65, H 4.75. Found: C 54.51, N 11.96, H 4.95. ESI-MS: *m/z*: 452 [M²⁺], 301 [M²⁺+H⁺]. ¹H NMR (300 MHz, DMSO, 298 K): δ = 8.61 (d, 2H; I33''), 7.99 (t, 2H; I44''), 7.48 (t, 2H; I55''), 8.67 (d, 2H; I66''), 8.03 (s, 2H; I3'5'), 4.51 (t, 2H; 1), 4.06 (t, 2H; 2), 8.87 (d, 2H; I'33''), 7.97 (t, 2H; I'44''), 7.21 (t, 2H; I'55''), 7.36 (d, 2H; I'66''), 8.87 (s, 2H; I'3'5'), 4.77 (t, 2H; 1'), 4.15 (t, 2H; 2'), 8.83 (d, 2H; II33''), 7.98 (t, 2H; II44''), 7.25 (t, 2H; II55''), 7.51 (d, 2H; II66''), 9.08 (d, 2H; II3'5'), 8.48 ppm (t, 1H; II4').

[(tpy)Ru(dtdeg)RuCl₃]Cl₂, (2): 1 (0.190 g; 0.195 mmol) was dissolved in 60 mL of MeOH. At reflux temperature, 4 mL of the 0.1 M ruthenium(III) solution (0.4 mmol) was added to the solution. The mixture was refluxed for 3 hours and the resulting precipitate was filtered off at RT. The residue was dissolved in 1000 mL of hot MeOH and filtered to remove any insoluble species (probably ruthenium-oxo species). The filtrate was concentrated *in vacuo*, and the product was precipitated with diethyl ether. After filtration of the mixture, the residue was extensively washed with diethyl ether, which resulted in pure product. Yield: 0.082 g (36 %). Elemental analysis (%) calculated for C₄₉H₃₉Cl₅N₉O₃Ru₂·8H₂O·0.5HCl (Besides water (*vide supra*), HCl was used to fit the elemental analysis, as the product precipitates from an acidic solution and an aqueous solution of the product is slightly acidic): C 43.80, N 9.38, H 4.16, Cl 14.51. Found: C 43.45, N 9.17, H 3.28, Cl 14.60. ¹H NMR (300 MHz, DMSO, 320 K): δ = -8.44 (s, 2H; I33''), 0.94 (s, 2H; I44''), -9.89 (s, 2H; I55''), -30.19 (s, 2H; I66''), 4.79 (s, 2H; I3'5'), 14.43 (s, 2H; 1), 4.12 (s, 2H; 2), 9.26 (s, 2H; I'33''), 8.09 (s, 2H; I'44''), 7.27 (s, 2H; I'55''), 7.82 (s, 2H; I'66''), 9.44 (s, 2H; I'3'5'), 5.26 (s, 2H; 1'), 4.41 (s, 2H; 2'), 8.90 (d, 2H; II33''), 8.09 (s, 2H; II44''), 7.27 (s, 2H; II55''), 7.53 (d, 2H; II66''), 9.15 (d, 2H; II3'5'), 8.54 ppm (t, 1H; II4').

2.3 Results and discussion

2.3.1 Characterization of the diamagnetic precursor **1** by ^1H NMR spectroscopy

Complex **1** is water soluble. However, the ^1H NMR spectrum of **1** is shown in $\text{dms-}d_6$ for comparison with **2** (Figure 2.2, assignments are reported in the experimental section). The appearance of four individual resonances in the region between 4 and 5 ppm for the linker protons 1, 2, 1' and 2' clearly indicates the presence of a non-symmetric species consisting of two different moieties. This is further confirmed by the fact that three sets of signals are recognized for the three inequivalent terpyridine ligands I, I' and II in the aromatic region by 2D ^1H NMR experiments (data not shown). Symmetry is displayed within each unit due to the occurrence of a C_2 symmetry axis, which is aligned along the linking diethylene glycol ether chain and passes through the ruthenium center. Therefore, only half of the resonances for each terpyridine ligand are observed. The signals for the 66'' protons have been identified by the small J value as compared to that of the 33'' protons (~ 5 Hz *versus* ~ 9 Hz for the 66'' and 33'' protons, respectively). The terpyridine ligand II has been distinguished from the other terpyridine ligands by the signal for the II4' proton, since it is the only signal with a relative intensity of 1. The terpyridine ligands I and I' have been differentiated by the chemical shift of the 66'' protons. The I'66'' resonance is shifted upfield compared to the I66'' signal, due to shielding of the former by the terpyridine ligand II.

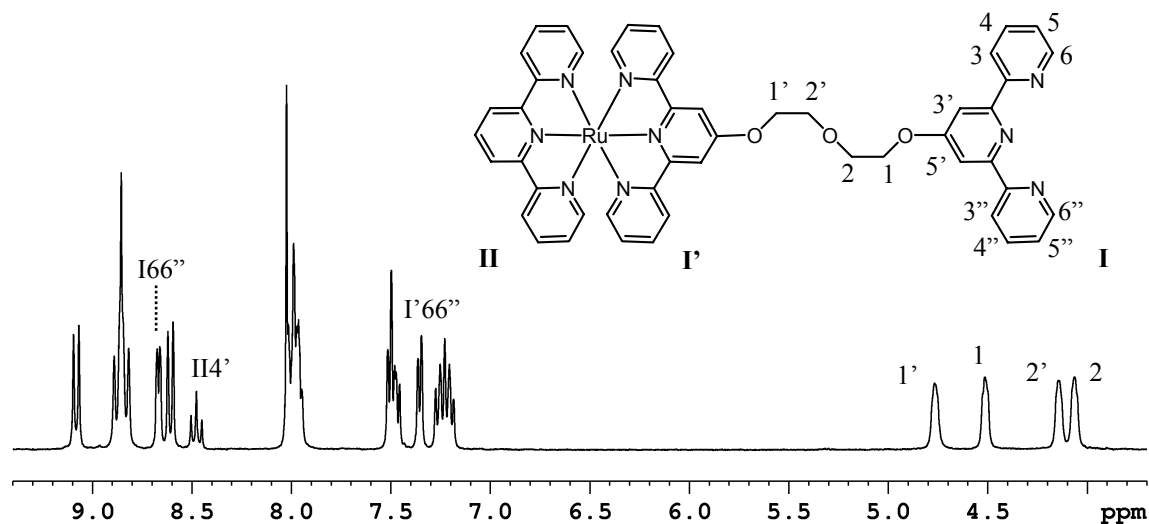


Figure 2.2 Schematic representation and 1D ^1H NMR spectrum of the cation of **1** in $\text{DMSO-}d_6$ at 298 K with some assignments. The numbering scheme given for terpyridine ligand I is also applicable to ligands I' and II.

2.3.2 ^1H NMR assignment strategy for the paramagnetic complex **2**

Complex **2** is, like its precursor **1**, soluble in water. Since hydrolysis of **2** occurs in water, its 1D ^1H NMR spectrum is shown in $\text{dms}\text{-}d_6$ (Figure 2.3). The spectrum has been acquired at 320 K. At this temperature, the “paramagnetic” signals, *i.e.* the resonances of the paramagnetic ruthenium(III) moiety, do not overlap. The effect of the unpaired electron of the paramagnetic species **2** is clearly recognized in the ^1H NMR spectrum. Most signals are observed in the normal diamagnetic envelope from 0 to 12 ppm, but some signals are greatly shifted upfield or downfield. The unpaired electron influences the magnetic field sensed by a proton, since a significant magnetic dipolar field is associated with the large magnetic moment of the unpaired electron, which is 658 times that of a proton.^[8] The broadened and shifted resonances, which also display relatively short longitudinal relaxation times, have been classified as signals of protons of the paramagnetic trichlororuthenium(III) moiety. The signal at 4.79 ppm has also been established as a “paramagnetic” signal, since it exhibits short T_1 and T_2 values. Only 5 resonances are observed for the ruthenium(III) unit, because of the C_2 symmetry. The resonances appearing in the aromatic region have been assigned to the protons of the diamagnetic ruthenium(II) unit. This is fully consistent with the fact that the unpaired electron resides on the ruthenium(III) ion, and influences the nuclei closest to it the most. The striking similarities in chemical shift between the resonances for the terpyridine ligand I protons and the analogous resonances of the mononuclear parental complex $[\text{Ru}(\text{tpy})\text{Cl}_3]$ at the same temperature (Table 2.1), further confirm the assignment.

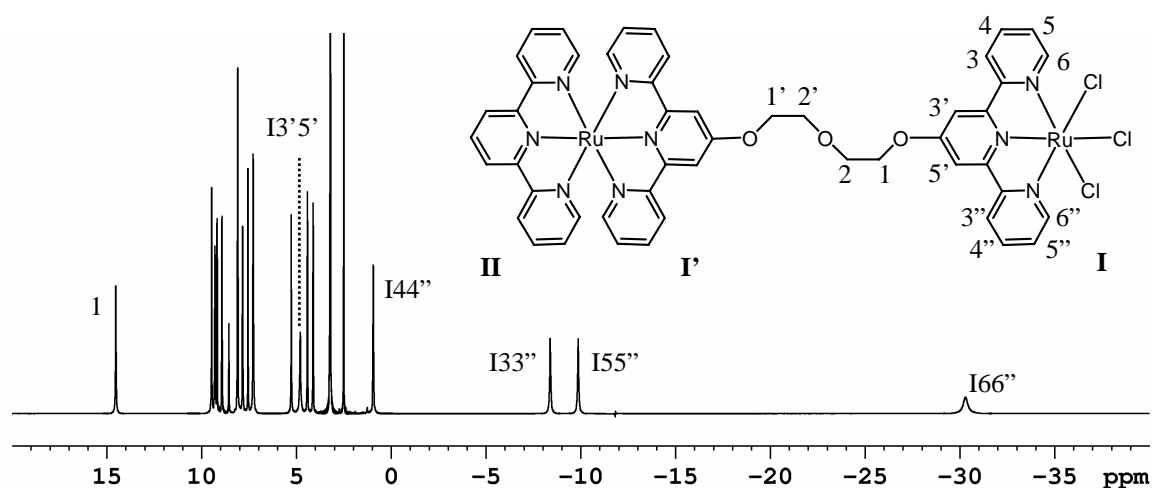


Figure 2.3 Schematic representation and 1D ^1H NMR spectrum of the cation of **2** in $\text{DMSO-}d_6$ at 320 K with some assignments. The numbering scheme given for terpyridine ligand I is also applicable to terpyridine ligands I' and II.

At 320 K, nine resonances, of which two have a relative intensity of 4, are observed in the aromatic region of the ^1H NMR spectrum of **2** (Figure 2.4). Thus, a total of eleven resonances are identified, which agrees with the structure and C_2 symmetry of the bis(terpyridyl)-ruthenium(II) moiety. The resonances of the terminal terpyridine ligand II appear as doublets and triplets, with exception of those that overlap with resonances of the I' terpyridine ligand. In contrast, all the resonances of the terpyridine ligand I' are significantly broadened. These signals also display relatively short longitudinal relaxation times. Fast relaxation rates result in a loss of magnetization during the various steps of the sequences of NMR experiments, which may cause a dramatic decrease in signal intensity.^[8] For a 2D ^1H COSY NMR experiment of **2**, a relaxation delay of 20 ms resulted in a best signal-to-noise ratio in the aromatic region, as well as in the upfield region where most paramagnetic signals occur (*vide infra*). Since short acquisition times are a consequence of a short relaxation delay, a larger number of points (1024 in both dimensions) have been acquired in the same experimental time ensuing better resolution and signal intensity as well.

The resonances of the terpyridine ligand II have been assigned starting from its II4' proton, which displays a relative intensity of 1, using 2D ^1H COSY and NOESY experiments (data not shown). The I'3'5' resonance has been identified at 9.44 ppm, because no crosspeaks appear in the 2D COSY ^1H NMR. From the two signals at 9.26 and 7.81 ppm, the first most likely originates from the I'33'' protons. The more upfield shifted signal at 7.81 ppm is expected to arise from the I'66'' protons, since these protons are shielded by the terpyridine ligand II. A NOE between the I'3'5' and I'33'' signals is not observed in 2D ^1H NOESY experiments, because the resonance positions are too close to resolve the crosspeak from the diagonal. In analogy with **1**, the signal at 5.26 ppm has been assigned to the linker protons I'.

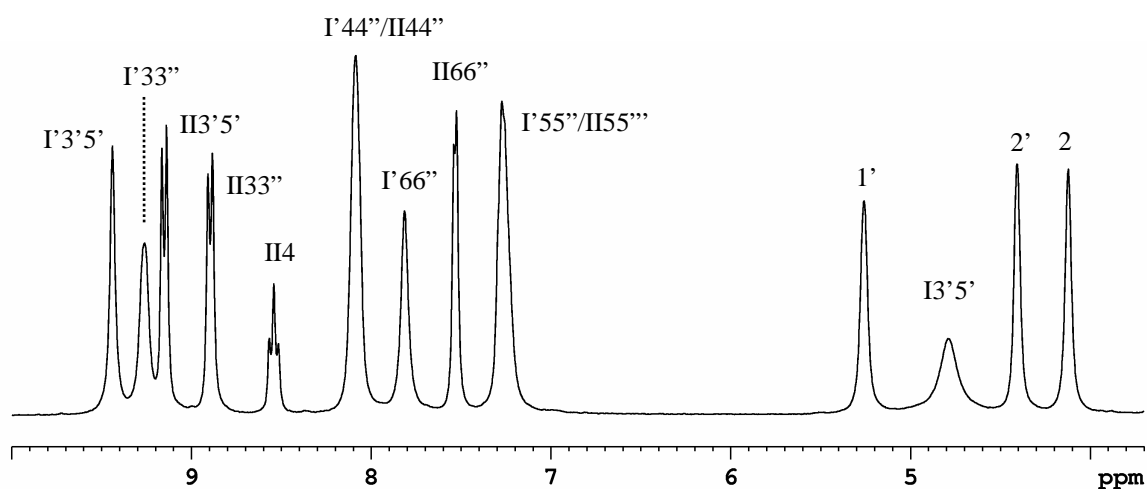


Figure 2.4 Part of the ^1H NMR spectrum of **2** in $\text{DMSO-}d_6$ at 320 K with assignments.

For the most “paramagnetic” signals of the paramagnetic species **2**, the success of a COSY experiment can be severely hampered by short transverse relaxation times T_2 .^[8] Indeed, the signal at -30.19 ppm appears to be too broad ($T_2 = 1/\pi(\text{fwh})$, in which fwh is the full width at half height) to show crosspeaks in a ^1H COSY NMR spectrum. The signal is expected to arise from the I66” protons, since these protons are closest to the paramagnetic ruthenium(III) ion. This signal is not only shifted and broadened the most, but also displays the shortest relaxation time T_1 . The assumption is confirmed by 1D NOE experiments (*vide infra*). In the upfield portion of the 2D COSY ^1H NMR spectrum a three-spins system is displayed (Figure 2.5). Taking into account the above assignment, the considered resonances can be assigned to the I33”, I44” and I55” protons. The resonance at 0.94 ppm must arise from the I44” protons, as it displays crosspeaks to both resonances at -8.44 and -9.89 ppm. The latter resonances, corresponding to the I33” and I55” protons, cannot be distinguished from one another yet.

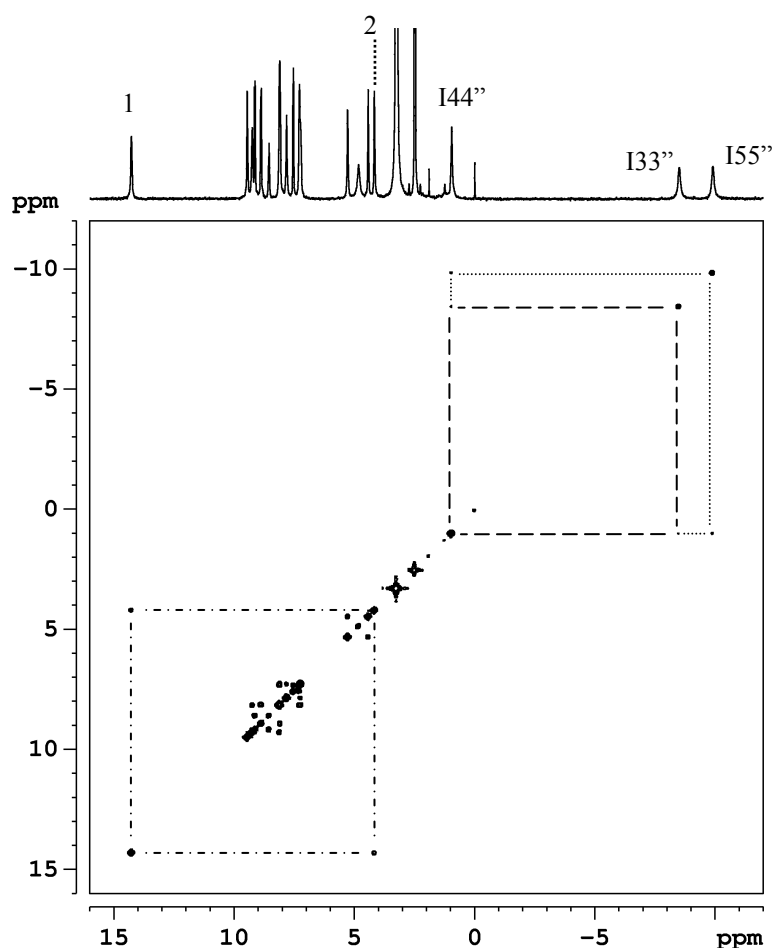


Figure 2.5 2D ^1H COSY NMR spectrum of **2** in $\text{DMSO-}d_6$ at 320 K with some assignments and crosspeaks indicated.

An additional spin-spin connectivity patterns involves the resonances at 14.43 and 4.12 ppm, which assigns these signals to the protons of the diethylene glycoether linker. The signal at 14.43 ppm is attributed to the 1 protons, *i.e.* the linker protons, which are closest to the ruthenium(III) ion.

Further assignments cannot be achieved without specific chemical substitution, which would require laborious syntheses, or interpretation of proton longitudinal relaxation times in correlation with distances between protons and the ruthenium(III) center. The latter are available from an earlier published^[17] crystal structure of [Ru(tpy)Cl₃]. However, the distance to the metal determined for a proton using T₁ values may appear shorter than it really is when delocalized spin density is effective in relaxing the nucleus,^[8] as may be the case for **2** (*vide infra*). 1D steady-state NOE studies are likely to be the only resource for examining dipolar contacts of the protons close to the metal, since a maximum intensity of the NOE is obtained. The mixing time of a 2D NOESY experiment is relative short, and therefore the 2D NOESY response is less than that of a 1D NOE. 1D NOE difference experiments are often used to probe metalloprotein active-site structures, but have scarcely been used to study paramagnetic metal complexes. The NOE intensity for paramagnetic compounds is proportional to the rotational correlation time and inversely proportional to the longitudinal relaxation rate.^[8] Therefore, the relatively small size and small T₁ values of paramagnetic complexes usually prevent the use of NOE techniques.

However, 1D NOE difference experiments have successfully been applied to characterize the paramagnetic ruthenium(III) complex **2**. Upon irradiation of the “paramagnetic” signal at 4.79 ppm, negative NOEs are displayed by the resonances at 14.43 and –8.44 ppm (upper spectrum, Figure 2.6). These signal enhancements clearly prove that the irradiated resonance originates from the I3’5’ protons, and that the resonances exhibiting NOEs arise from the linker 1 protons and the I33” protons, respectively. Using a 10 mM concentration and a great number of scans, irradiation of the I66” signal produces a signal enhancement at –9.89 ppm despite its short T₁ value. The NOE unambiguously confirms the assignment of the I66” protons, as well as that of the I55” protons, and completes successfully the full characterization of the paramagnetic species **2** by ¹H NMR. All “paramagnetic” signals have been irradiated and the observed NOEs confirm the assignments done by 2D COSY NMR. For the I3’5’ and I66” signals, NOEs are only observed upon irradiation of these resonances, but are not displayed upon irradiation of the I33” or 1 resonance, and the I55” signal, respectively. It has been recognized that larger NOEs occur upon saturation of the signal with a smaller T₁ value.^[8]

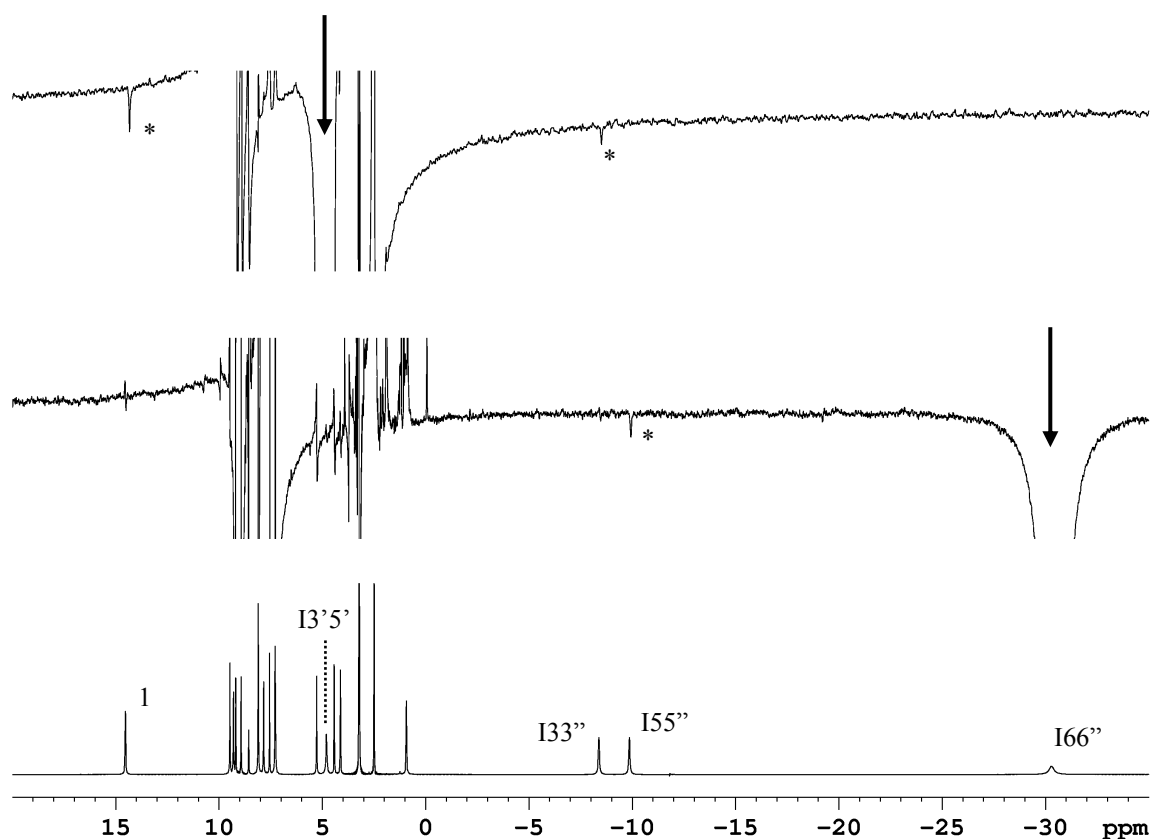


Figure 2.6 1D ^1H NOE difference NMR spectra (upper and center), and 1D ^1H NMR spectrum (bottom) of **2** in $\text{DMSO-}d_6$ at 320 K. Irradiated signals are indicated with an arrow. NOEs are indicated with an asterisk.

2.3.3 Temperature dependence of the chemical shift

Spectra of **2** were monitored by variable-temperature measurements over the temperature range 300 to 360 K (Figure 2.7). The chemical shifts of the paramagnetic protons are all temperature sensitive. They shift to the diamagnetic region upon an increase of the temperature.

The observed chemical shifts of the paramagnetic signals of **2** have been plotted against $1/T$ over the temperature range from 300 to 360 K (Figure 2.8). This Figure illustrates that the hyperfine shift linearly decreases upon a stepwise decrease of $1/T$, which indicates Curie behavior. Curie's law ($M = \text{constant} \times H/T$) states that magnetization (M) increases with an increase of the applied magnetic field (H), but decreases if the temperature increases.

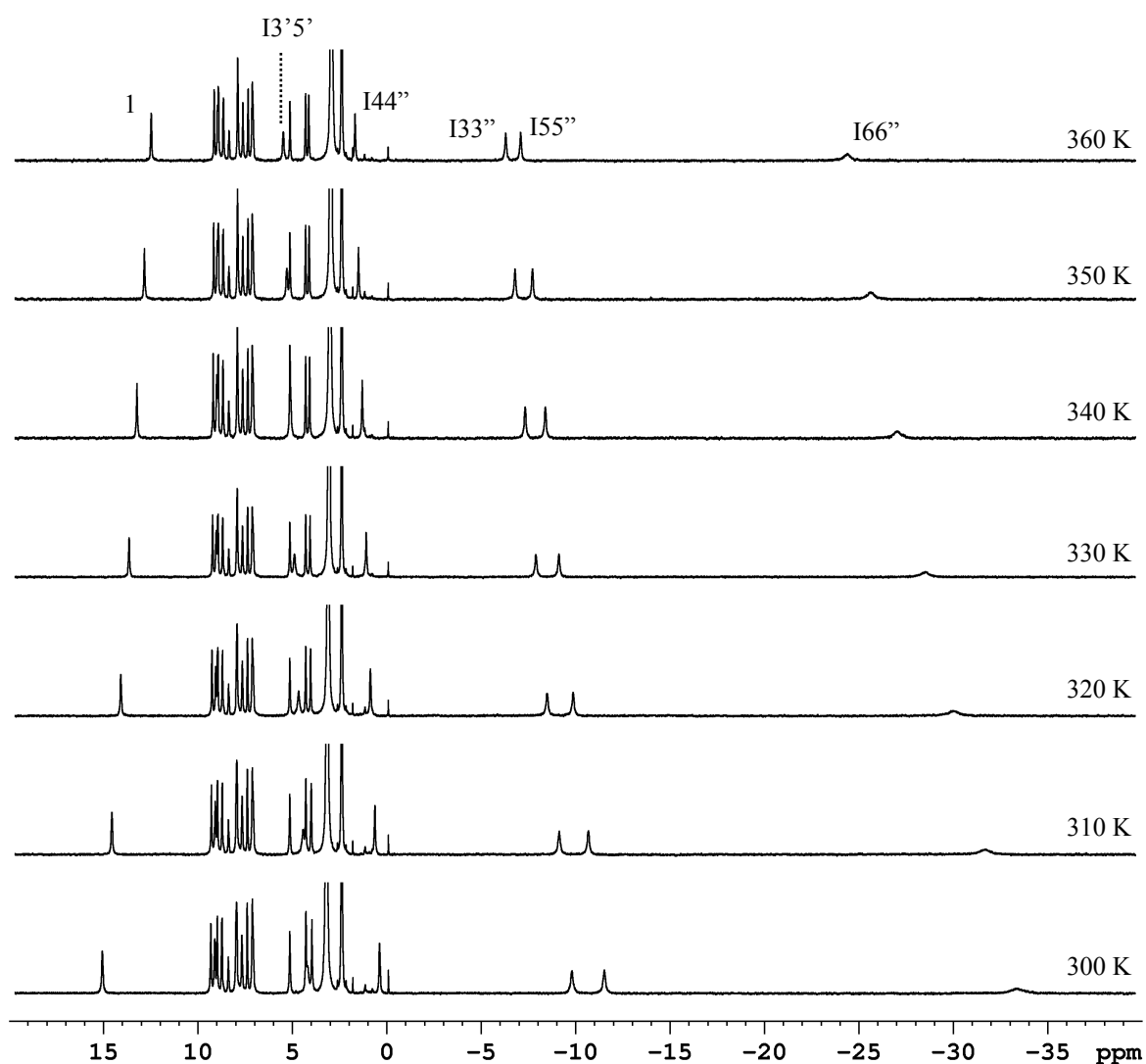


Figure 2.7 Variable temperature 1D ^1H NMR spectra for **2** in $\text{DMSO-}d_6$ in the temperature range from 300 to 360 K.

The equations (3) and (4) for the contact and dipolar shift, respectively (*vide infra*), indicate the linear dependency between the shift and the inverse of the temperature. From both equations it can be inferred that the observed chemical shift will approach the diamagnetic value as $1/T$ approaches zero. This behavior is also specified by the Curie law, which predicts zero magnetism at infinite temperatures. The intercepts obtained after extrapolation to infinite temperature for most of the signals differ only slightly from the expected diamagnetic shifts, which are in the aromatic region from 7 to 10 ppm. However, some intercepts deviate appreciably from their diamagnetic values. For example, the intercepts for I66'' and I55'' are 20.65 and 15.29 ppm, respectively. The reasons for a deviation from Curie behavior have not been studied here.

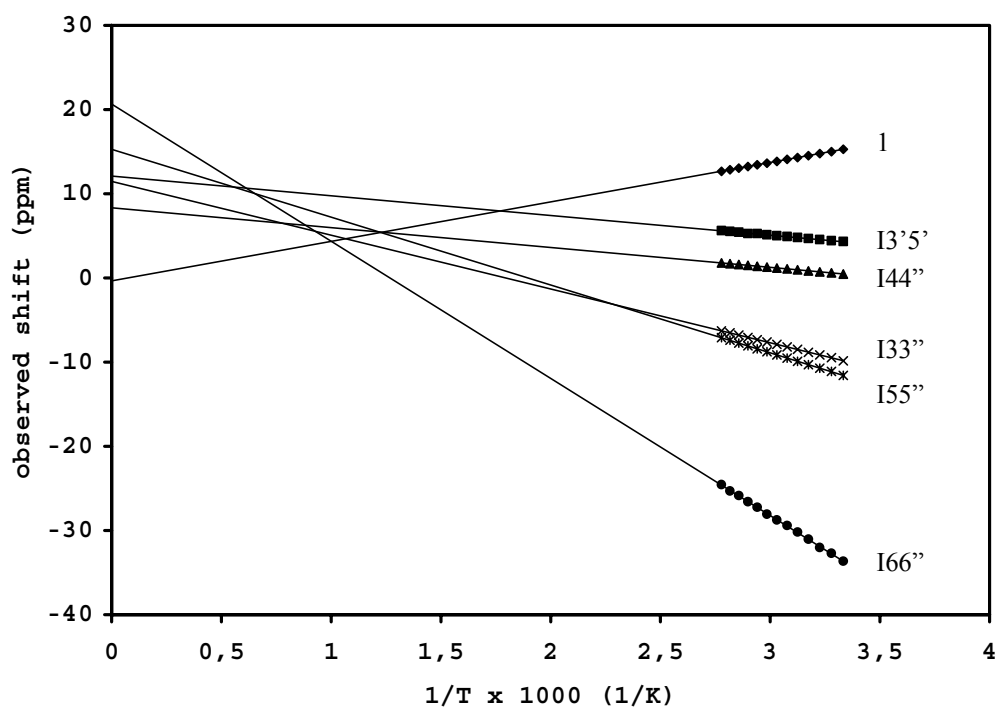


Figure 2.8 Plots of the chemical shift *versus* 1/T for 2.

2.3.4 The hyperfine shift

For a proton of a paramagnetic species the observed ^1H chemical shift is different from its diamagnetic value because of the interaction between the proton nucleus and the unpaired electron, *i.e.* the hyperfine interaction (equation (1)). Contact (through bond) and dipolar (through space) couplings contribute to the hyperfine shift (equation (2)). The contact contribution to the hyperfine or isotropic shift is given^[8] by equation (3), where A is the contact coupling constant, g_e is the free electron g -value, μ_B is the Bohr magneton, S is the spin quantum number of the spinning electron, \hbar is Planck's constant divided by 2π , γ is the proton gyromagnetic ratio, k_B is the Boltzmann constant and T is the absolute temperature.

The contact shift is given by an additional magnetic field, which is generated at the nucleus by spin delocalization of the unpaired electron. The unpaired spin density is transmitted through antibonding molecular orbitals of the complex. Spin density may reach the nucleus by two different mechanisms. Direct spin delocalization occurs owing to the hydrogen contribution to the molecular orbitals that have unpaired electrons. The contribution to the hyperfine shift through this mechanism decreases rapidly as the number of chemical bonds between the metal and the resonating nucleus increases. Spin polarization arises, because the presence of an unpaired electron in a molecular orbital polarizes the paired electrons in a different molecular

orbital. Spin polarization can result in alternating positive and negative shifts in an aromatic system to yield zero spin density over the entire system per doubly occupied MO. Both the direct delocalization and polarization mechanism can occur through σ and π orbitals.

The dipolar or pseudocontact shift is given by equation (4), which is defined^[8] for axially symmetric systems. The unpaired electron is considered to be localized on the metal in a paramagnetic complex. The shift is evaluated by expressing the principal molecular magnetic susceptibility values as a function of the principal g values, which holds when the spin multiplet ground state is well isolated from excited electronic states and zero-field splitting is negligible. μ_0 is the magnetic permeability of a vacuum, g_{\parallel} and g_{\perp} are the principal parallel and perpendicular g values, respectively, r is the metal-proton distance, and θ is the angle between the metal-nucleus vector r and the z component of the magnetic susceptibility tensor.

$$\delta_{\text{observed}} = \delta_{\text{diamagnetic}} + \delta_{\text{hyperfine}} \quad (1)$$

$$\delta_{\text{hyperfine}} = \delta_{\text{contact}} + \delta_{\text{dipolar}} \quad (2)$$

$$\delta_{\text{contact}} = \frac{A}{\hbar} \frac{g_e \mu_B S(S+1)}{3\gamma_i kT} \quad (3)$$

$$\delta_{\text{dipolar}} = \frac{\mu_0}{4\pi} \frac{\mu_B^2 S(S+1)}{9kT} (g_{\parallel}^2 - g_{\perp}^2) \frac{1}{r^3} (3 \cos^2 \theta - 1) \quad (4)$$

2.3.5 Contact and dipolar contributions to the chemical shifts of **2**

The I33'', I44'', I55'' and I66'' protons of the trichlororuthenium(III) moiety of **2** display hyperfine shifts which agree with the metal-proton distances, as well as with the number of chemical bonds to the metal center. The protons closest to the paramagnetic ruthenium(III) ion (*i.e.* the I66'' protons) display the largest hyperfine shift, whereas the protons furthest away from the unpaired electron (the I44'' protons) show a relatively small hyperfine shift. These observations suggest that dipolar interactions or direct delocalization of spin density (or both) influences the shifts of these protons. In contrast, the I3'5' protons of the central pyridine ring of ligand I display a downfield shift with respect to the I33'' and I55'' signals, for which the metal-proton distances are approximately similar to that of the I3'5' protons. The shift of the I3'5' resonance agrees with^[12] the signal of the same protons of the

mononuclear complex $[\text{Ru}(\text{tpy})\text{Cl}_3]$. Interestingly, the 4' proton of the latter displays^[12] a large upfield shift (-20.99 ppm) in comparison to its 44'' signal, and the I44'' resonance of **2**. Upfield shifts for *ortho* and *para* protons versus downfield shifts for *meta* protons have been observed before in six-membered π systems of paramagnetic molecules.^[18] The shifts indicate that spin delocalization into the central pyridine ring of trichlororuthenium(III) terpyridyl complexes at least partly occurs by a spin polarization mechanism.

The unpaired electron of the low-spin ruthenium(III) ion occupies one of the t_{2g} orbitals, which have the correct symmetry for π bonding. Therefore, π delocalization of spin density is likely to occur. Once some unpaired spin density is present in a π system, it can spin-polarize the electrons of the C–H σ bond. The alternating chemical shifts of the pyridyl (Chapter 6) and phenyl^[12] protons of $[\text{Ru}(\text{qpy})\text{Cl}_3]$ and $[\text{Ru}(\text{phtpy})\text{Cl}_3]$ (qpy = 4'-pyridyl-2,2':6'2''-terpyridine and phtpy = 4'-phenyl-2,2':6'2''-terpyridyl), support that spin polarization occurs in the central part of the terpyridine ligand.

Direct delocalization of spin density may occur into the outer pyridines of the terpyridine ligand I, because the ruthenium(III)-nitrogen coordination bonds are not orthogonal. The N–Ru–N'' angle has been found^[17] to be $\sim 158.3(3)^\circ$ for $[\text{Ru}(\text{tpy})\text{Cl}_3]$. Therefore, overlap is expected between the ruthenium-nitrogen molecular orbitals and the t_{2g} metal orbital, which is located in the plane of the terpyridine ligand. Such overlap may cause transfer of unpaired spin density through σ bonds.

The relative weight of the dipolar or pseudocontact shift can be evaluated when both g values and structural information are available. For low-spin, d^5 metal complexes of octahedral symmetry EPR spectra can only be seen at temperatures close to liquid helium, because of the large spin-orbit coupling present. At the time of writing, no such measurements could be performed for **2**. However, EPR data of $[\text{Ru}(\text{tpy})\text{Cl}_3]$ have shown two g values (2.36 and 1.86), which indicates pseudo-axial symmetry. From the crystal structure of $[\text{Ru}(\text{tpy})\text{Cl}_3]$, which has previously been published,^[17] metal-proton distances can be derived (Table 2.1). Hence, the contribution to the dipolar shift can be estimated. Using the known parameters of equation (4) gives $\delta_{\text{dipolar}} = 162.31/r^3 (g_{\parallel}^2 - g_{\perp}^2) (3 \cos^2 \theta - 1)$ ppm at 320 K (with r in Å). Taking into account that the geometric factor $(3 \cos^2 \theta - 1)$ can have a maximum value of 2, appreciable contributions to the pseudocontact shifts are possible. For example, the 66'' protons, which are at ~ 3.1 Å from the ruthenium atom in $[\text{Ru}(\text{tpy})\text{Cl}_3]$, can have a maximum dipolar shift of 23 ppm. Large dipolar contributions to the shift have been reported for low-spin d^5 ruthenium.^[19] Exact calculations of the dipolar shift require that the principal g directions are available. These can be obtained from single-crystal EPR measurements. The principal g directions may also be guessed from the symmetry of the molecule, which has not been achieved in this study.

The linker protons 1, which are relatively far from the paramagnetic center, show a relatively large downfield shift. Contact contributions to the shift through σ bonds are negligible, because of the large metal-proton distances. The shift may be due to a large contribution of the dipolar shift, or to a spin polarization mechanism, although it has been found for nickel(III) complexes that spin density cannot be transmitted through ethereal oxygen atoms.^[20] Moreover, the chemical shifts of the terpyridine I' protons of the diamagnetic ruthenium(II) moiety differ significantly from those of the corresponding protons of the diamagnetic precursor **1** (*i.e.* 0.64 ppm for the I'3'5' signal; see experimental section). The ruthenium(II) moiety may closely approach the paramagnetic ruthenium(III) center, because of the high flexibility of the linker. This approach can result in dipolar interactions between the paramagnetic unit and the diamagnetic unit. However, the shifted and broadened signals of the protons of the diamagnetic unit can also originate from intermolecular interactions. Concentration-dependent ¹H NMR studies have not been performed to study these interactions. The fact that the protons of the terminal terpyridine ligand II are less affected by the paramagnetic metal center than the terpyridine I' signals, indicates a distance dependence of the influence of the unpaired electron, which supports intramolecular interactions are of importance.

2.3.6 Relaxation properties of **2**

In Table 2.1, the chemical shifts and relaxation data are summarized for **2**. The shifts and T_1 and T_2 values of [Ru(tpy)Cl₃] are also reported here, as well as metal-proton distances, which have been derived from crystal structure data^[17] of [Ru(tpy)Cl₃]. The I66'' protons of **2**, which are closest to ruthenium, have a very short T_1 value (2.80 ms) and a broad line width ($T_2 = 1.75$ ms), whereas protons further away have longer T_1 s and narrower line widths. This is expected because both T_1 and T_2 are dependent on r^{-6} due to dipolar relaxation contributions.^[8] Thus, protons closer to the ruthenium center experience a stronger paramagnetic effect.

However, for the I3'5' protons the T_1 value is much shorter than that expected. Whereas the distance of the considered protons to the metal center is in between that of the I33'' and I55'' protons, T_1 is appreciably smaller (10.7 ms *versus* 17.7 and 28.5 ms, respectively). Delocalized π spin density onto the central pyridine clearly affects the relaxation of the I3'5' protons. In fact, the ratios between the T_1^{-1} values of all the different nuclei do not follow the ratios of the sixth power of the metal to nucleus distances. This indicates that also for the outer pyridines other contributions than dipolar interactions influence the relaxation.

Table 2.1 Chemical shifts and relaxation data for **2** and [Ru(tpy)Cl₃] at 320 K, 300 MHz, as well as metal-proton distances^[17] for [Ru(tpy)Cl₃].

protons	2			[Ru(tpy)Cl₃]			
	δ_{obs} (ppm)	T ₁ (ms)	T ₂ (ms)	δ_{obs} (ppm)	T ₁ (ms)	T ₂ (ms)	$r_{\text{Ru-H}}$ (Å)
I66''	-30.19	2.80	1.75	-31.62	4.81	3.41	3.1
I55''	-9.89	28.6	9.2	-6.63	39.9	15.4	5.2
I44''	0.94	46.8	18.1	-2.48	54.5	20.3	5.7
I33''	-8.44	17.5	9.2	-7.87	31.6	15.8	4.9
I3'5'	4.79	10.7	8.8	5.90	20.3	15.4	5.1
I4'	-	-	-	-20.99	13.5	7.6	5.8
1	14.43	51.0	18.5	-	-	-	-
2	4.12	100.9	30.5	-	-	-	-

2.4 Concluding remarks

The preparations of the water-soluble ruthenium(II) complex [(tpy)Ru(dtdeg)]Cl₂ (**1**) and the water-soluble ruthenium(II)-ruthenium(III) complex [(tpy)Ru(dtdeg)RuCl₃]Cl₂ (**2**) are presented. Characterization of the paramagnetic complex **2** has been achieved in a straightforward manner by ¹H NMR spectroscopy. The data demonstrate that characterization of trichlororuthenium terpyridine complexes is feasible without laborious chemical substitution, elaborate examination of T₁ and T₂ relaxation times, or theoretical studies to calculate the different contributions to the chemical shift and nuclear relaxation rates. In fact complex **2** represents the first example of a paramagnetic ruthenium(III) complex, which has been fully characterized using 1D NOE difference experiments, despite relatively short relaxation times. The technique might be widely applicable to other paramagnetic inorganic complexes. Analysis of the chemical shift behavior *versus* temperature for the terpyridine I protons of the ruthenium(III) unit indicates Curie behavior. Both dipolar and contact interactions are suggested to contribute to the hyperfine shift of the different protons. Spin polarization is probably affecting the chemical shift of the I3'5' protons. Comparison of T₁ and T₂ values with the metal-proton distances indicate that relaxation is determined by different unpaired-electron proton interactions. The chemical shifts of the protons of the diamagnetic ruthenium(II) unit are also influenced by the paramagnetic ruthenium(III) center. The shifts possibly originate from intramolecular interactions between the two moieties. Biological properties of **2** will be presented in Chapter 3.

2.5 References

- [1] (a) Wheate, N. J.; Collins, J. G., *Coord. Chem. Rev.* **2003**, *241*, 133-145. (b) Reedijk, J., *Proc. Natl. Acad. Sci. U. S. A.* **2003**, *100*, 3611-3616.
- [2] Reedijk, J., *Chem. Rev.* **1999**, *99*, 2499-2510.
- [3] Clarke, M. J., *Coord. Chem. Rev.* **2003**, *236*, 209-233.
- [4] (a) Iengo, E.; Mestroni, G.; Geremia, S.; Calligaris, M.; Alessio, E., *J. Chem. Soc.-Dalton Trans.* **1999**, 3361-3371. (b) Serli, B.; Iengo, E.; Gianferrara, T.; Zangrando, E.; Alessio, E., *Metal-Based Drugs* **2001**, *8*, 9-18.
- [5] (a) Önfelt, B.; Lincoln, P.; Nordén, B., *J. Am. Chem. Soc.* **1999**, *121*, 10846-10847. (b) Wilhelmsson, L. M.; Westerlund, F.; Lincoln, P.; Nordén, B., *J. Am. Chem. Soc.* **2002**, *124*, 12092-12093. (c) Brodkorb, A.; Kirsch-De Mesmaeker, A.; Rutherford, T. J.; Keene, F. R., *Eur. J. Inorg. Chem.* **2001**, 2151-2160.
- [6] Allardyce, C. S.; Dyson, P. J., *Platinum Metals Rev.* **2001**, *45*, 62-69.
- [7] (a) Clarke, M. J.; Bitler, S.; Rennert, D.; Buchbinder, M.; Kelman, A. D., *J. Inorg. Biochem.* **1980**, *12*, 79-87. (b) Clarke, M. J.; Zhu, F. C.; Frasca, D. R., *Chem. Rev.* **1999**, *99*, 2511-2533.
- [8] Bertini, I.; Luchinat, C., *NMR of paramagnetic substances, Coord. Chem. Rev. Vol. 150* (Ed.: Lever, A. B. P.), Elsevier, Amsterdam, **1996**.
- [9] Bertini, I.; Luchinat, C.; Piccioli, M., in *Nuclear Magnetic Resonance of Biological Macromolecules, Pt B*, **2001**, *339*, 314-340.
- [10] (a) Steiner, U. E.; Serebrennikov, Y. A., *J. Chem. Phys.* **1994**, *100*, 7503-7507. (b) Serebrennikov, Y. A.; Steiner, U. E., *J. Chem. Phys.* **1994**, *100*, 7508-7514.
- [11] Nováková, O.; Kašpárková, J.; Vrána, O.; Van Vliet, P. M.; Reedijk, J.; Brabec, V., *Biochemistry* **1995**, *34*, 12369-12378.
- [12] Velders, A. H., Ph.D. thesis, Leiden University (Leiden), **2000**.
- [13] Van Vliet, P. M.; Toekimin, S. M. S.; Haasnoot, J. G.; Reedijk, J.; Nováková, O.; Vrána, O.; Brabec, V., *Inorg. Chim. Acta* **1995**, *231*, 57-64.
- [14] (a) Potts, K. T.; Konwar, D., *J. Org. Chem.* **1991**, *56*, 4815-4816. (b) Holbrey, J. D.; Tiddy, G. J. T.; Bruce, D. W., *J. Chem. Soc.- Dalton Trans.* **1995**, 1769. (c) Constable, E. C.; Ward, M. D., *J. Chem. Soc.- Dalton Trans.* **1990**, 1405. (d) Sullivan, B. P.; Calvert, J. M.; Meyer, T. J., *Inorg. Chem.* **1980**, *19*, 1404-1407.
- [15] Sauvage, J. P.; Collin, J. P.; Chambron, J. C.; Guillerez, S.; Coudret, C.; Balzani, V.; Barigelli, F.; Decola, L.; Flamigni, L., *Chem. Rev.* **1994**, *94*, 993-1019.
- [16] (a) Dugad, L. B.; Lamar, G. N.; Banci, L.; Bertini, I., *Biochemistry* **1990**, *29*, 2263-2271. (b) Banci, L.; Bertini, I.; Luchinat, C.; Piccioli, M.; Scozzafava, A.; Turano, P., *Inorg. Chem.* **1989**, *28*, 4650-4656.
- [17] Laurent, F.; Plantalech, E.; Donnadieu, B.; Jimenez, A.; Hernandez, F.; Martinez-Ripoll, M.; Biner, M.; Llobet, A., *Polyhedron* **1999**, *18*, 3321-3331.
- [18] (a) Ming, L. J.; Banci, L.; Luchinat, C.; Bertini, I.; Valentine, J. S., *Inorg. Chem.* **1988**, *27*, 4458-4463. (b) Lamar, G. N., *J. Am. Chem. Soc.* **1965**, *87*, 3567-&.
- [19] Clarke, M. J.; Bailey, V. M.; Doan, P. E.; Hiller, C. D.; LaChance-Galang, K. J.; Daghlian, H.; Mandal, S.; Bastos, C. M.; Lang, D., *Inorg. Chem.* **1996**, *35*, 4896-4903.
- [20] (a) Eaton, D. R.; Josey, A. D.; Benson, R. E.; Phillips, W. D.; Cairns, T. L., *J. Am. Chem. Soc.* **1962**, *84*, 4100. (b) Eaton, D. R.; Josey, A. D.; Phillips, W. D.; Benson, R. E., *J. Chem. Phys.* **1962**, *37*, 347.

Chapter 3

Dinuclear ruthenium(II) complexes with long and flexible linkers: rotational behavior of coordinated 9-ethylguanine and biological properties

Abstract – The dinuclear ruthenium(II) complexes $[\text{Cl}(\text{bpy})\text{Ru}(\text{dtdeg})\text{Ru}(\text{bpy})\text{Cl}]\text{Cl}_2$ (**1**), $[(\text{tpy})\text{Ru}(\text{dtdeg})\text{Ru}(\text{bpy})\text{Cl}]\text{Cl}_3$ (**2**), and $[(\text{tpy})\text{Ru}(\text{dtdeg})\text{Ru}(\text{tpy})]\text{Cl}_4$ (**3**) are described (bpy = 2,2'-bipyridine, dtdeg = bis[4'-(2,2':6',2''-terpyridyl)]-diethyleneglycolether, tpy = 2,2':6',2''-terpyridine). The bifunctional complex **1** has been studied for its hydrolysis and interaction with the guanine derivative 9-ethylguanine (9egua). Hydrolysis of a 1 mM solution of **1** in D_2O at 310 K proceeds fast, but not completely. After approximately 2.5 hours equilibrium is accomplished, in which the mono aqua species $[(\text{D}_2\text{O})(\text{bpy})\text{Ru}(\text{dtdeg})\text{Ru}(\text{bpy})\text{Cl}]^+$ (**4**) and the diaqua species $[(\text{D}_2\text{O})(\text{bpy})\text{Ru}(\text{dtdeg})\text{Ru}(\text{bpy})(\text{D}_2\text{O})]^{2+}$ (**5**) are present *in situ* in a ratio of $\sim 3:7$. At this point the dichloro complex is not present in solution anymore. Upon reaction of **1** with 9egua, the monoadduct $[\text{Cl}(\text{bpy})\text{Ru}(\text{dtdeg})\text{Ru}(\text{bpy})(9\text{egua})]\text{Cl}_3$ (**6**) and the bisadduct $[(9\text{egua})(\text{bpy})\text{Ru}(\text{dtdeg})\text{Ru}(\text{bpy})(9\text{egua})]\text{Cl}_4$ (**7**) are formed, which both have been isolated and characterized by variable temperature ^1H NMR experiments. The coordinated base is hindered for free rotation at RT. At 248 K, 9egua is flipping between two enantiomeric rotamers, in which it is positioned in such a way that the keto group is wedged between the bpy and tpy ligands. Biological properties (*i.e.* cytotoxicity, cell uptake and adhesion) of the complexes **1**, **2**, and **3**, and the dinuclear complex $[(\text{tpy})\text{Ru}(\text{dtdeg})\text{RuCl}_3]\text{Cl}_2$ (labeled as **8** in this Chapter), which has been introduced in Chapter 2, are discussed.

3.1 Introduction

Polynuclear platinum complexes, which are linked by long and flexible α,ω -diaminoalkane linkers, have shown great potential as antitumor agents.^[1] Their high activity is thought^[2] to be due to the formation of long-range adducts with DNA, which is generally believed to be the ultimate target of anticancer platinum complexes.^[3] Structure-activity relationships state that polynuclear complexes with monofunctional platinum centers are more active than the isomers with bifunctional platinum moieties.^[4] It has been demonstrated that the bifunctional complexes [$\{trans\text{-PtCl}(\text{NH}_3)_2\}_2(\text{H}_2\text{N}(\text{CH}_2)_6\text{NH}_2)]^{2+}$ (1,1/t,t) and [$\{trans\text{-PtCl}(\text{NH}_3)_2\}_2\{\mu\text{-trans-Pt}(\text{NH}_3)_2(\text{H}_2\text{N}(\text{CH}_2)_6\text{NH}_2)_2\}]^{4+}$ (1,0,1/t,t,t or BBR3464) form 1,4-interstrand adducts, which consist of two conformers.^[5, 6] For 1,1/t,t these conformers are interconvertible.^[5] It has been suggested that delocalization of the lesion can represent an extremely efficient block to excision repair.

Ruthenium complexes are also known for their anticancer activity, and polynuclear derivatives are under study.^[7, 8] A series of dinuclear ruthenium complexes have been synthesized inspired by the mononuclear antimetastatic complex NAMI-A ($trans\text{-}(\text{H}_2\text{im})[\text{RuCl}_4(\text{dmsO})(\text{Him})]$).^[9] It appears that its antimetastatic activity is not related to DNA binding,^[10] although NAMI-A has been shown to interact with DNA *in vitro*.^[11] Dinuclear photoreactive ruthenium complexes have been designed, as it is thought that the greater size, higher charge and variation in shape increase DNA-binding affinity and specificity in comparison to the mononuclear complexes.^[12] These complexes mainly interact with the DNA by electrostatic interactions and intercalation. A relation between DNA binding and cytotoxicity has not yet been established for this new class of complexes.

In this Chapter, the dinuclear ruthenium(II) complexes [$\text{Cl}(\text{bpy})\text{Ru}(\text{dtdeg})\text{Ru}(\text{bpy})\text{Cl}]\text{Cl}_2$ (**1**), [$(\text{tpy})\text{Ru}(\text{dtdeg})\text{Ru}(\text{bpy})\text{Cl}]\text{Cl}_3$ (**2**), and [$(\text{tpy})\text{Ru}(\text{dtdeg})\text{Ru}(\text{tpy})]\text{Cl}_4$ (**3**) are described (Figure 3.1) (bpy = 2,2'-bipyridine, dtdeg = bis[4'-(2,2':6',2''-terpyridyl)]-diethyleneglycolether, tpy = 2,2':6',2''-terpyridine). The complexes have been synthesized using the long and flexible dtdeg linker to allow the formation of long-range DNA adducts. The design and development of complex **1** is based on the mononuclear complex [$\text{Ru}(\text{tpy})(\text{bpy})\text{Cl}]\text{Cl}$, which has been reported to monofunctionally coordinate to DNA by substitution of the relatively labile chloride ligand.^[13] Complex **1** may form bisadducts with DNA by monofunctional coordination of both metal units. Complexes **2** and **3** have been synthesized by substitution with the inert ligand terpyridine at one or both metal moieties. Substitution-inert ruthenium polypyridyl complexes are known to bind to DNA by electrostatic or surface binding, or partial intercalation.^[14, 15]

Since it is thought that hydrolysis occurs before coordination to DNA,^[16] the hydrolysis of **1** into the mono- and di-aqua species $[(D_2O)(bpy)Ru(dtdeg)Ru(bpy)Cl]^+$ (**4**) and $[(D_2O)(bpy)Ru(dtdeg)Ru(bpy)(D_2O)]^{2+}$ (**5**) has been studied *in situ* by 1H NMR. The interaction of **1** with the DNA-model base 9-ethylguanine (9egua) is also described. The characterization of the monoadduct $[Cl(bpy)Ru(dtdeg)Ru(bpy)(9egua)]Cl_3$ (**6**) and the bisadduct $[(9egua)(bpy)Ru(dtdeg)Ru(bpy)(9egua)]Cl_4$ (**7**) by variable temperature 1H NMR experiments is presented. Biological properties (*i.e.* cytotoxicity, cell uptake and adhesion) of the complexes **1**, **2**, and **3**, and of the dinuclear complex $[(tpy)Ru(dtdeg)RuCl_3]Cl_2$ (labeled as **8** in this Chapter), which has been introduced in Chapter 2, will be discussed as well.

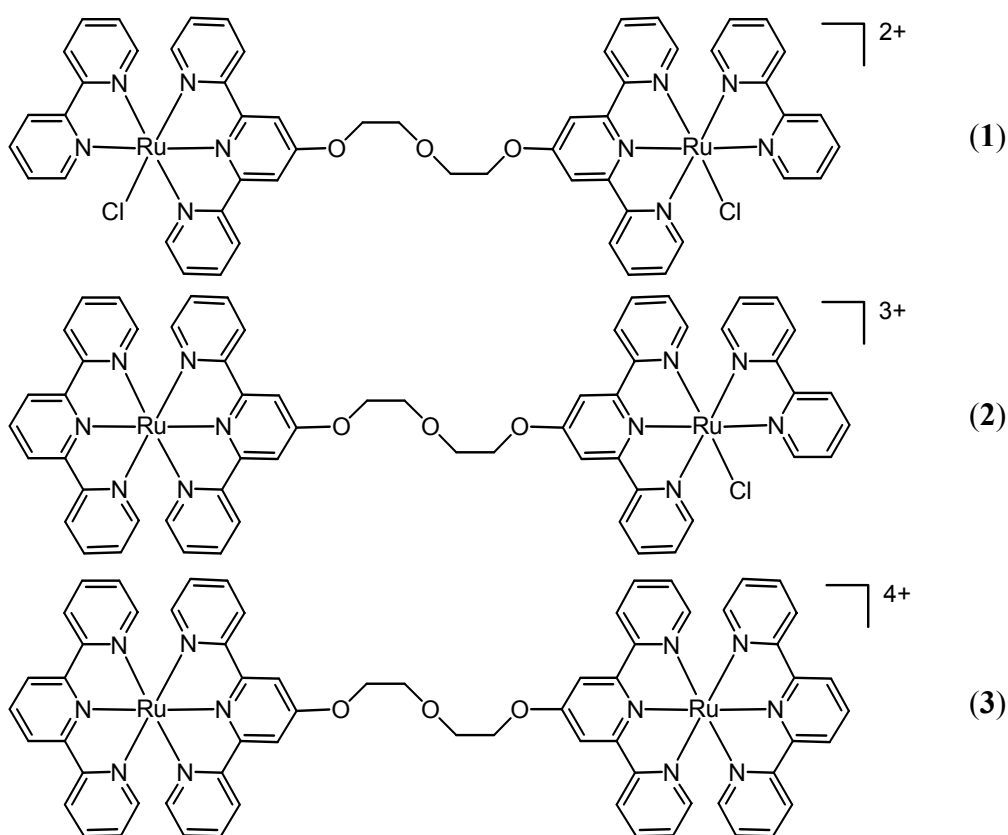


Figure 3.1 The cationic dinuclear ruthenium(II) complexes **1**, **2**, and **3**.

3.2 Experimental section

3.2.1 General methods and starting materials

^1H NMR spectra were acquired on a Bruker DPX 300 and DMX 600 spectrometer. Spectra were recorded in deuterated DMSO, water, or methanol and calibrated on residual solvent peaks at δ 2.49, δ 4.78 (298 K) and δ 3.30, respectively. Elemental analyses on C, H and N were performed on a Perkin Elmer series II CHNS/O Analyzer 2400. Electrospray mass spectra were recorded on a Finnigan TSQ-quantum instrument with an electrospray interface (ESI). Hydrated $\text{RuCl}_3 \cdot x\text{H}_2\text{O}$ ($x \sim 3$) was used as received from Johnson & Matthey. The ligands tpy and bpy were obtained from Sigma. The complex $[\text{Ru}(\text{tpy})\text{Cl}_3]$ was synthesized following a known procedure.^[17] The synthesis of the ligand dtdeg, the 0.1 M ruthenium(III) solution, and the complex $[(\text{tpy})\text{Ru}(\text{dtdeg})\text{RuCl}_3]\text{Cl}_2$ are described in Chapter 2, section 2.2.3. The complexes $[\text{Cl}_3\text{Ru}(\text{dtdeg})\text{RuCl}_3]$ and $[\text{Cl}(\text{bpy})\text{Ru}(\text{dtdeg})\text{Ru}(\text{bpy})\text{Cl}]\text{Cl}_2$ (**1**) have previously been synthesized,^[18] but the procedures will also be reported here for convenience. The species $[(\text{D}_2\text{O})(\text{bpy})\text{Ru}(\text{dtdeg})\text{Ru}(\text{bpy})\text{Cl}]^+$ (**4**) and $[(\text{D}_2\text{O})(\text{bpy})\text{Ru}(\text{dtdeg})\text{Ru}(\text{bpy})(\text{D}_2\text{O})]^{2+}$ (**5**) were formed *in situ* in D_2O at 310 K.

3.2.2 Syntheses

$[\text{Cl}_3\text{Ru}(\text{dtdeg})\text{RuCl}_3]$:^[18] A mixture of dtdeg (300 mg; 0.53 mmol), LiCl (300 mg; 7.08 mmol) and 21.1 mL of 0.1 M ruthenium(III) solution (2.11 mmol) in 40 mL of DMF were stirred at 353 K for 2 hours. After filtration, the residue was washed with DMF, EtOH and diethyl ether. The product was partly purified by reflux in 200 mL of acetone for 4 hours. Yield: 470 mg (91 %). ^1H NMR (300 MHz, DMSO, 298 K): $\delta = -9.96$ (s, 4H; I33''), 1.05 (s, 4H; I44''), -11.48 (s, 4H; I55''), -34.27 (s, 4H; I66''), 4.75 (s, 4H; I3'5'), 16.62 (s, 4H; I1), 4.08 ppm (s, 4H; I2).

$[\text{Cl}(\text{bpy})\text{Ru}(\text{dtdeg})\text{Ru}(\text{bpy})\text{Cl}]\text{Cl}_2$ (1**)**:^[18] A mixture of $[\text{Cl}_3\text{Ru}(\text{dtdeg})\text{RuCl}_3]$ (100 mg; 0.10 mmol), bpy (32 mg; 0.20 mmol), LiCl (43 mg; 1.01 mmol) and triethylamine 37 mg; 0.37 mmol) in 20 mL of EtOH 98 % were refluxed for 3 hours. The base triethylamine assisted in the reduction of ruthenium(III) by EtOH. After filtration and evaporation *in vacuo*, the product was purified by column chromatography on neutral alumina with chloroform/EtOH (v:v = 1:1) as the eluents. The purple band was collected in two fractions. From the second fraction pure product was obtained. Yield: 99 mg (79 %). ^1H NMR (300 MHz, DMSO, 298 K): $\delta = 8.70$ (d, 4H; I33''), 7.90 (t, 4H; I44''), 7.31 (t, 4H; I55''), 7.58 (d, 4H; I66''), 8.58 (s, 4H; I3'5'), 4.71 (t, 4H; 1), 4.13 (t, 4H; 2), 8.88 (d, 2H; II3), 8.31 (t, 2H;

II4), 8.02 (t, 2H; II5), 10.09 (d, 2H; II6), 8.63 (d, 2H; II3'), 8.75 (t, 2H; II4'), 7.09 (t, 2H; II5'), 7.42 ppm (d, 2H; II6').

[(tpy)Ru(dtdeg)Ru(bpy)Cl]Cl₃, (2): A mixture of a crude batch of [(tpy)Ru(dtdeg)RuCl₃]Cl₂ (800 mg; 0.68 mmol), bpy (159 mg; 1.02 mmol), LiCl (143 mg; 3.37 mmol) and triethylamine (250 mg; 2.48 mmol) were refluxed for 2.5 hours in 135 mL of absolute EtOH. After filtration and evaporation *in vacuo*, the product was purified by column chromatography on neutral alumina with acetone/EtOH (v:v = 6:4) as the eluents. From the brown third band, pure product was isolated by precipitation of the particular fraction with diethyl ether. Yield: 155 mg (18 %). Elemental analysis (%) calculated for C₅₉H₄₇Cl₄N₁₁O₃Ru₂·7H₂O: C 49.62, N 10.79, H 4.31. Found: C 49.15, N 10.44, H 4.16. ¹H NMR (300 MHz, DMSO, 298 K): δ = 8.77 (d, 2H; I33''), 7.87 (t, 2H; I44''), 7.31 (t, 2H; I55''), 7.59 (d, 2H; I66''), 8.67 (s, 2H; I3'5'), 4.78 (t, 2H; 1), 4.19 (t, 2H; 2), 8.93 (d, 2H; I'33''), 7.95 (t, 2H; I'44''), 7.20 (t, 2H; I'55''), 7.36 (d, 2H; I'66''), 8.90 (s, 2H; I'3'5'), 4.78 (t, 2H; 1'), 4.19 (t, 2H; 2'), 8.88 (d, 1H; II3), 8.31 (t, 1H; II4), 8.02 (t, 1H; II5), 10.06 (d, 1H; II6), 8.63 (d, 1H; II3'), 8.76 (t, 1H; II4'), 7.09 (t, 1H; II5'), 7.45 (d, 1H; II6'), 8.84 (d, 2H; III33''), 8.01 (t, 2H; III44''), 7.26 (t, 2H; III55''), 7.54 (d, 2H; III66''), 9.08 (d, 2H; III3'5'), 8.48 ppm (t, 1H; III4').

[(tpy)Ru(dtdeg)Ru(tpy)]Cl₄, (3): An excess of AgBF₄ (2.4 g; 12.33 mmol) was dissolved in 100 mL of acetone and filtered. [Ru(tpy)Cl₃] (405 mg; 0.92 mmol) was added to the filtrate and the mixture was refluxed for 16 hours to remove the chloride ions from ruthenium. After filtration to remove precipitated AgCl, the filtrate was evaporated *in vacuo*, which resulted in a green oil (~ 3 mL). The ligand dtdeg (210 mg; 0.37 mmol) was added and the mixture was refluxed for 1 hour in 120 mL DMF, which acted as reducing agent. The reaction mixture was filtered and the filtrate evaporated *in vacuo* until ~ 3 mL of a red oil resulted. The product was purified by column chromatography on neutral alumina with a mixture of CH₃CN/aqueous saturated KNO₃ solution/H₂O (v:v:v = 35:5:6) as the eluents. The nitrate salt of the product was obtained from the fraction containing the first orange red band. The chloride salt of the product was synthesized to be able to compare results with complexes **1** and **2**, which are chloride salts as well. 30 mL of a saturated LiCl solution in MeOH was added to a concentrated solution of the complex in MeOH. The product was obtained by precipitation with a large amount of acetone (2 L). Column chromatography on neutral alumina and EtOH yielded pure complex. Yield: 160 mg (31 %). Elemental analysis (%) calculated for C₆₄H₅₀Cl₄N₁₂O₃Ru₂·8H₂O: C 50.46, N 11.03, H 4.37. Found: C 49.97, N 10.70, H 4.13. ¹H NMR (300 MHz, DMSO, 298 K): δ = 9.01 (d, 4H; I33''), 7.93 (t, 4H; I44''), 7.21 (t, 4H; I55''), 7.37 (d, 4H; I66''), 8.99 (s, 4H; I3'5'), 4.87 (t, 4H; 1), 4.24 (t, 4H; 2), 8.85 (d, 4H; II33''), 8.01 (t, 4H; II44''), 7.29 (t, 4H; II55''), 7.55 (d, 4H; II66''), 9.10 (d, 4H; II3'5'), 8.49 ppm (t, 2H; II4').

[Cl(bpy)Ru(dtdeg)Ru(bpy)(9egua)]Cl₃, (6): [Cl(bpy)Ru(dtdegRu(bpy)Cl)]Cl₂ (90 mg; 0.07 mmol) and an excess of 9egua (53 mg; 0.30 mmol) were stirred in 54 mL of H₂O, at 310 K for 24 hours. The mixture was concentrated *in vacuo* and filtered to remove free 9egua. The mixture was passed to EtOH by coevaporation with EtOH twice. Column chromatography on neutral alumina with CHCl₃/EtOH (v:v = 1:1) separated **6** from the bisadduct **7**. From the brown pink third band the monoadduct **6** was isolated by precipitation of the fraction with diethyl ether. Yield: 4 mg (4 %). ¹H NMR (600 MHz, MeOH, 248 K): δ = 8.34 (d, 1H; I3), 7.82 (t, 1H; I4), 7.19 (t, 1H; I5), 8.21 (d, 1H; I6), 8.28 (s, 1H; I3'), 8.52 (s, 1H; I5'), 8.73 (d, 1H; I3''), 8.02 (t, 1H; I4''), 7.36 (t, 1H; I5''), 7.61 (d, 1H; I6''), 4.70 (t, 2H; 1), 4.18 (t, 2H; 2), 8.79 (d, 1H; II3), 8.27 (t, 1H; II4), 7.78 (t, 1H; II5), 9.18 (d, 2H; II6), 8.59 (d, 1H; II3'), 7.81 (t, 1H; II4'), 7.10 (t, 1H; II5'), 7.36 (d, 2H; II6'), 6.86 (s, 1H; H8(9egua)), 3.82 (q, 2H; CH₂(9egua)), 1.07 ppm (t, 3H, CH₃(9egua)), 8.58 (d, 1H; I'3), 7.90 (t, 1H; I'4), 7.29 (t, 1H; I'5), 7.70 (d, 1H; I'6), 8.50 (s, 1H; I'3'), 8.48 (s, 1H; I'5'), 8.57 (d, 1H; I'3''), 7.84 (t, 1H; I'4''), 7.21 (t, 1H; I'5''), 7.69 (d, 1H; I'6''), 4.66 (t, 2H; 1'), 4.18 (t, 2H; 2'), 8.78 (d, 1H; II'3), 8.28 (t, 1H; II'4), 7.96 (t, 1H; II'5), 10.10 (d, 1H; II'6), 8.52 (d, 1H; II'3'), 7.73 (t, 1H; II'4'), 7.06 (t, 1H; II'5'), 7.52 ppm (d, 1H; II'6'). The monoadduct was not analyzed any further, due to the low yield.

[(9egua)(bpy)Ru(dtdeg)Ru(bpy)(9egua)]Cl₄, (7): After collecting the monoadduct **6** from the column, the eluens was changed to a mixture of EtOH and MeOH (v:v = 9:1). From the light orange band the bisadduct was isolated by precipitation of the fraction with diethyl ether. Yield: 14 mg (12 %). ¹H NMR (600 MHz, MeOH, 248 K): δ = 8.41 (d, 2H; I3), 7.84 (t, 2H; I4), 7.19 (t, 2H; I5), 8.21 (d, 2H; I6), 8.38 (s, 2H; I3'), 8.64 (s, 2H; I5'), 8.84 (d, 2H; I3''), 8.06 (t, 2H; I4''), 7.36 (t, 2H; I5''), 7.63 (d, 2H; I6''), 4.71 (t, 4H; 1), 4.19 (t, 4H; 2), 8.79 (d, 2H; II3), 8.26 (t, 2H; II4), 7.78 (t, 2H; II5), 9.19 (d, 2H; II6), 8.59 (d, 2H; II3'), 7.81 (t, 2H; II4'), 7.09 (t, 2H; II5'), 7.38 (d, 2H; II6'), 6.88 (s, 2H; H8(9egua)), 3.84 (q, 4H; CH₂(9egua)), 1.07 ppm (t, 6H, CH₃(9egua)). The bisadduct was not analyzed any further, due to the low yield.

3.2.3 Biological tests.

Cell cultures: KB carcinoma cells were maintained in Minimum Essential Medium (EuroClone, Whetherby, UK) containing 1.5 g/L sodium hydrogencarbonate and supplemented with 10 % fetal bovine serum (FBS) (Invitrogen Italia, Milano, Italy), 2 mM L-glutamine (EuroClone, Whetherby, UK), 100 units/mL penicillin and 100 µg/mL streptomycin (EuroClone, Whetherby, UK), 1 mM sodium pyruvate (EuroClone, Wetherby,

UK), 1 % non-essential aminoacids (EuroClone, Wetherby, UK), 1 mM HEPES solution, EuroClone, Wetherby, UK), in a humidified atmosphere with 5 % CO₂ at 310 K.

HBL-100, non tumorigenic epithelial cells, were maintained in McCoy's 5A medium (SIGMA, St. Louis, MO, USA) supplemented with 10 % fetal bovine serum (FBS), 2 mM L-glutamine, 100 UI/mL penicillin and 100 µg/mL streptomycin (EuroClone, Wetherby, UK), in a humidified atmosphere with 5 % CO₂ at 310 K.

A2780cis and A2780R cells (cisplatin sensitive and resistant human ovarian carcinoma, respectively) were maintained in Dulbecco's modified Eagle's Medium (DMEM: Gibco BRL™, Invitrogen Corporation, The Netherlands) supplemented with 10 % fetal calf serum (Perbio Science, Belgium), penicillin (100 units/mL: Duchefa Biochemie BV, The Netherlands) and streptomycin (100 µg/mL: Duchefa Biochemie BV, The Netherlands) in a humidified 6 % CO₂, 94 % air atmosphere. L1210/0 and L1210/2 cells (cisplatin sensitive and resistant mouse leukemia, respectively) were grown (partly in suspension and partly weakly adherent to the flasks) under the above mentioned conditions for maintenance of A2780 cell growth.

Cells from confluent monolayers were removed from flasks by 0.05 % trypsin solution (SIGMA, St. Louis, MO, USA); cell viability was determined by the trypan blue exclusion test.

***In vitro* cytotoxicity evaluation:** Cell growth was determined by the MTT assay, a colorimetric assay based on the ability of viable cells to reduce the soluble yellow 3-(4,5-dimethylthiazol-2-yl)-2,5-diphenyl-2H-tetrazolium bromide to blue formazan crystals by the mitochondria.^[19] Cells were seeded between 1000 and 5000 cells/well (depending on the cell type) onto 96-well plates (Corning Costar®) in 100 µl of complete medium with 5 to 10 % of FBS. KB and HBL-100 cells were treated 24 hours after the sowing by adding 100 µL of complete medium containing the test compounds at the appropriate concentrations. A2780 and L1210 cells were treated 48 hours after sowing.

Final tested concentrations ranged between 1 µM and 100 µM and have been obtained by several dilutions with complete medium from stock solutions (1 mM) in sterile water. After 24, and 72 hours of incubation, cells were incubated with 1 mg/mL MTT solution for 2 to 4 hours at 310 K. Subsequently, the medium was discarded and the formed crystals were dissolved in 100 µL DMSO per well. Optical density (OD) was measured at 570 nm with a spectrophotometer Spectra Count Packard® Bell (Meriden, CT, USA), and at 590 nm using a Biorad 550 microplate reader. The OD is directly proportional to the number of living cells, which are compared to the control (untreated cells).

Atomic absorption spectroscopy: Cells were sown in 6-well plates and treated with 100 µM of the ruthenium compounds in Dulbecco Phosphate Buffer Saline (DPBS) at pH= 7.4 for 1

hour at 310 K. At the end of treatment the cells were extensively washed and harvested with a solution of Trypsin-EDTA. Cell specimens, counted by trypan blue exclusion test were dried overnight at 353 K and then at 378 K in Nalgene[®] cryovials. Cell decomposition was facilitated by addition of an aliquot of tetramethylammonium hydroxide (25 % in water) (Aldrich Chimica, Gallarate, Milano, Italy) and of milliQ water at a ratio 1:1 directly to each vial, at room temperature and under shaking (modified from Tamura and Arai). Final volumes were adjusted to 1 mL with milliQ water. The ruthenium concentration was measured using a Graphite Furnace Atomic Absorption Spectrometer (GFAAS), model SpectrAA-220Z, supplied with the GTA 110Z power and with a specific ruthenium emission lamp (Hollow cathode lamp P/N 56-101447-00) (Varian, Mulgrave, Victoria, Australia). The quantification of ruthenium was carried out in 10 μ L samples at 349.9 nm with an atomizing temperature of 2773 K, using argon as carrier gas at a flow rate of 3.0 L min⁻¹. Before each daily analysis session, a five-point calibration curve was obtained using Ruthenium Custom-Grade Standard 998 μ g mL⁻¹ (Inorganic Ventures Inc., Saint Louis, MO, USA).

Adhesion assay: To evaluate pro-adhesive effects of the ruthenium compounds, cells were sown in 96-well plates (Corning Costar, Milano, Italy) in complete medium. Two days later cells were treated with each ruthenium compound for 1 hour in complete medium at the concentrations of 1, 10, 100 μ M at 310 K. The pro-adhesive effect was determined as the resistance of cells to the action of a trypsin solution (0.05 % w:v for 30 min at 310 K). After this time cells were washed twice with PBS (Phosphate Buffer Saline pH = 7.4). Cells, which remained attached, were fixed and stained with 50 μ l of sulforhodamine B (Sigma Chemical Co.) for 1 hour at room temperature (Skehan et al, 1990). After removal of the unreacted dye, cells were washed twice with a solution of 1 % (v:v) acetic acid and left to air dry. Sulforhodamine B bound to cells was dissolved with a 10 mM solution of Tris base (Sigma Chemical Co.) at pH = 10.5, and the absorbance was measured at 570 nm using a spectrophotometer Spectra Count Packard Bell (Meridien, CT,USA). In each experiment controls, which were not subjected to incubation with the compounds and trypsinization, were added.

Morphological analysis: To evaluate a possible modification of cell structure, KB and HBL-100 cells were treated for 1 hour with 100 μ M of the compounds in complete medium. At the end of treatment cells were fixed with 4 % paraformaldehyde for 10 min, and were washed twice with DPBS. Cell structure was evaluated with a phase contrast microscope, with a magnification of 200X.

Statistical analysis: Data were submitted to computer-assisted statistical analysis using ANOVA analysis of variance and Dunnett post-test or Student t-test.

3.3 Results and discussion

3.3.1 Characterization of complexes **1**, **2** and **3** by ^1H NMR spectroscopy

^1H NMR characterization of **1** has been performed previously.^[18] For convenience, its ^1H NMR spectrum in $\text{DMSO-}d_6$ is shown in Figure 3.2 (top). The appearance of two individual resonances in the region between 4 and 5 ppm for the linker protons of **1** clearly indicates the presence of a symmetric species consisting of two identical moieties. Symmetry is also displayed within each unit due to the occurrence of a second C_2 symmetry axis. The eight signals of the bipyridine ligand II are easily recognized, because of the relative intensity of 2 caused by the fact that the ligand is located in the plane of symmetry. For comparison, the terpyridine I signals have a relative intensity of 4. The II6 bipyridine signal is shifted relatively downfield, due to the deshielding effect of the nearby chloride ligand. In contrast, the II6' resonance is shifted relatively upfield as these protons are shielded by terpyridine ligand I.

The ^1H NMR spectrum of **2** in $\text{DMSO-}d_6$ is also depicted in Figure 3.2 (middle). The assignment of the ^1H NMR data has been done by 2D COSY and NOESY experiments (data not shown). In the upfield region of the spectrum, four different resonances are not clearly observed for the linker protons. However, four sets of signals are identified in the aromatic region for the four nonequivalent polypyridine ligands I, I', II and III, which indicates the presence of two different metal moieties. The signals for the pyridine 6 protons have been identified by the small J value, as compared to that of the pyridine 3 protons (~ 5 Hz versus ~ 9 Hz, respectively). The eight resonances of the bipyridine ligand II protons are recognized through their relative intensity of 1. The II6 and II6' signal have been distinguished by the relative downfield shift of the former. From the relative double intensity of the terpyridine protons of **2**, the presence of a C_2 symmetry axis within each unit can be inferred. The terpyridine ligand III has been distinguished from the terpyridine ligands I and I' by the signal for the III4' proton, since it is the only terpyridine signal with a relative intensity of 1. The terpyridine ligands I and I' have been differentiated by the II6-II6'' interligand NOE crosspeak.

Characterization of **3** by ^1H NMR has been performed similarly to that of **1** and **2**. Therefore, it will not be discussed in detail. The 1D spectrum is displayed in Figure 3.2 (bottom). Characteristic features are the presence of only two resonances in the upfield region between 4 and 5 ppm, and the relative intensity of 4 for the two sets of terpyridine signals observed in the aromatic region. These indicate the C_2 symmetry of the species. The signals of the terminal terpyridine ligand II have been identified by the resonance of the II4' proton.

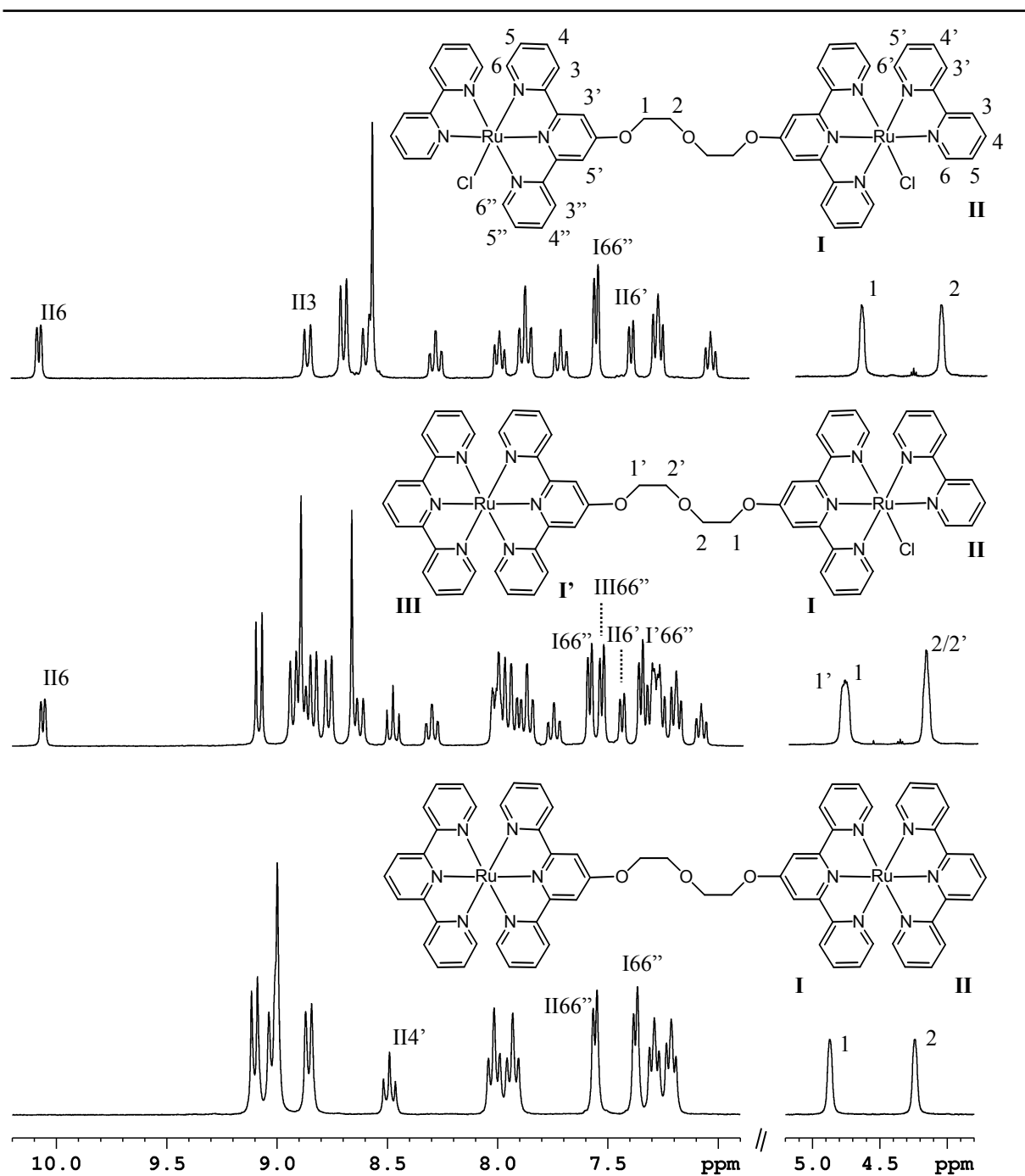


Figure 3.2 1D ^1H NMR spectra of **1** (top), **2** (middle), and **3** (bottom) in $\text{DMSO-}d_6$ at 298 K with some assignments, and schematic representations of the cations of **1**, **2**, and **3**. The numbering scheme given for the cation of **1** is also applicable to those of **2** and **3**.

3.3.2 Hydrolysis of the dinuclear compounds in D₂O

It is generally believed that hydrolysis of the chloride ligands of cisplatin occurs before it coordinates to DNA.^[16] Since a similar reaction pathway is suggested for ruthenium anticancer complexes,^[7, 20] the hydrolysis of 1 mM solutions of the dinuclear complexes has been studied at 310 K. The hydrolysis of **1** can easily be followed by monitoring the resonances of the H6 bipyridine protons in the 1D ¹H NMR spectra at 310 K (Figure 3.3), as these protons are shifted relatively downfield and are well isolated from other resonances.

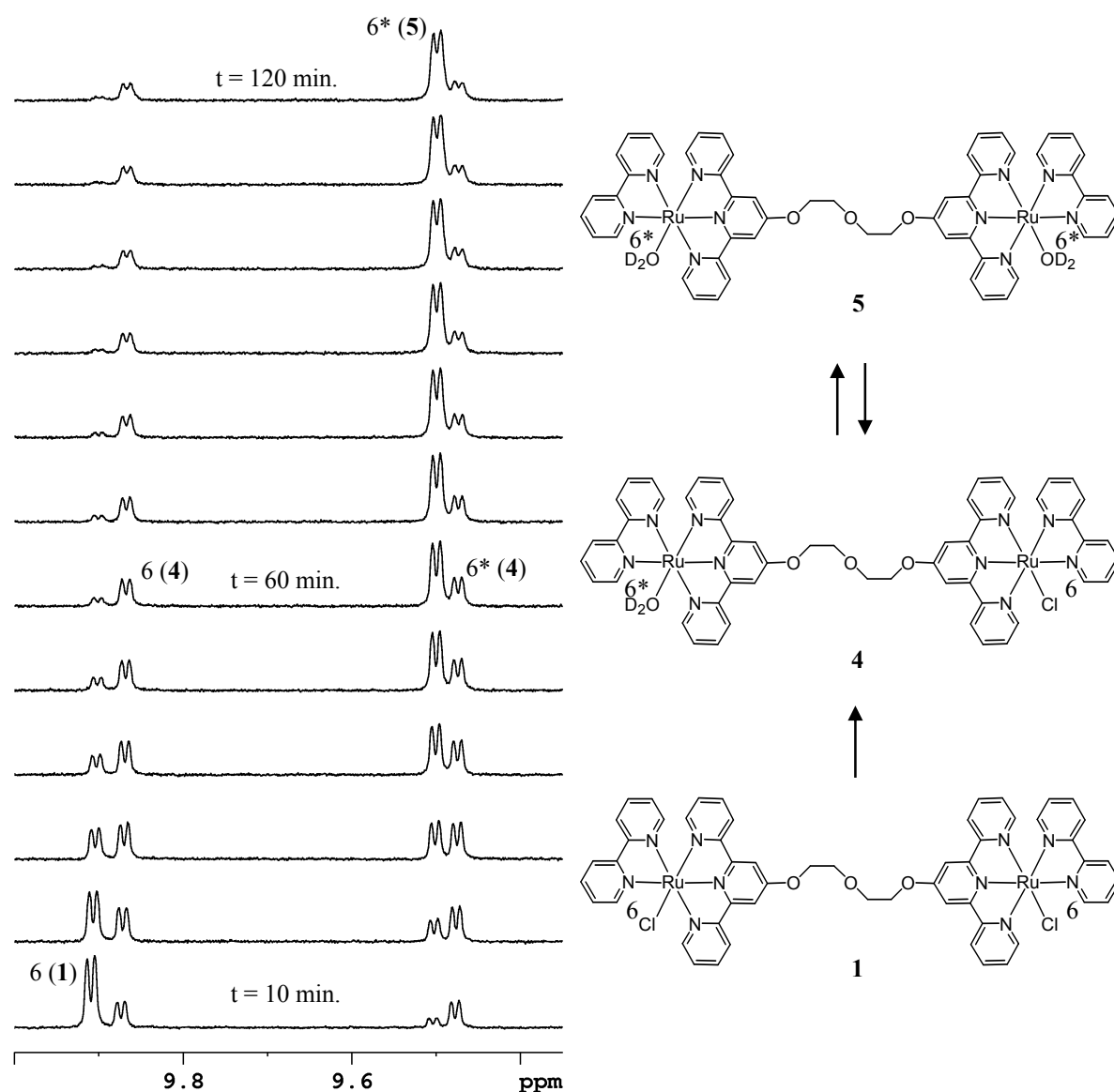


Figure 3.3 Downfield region of the ¹H NMR spectra (600 MHz) of **1** in D₂O (1 mM) at 310 K at different times *t*, with intervals of 10 minutes.

The bipyridine 6 resonance of **1** is found relatively downfield in D₂O at t = 0, because of the deshielding effect of the coordinated chloride ions. Upon hydrolysis of the first chloride ion, an asymmetric species results, *i.e.* [Cl(bpy)Ru(dtdeg)Ru(bpy)(D₂O)]³⁺ (**4**). The species is observed in ¹H NMR by the appearance of two signals of identical intensity for the two different bipyridine protons 6 and 6*. The resonance of the bipyridine proton close to the coordinated D₂O molecule (6*), experiences an upfield shift of 0.44 ppm in comparison with that of the corresponding resonance of the intact ruthenium moiety. Already after 15 minutes, the relative occurrence of the mono-aqua species amounts to 45 %. The diaqua species is present then as well for approximately 10 %, which is inferred from the relative intensity of the new signal at 9.5 ppm. This resonance arises from the two identical bipyridine 6* protons of the fully hydrolyzed symmetric species, [(D₂O)(bpy)Ru(dtdeg)Ru(bpy)(D₂O)]⁴⁺ (**5**), and increases with time. The chemical shift of the bipyridine 6* signal of **5** is shifted upfield with respect to the bipyridine 6 signal of **1**, but remains in the downfield region of the spectrum. The shift may indicate coordination of a hydroxide anion in stead of water. However, the pH of the solution has not been measured during the hydrolysis experiment to examine this possibility.

The relative intensity of the different species present in solution has been plotted against time in Figure 3.4. The abundance of the dichloro species decreases rapidly. Within 12 minutes, half of the original complex is hydrolyzed, and both the mono-aqua species and the fully hydrolyzed complex are observed. For the first 20 minutes, the mono-aqua species is formed relatively fast in comparison to the diaqua complex. After half an hour the presence of the mono-aqua species starts to decrease, but it does not disappear completely in time. After about 2.5 hours equilibrium is accomplished, in which the mono-aqua and di-aqua species are present in a ratio of ~ 3:7 and the dichloro complex is absent.

Hydrolysis of **2** only occurs at one metal moiety. Similarly to **1**, the hydrolysis has been followed by monitoring the chemical shift of the H6 resonance (data not shown). Hydrolysis of **2** proceeds almost completely, *i.e.* 95 % of the aqua species is formed from a 1 mM solution of **2** in D₂O after 2.5 hours at 310 K. These results indicate that for **1** hydrolysis of the first chloride ion decreases the rate and thermodynamic equilibrium of hydrolysis of the second chloride ion. Since **3** does not have labile leaving groups coordinated to ruthenium, hydrolysis does not occur and its ¹H NMR spectrum is stable with time.

Hydrolysis of the complexes also seems to be dependent on the concentration of the complexes, *i.e.* hydrolysis of a higher concentrated solution is relatively slow. Furthermore, complexes **1** and **2** are poorly soluble in physiological solutions containing 0.9 % of NaCl. The chloride counter ions probably affect hydrolysis and solubility. Hydrolysis of the complexes has not been studied at different ionic strengths or in buffer solution.

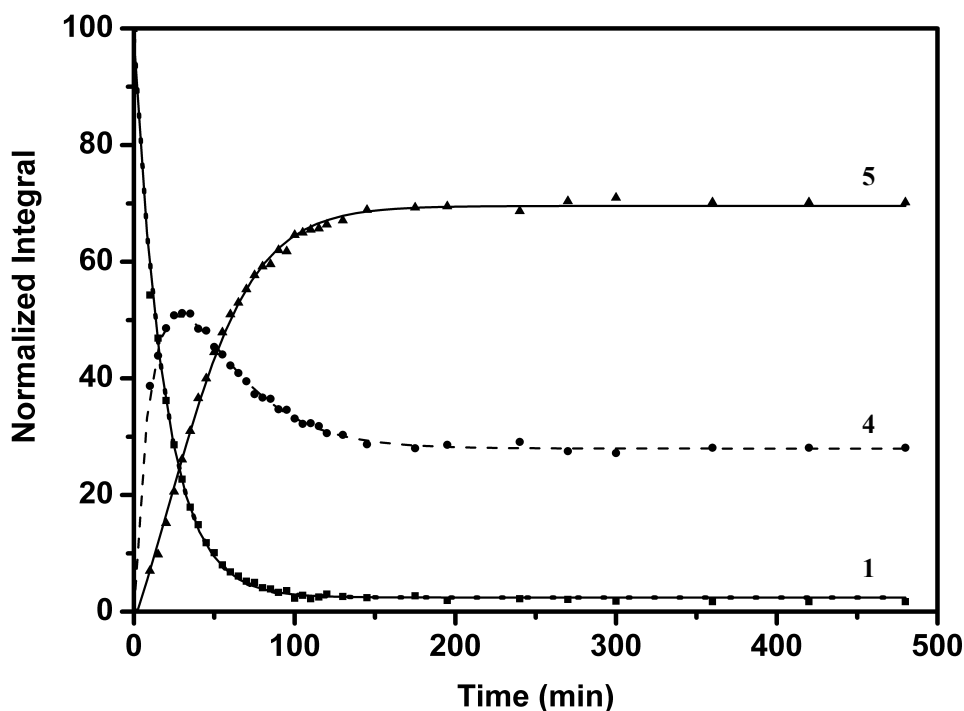


Figure 3.4 Plots of the normalized integral of the bipyridine 6 and 6* resonances *versus* time in minutes for the dichloro (1), mono-aqua (4) and di-aqua species (5).

3.3.3 Characterization of the bisadduct 7

The reaction of 1 with 9egua has been performed in water with a twofold excess of 9egua, and resulted in a mixture of monoadduct (6) and bisadduct (7), and hydrolyzed species. The fact that 1 not fully hydrolyzes probably influences the reactivity towards 9egua. Moreover, 9egua was found to dissociate from ruthenium at RT upon removal of the excess of 9egua. Dissociation of 9egua was particularly fast in water, as hydrolyzed species were formed. As a result, complexes 6 and 7 were obtained in low yield and not completely pure. However, it has been possible to characterize the 9egua adducts by 1D and 2D ^1H NMR spectroscopy. Since the bisadduct displays a relatively simple ^1H NMR spectrum with respect to that of the monoadduct, it will be discussed first. ^1H NMR experiments were performed in $\text{MeOH-}d_4$ to prevent the dissociation of the base from ruthenium.

Parts of the ^1H NMR spectra of $[(9\text{egua})(\text{bpy})\text{Ru}(\text{dtdeg})\text{Ru}(\text{bpy})(9\text{egua})]\text{Cl}_4$ (7) in $\text{MeOH-}d_4$ at 298 K (top) and 248 K (bottom) are shown in Figure 3.5. At both temperatures, only two resonances of intensity four are observed for the linker protons between 4 and 5 ppm, indicating that the two metal moieties are identical. At 248 K, a double intensity for each signal in the aromatic region is observed. Resonances of 9egua at 6.88, 3.84 and 1.07 ppm for

the H8, CH₂ and CH₃ protons, respectively, have shifted from the corresponding values for free 9egua (7.71, 4.08 and 1.43 ppm), which prove coordination of the DNA-model base to ruthenium. The relative intensity of the H8 signal confirms the formation of the bisadduct. The large upfield chemical shift of the H8 in comparison with that of free 9egua clearly indicates N7 coordination to ruthenium. In the aromatic region of the spectrum at RT, sharp signals are observed for the bipyridine protons, whereas broad resonances are seen for the terpyridine protons. The broad resonances suggest hindered rotational behavior of coordinated 9egua, which affects the terpyridine resonances exclusively. Variable temperature ¹H NMR experiments have been performed to study this behavior.

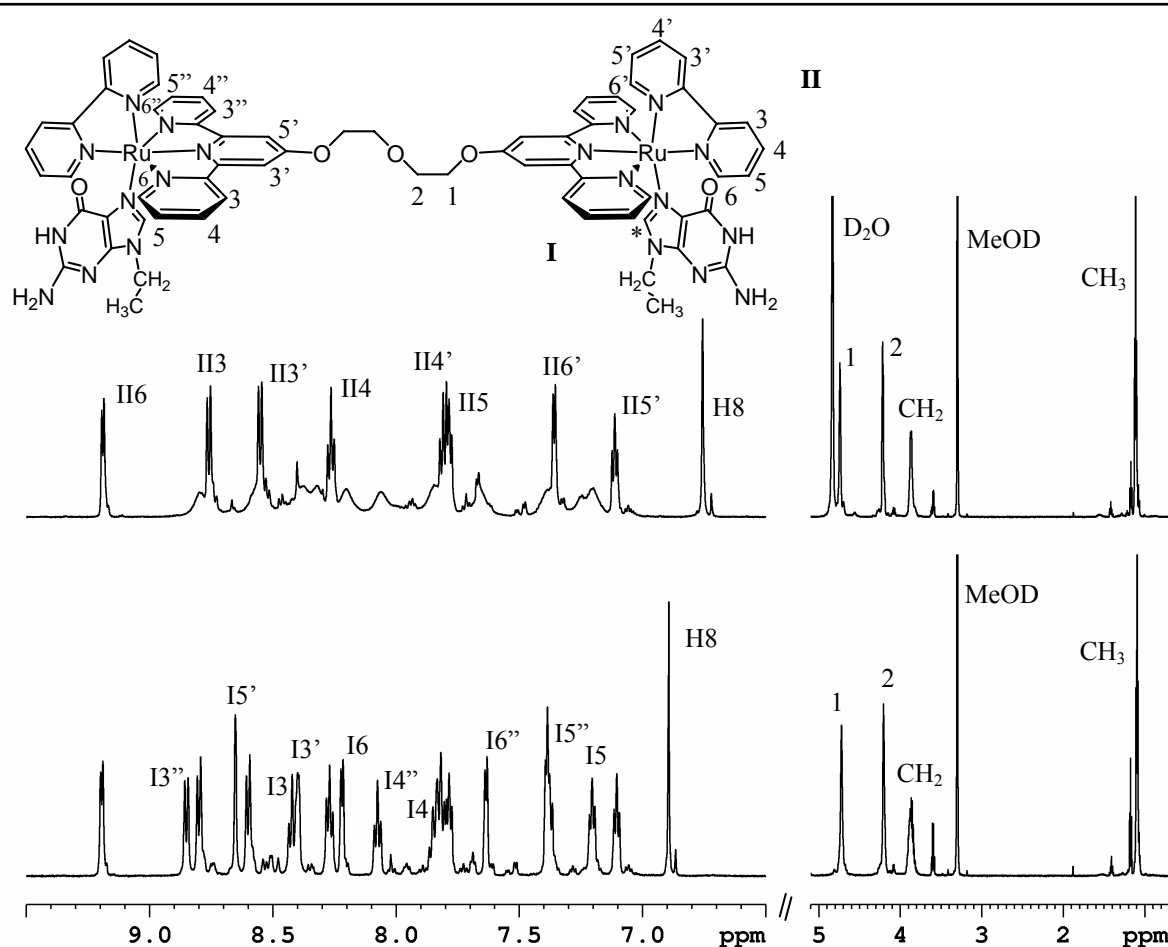


Figure 3.5 Parts of the ¹H NMR spectra of **7** at 298 K (top) and 248 K (bottom) in MeOH-*d*₄, and schematic representation of the bisadduct **7**. A numbering scheme is only given for the terpyridine ligand I, the bipyridine ligand II and the linker protons 1 and 2, because the two metal moieties are identical. The H8 proton of 9egua is indicated with an asterisk in the schematic representation of the adduct. In the spectrum at 298 K, the bipyridine resonances are indicated. In the spectrum at 248 K, assignments of the terpyridine protons are given. At 248 K, the D₂O signal has shifted beyond the shown region.

At low temperatures, 9egua is not expected to rotate, which would result in sharp resonances for all protons. At high temperatures 9egua is expected to rotate fast at the NMR time scale. Then, all protons sense an average of the rotating 9egua, which would result in sharp resonances as well. Upon decreasing the temperature in ^1H NMR measurements of **7**, all resonances sharpen rather fast, *i.e.* at 278 K the individual terpyridine signals are already recognized. Thus, the 9egua base may be in a fixed position at relatively high temperatures. The terpyridine signals have a maximum intensity at 248 K. At this temperature, a total of eighteen sharp signals of double intensity are observed in the aromatic region (Figure 3.5). Using 2D COSY and NOESY experiments all signals have been assigned at 248 K. The particular J couplings for the 6 and 3 protons (*vide supra*) have been taken into account. The $\text{H}6'$ resonance is shifted relatively upfield in comparison to the $\text{H}6$ signal, because the $\text{H}6'$ protons are shielded by the terpyridine ligand. One set of eight signals with relative intensities of 2 has been assigned to the bipyridine ligand, and one set of ten signals with similar intensities has been attributed to the terpyridine protons. Thus, a signal is observed for every single terpyridine proton, indicating that no C_2 symmetry is present within the metal moieties. The model base 9egua is apparently not positioned in a plane of symmetry. The orientation of 9egua has been determined from $\text{H}8$ – $\text{I}5'$ and $\text{H}8$ – $\text{I}3''$ NOE crosspeaks (Figure 3.6). In Figure 3.6 clear NOEs are observed from the $\text{H}8$ signal to the $\text{H}6$, $\text{I}5'$ and $\text{I}6''$ resonances. The $\text{H}8$ – $\text{I}3''$ NOE is relatively weak. The $\text{H}8$ – $\text{I}5'$ and $\text{H}8$ – $\text{I}3''$ NOEs indicate that the orientation of 9egua is such that the keto group is located at a position between the bipyridine ligand and the $\text{I}6$ proton of the terpyridine ligand, as is indicated in the schematic representation of **7** given in Figure 3.5.

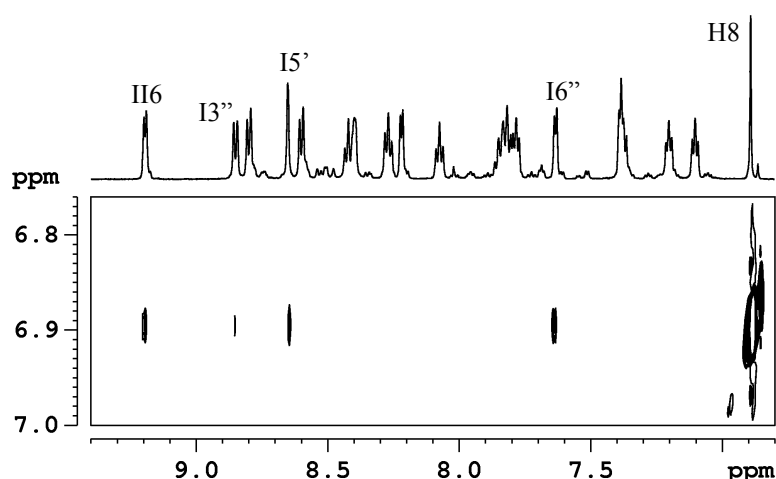


Figure 3.6 Part of the 2D ^1H NOESY spectrum of **7** in $\text{MeOH-}d_4$ at 248 K showing the $\text{H}8$ – $\text{I}3''$ and $\text{H}8$ – $\text{I}5'$ crosspeaks, as well as the $\text{H}8$ – $\text{H}6$ and $\text{H}8$ – $\text{I}6''$ NOEs.

The keto group is likely to be the least sterically hindered in this particular position, which agrees with the crystal structure^[21] of the known 9egua monoadduct $[\text{Ru}(\text{bpy})_2(9\text{egua})\text{Cl}]^+$. The relatively intense $\text{I6}''\text{-II6}$ NOE and the absence of a $\text{I6}\text{-II6}$ NOE confirm the orientation (Figure 3.7). The difference in intensity between the $\text{H8}\text{-I5}'$ and $\text{H8}\text{-I3}''$ NOEs may be explained by the fact that the H8 proton is located more close to the $\text{I5}'$ proton. The $\text{H8}\text{-I6}''$ and $\text{H8}\text{-II6}$ NOEs may result from flipping of the 9egua from one position to another, whereby the H8 proton passes rather closely along the II6 and $\text{I6}''$ protons. Only one species is observed in the ^1H NMR spectra, and therefore it is thought that the two rotamers are enantiomers. In the second rotamer the keto group of 9egua is wedged in between the bipyridine ligand and the $\text{I6}''$ proton of the terpyridine ligand. The observed $\text{I3}\text{-I3}''$, $\text{I4}\text{-I4}''$, $\text{I5}\text{-I5}''$, $\text{I6}\text{-I6}''$, and $\text{I3}'\text{-I5}'$ exchange peaks confirm this assumption (Figure 3.7). The terpyridine signals are interchanged by the flipping of 9egua (Figure 3.8).

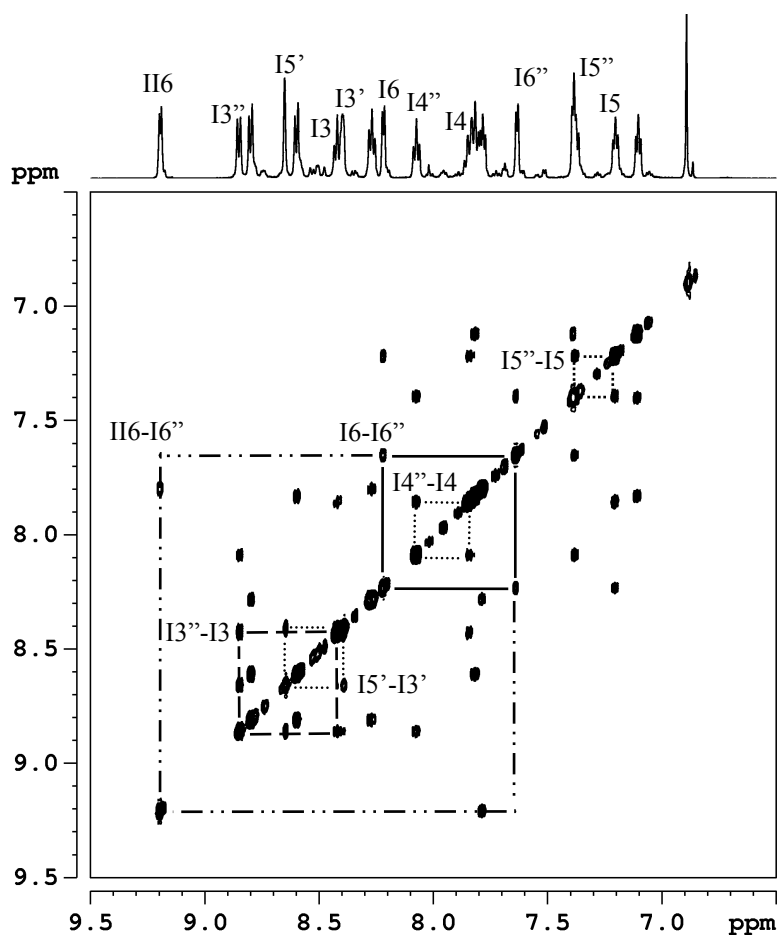


Figure 3.7 Part of the 2D ^1H NOESY spectrum of **7** in $\text{MeOH-}d_4$ at 248 K with the $\text{II6}\text{-I6}''$ NOE and the $\text{I3}\text{-I3}''$, $\text{I4}\text{-I4}''$, $\text{I5}\text{-I5}''$, $\text{I6}\text{-I6}''$, and $\text{I3}'\text{-I5}'$ exchange peaks indicated. H8 NOEs are not evident here, due to their low intensities.

Two similar rotamers have also been found for the bis(methylbenzimidazole) adduct of **1**, albeit at 183 K.^[18] Clearly, 9egua is more sterically demanding than methylbenzimidazole, and stops rotating at relatively high temperatures. A space-filling model of the cation $[\text{Ru}(\text{bpy})_2(9\text{egua})\text{Cl}]^+$, which is structurally rather similar to a single metal moiety of **7**, has indicated a potential energy barrier for rotation around the ruthenium N7 bond.^[21] The keto group of 9egua appears to be sterically hampered for rotation by the bipyridine ligand, to which the base is coordinated in a *trans* position. From studies with the mononuclear complex $[\text{Ru}(\text{tpy})(\text{bpy})(9\text{egua})]^{2+}$ it is also known that steric interactions of the bipyridine ligand hinder rotation of 9egua.^[22] Therefore, flipping most likely occurs in such a way that the keto group passes under the terpyridine ligand (Figure 3.8). The fact that H8–I6'' and H8–II6 NOEs are observed confirm such passage.

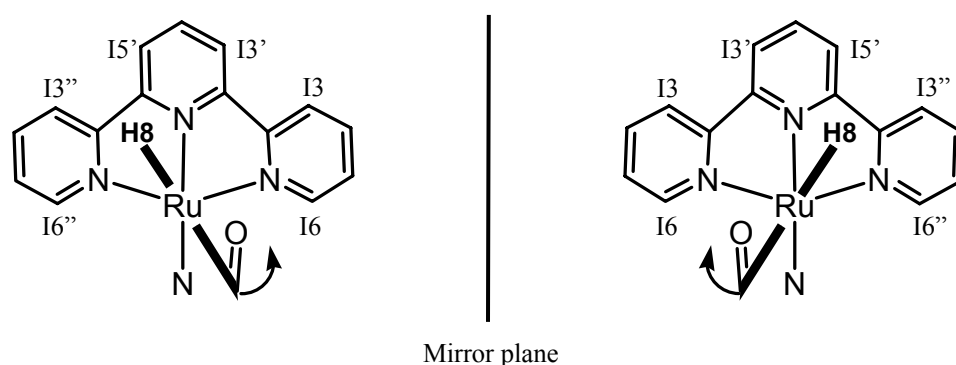


Figure 3.8 Schematic representation of the metal moieties of the two enantiomeric rotamers of **7**. The structures are viewed from above along the bpy-ruthenium-9egua axis. Thus, the bpy ligand is pointing towards the reader, with its plane parallel to the mirror plane. The tpy ligand is positioned in the plane of the paper. The 9egua base coordinates to ruthenium from below, and is located under the tpy plane. The base is represented by the bar with its H8 and keto group indicated. The tpy signals are interchanged by the flipping of 9egua, because the two rotamers are mirror images.

Since the bpy protons are in the plane of symmetry, they experience either an average of the presence of the rotating 9egua or see the presence of 9egua in a single position, which is actually degenerate. Both possibilities yield sharp resonances for all bpy protons. 2D NOESY experiments have not been performed at temperatures below 248 K. Therefore, it cannot be inferred whether 9egua is still flipping at these temperatures or is fixed in one of the positions. Upon slightly increasing the temperature to 308 K, the terpyridine signals broaden beyond recognition (Figure 3.9). Sharp terpyridine signals are not observed within the measured temperature range, which has been limited to a maximum of 328 K due to the low boiling point of MeOD. Fast rotation of 9egua is clearly not occurring at this temperature.

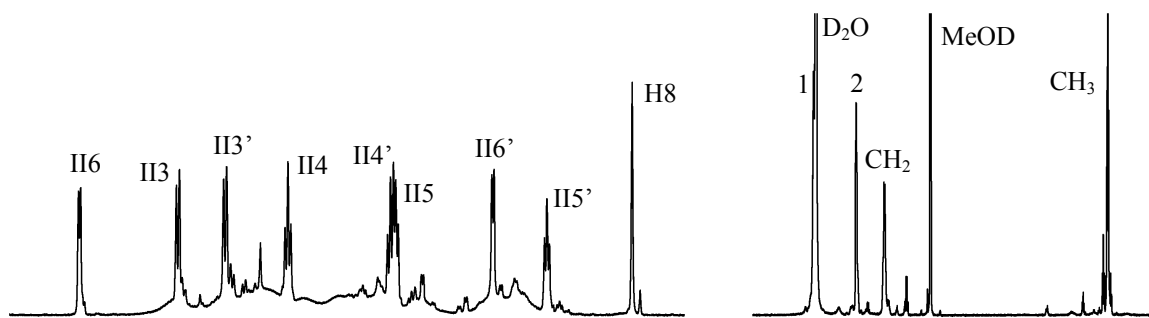


Figure 3.9 Parts of the ^1H NMR spectrum of **7** in $\text{MeOH-}d_4$ at 308 K with some assignments. The tpy signals are broadened beyond recognition.

3.3.4 Characterization of the monoadduct **6**

The monoadduct $[\text{Cl}(\text{bpy})\text{Ru}(\text{dtdeg})\text{Ru}(\text{bpy})(\text{9egua})]\text{Cl}_3$ (**6**) has also been identified and characterized by 1D and 2D COSY and NOESY ^1H NMR in $\text{MeOH-}d_4$ at 248 K. The ^1H NMR spectra at RT (top) and 248 K (bottom) are shown in Figure 3.10. A similar temperature dependence of the motion of **9egua** as in **7** has been observed for **6**. Therefore, the characterization will not be discussed in detail.

Characteristic features are the four different signals for the linker protons (data not shown), as well as two resonances for the two different bipyridine II6 and II'6 protons in the downfield region. Both indicate the presence of two inequivalent metal moieties. The II'6 resonance is shifted downfield in comparison to the II6 signal, due to the nearby deshielding chloride ion. An interesting feature to note is the fact that only the terpyridine resonances of the moiety to which **9egua** is coordinated are broadened at RT. The chloride moiety displays sharp signals for all protons at this temperature. At 248 K sharp signals of intensity one are observed in the aromatic region for all protons, including those of the chloride moiety. Thus, C_2 symmetry is not present within both metal moieties. The terpyridine protons of the chloride unit also display exchange signals in a 2D NOESY experiment, like the terpyridine signals of the **9egua** moiety.

The exchange rate can be calculated for both metal units from the line widths of the resonances, which are in exchange, at the different temperatures. A similar exchange rate for both metal units may indicate that the chloride moiety is affected by the rotational behavior of the **9egua** ligand, which is coordinated to the other ruthenium moiety. The flexible linker can allow close approach of the two different metal units, thereby facilitating the interaction. The exchange rates have, however, not been calculated.

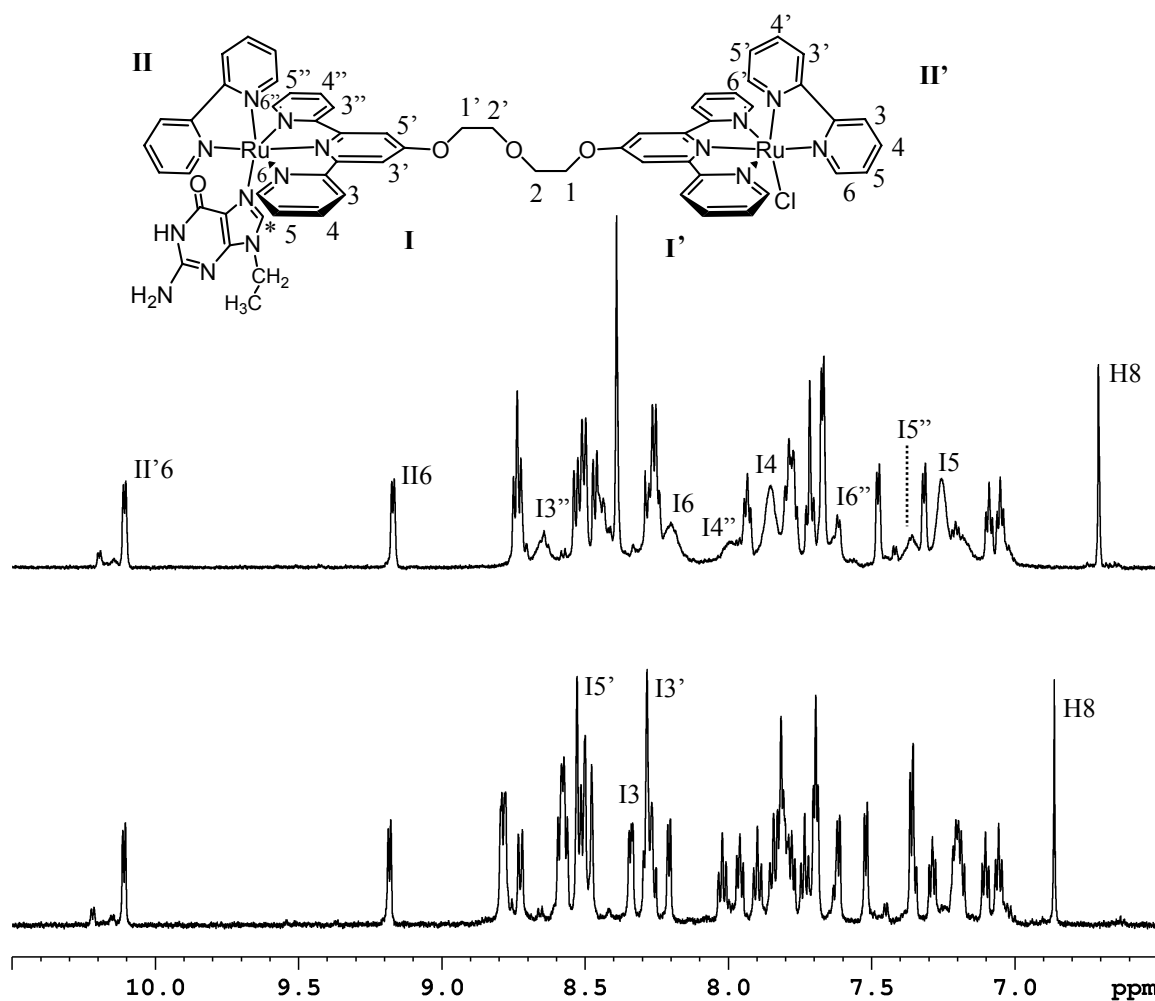


Figure 3.10 Schematic representation of **6** with its numbering scheme, and the aromatic region of the ^1H NMR spectra of **6** at RT (upper) and 248 K (lower) with some assignments. Only the tpy resonances of the metal moiety to which 9egua is coordinated are broadened.

3.3.4 Biological properties of the dinuclear complexes

Cytotoxicity has been evaluated on human KB carcinoma cells and HBL-100 epithelial non-tumor cells for 24 and 72 hours. Cytotoxicity has also been evaluated on cisplatin-sensitive and cisplatin-resistant mouse leukemia L1210 cells and human ovarian carcinoma A2780 cells for 72 hours. Complexes **1** and $[(\text{tpy})\text{Ru}(\text{dtdeg})\text{RuCl}_3]\text{Cl}_2$ (**8**) reach approximately 40 % of cell growth inhibition of KB cells at the highest concentration used (100 μM) after 24 hours. Complexes **2** and **3** are slightly less potent as only 30 % of inhibition is reached at 100 μM . Prolonging cell exposure from 24 to 72 hours results in a slight increase (up to 50-60 % of inhibition) of the anti-proliferative activity of the tested complexes. Against the

HBL-100 cell line, about 50 % of growth inhibition is displayed by complexes **1**, **2**, and **8** after 24 hours at 100 μ M. After 72 hours, anti-proliferative activity up to 60 % is shown. Complex **3** is devoid of any activity against HBL-100 cells.

Complex **1** shows an inhibition of cell growth of 50 % at a concentration of 33 μ M against L1210/0 and L1210/R cells, but anti-proliferative activity does not increase with higher concentrations. Complexes **2** and **3** are less active, 50 % of inhibition is reached at concentrations of 100 μ M. The complexes are less active against A2780 cells. Complex **8** is not active against the A2780 and the L1210 cell lines.

Thus, in general none of the complexes displays significant cytotoxicity. The IC₅₀ values given in Table 3.1 are only an indication of cytotoxicity, since only one concentration shows an effect slightly higher than 50 % of cell growth inhibition. IC₅₀ values are only shown for cell exposure of 72 hours. Only **8** inhibits cell growth of KB and HBL-100 cells for more than 50 % already after 24 hours at a concentration of 100 μ M (IC₅₀ ~ 74 μ M).

Table 3.1 Indication of IC₅₀ values for the series of dinuclear ruthenium complexes calculated after 72 hours of treatment.

complex	IC ₅₀					
	KB	HBL-100	L1210cis	L1210R	A2780cis	A2780R
1	68	34	33	33	> 100	> 100
2	57	87	~ 100	~ 100	> 100	> 100
3	93	> 100	~ 100	~ 100	>100	> 100
8	> 100	74	> 100	> 100	> 100	> 100

Ruthenium cell uptake has been studied using KB and HBL-100 cells, which were treated with 100 μ M of the dinuclear complexes in DPBS for 1 hour at 310 K. Complexes **1** and **8** are taken up by KB and HBL-100 cells to the same extent, reaching intracellular concentrations much higher than the concentrations used to treat the cells (3 mM and 7 mM, respectively). Compared to **1** and **8**, complexes **2** and **3** are not significantly taken up by both type of cells. Intracellular concentrations approximately similar to the treated concentrations are attained. For comparison, under the same experimental conditions NAMI-A is taken up by cells reaching concentrations 4 to 5 times that used to treat the cells. The results indicate that uptake of the complexes is not per se hindered by the dinuclear nature of the complexes. However, uptake of the different complexes is unrelated to the anti-proliferative effects.

Pro-adhesive effects have been studied as well. The pro-adhesive effect is the percentage of increase in adhesion strength of treated cells *versus* control cells. The adhesion assay has been developed to study the anti-metastatic activity^[23] of the mononuclear ruthenium complex

NAMI-A. Increased adhesion may indicate a decrease in the cell's capability to dissociate from the solid tumor to invade other tissues. The pro-adhesive effect was studied using KB and HBL-100 cells, since particularly complex **2** showed a change of the cells shape in the tests with human ovarian A2780 cisplatin-sensitive cells. The A2780cis cells were spread on the wells bottom after treatment with **2**, indicating increased adherence to the well.

In general, all complexes show dose-dependent pro-adhesive effects, which are strongest on KB cells. However, effects are not dose dependent for **1** on both cell lines and not for **3** on HBL-100 cells. Increase in adhesion is strongest for **2** on KB cells, *i.e.* at 100 μM an increase of about 300 % is observed, which is comparable to that observed for NAMI-A. A significant increase is also displayed by **8**. At 10 μM an increase of 200 % is displayed, but adhesion does not increase much further at higher dose.

Morphological analysis of the KB and HBL-100 cell line did not show a significant modification of the cell shape upon incubation with the complexes.

3.4 Concluding remarks

The dinuclear ruthenium(II) complexes $[\text{Cl}(\text{bpy})\text{Ru}(\text{dtdeg})\text{Ru}(\text{bpy})\text{Cl}]\text{Cl}_2$ (**1**), $[(\text{tpy})\text{Ru}(\text{dtdeg})\text{Ru}(\text{bpy})\text{Cl}]\text{Cl}_3$ (**2**), and $[(\text{tpy})\text{Ru}(\text{dtdeg})\text{Ru}(\text{tpy})]\text{Cl}_4$ (**3**) are described. The hydrolysis of **1** has been studied, as well as its binding to the DNA-model base 9-ethylguanine. At 310 K and 1 mM hydrolysis of **1** proceeds fast, but not completely. After about 2.5 hours, equilibrium is accomplished, in which the monoaqua and diaqua species are present in a ratio of $\sim 3:7$. The partial hydrolysis of **1** is likely to have an effect on the reactivity towards 9egua. Although 9egua easily dissociates from ruthenium at RT in the absence of excess 9egua, both the monoadduct $[\text{Cl}(\text{bpy})\text{Ru}(\text{dtdeg})\text{Ru}(\text{bpy})(9\text{egua})]\text{Cl}_3$ (**6**) and the bisadduct $[(9\text{egua})(\text{bpy})\text{Ru}(\text{dtdeg})\text{Ru}(\text{bpy})(9\text{egua})]\text{Cl}_4$ (**7**) have been isolated and characterized by variable temperature ^1H NMR experiments. The base is hindered for free rotation at RT. At 248 K, flipping of 9egua between two enantiomeric rotamers is seen. Unfortunately, the dinuclear complexes **1**, **2**, **3**, and $[(\text{tpy})\text{Ru}(\text{dtdeg})\text{RuCl}_3]\text{Cl}_2$ (**8**) do not display cytotoxicity against a variety of cancer cells. High cellular uptake of **1** and **8** has been found, but is not related to cytotoxicity. Complexes **2** and **8** significantly increase adhesion of KB tumor cells, but morphological changes of the cell's shape are small.

Concluding, the dinuclear ruthenium complexes represent the first of a new class of polynuclear ruthenium polypyridyl compounds as potential anticancer agents. Variation of the metal, terminal ligands or the linker can provide a wealth of polypyridyl polynuclear complexes, which may display significant cytotoxicity.

3.5 References

- [1] (a) Wheate, N. J.; Collins, J. G., *Coord. Chem. Rev.* **2003**, *241*, 133-145. (b) Reedijk, J., *Proc. Natl. Acad. Sci. U. S. A.* **2003**, *100*, 3611-3616.
- [2] Farrell, N.; Qu, Y.; Bierbach, U.; Valsecchi, M.; Menta, E., in *Cisplatin. Chemistry and Biochemistry of a Leading Anticancer Drug* (Ed.: Lippert, B.), Verlag Helvetica Chimica Acta, Zurich, Wiley-VCH, Weinheim, **1999**, 479-496.
- [3] Reedijk, J., *Chem. Rev.* **1999**, *99*, 2499-2510.
- [4] Farrell, N.; Qu, Y.; Feng, L.; Van Houten, B., *Biochemistry* **1990**, *29*, 9522-9531.
- [5] Cox, J. W.; Berners-Price, S.; Davies, M. S.; Qu, Y.; Farrell, N., *J. Am. Chem. Soc.* **2001**, *123*, 1316-1326.
- [6] Hegmans, A.; Berners-Price, S. J.; Davies, M. S.; Thomas, D. S.; Humphreys, A. S.; Farrell, N., *J. Am. Chem. Soc.* **2004**, *126*, 2166-2180.
- [7] Clarke, M. J., *Coord. Chem. Rev.* **2003**, *236*, 209-233.
- [8] (a) Alessio, E.; Mestroni, G.; Bergamo, A.; Sava, G., *Metal Ions in Biological Systems* **2004**, *42*, 323-351. (b) Galanski, M.; Arion, V. B.; Jakupec, M. A.; Keppler, B. K., *Curr. Pharm. Design* **2003**, *9*, 2078-2089.
- [9] (a) Iengo, E.; Mestroni, G.; Geremia, S.; Calligaris, M.; Alessio, E., *J. Chem. Soc.-Dalton Trans.* **1999**, 3361-3371. (b) Serli, B.; Iengo, E.; Gianferrara, T.; Zangrando, E.; Alessio, E., *Metal-Based Drugs* **2001**, *8*, 9-18.
- [10] Zorzet, S.; Bergamo, A.; Cocchietto, M.; Sorc, A.; Gava, B.; Alessio, E.; Iengo, E.; Sava, G., *J. Pharmacol. Exp. Ther.* **2000**, *295*, 927-933.
- [11] Sava, G.; Alessio, E.; Bergamo, A.; Mestroni, G., in *Top. Biol. Inorg. Chem.* (Eds.: Clarke, M. J.; Sadler, P. J.), Springer, Berlin, **1999**, *1*, 143-169.
- [12] (a) Önfelt, B.; Lincoln, P.; Nordén, B., *J. Am. Chem. Soc.* **1999**, *121*, 10846-10847. (b) Wilhelmsson, L. M.; Westerlund, F.; Lincoln, P.; Nordén, B., *J. Am. Chem. Soc.* **2002**, *124*, 12092-12093. (c) Brodkorb, A.; Kirsch-De Mesmaeker, A.; Rutherford, T. J.; Keene, F. R., *Eur. J. Inorg. Chem.* **2001**, 2151-2160.
- [13] Nováková, O.; Kašpárková, J.; Vrána, O.; Van Vliet, P. M.; Reedijk, J.; Brabec, V., *Biochemistry* **1995**, *34*, 12369-12378.
- [14] (a) Barton, J. K., *Science* **1986**, *233*, 727-734. (b) Erkkila, K. E.; Odom, D. T.; Barton, J. K., *Chem. Rev.* **1999**, *99*, 2777-2795. (c) Pyle, A. M.; Rehmann, J. P.; Meshoyrer, R.; Kumar, C. V.; Turro, N. J.; Barton, J. K., *J. Am. Chem. Soc.* **1989**, *111*, 3051-3058.
- [15] Kelly, J. M.; Tossi, A. B.; McConnell, D. J.; Ohuigin, C., *Nucleic Acids Res.* **1985**, *13*, 6017-6034.
- [16] Reedijk, J., *Chem. Commun.* **1996**, 801-806.
- [17] Sullivan, B. P.; Calvert, J. M.; Meyer, T. J., *Inorg. Chem.* **1980**, *19*, 1404-1407.
- [18] Velders, A. H., Ph.D. thesis, Leiden University (Leiden), **2000**.
- [19] (a) Tada, H.; Shiho, O.; Kuroshima, K.; Koyama, M.; Tsukamoto, K., *J. Immunol. Methods* **1986**, *93*, 157-165. (b) Mosmann, T., *J. Immunol. Methods* **1983**, *65*, 55-63. (c) Alley, M. C.; Scudiero, D. A.; Monks, A.; Hursey, M. L.; Czerwinski, M. J.; Fine, D. L.; Abbott, B. J.; Mayo, J. G.; Shoemaker, R. H.; Boyd, M. R., *Cancer Res.* **1988**, *48*, 589-601.
- [20] Guo, Z. J.; Sadler, P. J., *Angew. Chem.-Int. Edit.* **1999**, *38*, 1513-1531.
- [21] Van Vliet, P. M.; Haasnoot, J. G.; Reedijk, J., *Inorg. Chem.* **1994**, *33*, 1934-1939.
- [22] Van Vliet, P. M., Ph.D. thesis, Leiden University (Leiden), **1996**.
- [23] Sava, G.; Zorzet, S.; Turrin, C.; Vita, F.; Soranzo, M.; Zabucchi, G.; Cocchietto, M.; Bergamo, A.; DiGiovine, S.; Pezzoni, G.; Sartor, L.; Garbisa, S., *Clin. Cancer Res.* **2003**, *9*, 1898-1905.

Chapter 4

Heterodinuclear ruthenium-platinum complexes with long and flexible linkers: crystal structure and cytotoxicity

Abstract – The complexes $[\text{Cl}_3\text{Ru}(\text{dtdeg})]$ (**1**) and $[\text{Cl}(\text{bpy})\text{Ru}(\text{dtdeg})]\text{Cl}$ (**2**) have been produced for the synthesis of the heterodinuclear ruthenium-platinum complexes $[\text{Cl}_3\text{Ru}(\text{dtdeg})\text{PtCl}]\text{Cl}$ (**3**), and $[\text{Cl}(\text{bpy})\text{Ru}(\text{dtdeg})\text{PtCl}]\text{Cl}_2$ (**4**) (bpy = 2,2'-bipyridine, dtdeg = bis[4'-(2,2':6',2''-terpyridyl)]-diethyleneglycolether). The complex $[(\text{tpy})\text{Ru}(\text{dtdeg})\text{PtCl}]\text{Cl}_3$ (**5**) has been synthesized from $[(\text{tpy})\text{Ru}(\text{dtdeg})]\text{Cl}_2$, which has been presented in Chapter 2 (tpy = 2,2':6',2''-terpyridine). The paramagnetic complexes **1** and **3** have been characterized by ^1H NMR spectroscopy, including 1D NOE difference experiments. The crystal structure of the cation of **5** has been elucidated, and shows self-stacking interactions of the platinum units. The distance between the ruthenium and platinum metals in the crystal structure is approximately 14.5 Å. Complex **5** has been reacted with the DNA-model base 9-ethylguanine (9egua). The adduct $[(\text{tpy})\text{Ru}(\text{dtdeg})\text{Pt}(9\text{egua})](\text{PF}_6)_4$ (**6**) has been isolated and characterized by ^1H NMR experiments. The results suggest that the platinum moiety is able to both intercalate and coordinate to the DNA, without being hindered by the dangling ruthenium moiety. The length and flexibility of the linker may allow the formation of long-range DNA adducts. The complexes have been tested for their cytotoxicity.

4.1 Introduction

Polynuclear platinum complexes constitute a class of compounds, which has been developed to circumvent resistance to the antitumor drug cisplatin.^[1, 2] It is believed these complexes can achieve a unique spectrum of anticancer activity, because they form radically different adducts to DNA, the known ultimate target of anticancer platinum complexes.^[3] Whereas cisplatin forms mainly 1,2-intrastrand adducts,^[4] the high cytotoxicity displayed by polynuclear α,ω -diaminoalkane-linked platinum complexes is thought to be due to the formation of long-range DNA-adducts.^[2] Mononuclear and polynuclear ruthenium complexes are also studied for their anticancer activities.^[5] One example is the series of dinuclear complexes based upon the mononuclear antimetastatic compound NAMI-A.^[6] The extension of the polynuclear concept to heteropolynuclear ruthenium-platinum complexes represents an interesting challenge. Mononuclear ruthenium and platinum anticancer complexes are known to display different mechanisms of action, which are intrinsic to their geometry, reactivity and biological pharmacology.^[4, 5, 7] Selective reactivity at each metal center may be achieved by the use of ruthenium and platinum for the different metal moieties of polynuclear anticancer complexes.

Only a few examples of heteropolynuclear ruthenium-platinum anticancer complexes have been reported so far. One example of a dinuclear ruthenium-platinum complex with a long and flexible linker has been reported, *i.e.* [*cis*-RuCl₂(dms_o)₃]₂H₂N(CH₂)₄NH₂[*cis*-PtCl₂(NH₃)₂].^[8] This complex has, however, been found to be too reactive to be used as a DNA-binding agent. A small class of dinuclear ruthenium-platinum complexes comprises polyazine bridged compounds. For these heterodinuclear complexes it is thought that light absorption of the ruthenium unit, and subsequent energy transfer, activates the platinum moiety for reaction with DNA.^[9] Biological data have not yet been reported.

In this Chapter, the synthesis of the complexes [Cl₃Ru(dtdeg)] (**1**) and [Cl(bpy)Ru(dtdeg)]Cl (**2**) is described (bpy = 2,2'-bipyridine, dtdeg = bis[4'-(2,2':6',2''-terpyridyl)]-diethyleneglycolether). They have been produced for the assembly of the heterodinuclear ruthenium-platinum complexes [Cl₃Ru(dtdeg)PtCl]Cl (**3**), and [Cl(bpy)Ru(dtdeg)PtCl]Cl₂ (**4**). The ruthenium-platinum complex [(tpy)Ru(dtdeg)PtCl]Cl₃ (**5**) is presented as well (tpy = 2,2':6',2''-terpyridine). The complexes have been synthesized using the long and flexible dtdeg linker to allow the formation of long-range DNA adducts. The design and subsequent development of the complexes have been inspired by the cytotoxic mononuclear complex [Pt(tpy)Cl]Cl·2H₂O, which can intercalate^[10] and coordinate^[11] to DNA. The ruthenium unit of the complexes has been varied in the number of relatively labile chloride ligands. The ruthenium moieties resemble the mononuclear complexes [Ru(tpy)Cl₃],

$[\text{Ru}(\text{tpy})(\text{bpy})\text{Cl}]^+$ and $[\text{Ru}(\text{tpy})_2]^{2+}$. The complex $[\text{Ru}(\text{tpy})\text{Cl}_3]$ has been reported to display antitumor activity, which is believed to be due to the coordination to two guanines of opposite DNA strands.^[12, 13] The complex $[\text{Ru}(\text{tpy})(\text{bpy})\text{Cl}]\text{Cl}$ has been shown to bind monofunctionally to DNA.^[12] Substitution-inert ruthenium polypyridyl complexes are known to be able to bind to DNA by electrostatic or surface binding, or partial intercalation.^[14] The complexes, including the paramagnetic compounds **1** and **3**, have been characterized by different ^1H NMR experiments. A crystal structure of complex **5** is presented. This complex has also been studied for its interaction with the DNA-model base 9-ethylguanine (9egua). The characterization of the adduct $[(\text{tpy})\text{Ru}(\text{dtdeg})\text{Pt}(9\text{egua})](\text{PF}_6)_4$ (**6**) by ^1H NMR is described. The complexes have been tested for their cytotoxicity against cisplatin-sensitive and cisplatin-resistant human ovarian carcinoma and mouse leukemia cell lines.

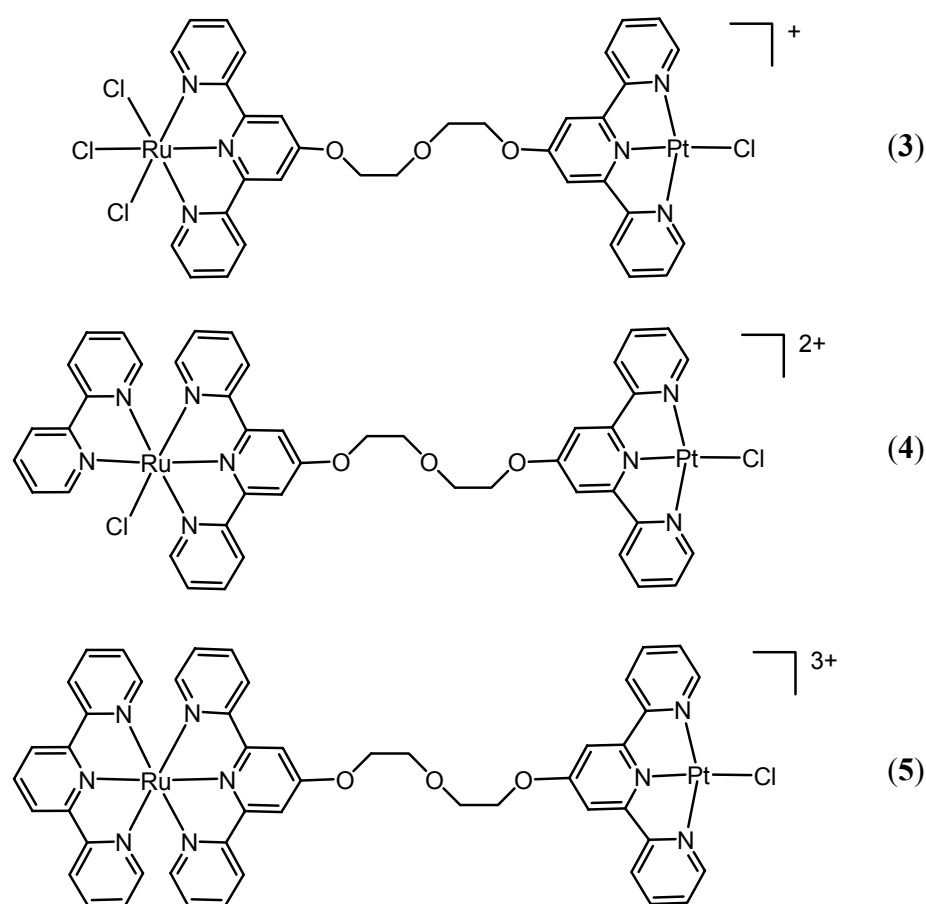


Figure 4.1 The cationic ruthenium-platinum complexes **3**, **4**, and **5**.

4.2 Experimental section

4.2.1 General methods and starting materials

Elemental analyses on C, H and N were performed on a Perkin Elmer series II CHNS/O Analyzer 2400. Electrospray mass spectra were recorded on a Finnigan TSQ-quantum instrument with an electrospray interface (ESI). Hydrated $\text{RuCl}_3 \cdot x\text{H}_2\text{O}$ ($x \sim 3$) and K_2PtCl_4 were used as received from Johnson & Matthey. The ligands bipyridine and terpyridine were obtained from Sigma. The complexes $[\text{Ru}(\text{tpy})\text{Cl}_3]$ and $[\text{Pt}(\text{cod})\text{Cl}_2]$ were produced according to literature procedures.^[15] The 0.1 M ruthenium(III) solution and the ligand dtdeg have previously been synthesized,^[16] the procedures are described in Chapter 2 for convenience. The complex $[\text{Cl}_3\text{Ru}(\text{dtdeg})]$ (**1**) has earlier been synthesized as well, but was not obtained pure.^[16] Therefore, its synthesis is described here. The synthesis of $[(\text{tpy})\text{Ru}(\text{dtdeg})]\text{Cl}_2$ is described in Chapter 2. The ruthenium-platinum complexes **3**, **4**, and **5** have been prepared by modification of a procedure known^[17] for the synthesis of $[\text{Pt}(\text{tpy})\text{Cl}]\text{Cl} \cdot 2\text{H}_2\text{O}$.

4.2.2 ^1H NMR measurements

NMR spectra were acquired on a Bruker DPX 300, a DMX 600, and an AV 400 MHz spectrometer. Spectra were recorded in deuterated DMSO, acetone and MeOH, and were calibrated on residual solvent peaks at δ 2.49, 2.06 and 3.30 ppm, respectively. The 1D ^1H NMR spectra of the paramagnetic complexes **1** and **3** were obtained using a 100 ppm spectral width. Longitudinal relaxation times were measured by the standard inversion-recovery method, with 7 s relaxation delay and a spectral width of 100 ppm. Variable delays ranged from 50 μs to 500 ms to define the T_1 values for the proton signals of the paramagnetic ruthenium(III) moiety, and from 100 ms to 5000 ms to define the T_1 values for the proton signals of the diamagnetic ruthenium(II) moiety. Magnetization recovery was exponential within experimental error. T_2 values were estimated from the peak half-widths. The COSY spectra were obtained by collecting $1024 F_2 \times 1024 F_1$ data points with a relaxation delay of 20 ms. 1D NOE difference experiments were carried out according to published procedures.^[18] These procedures include a WEFT pulse sequence, which was not applied here. The irradiation time used for the 1D NOE experiment was 500 ms, and the number of scans 16384.

4.2.3 Syntheses

[Cl₃Ru(dtdeg)], (1): 0.1 M ruthenium solution (1.77 mL; 0.18 mmol) was added to a hot solution of the ligand dtdeg (200 mg; 0.35 mmol) in 200 mL of EtOH 98 %. After 2 hours of reflux, the hot reaction mixture was filtered to remove unwanted [Cl₃Ru(dtdeg)RuCl₃]. The filtrate was cooled to RT for 24 hours. The formed precipitate was collected by filtration and was washed three times with ~ 10 mL of chloroform to remove excess dtdeg. The residue was subsequently washed with EtOH 98 %, acetone and diethyl ether. Yield 62 mg (45 %). Elemental analysis (%) calculated for C₃₄H₂₈Cl₃N₆O₃Ru·1CHCl₃: C 46.95, N 9.39, H 3.26. Found: C 46.42, N 9.70, H 3.20. ¹H NMR (300 MHz, DMSO, 340 K): δ = -7.38 (2H; I33''), 1.35 (2H; I44''), -8.28 (2H; I55''), -27.24 (2H; I66''), 5.07 (2H; I3'5'), 14.28 (t, 2H; 1), 3.74 (2H; 2), 8.85 (2H; I'33''), 7.62 (2H; I'44''), 8.13 (2H; I'55''), 8.91 (2H; I'66''), 8.18 (2H; I'3'5'), 4.65 (2H; 1'), 4.13 ppm (2H; 2').

[Cl(bpy)Ru(dtdeg)]Cl (2): [Cl₃Ru(dtdeg)] (95 mg; 0.12 mmol), 2,2'-bipyridine (19 mg; 0.12 mmol), triethylamine (22 mg; 0.22 mmol) and LiCl (11 mg; 0.26 mmol) were dissolved in 19 mL of EtOH 98 % and refluxed for 5 hours. After filtration at RT, the mixture was evaporated *in vacuo* and purified by column chromatography on neutral alumina using a mixture of EtOH 98 % and acetone (v:v = 1:1). The first fraction eluting, yielded pure product after precipitation with diethyl ether and filtration. Yield: 47 mg (43 %). Elemental analysis (%) calculated for C₄₄H₃₆Cl₂N₈O₃Ru·3H₂O: C 55.58, N 11.78, H 4.45. Found: C 55.22, N 11.78, H 3.91. ¹H NMR (300 MHz, DMSO, 298 K): δ = 8.68 (d, 2H; I33''), 7.93 (t, 2H; I44''), 7.32 (t, 2H; I55''), 7.58 (d, 2H; I66''), 8.59 (s, 2H; I3'5'), 4.65 (t, 2H; 1), 4.03 (t, 2H; 2), 8.68 (d, 2H; I'33''), 7.47 (t, 2H; I'44''), 7.98 (t, 2H; I'55''), 8.62 (d, 2H; I'66''), 8.03 (s, 2H; I'3'5'), 4.49 (t, 2H; 1'), 4.03 (t, 2H; 2'), 8.86 (d, 1H; II3), 8.29 (t, 1H; II4), 8.00 (t, 1H; II5), 10.07 (d, 1H; II6), 8.59 (d, 1H; II3'), 7.72 (t, 1H; II4'), 7.05 (t, 1H; II5'), 7.39 ppm (d, 1H; II6').

[Cl₃Ru(dtdeg)PtCl]Cl, (3): [Pt(cod)Cl₂] (88 mg; 0.23 mmol) was added to a hot solution of [Cl₃Ru(dtdeg)] (134 mg; 0.17 mmol) in 320 mL of a mixture of EtOH 98 % and MeOH (v:v = 1:1). After 6 hours of reflux, the mixture was cooled to RT. The formed precipitate was filtered and washed with acetone to remove unreacted [Pt(cod)Cl₂]. The residue was subsequently washed with diethyl ether. Yield: 106 mg (61 %). Elemental analysis (%) calculated for C₃₄H₂₈Cl₅N₆O₃RuPt·3H₂O: C 37.26, N 7.67, H 3.13. Found: C 36.70, N 8.13, H 2.79. ¹H NMR (300 MHz, DMSO, 310 K): δ = -9.13 (2H; I33''), 0.75 (2H; I44''), -10.58 (2H; I55''), -31.79 (2H; I66''), 4.63 (2H; I3'5'), 15.06 (t, 2H; 1), 3.89 (2H; 2), 8.83 (2H; I'33''), 8.19 (2H; I'44''), 8.91 (2H; I'55''), 9.08 (2H; I'66''), 8.91 (2H; I'3'5'), 5.03 (2H; 1'), 4.30 ppm (2H; 2'). ¹⁹⁵Pt NMR (300 MHz, MeOH, 298 K): δ = -2705 ppm.

[Cl(bpy)Ru(dtdeg)PtCl]Cl₂ (4): [Cl(bpy)Ru(dtdeg)]Cl (22 mg, 0.025 mmol) and [Pt(cod)Cl₂] (11 mg, 0.030 mmol) were refluxed for 6 hours in 18 mL of MeOH. The reaction mixture was cooled to RT and filtered. The filtrate was slowly precipitated with diethyl ether. Yield: 16 mg (55 %). Elemental analysis (%) calculated for C₄₄H₃₆Cl₄N₈O₃RuPt·3H₂O: C 43.43, N 9.21, H 3.48. Found: C 42.90, N 9.22, H 3.21. ¹H NMR (300 MHz, DMSO, 298 K): δ = 8.70 (d, 2H; I33''), 7.92 (t, 2H; I44''), 7.30 (t, 2H; I55''), 7.55 (d, 2H; I66''), 8.59 (s, 2H; I3'5'), 4.68 (t, 2H; 1), 4.07 (t, 2H; 2), 8.70 (d, 2H; I'33''), 8.46 (t, 2H; I'44''), 7.91 (t, 2H I'55''), 8.89 (d, 2H; I'66''), 8.43 (s, 2H; I'3'5'), 4.63 (t, 2H; 1'), 4.06 (t, 2H; 2'), 8.87 (d, 1H; II3), 8.30 (t, 1H; II4), 8.01 (t, 1H; II5), 10.06 (d, 1H; II6), 8.60 (d, 1H; II3'), 7.74 (t, 1H; II4'), 7.07 (t, 1H; II5'), 7.40 (d, 1H; II6'). ¹⁹⁵Pt NMR (300 MHz, MeOH, 298 K): δ = -2702 ppm.

[(tpy)Ru(dtdeg)PtCl]Cl₃ (5): [(tpy)Ru(dtdeg)]Cl₂ (100 mg; 0.10 mmol) and [Pt(cod)Cl₂] (50 mg; 0.15 mmol) were refluxed in 20 mL of MeOH for 6 hours. The reaction mixture was cooled to RT and filtered. Red plate-shaped crystals were obtained by slow precipitation of the filtrate with diethyl ether. Yield: 107 mg (88 %). Elemental analysis (%) calculated for C₄₉H₃₉Cl₄N₉O₃PtRu·7H₂O (A different batch than the obtained crystals was used. The presence of predominantly methanol molecules in the solvent region of the crystal structure of **5**, has clearly been indicated by the electron density of first models of the crystal structure. Importantly, the solvent region might – instead – also contain some water molecules but due to disorder the refinement of the solvent molecules has not been succeeded. Because the solvent region in the packing of the crystal structure of **5** is rather large and disordered, it is reasonable that in a different batch of crystals a different arrangement of solvent molecules is present in the solvent region. Water, which is present in methanol, was used instead of methanol to fit the elemental analysis as the C/N ratio of the analysis corresponds to the structural formula of the complex. The water molecules might also have been taken from the air after drying of the product *in vacuo* on P₂O₅, which has been done before elemental analysis.): C 43.09, N 9.23, H 3.91. Found: C 43.26, N 9.42, H 3.90. ESI-MS: *m/z*: 378 [M³⁺]. ¹H NMR (600 MHz, DMSO, 298 K): δ = 8.95 (d, 2H; I33''), 7.99 (t, 2H; I44''), 7.22 (t, 2H; I55''), 7.36 (d, 2H; I66''), 8.89 (s, 2H; I3'5'), 4.77 (t, 2H; 1), 4.14 (t, 2H; 2), 8.83 (d, 2H; I'33''), 8.46 (t, 2H; I'44''), 7.93 (t, 2H I'55''), 8.92 (d, 2H; I'66''), 8.55 (s, 2H; I'3'5'), 4.72 (t, 2H; 1'), 4.11 (t, 2H; 2'), 8.84 (d, 2H; II33''), 8.01 (t, 2H; II44''), 7.28 (t, 2H; II55''), 7.52 (d, 2H; II66''), 9.09 (d, 2H; II3'5'), 8.49 ppm (t, 1H; II4'). ¹⁹⁵Pt NMR (300 MHz, MeOH, 298 K): δ = -2701 ppm.

Crystal structure data for **5**·8CH₃OH: C₅₇H₆₃Cl₄N₉O₁₁PtRu, *M_r* = 1496.20, red plate-shaped crystal (0.03 x 0.13 x 0.30 mm), triclinic, space group $\overline{P1}$ with *a* = 8.8396(12) Å, *b* = 15.961(2) Å, *c* = 23.548(4) Å, α = 75.031(13)°, β = 88.528(13)°, γ = 78.975(17)°, *V* =

3149.4(8) Å³, $Z = 2$, $D_x = 1.578 \text{ g cm}^{-3}$, $\mu(\text{Mo K}\alpha) = 2.804 \text{ mm}^{-1}$. A total of 53838 reflections were measured (11287 independent, $R_{\text{int}} = 0.1061$, $\theta_{\text{max}} = 25.35^\circ$, $T = 150 \text{ K}$, Mo K α radiation, graphite monochromator, $\lambda = 0.71073$) on a Nonius Kappa CCD diffractometer on a rotating anode; data were corrected for absorption using PLATON/MULABS, T-range 0.741-0.929. The structure was solved by automated direct methods (SHELXS86). Full-matrix least-squares refinement of 577 parameters on F^2 (SHELXL-97) resulted in a final $R1$ value of 0.0470, $wR2 = 0.0927$, $S = 0.898$. H-atoms were introduced on calculated positions. A volume of 1257 Å³ per unit cell is filled with disordered methanol solvent molecules in which the chloride counter ions are positioned as well. Disorder models of solvent and counter ions suggest the presence of three chloride ions per ruthenium-platinum complex, one of which is disordered over two positions. However, these models proved to be unstable upon refinement. Using the PLATON/SQUEEZE method, a total of 379 e^- was found in the disordered region which corresponds to circa 8 methanol molecules per ruthenium-platinum complex. CCDC-230794 contains the supplementary crystallographic data for this paper. These data can be obtained online free of charge (or from the Cambridge Crystallographic Data Centre, 12, Union Road, Cambridge CB2 1EZ, UK; fax: (+44) 1223-336-033; or deposit@ccdc.cam.ac.uk).

[(tpy)Ru(dtdeg)Pt(9egua)](PF₆)₄ (6): **5** (55 mg; 0.044 mmol) and 9egua (12 mg; 0.066 mmol) were stirred in 20 mL of H₂O for 2 days at 310 K. An excess of an aqueous solution of NH₄PF₆ was added and the resulting precipitate was filtered off. The residue was recrystallized from acetone and diethyl ether. Yield: 37 mg (45 %). ESI-MS: m/z : 319 [M⁴⁺]. ¹H NMR (600 MHz, acetone, 293 K): δ = 8.81 (d, 2H; I33''), 8.04 (t, 2H; I44''), 7.28 (t, 2H; I55''), 7.65 (d, 2H; I66''), 8.71 (s, 2H; I3'5'), 4.84 (t, 2H; 1), 4.24 (t, 2H; 2), 8.72 (d, 2H; I'33''), 8.51 (t, 2H; I'44''), 7.83 (t, 2H I'55''), 8.37 (d, 2H; I'66''), 8.40 (s, 2H; I'3'5'), 4.84 (t, 2H; 1'), 4.24 (t, 2H; 2'), 8.80 (d, 2H; II33''), 8.07 (t, 2H; II44''), 7.35 (t, 2H; II55''), 7.80 (d, 2H; II66''), 9.05 (d, 2H; II3'5'), 8.54 ppm (t, 1H; II4'). ¹⁹⁵Pt NMR (300 MHz, acetone, 298 K): δ = -2690 ppm.

4.2.4 Cytotoxicity tests

Cell cultures: A2780cis and A2780R cells (cisplatin sensitive and resistant human ovarian carcinoma, respectively) were maintained in Dulbecco's modified Eagle's Medium (DMEM: Gibco BRL™, Invitrogen Corporation, The Netherlands) supplemented with 10 % fetal calf serum (Perbio Science, Belgium), penicillin (100 units/mL: Duchefa Biochemie BV, The Netherlands) and streptomycin (100 µg/mL: Duchefa Biochemie BV, The Netherlands) in a humidified 6 % CO₂, 94 % air atmosphere at 310 K. Cisplatin sensitive and resistant mouse

leukemia L1210/0 and L1210/2 cells were grown (partly in suspension and partly adherent to the flasks) under the above mentioned conditions.

Cells were removed from the flasks by a 0.05 % trypsin solution. Cell viability was determined by the trypan blue exclusion test.

***In vitro* cytotoxicity evaluation:** Between 1000 and 5000 cells were seeded per well (depending on the cell type) onto 96-well plates (Corning Costar[®]) in 100 μ L of complete medium with 5 to 10 % of FCS. Cells were treated 24 hours after sowing by addition of 100 μ L of the complex in complete medium at the appropriate concentration. Cell growth was determined after 72 hours of incubation by the MTT assay, a colorimetric assay based on the ability of viable cells to reduce the soluble yellow 3-(4,5-dimethylthiazol-2-yl)-2,5-diphenyl-2H-tetrazolium bromide to blue formazan crystals by the mitochondria.^[19]

Final tested concentrations ranged between 4 μ M and 100 μ M and have been obtained by several dilutions with complete medium from stock solutions (2 mM) in sterile water. Stock solutions of complexes **3** and [Ru(tpy)Cl₃] were prepared in DMSO due to poor water solubility. The highest tested concentration of **3** was only 10 μ M, which contained 3.3 % of DMSO. [Ru(tpy)Cl₃] was tested with 4 % of DMSO in the highest concentration (100 μ M). Control experiments with DMSO have been carried out and will be considered while discussing the cytotoxic activity of these complexes. After 72 hours of incubation at 310 K, cells were incubated with 1 mg/mL MTT solution for 2 to 4 hours at 310 K. Subsequently, the medium was discarded and the formed crystals were dissolved in 100 μ L DMSO per well. Optical density (OD) was measured at 590 nm with a Biorad 550 microplate reader. The OD is directly proportional to the number of living cells, which are compared to the control (untreated cells).

4.3 Results and discussion

4.3.1 Characterization of the paramagnetic complexes **1** and **3** by ¹H NMR spectroscopy

The paramagnetic complex [Cl₃Ru(dtdeg)] (**1**) contains both a paramagnetic ruthenium(III)-terpyridyl unit and a metal-free terpyridyl moiety. The resonances of the former are significantly broadened and shifted, due to the presence of the unpaired electron in the t_{2g} orbital of the ruthenium(III) ion (Figure 4.2). The signals of the latter are observed within the normal diamagnetic envelope, but are somewhat broadened. In Chapter 2 of this thesis, a strategy for the characterization of paramagnetic trichlororuthenium(III)-terpyridine complexes by ¹H NMR spectroscopy has been presented using the complex

$[(\text{tpy})\text{Ru}(\text{dtdeg})\text{RuCl}_3]^{2+}$ as a model compound. A similar strategy will be used for the characterization of **1** (and **3**).

The ^1H NMR spectrum of **1** has been acquired at 340 K. At this temperature the “paramagnetic” signals, *i.e.* the resonances of the paramagnetic ruthenium(III) moiety, do not overlap. The signal at 5.07 ppm has also been established as a “paramagnetic” signal, since it exhibits short longitudinal (T_1) and transverse (T_2) relaxation times. Five resonances of similar intensity are observed in the aromatic region of the ^1H NMR spectrum for the terpyridine I' signals of the diamagnetic ruthenium(II) unit of **1**, which indicates the presence of a C_2 symmetry axis within the molecule. The resonances have been assigned by 2D COSY ^1H NMR experiments at 340 K using a mixing time of 20 ms (Figure 4.3). The signal at 8.91 ppm has been assigned to the I'66' protons, since it is observed as a doublet. The resonance displays a J value (~ 7 Hz), which is too small for that of 33'' pyridyl protons. For the latter, a J value of ~ 9 Hz is usually observed in diamagnetic species. The signal at 8.18 ppm does not show a crosspeak in the COSY spectrum. Therefore, it has been assigned to the I'3'5' protons.

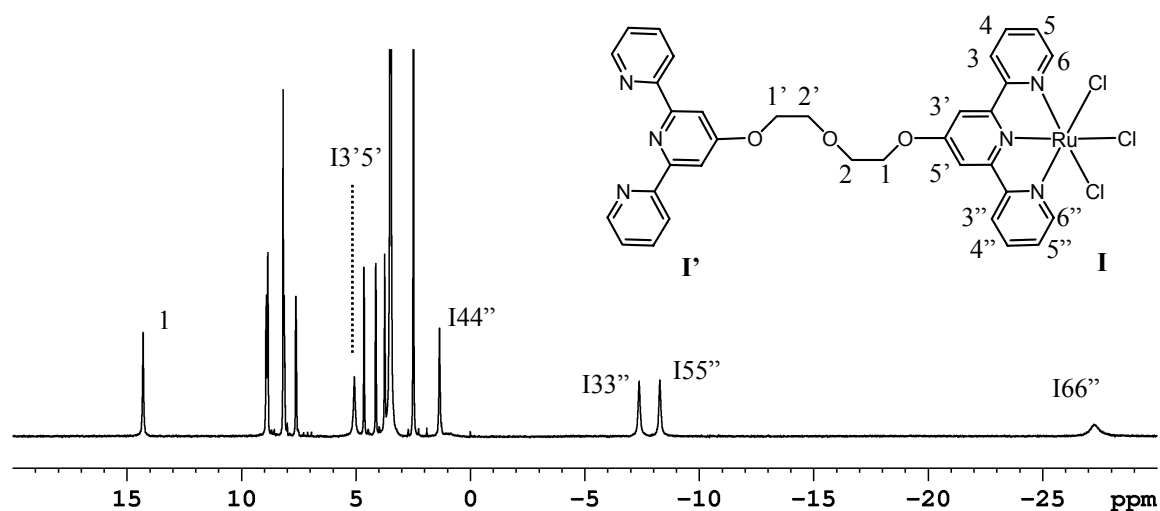


Figure 4.2 Schematic representation of the structure of **1**, and its 1D ^1H NMR spectrum at 340 K in $\text{DMSO-}d_6$ with the paramagnetic signals indicated. The numbering scheme given for the terpyridine protons **I**, can also be applied to the **I'** protons.

In agreement with the double C_2 symmetry of the complex, five resonances have also been found for the **I** protons of the paramagnetic ruthenium(III) unit. They have partly been assigned by 2D COSY ^1H NMR (Figure 4.3). The signal at -27.24 ppm appears to be too broad to show crosspeaks. In analogy with the complexes $[(\text{tpy})\text{Ru}(\text{dtdeg})\text{RuCl}_3]^{2+}$ (Chapter 2) and $[\text{Ru}(\text{tpy})\text{Cl}_3]$,^[16] the signal has been assigned to the I66'' protons. These are the protons

closest to the paramagnetic ruthenium(III) center, and can therefore be expected to shift the most. The paramagnetic resonance at 1.35 ppm displays crosspeaks to the signals at -7.38 and -8.28 ppm. Hence, it has been attributed to the I44'' protons. The I33'' and I55'' protons can not be assigned, yet. A two-spins system is shown by the resonances at 14.28 and 3.74 ppm, which assigns these signals to the diethylene protons 1 and 2. The resonance at 14.28 ppm has been ascribed to the linker protons 1, since they are closest to the paramagnetic center.

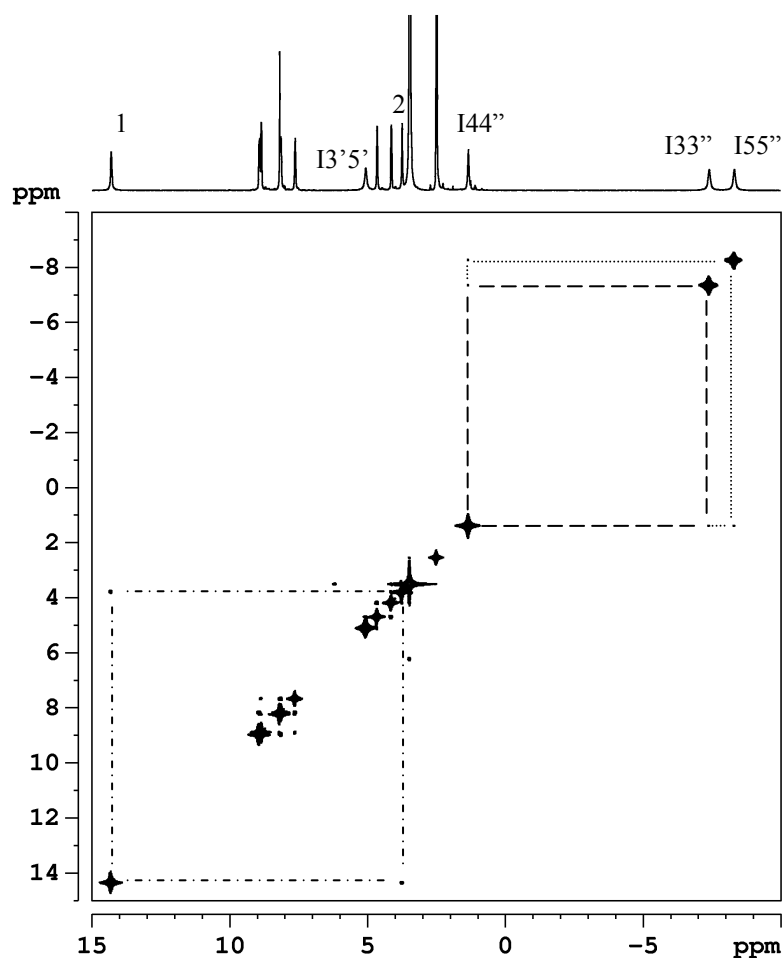


Figure 4.3 2D ^1H COSY NMR spectrum of **1** in $\text{DMSO-}d_6$ at 340 K with some crosspeaks indicated, and assignments given.

1D NOE difference experiments (Figure 4.4) complete the assignment of **1**. Upon irradiation of the paramagnetic signal at 5.07 ppm, signal enhancements are displayed by the diethylene protons 1 at 14.28 ppm, and by the resonance at -7.38 ppm. As a result, the signal at 5.07 ppm has been assigned to the I3'5' protons. Thereby, the signal at -7.38 ppm can be ascribed to the I33'' protons. Irradiation of the largely shifted and broadened I66'' resonance at -27.24 ppm results in a NOE of the signal at -8.28 ppm. This NOE unambiguously proves the

assignment of the I66'' and I55'' protons. The 1' and 2' resonances have been assigned by a I'3'5'-1' crosspeak (data not shown).

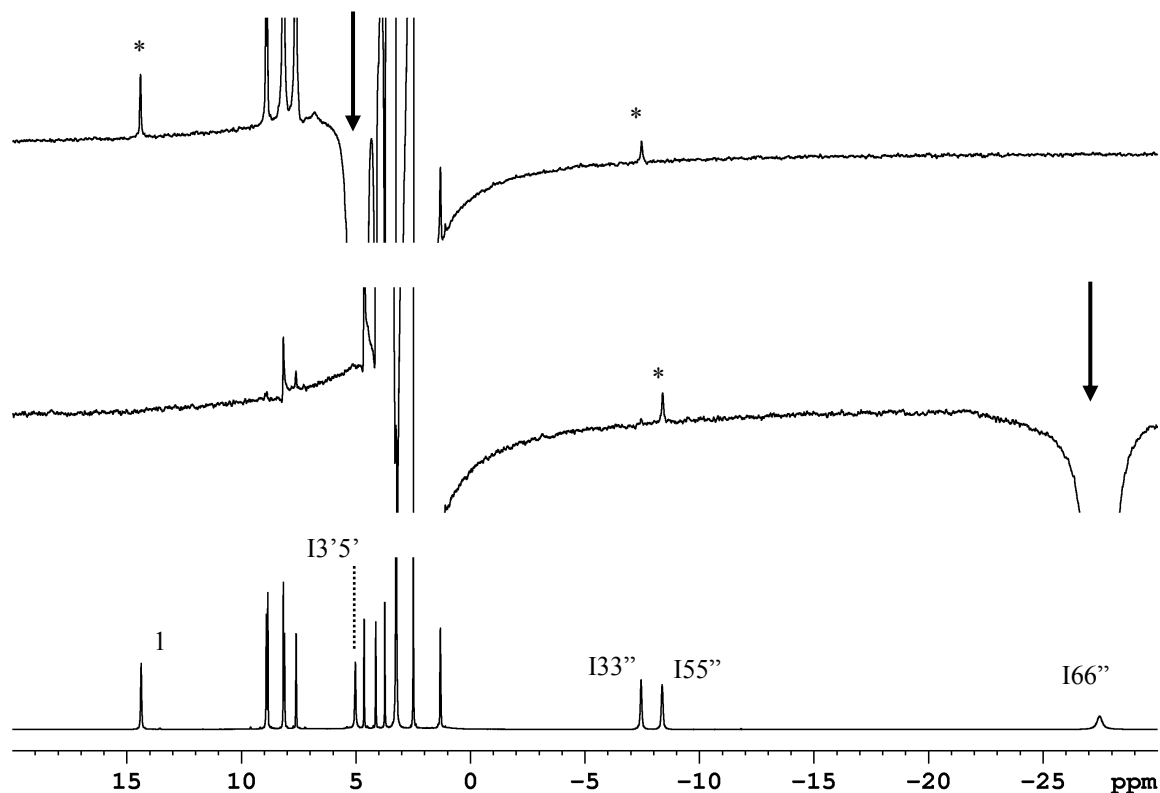


Figure 4.4 1D ^1H NOE difference NMR spectra (top and middle) and 1D ^1H NMR spectrum (bottom) of **1** in $\text{DMSO-}d_6$ at 340 K. Irradiated signals are indicated with an arrow. NOEs are indicated by an asterisk.

The 1D ^1H NMR spectrum of the paramagnetic complex $[\text{Cl}_3\text{Ru}(\text{dtdeg})\text{PtCl}]\text{Cl}$ (**3**) in $\text{DMSO-}d_6$ is depicted in Figure 4.5. The complex displays a similar spectrum to that of its precursor **1**. The paramagnetic signals of the ruthenium(III) moiety are observed outside the diamagnetic region, whereas the signals of the diamagnetic platinum(II) moiety are found within this region. For both metal moieties five signals are observed for the aromatic protons, which indicates that C_2 symmetry is displayed within each unit. The chemical shifts of the platinum-terpyridine protons have shifted in comparison to the corresponding signals of **1** ($\delta = 8.83, 8.19, 8.91, 9.08, \text{ and } 8.91$ versus $8.89, 7.70, 8.25, 8.89, \text{ and } 8.25$ for the I'33'', I'44'', I'55'', I'66'', and I'3'5' protons of **3** and **1**, respectively). The differences in shifts indicate coordination of platinum to the free terpyridyl unit of **1**. The ^{195}Pt NMR shift of **3** proves coordination (see experimental section).

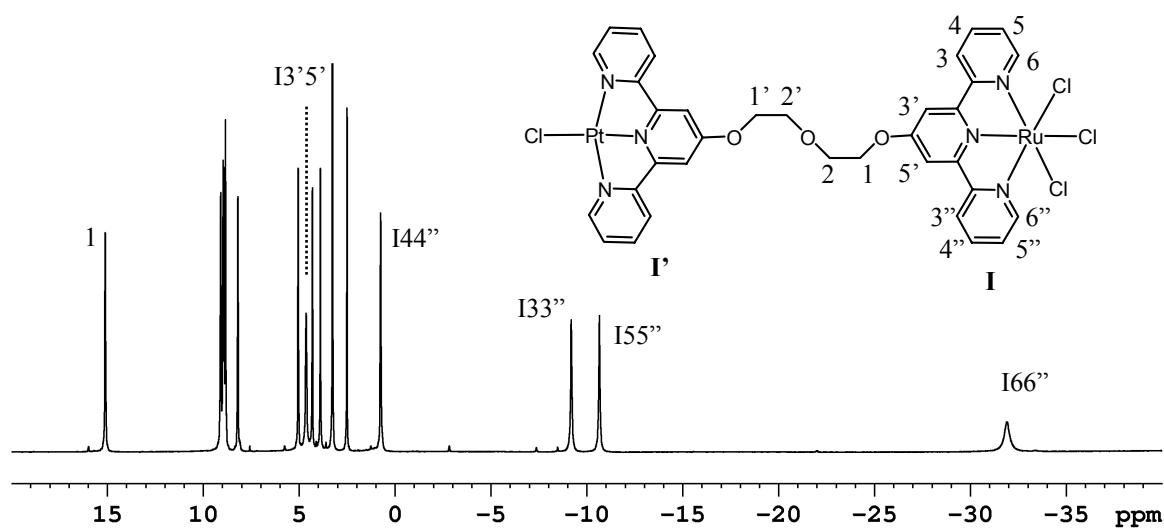


Figure 4.5 1D ^1H NMR spectrum of **3** at 310 K in $\text{DMSO-}d_6$ with the paramagnetic signals indicated, and schematic representation of the structure of the cation of **3**. The numbering scheme given for the terpyridine protons **I**, can also be applied to the **I'** protons.

The ^1H NMR spectrum of **3** has been acquired at 310 K. At this temperature the “paramagnetic” signals, *i.e.* the resonances of the paramagnetic ruthenium(III) moiety, do not overlap. The paramagnetic signals of **3** show crosspeaks comparable to those of **1** in the 2D COSY NMR spectrum. Therefore, these data are not shown. 1D NOE difference experiments are depicted in Figure 4.6. Similar to **1**, signal enhancements of the diethylene protons **1** and **I33''** are seen upon irradiation of the paramagnetic signal at 4.63 ppm. Thereby, the latter can be attributed to the **I3'5'** protons. A NOE of the **I55''** signal upon saturation of the **I66''** signal has not been observed. In contrast to **1**, the **I3'5'-1** and **I3'5'-I33''** NOEs are identical in sign as the saturated signal. This difference shows that the NOE values are a function of the rotational correlation time. The latter is dependent on the molecular size of the species. The observed NOEs are rather small in comparison to those observed for **1**, which may be caused by concentration differences of the samples. However, the values of the NOEs may be close to zero, because the function of the NOE value first decreases to zero upon decreasing rotational correlation times (which decreases upon an increase of molecular weight), and subsequently becomes negative. The sign of the NOEs for **3** is similar to that observed for the complex $[(\text{tpy})\text{Ru}(\text{dtdeg})\text{RuCl}_3]^{2+}$, which is described in Chapter 2.

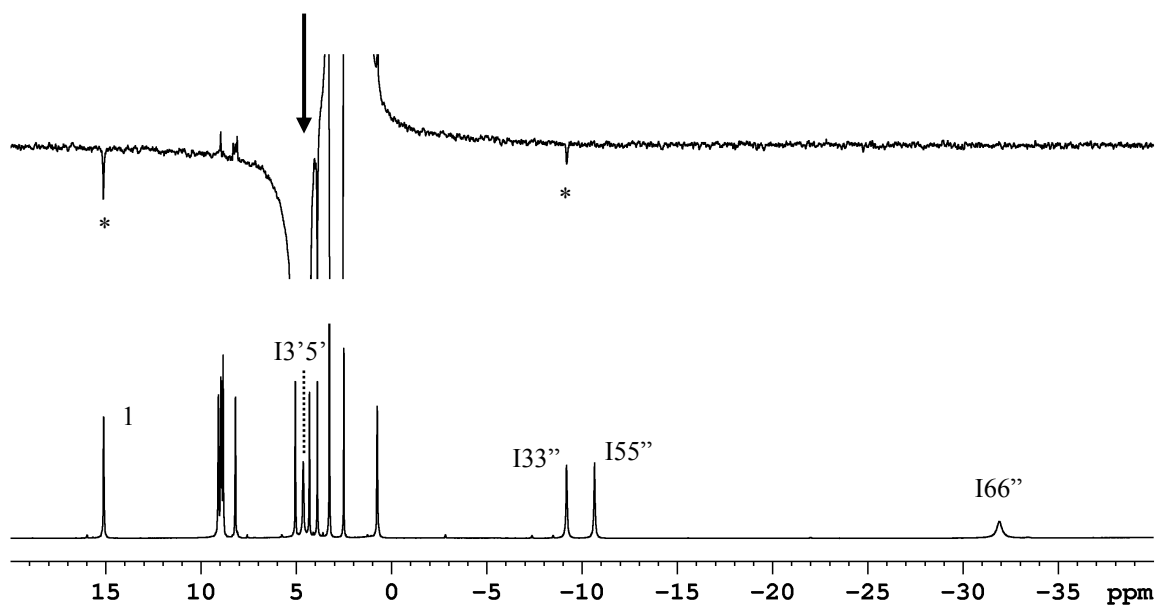


Figure 4.6 1D NOE difference ^1H NMR spectrum (top) and 1D ^1H NMR spectrum (bottom) of **3** in $\text{DMSO-}d_6$ at 310 K. Irradiated signals are indicated with an arrow. NOEs are indicated by an asterisk.

4.3.2 Characterization of the diamagnetic complexes **2**, **4**, and **5** by ^1H NMR spectroscopy

The 1D ^1H NMR spectra of $[\text{Cl}(\text{bpy})\text{Ru}(\text{dtdeg})]\text{Cl}$ (**2**) and $[\text{Cl}(\text{bpy})\text{Ru}(\text{dtdeg})\text{PtCl}]\text{Cl}_2$ (**4**) in $\text{DMSO-}d_6$ are shown in Figure 4.7. The assignment of the ^1H NMR data has been performed by 2D COSY and NOESY ^1H NMR experiments (see experimental section). The appearance of four individual resonances in the region between 4 and 5 ppm for the linker protons of **2** and **4**, indicates the presence of two different moieties for both complexes. This is confirmed by the fact that three sets of signals are identified in the aromatic region for the three nonequivalent polypyridine ligands of both **2** and **4**. Symmetry is displayed within each unit, due to the occurrence of a C_2 symmetry axis. The bipyridine ligand is located in the plane of symmetry, and therefore individual resonances of intensity 1 are observed for all its protons. The terpyridine signals have a relative intensity of 2. The II6 bipyridine signal has been recognized by its significant downfield shift, due to the deshielding effect of the nearby chloride ligand. The signals for the pyridine 6 protons and pyridine 3 protons have been identified by their J values of ~ 5 Hz and ~ 9 Hz, respectively. The two terpyridine ligands I and I' have been distinguished by the interligand I66''-II6 NOE crosspeak.

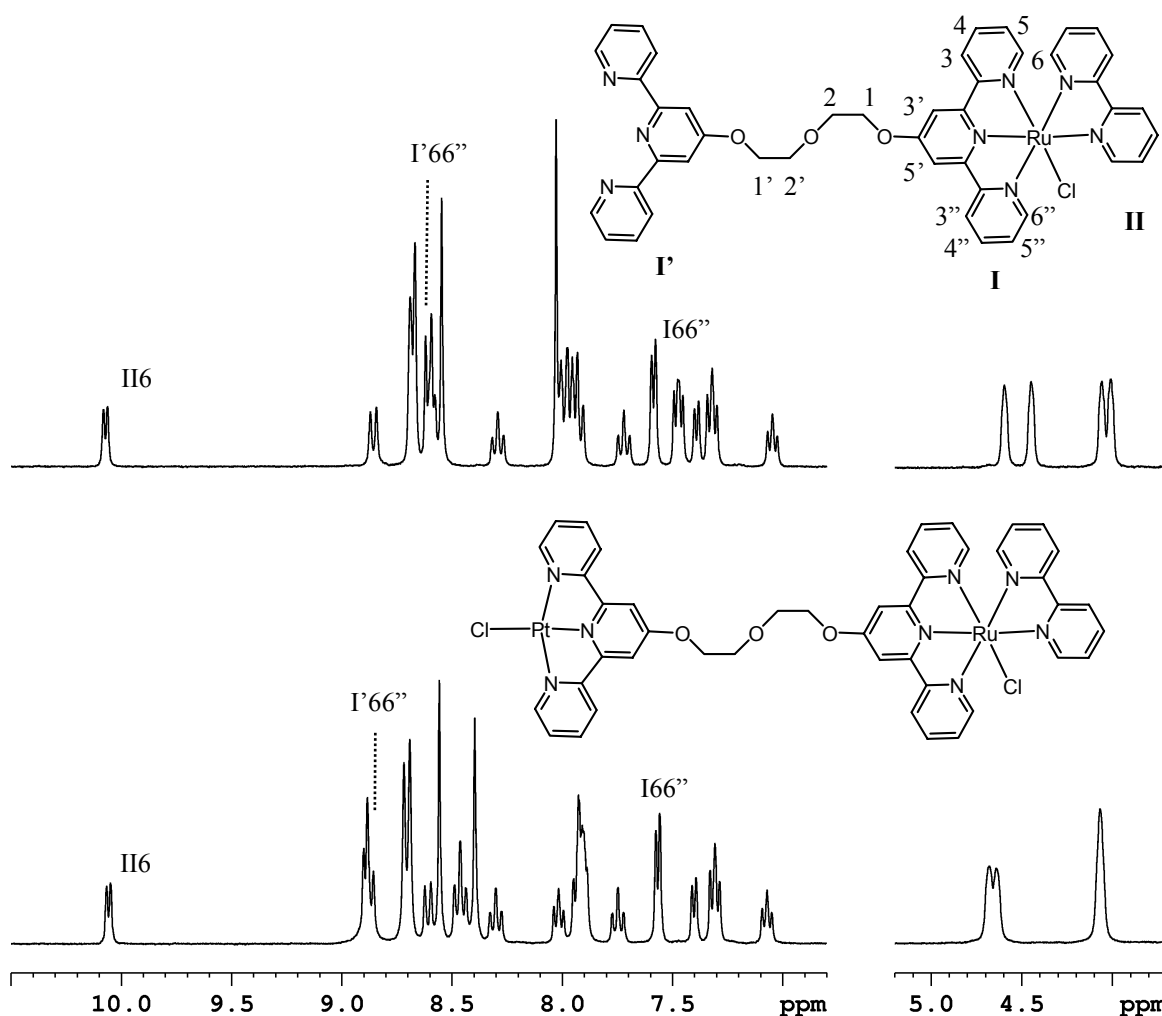


Figure 4.7 1D ^1H NMR spectra of **2** (top) and **4** (bottom) at 298 K in $\text{DMSO-}d_6$ with some assignments, and schematic representations of the cations of **2** and **4**. The numbering scheme given for the terpyridine protons I, can also be applied to the I' protons, and to those of **4**.

The downfield shift of the I'66'' signal of **4** in comparison to the analogous signal of **2**, indicates coordination of platinum to the free terpyridyl moiety. Coordination of platinum has been confirmed by the signal at -2700 in ^{195}Pt NMR.

The characterization of $[(\text{tpy})\text{Ru}(\text{dtdeg})\text{PtCl}]\text{Cl}_3$ (**5**) is very similar to that of complexes **2** and **4**. The ^1H NMR spectrum of **5**, measured at 600 MHz, is shown in Figure 4.8. The appearance of four distinct signals between 4 and 5 ppm for the linker protons indicates the presence of two different metal moieties. In the aromatic region, three sets of signals are observed for the three inequivalent terpyridine ligands I, I' and II. C_2 symmetry is displayed within each unit. All signals exhibit an intensity of two except for the triplet appearing at 8.49 ppm. This signal shows an intensity of 1, and has therefore been attributed to proton II4'.

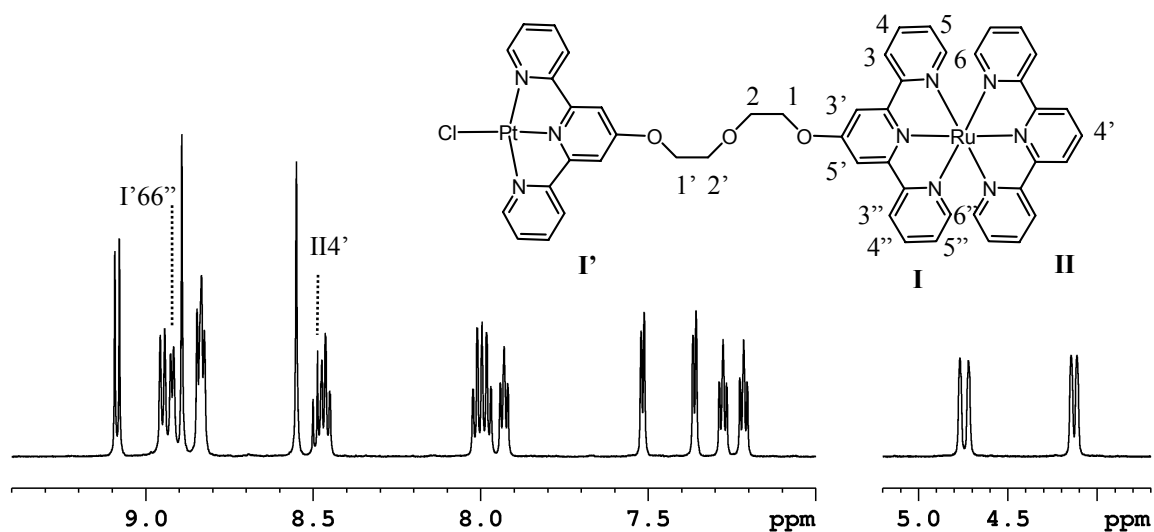


Figure 4.8 1D ^1H NMR spectrum of **5** at 298 K in $\text{DMSO-}d_6$ (600 MHz) with some assignments, and schematic representation of the cation of **5**. The numbering scheme given for the terpyridine protons I, can also be applied to the I' and II protons.

With the identification of the II4' signal, the signals of the terpyridyl ligand II have been assigned next by 2D ^1H COSY and NOESY NMR. A characteristic downfield shift of the I'66'' signal is seen, because of coordination of platinum to terpyridine ligand I. The recognition of the I'66'' signal has been used to assign the two remaining sets of signals for the protons of terpyridyl ligands I and I' taking into account the specific J values of the 33'' and 66'' pyridine protons as well. A typical shift of approximately -2700 ppm in ^{195}Pt NMR has also been observed.

4.3.3 Crystal structure of **5**

Red plated-shaped crystals of **5** have been obtained by slow precipitation from the reaction mixture with diethyl ether. The crystal structure has been elucidated (Figure 4.9) confirming unambiguously the molecular structure of the cation of **5**. Due to disorder, the coordinates of the chloride counter ions could not be refined (see experimental section). No crystal structures of heterodinuclear ruthenium-platinum complexes, in which the two metal moieties are linked through a long and flexible linker, have been reported to date. Bond lengths and angles are in agreement with literature data for parental cationic mononuclear complexes.^[20, 21] The intramolecular $\text{Ru}\cdots\text{Pt}$ distance is 14.547(3) Å. For comparison, the intramolecular $\text{Ru}\cdots\text{Pt}$ distance in the crystal structure of $[\text{Ru}(\text{bpy})_2(\mu\text{-}2,3\text{-dpp})\text{PtCl}_2](\text{PF}_6)_2$, in which dpp is the short and rigid bridging ligand 2,3-bis(2-pyridyl)pyrazine, is 6.7 Å.^[22] Given that the

diethyleneglycolether linker of **5** is somewhat folded in the crystal structure, the length over which both metal moieties can interact with DNA might even be larger. Long-range binding from the minor to the major groove of the DNA has been shown^[23] for the trinuclear platinum compound [*trans*-PtCl(NH₃)₂]₂μ-{H₂N(CH₂)₆NH₂}₂Pt(NH₃)₂](NO₃)₄, BBR3464, bound to a self-complementary DNA octamer 5'-d(ATG*TACAT)₂-3'. The two *trans*-PtCl(NH₃)₂ units coordinate in the major groove at the N7 positions of guanines on opposite DNA strands, whereas the central tetraamine linker is located in, or close to, the minor groove. Considering the length of the linker of **5**, either intercalative binding or coordination of the platinum moiety of **5** might occur in the major groove of the DNA after pre-association, which is largely stabilized by electrostatic forces, by binding of the 2+ charged ruthenium unit in the minor groove.

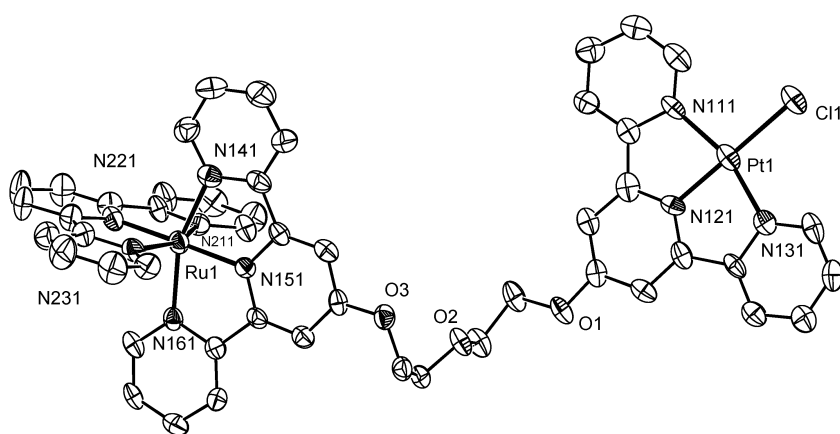


Figure 4.9 Displacement ellipsoid (50 % probability) plot of the structure of the cation of **5**. Counter ions and solvent molecules are not shown. Hydrogen atoms are omitted for clarity.

The crystal structure of **5** shows intermolecular stackings between the platinum moieties despite the linked, rather bulky ruthenium units (Figure 4.10). The platinum units stack in a head-to-tail fashion (Figure 4.11) with alternating short and long Pt...Pt distances of 3.4935(7) and 6.7337(12) Å, respectively. The short Pt...Pt distances are indicated with dashed lines in Figure 4.10. The packing of the crystal structure of **5** is such that chains of alternating platinum units related by inversion symmetry are situated in between the ruthenium units. Along the platinum-terpyridine chain, a continuous π - π stacking is displayed. The perpendicular distances of the center of geometry of one ring to the least-squares plane of the other ring are approximately 3.38 and 3.45 Å for the short and long pair, respectively. The short Pt...Pt distance of 3.49 Å might even allow $d_{z^2} - d_{z^2}$ interactions.^[24] Aggregation via weak bonding interactions into metal-bound $d^8 - d^8$ pairs in an infinite π - π

stack has indeed been reported for the perchlorate salt of the parental mononuclear $[\text{Pt}(\text{tpy})\text{Cl}]^+$ cation.^[21] Studies to examine the Pt-Pt interactions of **5** have not been undertaken.

The self-stacking interactions suggest that the platinum unit of **5** is able to intercalate in the DNA, like its mononuclear counterpart. Intercalation into DNA has been shown to occur for substitution-inert platinum(II) terpyridine analogues of the parental mononuclear complex $[\text{Pt}(\text{tpy})\text{Cl}]^+$, such as 2-hydroxyethanethiolate and 4-picoline terpyridine-platinum complexes.^[10, 25] A crystal structure^[26] of a double helical fragment with the 2-hydroxyethanethiolate derivative, has revealed stacking of the metallo-intercalator between two Watson-Crick GC base pairs with the DNA unwinding angle being 23° . Chloroterpyridineplatinum(II) has been illustrated to have two adenosine-5'-monophosphate molecules, which base pair in a rarely observed hybrid Watson-Crick-Hoogsteen variety, intercalated between two platinum complexes.^[27] Intercalation may subsequently result in coordination to DNA, since DNA coordination has been reported to be the thermodynamically more favorable mode of binding for mononuclear platinum terpyridine complexes containing a fourth relatively labile ligand like chloride or hydroxide.^[11, 28]

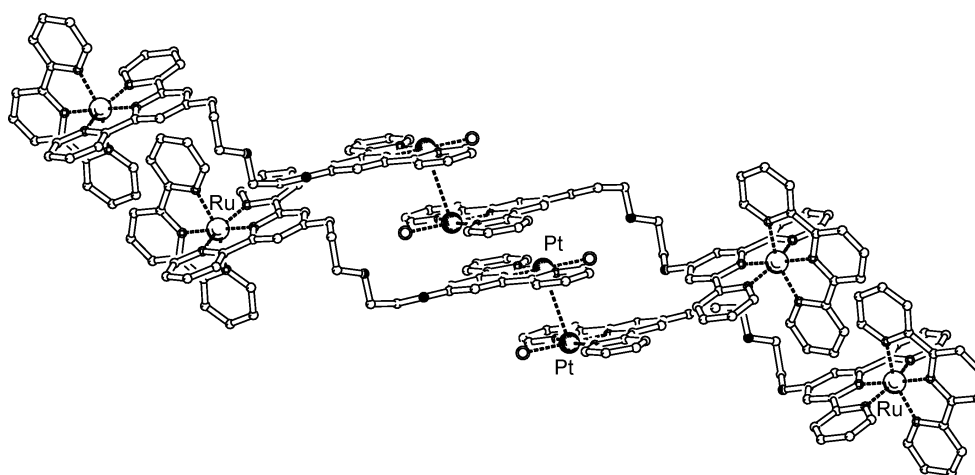


Figure 4.10 View of the packing of the crystal structure of the cation of **5** in which alternating short and long Pt...Pt distances are displayed by the platinum units. A short intermolecular Pt...Pt $[2-x,-y,-z]$ distance (dashed lines) of $3.4935(7)$ Å is observed between two platinum terpyridine units that are exactly orientated in a head-to-tail fashion. The long intermolecular Pt...Pt $[1-x,-y,-z]$ distance is caused by a lateral shift of one Pt-tpy unit with respect to the short Pt...Pt $[2-x,-y,-z]$ vector. Counter ions and solvent molecules are not shown.

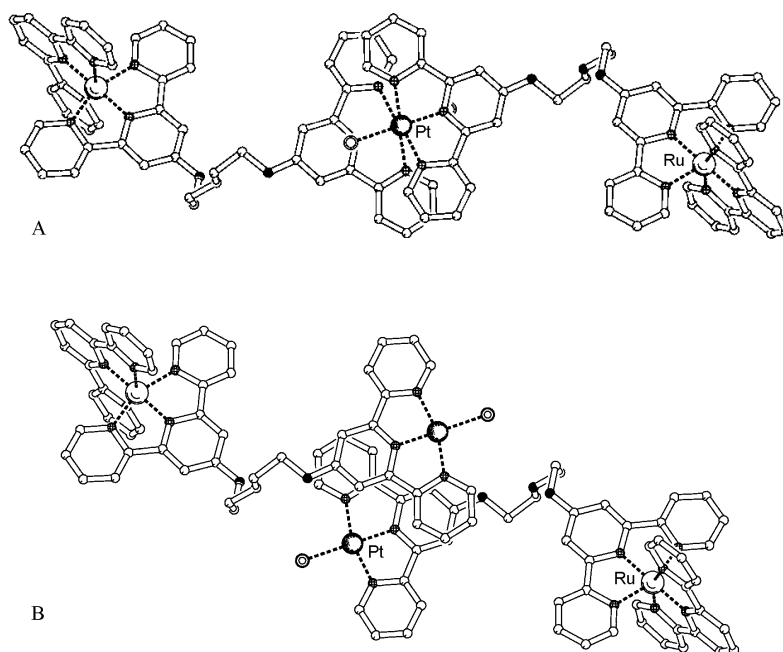


Figure 4.11 View in the direction of the short Pt····Pt [2-*x*, -*y*, -*z*] vector showing the π - π stacking interactions along the Pt-tpy chain: A, Pt····Pt = 3.4935(7) Å; B, Pt····Pt = 6.7337(12) Å. The planes through the rings are nearly parallel for both dimers, the dihedral angle between the planes being 1.1° and 2.4° for A and B, respectively. The perpendicular distances of the geometrical center of one ring to the least-squares plane through the other ring system are nearly identical for interaction A (approximately 3.38 Å) and interaction B (approximately 3.45 Å).

4.3.4 Binding of **5** to the DNA-model base 9-ethylguanine

Mononuclear platinum terpyridine complexes are known to bind preferentially to the DNA base guanine.^[29] To study whether the platinum unit of **5** is capable of coordination to DNA, the reaction with the DNA-model base 9-ethylguanine has been performed in water at 310 K for 2 days.

The monoadduct [(tpy)Ru(dtdeg)Pt(9egua)](PF₆)₄ (**6**) has been isolated as the hexafluorophosphate salt. The hexafluorophosphate salt of the adduct is not soluble in water. Therefore, the 1D ¹H NMR spectrum of **6** has been acquired in acetone-*d*₆, and is shown in Figure 4.12. Assignments of the terpyridyl signals have been done in analogy to those of **5**. The chemical shifts in acetone-*d*₆ of the 9egua protons of **6** compared to those of the free

DNA-model base ($\delta = 1.61, 4.36, 6.68$ and 8.90 versus $1.40, 4.06, 5.98$ and 7.60 ppm for CH_2 , CH_3 , NH_2 and H_8 , respectively) indicate binding of 9egua to the complex. Binding of 9egua is in agreement with the large upfield shift of the platinum terpyridine I'66'' protons of **6** compared to that of the chloride complex **5** ($\delta = 8.37$ versus 8.92 ppm), which is due to substitution of the relatively labile, deshielding chloride ligand. The relative intensity of 1 for the H_8 signal demonstrates binding occurs in a ratio of 1:1 of 9egua to **5**. N7 coordination is proven by the large shift of the H_8 signal in particular, and the observed I66''- H_8 NOE crosspeak in 2D ^1H NOESY experiments (Figure 4.13). No significant shift of **6** compared to **5** is displayed in ^{195}Pt NMR.

The resonance of the H_8 proton and its NOE to the I'66'' signal are in agreement with data reported for the N7 coordinated guanosine adduct of $[\text{Pt}(\text{tpy})(4\text{-picoline})]^{2+}$, in which the picoline ligand has been substituted by the DNA base.^[29, 30] Recently, a crystal structure of the guanosine-5'-monophosphate platinum terpyridine adduct has proven N7 coordination of the base to the platinum atom.^[31]

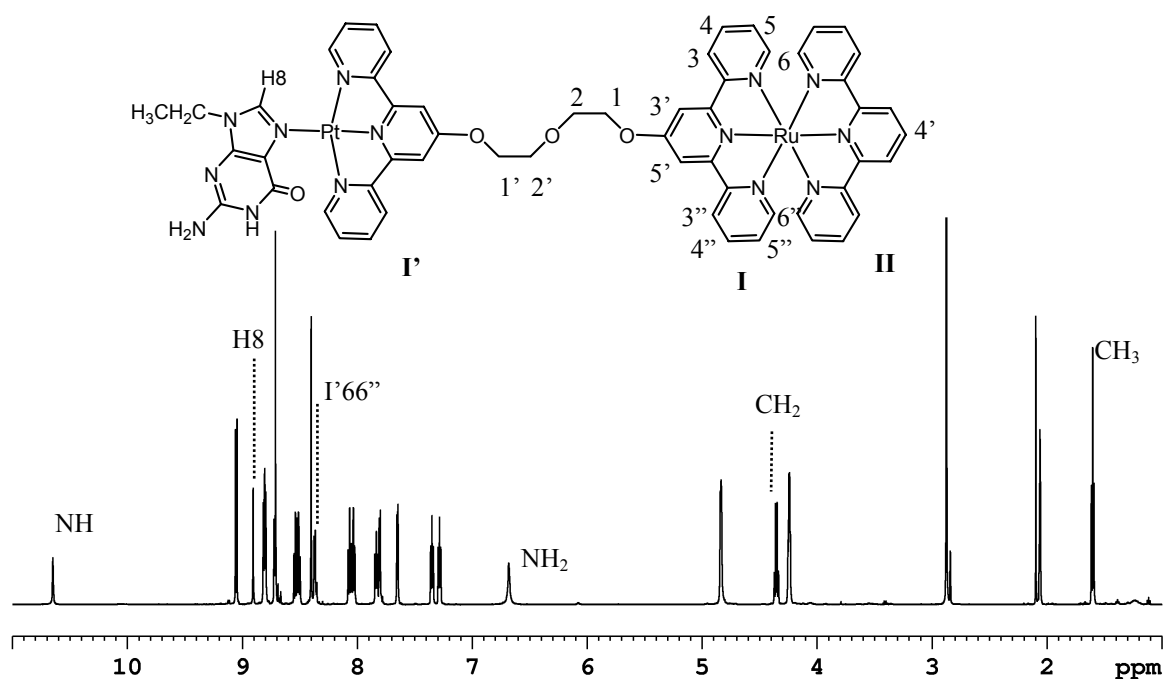


Figure 4.12 1D ^1H NMR spectrum of the adduct **6** in acetone- d_6 at 293 K (600 MHz) with some assignments, and schematic representation of its 4+ charged cation.

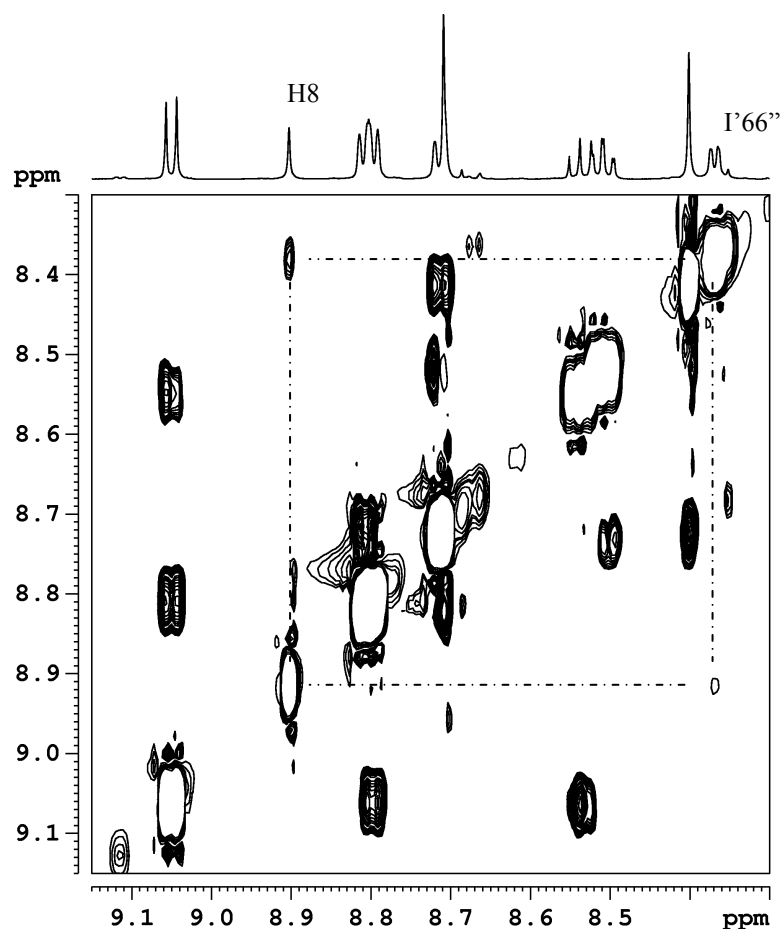


Figure 4.13 Part of the 2D ^1H NOESY NMR spectrum of **6** (600 MHz) in acetone- d_6 at 293 K with some assignments.

4.3.5 Biological activity

The complexes **3**, **4** and **5** do not display significant cytotoxicity against the cisplatin-sensitive and cisplatin-resistant human ovarian carcinoma cells A2780cis and A2780R, and the mouse leukemia cells L1210/0 and L1210/2. In terms of cell growth inhibition, only $[\text{Cl}(\text{bpy})\text{Ru}(\text{dtdeg})\text{PtCl}]\text{Cl}_2$ (**4**) shows moderate reduction of A2780R cell growth (55 %), but at a relatively high concentration of 100 μM . The complex $[\text{Cl}_3\text{Ru}(\text{dtdeg})\text{PtCl}]\text{Cl}$ (**3**) shows no inhibition of cell growth at concentrations (3 μM) at which the DMSO (necessary to dissolve **3**) percentage is negligible (1.5 %). Thus, whereas the mononuclear complex $[\text{Pt}(\text{tpy})\text{Cl}]\text{Cl}$ has IC_{50} values of approximately 1 μM , complexes **3**, **4** and **5** can be regarded as noncytotoxic. The inactivity of **3** is particularly surprising, since both its metal moieties are derived from promising anticancer agents.

It has been reported that dinuclear platinum terpyridine complexes, in which a long and flexible linker is attached to either the 4' position of the terpyridine ligand or to the 4' site of a coordinating fourth pyridine ligand, are not cytotoxic either.^[32, 33] In contrast, cytotoxicity is displayed by platinum-terpyridine complexes, which are linked through more short and rigid dipyrindyl linkers. An exception is a trinuclear compound in which two platinum-terpyridine moieties are linked through a trans-diammine bis(4,4'-dipyrindyl)platinum(II) unit by coordination to the dipyrindyl ligands. The charge of this linker has been suggested to be of importance for the activity of the complex.^[33]

4.4 Concluding remarks

The synthesis and characterization of the heterodinuclear ruthenium-platinum complexes $[\text{Cl}_3\text{Ru}(\text{dtdeg})\text{PtCl}]\text{Cl}$ (**3**), $[\text{Cl}(\text{bpy})\text{Ru}(\text{dtdeg})\text{PtCl}]\text{Cl}_2$ (**4**), and $[(\text{tpy})\text{Ru}(\text{dtdeg})\text{PtCl}]\text{Cl}_3$ (**5**) is presented. The paramagnetic dinuclear ruthenium(III)-platinum(II) complex **3** represents the first heterodinuclear ruthenium-platinum complex, which has been characterized by 1D NOE difference experiments. The crystal structure of the cation of **5** has been elucidated, and shows self-stacking interactions of the platinum moieties. The length of the linker is 14.5 Å, which may allow the formation of long-range DNA adducts. The adduct of **5** with the DNA-model base 9-ethylguanine has been isolated and characterized by ¹H NMR. The results suggest that the platinum moiety of the complexes is able to both intercalate and coordinate to the DNA, without being hindered by the dangling ruthenium unit. However, none of the complexes shows significant activity against A2780 and L1210 cisplatin sensitive and resistant cells. The lack of anticancer activity may have its origin in the nature and length of the linker. In Chapter 5, polynuclear complexes with linkers of variable length and charge are described.

4.5 References

- [1] (a) Reedijk, J., *Proc. Natl. Acad. Sci. U. S. A.* **2003**, *100*, 3611-3616. (b) Wheate, N. J.; Collins, J. G., *Coord. Chem. Rev.* **2003**, *241*, 133-145.
- [2] Farrell, N.; Qu, Y.; Bierbach, U.; Valsecchi, M.; Menta, E., in *Cisplatin. Chemistry and Biochemistry of a Leading Anticancer Drug* (Ed.: Lippert, B.), Verlag Helvetica Chimica Acta, Zurich, Wiley-VCH, Weinheim, **1999**, 479-496.
- [3] Reedijk, J., *Chem. Rev.* **1999**, *99*, 2499-2510.
- [4] Jamieson, E. R.; Lippard, S. J., *Chem. Rev.* **1999**, *99*, 2467-2498.
- [5] Clarke, M. J., *Coord. Chem. Rev.* **2003**, *236*, 209-233.
- [6] (a) Alessio, E.; Mestroni, G.; Bergamo, A.; Sava, G., *Metal Ions in Biological Systems* **2004**, *42*, 323-351. (b) Iengo, E.; Mestroni, G.; Geremia, S.; Calligaris, M.; Alessio, E., *J. Chem. Soc.-Dalton Trans.* **1999**, 3361-3371. (c) Serli, B.; Iengo, E.; Gianferrara, T.; Zangrando, E.; Alessio, E., *Metal-Based Drugs* **2001**, *8*, 9-18.

- [7] (a) Allardyce, C. S.; Dyson, P. J., *Plat. Met. Rev.* **2001**, *45*, 62-69. (b) Sun, H. Z.; Li, H. Y.; Sadler, P. J., *Chem. Rev.* **1999**, *99*, 2817-2842. (c) Reedijk, J., *Chem. Commun.* **1996**, 801-806.
- [8] (a) Qu, Y.; Farrell, N., *Inorg. Chem.* **1995**, *34*, 3573-3576. (b) Van Houten, B.; Illenye, S.; Qu, Y.; Farrell, N., *Biochemistry* **1993**, *32*, 11794-11801.
- [9] (a) Milkevitch, M.; Storrie, H.; Brauns, E.; Brewer, K. J.; Shirley, B. W., *Inorg. Chem.* **1997**, *36*, 4534-4538. (b) Williams, R. L.; Toft, H. N.; Winkel, B.; Brewer, K. J., *Inorg. Chem.* **2003**, *42*, 4394-4400.
- [10] Jennette, K. W.; Lippard, S. J.; Vassiliades, G. A.; Bauer, W. R., *Proc. Natl. Acad. Sci. U. S. A.* **1974**, *71*, 3839-3843.
- [11] Howe-Grant, M.; Wu, K. C.; Bauer, W. R.; Lippard, S. J., *Biochemistry* **1976**, *15*, 4339-4346.
- [12] Nováková, O.; Kašpárková, J.; Vrána, O.; Van Vliet, P. M.; Reedijk, J.; Brabec, V., *Biochemistry* **1995**, *34*, 12369-12378.
- [13] Van Vliet, P. M.; Toekimin, S. M. S.; Haasnoot, J. G.; Reedijk, J.; Nováková, O.; Vrána, O.; Brabec, V., *Inorg. Chim. Acta* **1995**, *231*, 57-64.
- [14] (a) Barton, J. K., *Science* **1986**, *233*, 727-734. (b) Erkkila, K. E.; Odom, D. T.; Barton, J. K., *Chem. Rev.* **1999**, *99*, 2777-2795. (c) Pyle, A. M.; Rehmann, J. P.; Meshoyrer, R.; Kumar, C. V.; Turro, N. J.; Barton, J. K., *J. Am. Chem. Soc.* **1989**, *111*, 3051-3058. (d) Kelly, J. M.; Tossi, A. B.; McConnell, D. J.; Ohuigin, C., *Nucleic Acids Res.* **1985**, *13*, 6017-6034.
- [15] (a) Sullivan, B. P.; Calvert, J. M.; Meyer, T. J., *Inorg. Chem.* **1980**, *19*, 1404-1407. (b) McDermott, J. X.; White, J. F.; Whitesides, G. M., *J. Am. Chem. Soc.* **1976**, *98*, 6521-6528.
- [16] Velders, A. H., Ph.D. thesis, Leiden University (Leiden), **2000**.
- [17] Annibale, G.; Brandolisio, M.; Pitteri, B., *Polyhedron* **1995**, *14*, 451-453.
- [18] Dugad, L. B.; Lamar, G. N.; Banci, L.; Bertini, I., *Biochemistry* **1990**, *29*, 2263-2271.
- [19] (a) Tada, H.; Shiho, O.; Kuroshima, K.; Koyama, M.; Tsukamoto, K., *J. Immunol. Methods* **1986**, *93*, 157-165. (b) Mosmann, T., *J. Immunol. Methods* **1983**, *65*, 55-63. (c) Alley, M. C.; Scudiero, D. A.; Monks, A.; Hursey, M. L.; Czerwinski, M. J.; Fine, D. L.; Abbott, B. J.; Mayo, J. G.; Shoemaker, R. H.; Boyd, M. R., *Cancer Res.* **1988**, *48*, 589-601.
- [20] Lashgari, K.; Kritikos, M.; Norrestam, R.; Norrby, T., *Acta Crystallogr. Sect. C-Cryst. Struct. Commun.* **1999**, *55*, 64-67.
- [21] Bailey, J. A.; Hill, M. G.; Marsh, R. E.; Miskowski, V. M.; Schaefer, W. P.; Gray, H. B., *Inorg. Chem.* **1995**, *34*, 4591-4599.
- [22] Yam, V. W. W.; Lee, V. W. M.; Cheung, K. K., *J. Chem. Soc.-Chem. Commun.* **1994**, 2075-2076.
- [23] Qu, Y.; Scarsdale, N. J.; Tran, M. C.; Farrell, N. P., *J. Biol. Inorg. Chem.* **2003**, *8*, 19-28.
- [24] Field, J. S.; Gertenbach, J. A.; Haines, R. J.; Ledwaba, L. P.; Mashapa, N. T.; McMillin, D. R.; Munro, O. Q.; Summerton, G. C., *Dalton Trans.* **2003**, 1176-1180.
- [25] McCoubrey, A.; Latham, H. C.; Cook, P. R.; Rodger, A.; Lowe, G., *FEBS Lett.* **1996**, *380*, 73-78.
- [26] Wang, A. H. J.; Nathans, J.; Van der Marel, G.; Van Boom, J. H.; Rich, A., *Nature* **1978**, *276*, 471-474.
- [27] Wong, Y.; Lippard, S. J., *J. Chem. Soc.-Chem. Commun.* **1977**, 824-825.
- [28] Peyratout, C. S.; Aldridge, T. K.; Crites, D. K.; McMillin, D. R., *Inorg. Chem.* **1995**, *34*, 4484-4489.
- [29] Lowe, G.; McCloskey, J. A.; Ni, J. S.; Vilaivan, T., *Bioorg. Med. Chem.* **1996**, *4*, 1007-1013.
- [30] Lowe, G.; Vilaivan, T., *Journal of the Chemical Society-Perkin Transactions 1* **1996**, 1499-1503.
- [31] Bugarcic, Z. D.; Heinemann, F. W.; van Eldik, R., *Dalton Trans.* **2004**, 279-286.
- [32] (a) Chan, H.-L.; Ma, D.-L.; Yang, M.; Che, C.-M., *ChemBiochem* **2003**, *4*, 62-68. (b) Chan, H.-L.; Ma, D.-L.; Yang, M.; Che, C.-M., *J. Biol. Inorg. Chem.* **2003**, *8*, 761-769. (c) Lowe, G.; Droz, A. S.; Park, J. J.; Weaver, G. W., *Bioorganic Chem.* **1999**, *27*, 477-486.
- [33] Lowe, G.; Droz, A. S.; Vilaivan, T.; Weaver, G. W.; Park, J. J.; Pratt, J. M.; Tweedale, L.; Kelland, L. R., *J. Med. Chem.* **1999**, *42*, 3167-3174.

Chapter 5

Trinuclear and tetranuclear ruthenium and platinum complexes with long and flexible linkers: syntheses, characterization and biological properties

Abstract – The complexes [(dtdeg)Ru(dtdeg)]Cl₂ (**1**) and [(dtdeg)Ru(dtdeg)Ru(dtdeg)]Cl₄ (**2**) (dtdeg = bis[4'-(2,2':6',2'')-terpyridyl]-diethyleneglycolether) have been used for the synthesis of the trinuclear and tetranuclear ruthenium(II)-ruthenium(III) complexes [Cl₃Ru(dtdeg)Ru(dtdeg)RuCl₃]Cl₂ (**3**) and [Cl₃Ru(dtdeg)Ru(dtdeg)Ru(dtdeg)RuCl₃]Cl₄ (**4**), and the ruthenium(II)-platinum(II) mixed-metal compounds [ClPt(dtdeg)Ru(dtdeg)PtCl]Cl₄ (**5**) and [ClPt(dtdeg)Ru(dtdeg)Ru(dtdeg)PtCl]Cl₆ (**6**). The paramagnetic complexes **3** and **4** have been characterized by ¹H NMR spectroscopy, including 1D ¹H NOE difference experiments. The hyperfine shifts of the paramagnetic signals of **3** and **4** display Curie behavior, and are suggested to be mainly dipolar of origin. The characterization of complexes **5** and **6** is also presented.

In general, the complexes do not show significant cytotoxicity against different cancer cell lines. However, inhibition of cell growth is observed, and is highest for the tetranuclear complexes. Complex **4** exhibits an IC₅₀ value of 8 μM against A2780cis cells, and displays moderate activity against the A2780R cell line. Complex **6** displays moderate activity against A2780 and L1210 cells. Interestingly, A2780cis cells adhere together and form clots upon incubation with **4**. This effect appears to be characteristic for the molecular structure of **4** and the A2780cis cell line.

5.1 Introduction

The development of polynuclear platinum complexes as anticancer agents is a productive field of research.^[1] The α,ω -diaminoalkane-linked polynuclear platinum complexes developed by Farrell *et al.* have extensively been examined.^[2] It appears that chain length and flexibility, and charge and hydrogen-bonding capabilities are of importance for their activity. The long and flexible linker has been found to allow the formation of long-range adducts on DNA,^[2] which is the target of platinum anticancer complexes.^[3] The positive charge of these promising class of polynuclear complexes has been shown to assist in DNA binding by preassociation to the duplex through electrostatic interactions.^[4] The trinuclear complex BBR3464, $[\{trans\text{-PtCl}(\text{NH}_3)_2\}_2\{\mu\text{-trans-Pt}(\text{NH}_3)_2(\text{H}_2\text{N}(\text{CH}_2)_6\text{NH}_2)_2\}]^{4+}$ (1,0,1/t,t,t), is the most active complex within the series, and has entered clinical trials.^[5] Compared to the dinuclear derivatives, BBR3464 contains a positively charged tetraamine-platinum linker. This linker supports an extraordinary way of DNA binding, *i.e.* it preassociates in the minor groove, whereas the outer platinum units of the trinuclear complex subsequently coordinate in the major groove.^[6]

Results from studies with polynuclear terpyridine platinum complexes have also indicated the importance of a charged linker.^[7] These dinuclear complexes display less activity against different cell lines upon increasing the length of their dipyridyl linker, which has ethynyl bonds of variable lengths, with or without phenyl groups in between. However, a trinuclear complex, in which a positively charged diaminedi(4,4'-bipyridine)platinum unit links the two platinum terpyridine units, does show high activity.

A small variety of polynuclear ruthenium^[8, 9] and heteropolynuclear ruthenium-platinum complexes have also been designed and studied as anticancer agents.^[10, 11] The relatively long and flexible linker dtdeg (dtdeg = bis[4'-(2,2':6',2''-terpyridyl)]-diethyleneglycolether) has been used for the syntheses of dinuclear polypyridyl ruthenium complexes, as presented in Chapters 2 and 3. The complexes consist of at least one substitution-inert ruthenium moiety, or of two units which are capable of monofunctional coordination after dissociation of the labile chloride ligand. It has been demonstrated that the complexes do not display significant cytotoxicity against different cell lines. In Chapter 4, heterodinuclear ruthenium-platinum derivatives have been described, which were developed based upon the cytotoxic^[7] complex $[\text{Pt}(\text{tpy})\text{Cl}]\text{Cl}$ (tpy = 2,2':6',2''-terpyridine). These complexes do not show activity either. The data presented suggest that the platinum moiety is capable of both intercalation and coordination to the DNA.^[11] However, even when the platinum moiety is linked to the trichlororuthenium moiety, which is derived from the antitumor active^[12] complex $[\text{Ru}(\text{tpy})\text{Cl}_3]$, cytotoxicity is not achieved.

In this Chapter, the complexes $[(\text{dtdeg})\text{Ru}(\text{dtdeg})]\text{Cl}_2$ (**1**) and $[(\text{dtdeg})\text{Ru}(\text{dtdeg})\text{Ru}(\text{dtdeg})]\text{Cl}_4$ (**2**) are presented. They have been produced for the assembly of flexible and particularly long polynuclear ruthenium and platinum terpyridine complexes. The linker-complexes **1** and **2** contain one or two positively charged bis(terpyridyl)-ruthenium(II) moieties, respectively, to enhance water solubility and DNA affinity by electrostatic interactions. They have been used to join two ruthenium(III) or two platinum(II) units, which resemble the mononuclear complexes $[\text{Ru}(\text{tpy})\text{Cl}_3]$ and $[\text{Pt}(\text{tpy})\text{Cl}]\text{Cl}$, respectively. The antitumor activity of $[\text{Ru}(\text{tpy})\text{Cl}_3]$ has been suggested to be due to DNA coordination by interstrand binding to two guanines.^[12, 13] DNA intercalation and coordination have been reported^[7, 14] to account for the cytotoxicity of $[\text{Pt}(\text{tpy})\text{Cl}]\text{Cl}$. The synthesis and characterization of the trinuclear and tetranuclear ruthenium(II)-ruthenium(III) complexes $[\text{Cl}_3\text{Ru}(\text{dtdeg})\text{Ru}(\text{dtdeg})\text{RuCl}_3]\text{Cl}_2$ (**3**) and $[\text{Cl}_3\text{Ru}(\text{dtdeg})\text{Ru}(\text{dtdeg})\text{Ru}(\text{dtdeg})\text{RuCl}_3]\text{Cl}_4$ (**4**) (Figure 5.1), and of the ruthenium(II)-platinum(II) mixed-metal compounds $[\text{ClPt}(\text{dtdeg})\text{Ru}(\text{dtdeg})\text{PtCl}]\text{Cl}_4$ (**5**) and $[\text{ClPt}(\text{dtdeg})\text{Ru}(\text{dtdeg})\text{Ru}(\text{dtdeg})\text{PtCl}]\text{Cl}_6$ (**6**) (Figure 5.1), are presented in this Chapter. The complexes have been tested for their cytotoxicity using a variety of cancer cell lines.

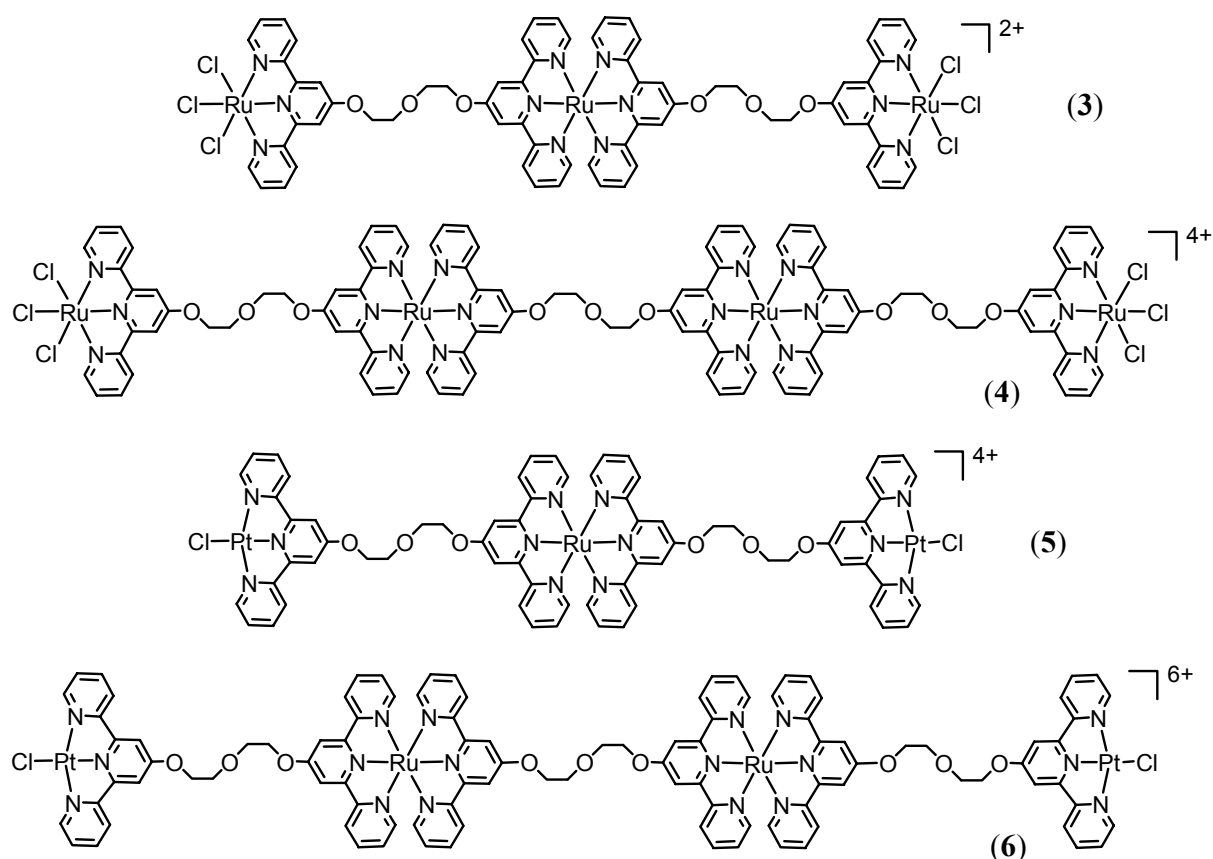


Figure 5.1 The polynuclear cationic ruthenium(II)-ruthenium(III) complexes **3** and **4**, and the polynuclear cationic ruthenium(II)-platinum(II) complexes **5** and **6**.

5.2 Experimental section

5.2.1 General methods and starting materials

Elemental analyses on C, H and N were performed on a Perkin Elmer series II CHNS/O Analyzer 2400. Electrospray mass spectra were recorded on a Finnigan TSQ-quantum instrument with an electrospray interface (ESI). Hydrated $\text{RuCl}_3 \cdot x\text{H}_2\text{O}$ ($x \sim 3$) and K_2PtCl_4 were used as received from Johnson & Matthey. The ligand dtdeg, the complex $[\text{Cl}_3\text{Ru}(\text{dtdeg})\text{RuCl}_3]$, and the 0.1 M ruthenium(III) solution have previously been synthesized,^[15] their synthesis is described in Chapter 2 for convenience.

5.2.2 ^1H NMR measurements

^1H NMR and ^{195}Pt NMR spectra were acquired on a Bruker DPX 300 and DMX 600 spectrometer. ^1H NOE difference spectra were measured on a Bruker DMX 600 spectrometer. Spectra were recorded in deuterated DMSO, and calibrated on residual solvent peak at δ 2.49 ppm. 1D ^1H spectra of the paramagnetic complexes were obtained using a 100 ppm spectral width. Longitudinal relaxation times were measured by the standard inversion-recovery method, with 7 s relaxation delay and a spectral width of 100 ppm. Variable delays ranged from 50 μs to 500 ms to define the T_1 values for the proton signals of the paramagnetic ruthenium(III) moiety, and from 100 ms to 5000 ms to define the T_1 values for the proton signals of the diamagnetic ruthenium(II) moiety. Magnetization recovery was exponential within experimental error. T_2 values were estimated from the peak half-widths. The COSY spectra were obtained by collecting 1024 $F_2 \times 1024 F_1$ data points with a relaxation delay of 20 ms. 1D NOE experiments were carried out according to published procedures.^[16] These procedures include a WEFT pulse sequence, which was not applied here. The irradiation time used for the 1D NOE experiment was 500 ms, and the number of scans 16384.

5.2.3 Syntheses

$[(\text{dtdeg})\text{Ru}(\text{dtdeg})]\text{Cl}_2$, (1): The ligand dtdeg (600 mg; 1.06 mmol), triethylamine (0.15 mL; 1.16 mmol), and 3 mL of the 0.1 M ruthenium(III) solution (0.30 mmol) were stirred under nitrogen for 20 minutes in 100 mL of a EtOH/ H_2O mixture (v:v = 3:1). Subsequently, the mixture was refluxed for 18 hours under nitrogen. The mixture was evaporated *in vacuo* with EtOH for three times. The resulting precipitate (mainly unreacted dtdeg) was filtered off, and the filtrate was concentrated *in vacuo*. The product was purified by column chromatography

on neutral alumina with EtOH/CH₃CN (v:v = 1:1) as the eluents. From the first part of the red band, pure product was isolated by precipitation of the particular fraction with diethyl ether. Yield: 89 mg (23 %). Elemental analysis (%) calculated for C₆₈H₅₆Cl₂N₁₂O₆Ru·5H₂O (water, originating from the used solvents, was used to fit the elemental analysis as the C/N ratio of the analysis corresponds to the structural formula of the complex): C 58.37, N 12.01, H 4.75. Found: C 58.05, N 12.03, H 5.09. ESI-MS: *m/z*: 619 [M²⁺], 413 [M²⁺+H⁺]. ¹H NMR (600 MHz, DMSO, 310 K): δ = 8.60 (d, 4H; I33''), 7.97 (t, 4H; I44''), 7.47 (t, 4H; I55''), 8.66 (d, 4H; I66''), 8.02 (s, 4H; I3'5'), 4.51 (t, 4H; 1), 4.06 (t, 4H; 2), 8.80 (d, 4H; I'33''), 7.94 (t, 4H; I'44''), 7.19 (t, 4H; I'55''), 7.43 (d, 4H; I'66''), 8.78 (s, 4H; I'3'5'), 4.74 (t, 4H; 1'), 4.14 ppm (t, 4H; 2').

[(dtdeg)Ru(dtdeg)Ru(dtdeg)]Cl₄, (2): An excess of AgBF₄ (580 mg) was dissolved in 45 mL of acetone and filtered. [Cl₃Ru(dtdeg)RuCl₃] (150 mg; 0.15 mmol) was added to the filtrate and the mixture was refluxed in the dark for 16 hours to remove the chloride ions from ruthenium. After filtration to remove precipitated AgCl, the filtrate was evaporated *in vacuo*, which resulted in a green oil (~ 1.5 mL). The ligand dtdeg (340 mg; 0.60 mmol) was added and the mixture was refluxed for 1 hour in 35 mL of DMF, which acted as the reducing agent. The red reaction mixture was filtered, and the filtrate was evaporated *in vacuo* until a red oil resulted (~ 1.5 mL). To synthesize the chloride salt of the product, 12 mL of a saturated LiCl solution in EtOH was added to the oil. The desired product was obtained by precipitation with 350 mL of acetone. Column chromatography on neutral alumina with acetone/MeOH/EtOH (v:v:v = 7:1:2) yielded pure product from the first fraction by precipitation with diethyl ether. Yield: 51 mg (16 %). Elemental analysis (%) calculated for C₁₀₂H₈₄Cl₄N₁₈O₉Ru₂·8H₂O (water, originating from the used solvents, was used to fit the elemental analysis as the C/N ratio of the analysis corresponds to the structural formula of the complex): C 55.84, N 11.49, H 4.59. Found: C 54.12, N 11.15, H 4.00. ESI-MS: *m/z*: 477 [M⁴⁺], 382 [M⁴⁺+H⁺]. ¹H NMR (600 MHz, DMSO, 293 K): δ = 8.62 (d, 4H; I33''), 8.02 (t, 4H; I44''), 7.49 (t, 4H; I55''), 8.68 (d, 4H; I66''), 8.04 (s, 4H; I3'5'), 4.49 (t, 4H; 1), 4.04 (t, 4H; 2), 8.88 (d, 4H; I'33''), 7.98 (t, 4H; I'44''), 7.24 (t, 4H; I'55''), 7.50 (d, 4H; I'66''), 8.86 (s, 4H; I'3'5'), 4.72 (t, 4H; 1'), 4.11 ppm (t, 4H; 2'), 8.97 (d, 4H; II33''), 7.91 (t, 4H; II44''), 7.21 (t, 4H; II55''), 7.47 (d, 4H; II66''), 8.95 (s, 4H; II3'5'), 4.81 (t, 4H; 1''), 4.20 ppm (t, 4H; 2'').

[Cl₃Ru(dtdeg)Ru(dtdeg)RuCl₃]Cl₂, (3): **1** (70 mg; 0.054 mmol) was dissolved in 27 mL of MeOH. At reflux temperature, 2 mL of 0.1 M ruthenium(III) solution was added to the solution. The mixture was refluxed for 3 hours and the resulting precipitate was filtered at RT. To remove any insoluble species (probably ruthenium-oxo species), the crude product was dissolved in 400 mL of hot MeOH, and filtered. The filtrate was concentrated *in vacuo* and the product was precipitated with diethyl ether. After filtration of the mixture, the residue was

extensively washed with diethyl ether resulting in pure product. Yield: 53 mg (57 %). Elemental analysis (%) calculated for $C_{68}H_{56}Cl_8N_{12}O_6Ru_3 \cdot 6H_2O \cdot HCl$ (Besides water (*vide supra*), HCl was used to fit the elemental analysis, as the product precipitates from an acidic solution and an aqueous solution of the product is slightly acidic): C 43.71, N 8.99, H 3.72. Found: C 43.43, N 8.89, H 3.67. ESI-MS: m/z : 826 $[M^{2+}]$. 1H NMR (600 MHz, DMSO, 327 K): δ = -8.52 (s, 4H; I33''), 0.96 (s, 4H; I44''), -9.91 (s, 4H; I55''), -30.25 (s, 4H; I66''), 4.80 (s, 4H; I3'5'), 14.20 (s, 4H; 1), 4.15 (s, 4H; 2), 9.26 (s, 4H; I'33''), 8.14 (s, 4H; I'44''), 7.21 (s, 4H; I'55''), 7.92 (s, 4H; I'66''), 9.48 (s, 4H; I'3'5'), 5.28 (s, 4H; 1'), 4.40 ppm (s, 4H; 2').

$[Cl_3Ru(dtdeg)Ru(dtdeg)Ru(dtdeg)RuCl_3]Cl_4$, (4): 2 (70 mg; 0.034 mmol) was dissolved in 30 mL of MeOH. At reflux temperature, 1.4 mL of the 0.1 M ruthenium(III) solution was added to the solution. The mixture was refluxed for 3 hours and the resulting precipitate was filtered at RT. To remove any insoluble species (probably ruthenium oxo species), the crude product was dissolved in 300 mL of hot MeOH, and filtered. The filtrate was concentrated *in vacuo* and the product was precipitated with diethyl ether. After filtration of the mixture, the residue was extensively washed with diethyl ether resulting in pure product. Yield: 60 mg (71 %). Elemental analysis (%) calculated for $C_{102}H_{84}Cl_{10}N_{18}O_9Ru_4 \cdot 12H_2O \cdot 1.5HCl$ (Besides water (*vide supra*), HCl was used to fit the elemental analysis, as the product precipitates from an acidic solution and an aqueous solution of the product is slightly acidic): C 44.78, N 9.22, H 4.03. Found: C 44.35, N 9.12, H 3.77. 1H NMR (600 MHz, DMSO, 315 K): δ = -8.41 (s, 4H; I33''), 1.08 (s, 4H; I44''), -9.99 (s, 4H; I55''), -30.88 (s, 4H; I66''), 4.93 (s, 4H; I3'5'), 15.04 (s, 4H; 1), 4.35 (s, 4H; 2), 9.59 (s, 4H; I'33''), 8.37 (s, 4H; I'44''), 7.60 (s, 4H; I'55''), 7.98 (s, 4H; I'66''), 9.76 (s, 4H; I'3'5'), 5.52 (s, 4H; 1'), 4.66 ppm (s, 4H; 2'), 9.38 (s, 4H; II33''), 8.29 (s, 4H; II44''), 7.50 (s, 4H; II55''), 8.09 (s, 4H; II66''), 9.36 (s, 4H; II3'5'), 5.23 (s, 4H; 1''), 4.57 ppm (s, 4H; 2'').

$[ClPt(dtdeg)Ru(dtdeg)PtCl]Cl_4$, (5): 1 (39 mg; 0.031 mmol) and $[Pt(cod)Cl_2]$ (32 mg; 0.087 mmol) were refluxed in 37 mL MeOH for 6 hours. The reaction mixture was cooled to RT and filtered. The product was obtained by slow precipitation of the filtrate with diethyl ether. Yield: 43 mg (76 %). Elemental analysis (%) calculated for $C_{68}H_{56}Cl_6N_{12}O_6Pt_2Ru \cdot 11H_2O$ (water, originating from the used solvents, was used to fit the elemental analysis as the C/N ratio of the analysis corresponds to the structural formula of the complex): C 40.05, N 8.24, H 3.85. Found: C 40.39, N 8.41, H 3.90. 1H NMR (600 MHz, DMSO, 312 K): δ = 8.85 (d, 4H; I33''), 8.46 (t, 4H; I44''), 7.93 (t, 4H; I55''), 8.90 (d, 4H; I66''), 8.55 (s, 4H; I3'5'), 4.74 (t, 4H; 1), 4.12 (t, 4H; 2), 8.95 (d, 4H; I'33''), 7.97 (t, 4H; I'44''), 7.23 (t, 4H; I'55''), 7.45 (d, 4H; I'66''), 8.87 (s, 4H; I'3'5'), 4.78 (t, 4H; 1'), 4.15 ppm (t, 4H; 2'). ^{195}Pt NMR (300 MHz, MeOH, 298 K): δ = -2702 ppm.

[ClPt(dtdeg)Ru(dtdeg)Ru(dtdeg)PtCl]Cl₆, (6): 2 (45 mg; 0.022 mmol) and [Pt(cod)Cl₂] (25 mg; 0.068 mmol) were refluxed in 40 mL MeOH for 6 hours. The reaction mixture was cooled to RT and filtered. **6** was obtained by slow precipitation of the filtrate with diethyl ether. Yield: 37 mg (62 %). Elemental analysis (%) calculated for C₁₀₂H₈₄Cl₈N₁₈O₉Pt₂Ru₂·12H₂O (water, originating from the used solvents, was used to fit the elemental analysis as the C/N ratio of the analysis corresponds to the structural formula of the complex): C 43.79, N 9.01, H 3.89. Found: C 43.95, N 9.30, H 4.15. ¹H NMR (600 MHz, DMSO, 298 K): δ = 8.86 (d, 4H; I33''), 8.44 (t, 4H; I44''), 7.90 (t, 4H; I55''), 8.74 (d, 4H; I66''), 8.52 (s, 4H; I3'5'), 4.71 (t, 4H; 1), 4.10 (t, 4H; 2), 9.01 (d, 4H; I'33''), 7.95 (t, 4H; I'44''), 7.23 (t, 4H; I'55''), 7.50 (d, 4H; I'66''), 8.94 (s, 4H; I'3'5'), 4.79 (t, 4H; 1'), 4.14 (t, 4H; 2'), 8.98 (d, 4H; II33''), 7.82 (t, 4H; II44''), 7.19 (t, 4H; II55''), 7.46 (d, 4H; II66''), 8.99 (s, 4H; II3'5'), 4.86 (t, 4H; 1''), 4.22 ppm (t, 4H; 2''). ¹⁹⁵Pt NMR (300 MHz, MeOH, 298 K): δ = -2699 ppm.

5.2.4 Cytotoxicity tests

Cell cultures: A2780cis and A2780R cells (cisplatin sensitive and resistant human ovarian carcinoma, respectively) were maintained in Dulbecco's modified Eagle's Medium (DMEM: Gibco BRL™, Invitrogen Corporation, The Netherlands) supplemented with 10 % fetal calf serum (Perbio Science, Belgium), penicillin (100 units/mL: Duchefa Biochemie BV, The Netherlands) and streptomycin (100 µg/mL: Duchefa Biochemie BV, The Netherlands) in a humidified 6 % CO₂, 94 % air atmosphere. L1210/0 and L1210/2 cells (cisplatin sensitive and resistant mouse leukemia, respectively) were grown (partly in suspension and partly weakly adherent to the flasks) under the same conditions as mentioned above.

Hs683 and U-373MG glioblastoma cells, HCT-15 and LoVo colorectal cancer cells, A549 lung cancer and MCF-7 breast cancer cells were cultured at 310 K in sealed (airtight) Falcon plastic dishes (Nunc, Gibco, Belgium) containing Eagle's minimal essential medium (MEM, Gibco) supplemented with 5 % fetal calf serum (FCS). All the media were supplemented with a mixture of 0.6 mg/mL glutamine (Gibco), 200 IU/mL penicillin (Gibco), 200 IU/mL streptomycin (Gibco) and 0.1 mg/mL gentamycin (Gibco). The FCS was heat-inactivated for 1 hour at 329 K.

Cells from confluent monolayers were removed from the flasks by a 0.05 % trypsin solution. Cell viability was determined by the trypan blue exclusion test.

In vitro cytotoxicity evaluation: Cell growth was determined by the MTT assay, a colorimetric assay based on the ability of viable cells to reduce the soluble yellow 3-(4,5-dimethylthiazol-2-yl)-2,5-diphenyl-2H-tetrazolium bromide to blue formazan crystals by the

mitochondria.^[17] Cells were seeded between 1000 and 5000 cells/well (depending on the cell type) onto 96-well plates (Corning Costar[®]) in 100 μ L of complete medium with 5 to 10 % of FCS. Cells were treated 24 hours after the sowing by adding 100 μ L of complete medium containing the test compounds at the appropriate concentrations.

Final tested concentrations ranged between 1 μ M and 50 μ M and have been obtained by several dilutions from stock solutions in sterile water. Stock solutions of 0.2 mM or 0.67 mM were prepared for the trinuclear and tetranuclear complexes, respectively. A 4 mM stock solution of [Ru(tpy)Cl₃] was prepared in DMSO, because of poor water solubility. A 40 μ M solution contained 1 % of DMSO, which was on average not of influence on cell growth. After 72 hours of incubation at 310 K, cells were incubated with 1 mg/mL MTT solution for 2 to 4 hours at 310 K. Subsequently, the medium was discarded and the formed crystals were dissolved in 100 μ L DMSO per well. Optical density (OD) was measured at 590 nm using a Biorad 550 microplate reader. The OD is directly proportional to the number of living cells, which are compared to the control (untreated cells).

5.3 Results and discussion

5.3.1 Characterization of the linker-complexes 1 and 2

The linker-complex [(dtdeg)Ru(dtdeg)]Cl₂ (**1**) has been characterized by ¹H NMR experiments in analogy with the characterization of [(dtdeg)Ru(dtdeg)Ru(dtdeg)]Cl₄ (**2**), which will be illustrated here. The 1D ¹H NMR spectrum of **2** in DMSO-*d*₆ is given in Figure 5.2. Assignments have been made by 2D ¹H NMR experiments. The six signals for the ethylene protons of the linker indicate the presence of a C₂ symmetry axis between the two ruthenium moieties. In the aromatic region, three sets of signals have been identified for the three inequivalent terpyridine ligands I, I' and II, which indicate a second C₂ symmetry axis. The 33'' signals and 66'' signals have been assigned by their specific J coupling constants of ~ 9 Hz and ~ 6 Hz, respectively. The aromatic signals of the terpyridine ligand I have been selected by the relatively downfield shift of the I66'' signal in comparison to that of I'66'' and II66''. The I'66'' protons are shielded by the aromatic terpyridine ligand II, and the II66'' protons are shielded by the terpyridine ligand I'. Therefore, both the I'66'' and II66'' resonances are shifted relatively upfield.

A I3'5'-I33'' NOE is not observed, probably because of fast rotation of the outer pyridine rings of the terpyridine ligand I. These pyridines are not in a fixed position, as they are not coordinated to the ruthenium ion. Fast rotation of the outer pyridine rings of I is clearly observed for **1**. The sign of a NOE cross peak in a NOESY spectrum depends on the

reciprocal of the rotational correlation time. Due to a difference in the rate of rotation between the outer pyridines of terpyridine ligand I and those of I', the I33''–I44'', I44''–I55'', I55''–I66'' and I3'5'–I' NOEs are of opposite sign (opposite to the diagonal) in comparison to the corresponding NOEs of terpyridine ligand I', which is coordinated to ruthenium. At 600 MHz, all NOEs displayed by **1** are of similar sign. This observation agrees with the fact that the strength of the magnetic field is also of influence on the sign of a NOE. The ¹H 2D NOESY NMR experiment of **2** has only been performed at 600 MHz, where a similar sign for all NOEs has been identified.

The I'3'5'–I'33'' and II3'5'–II33'' NOEs are not observed, presumably due to overlap with the diagonal. Therefore, the 33'' doublet at 8.88 ppm and the singlet at 8.86 ppm have been attributed to the similar terpyridine ligand (either I' or II), as well as the 33'' doublet and the singlet at 8.97 and 8.95 ppm, respectively. The singlet at 8.04 ppm has been assigned to the I3'5' protons. The terpyridine ligands I' and II have been distinguished using the 2-2' cross peak of the ethylene-linker protons, which is displayed in the NOESY spectrum of **2**. The I' resonances have subsequently been assigned via the 2'-1' COSY cross peak and the I'3'5'–I' NOE cross peak.

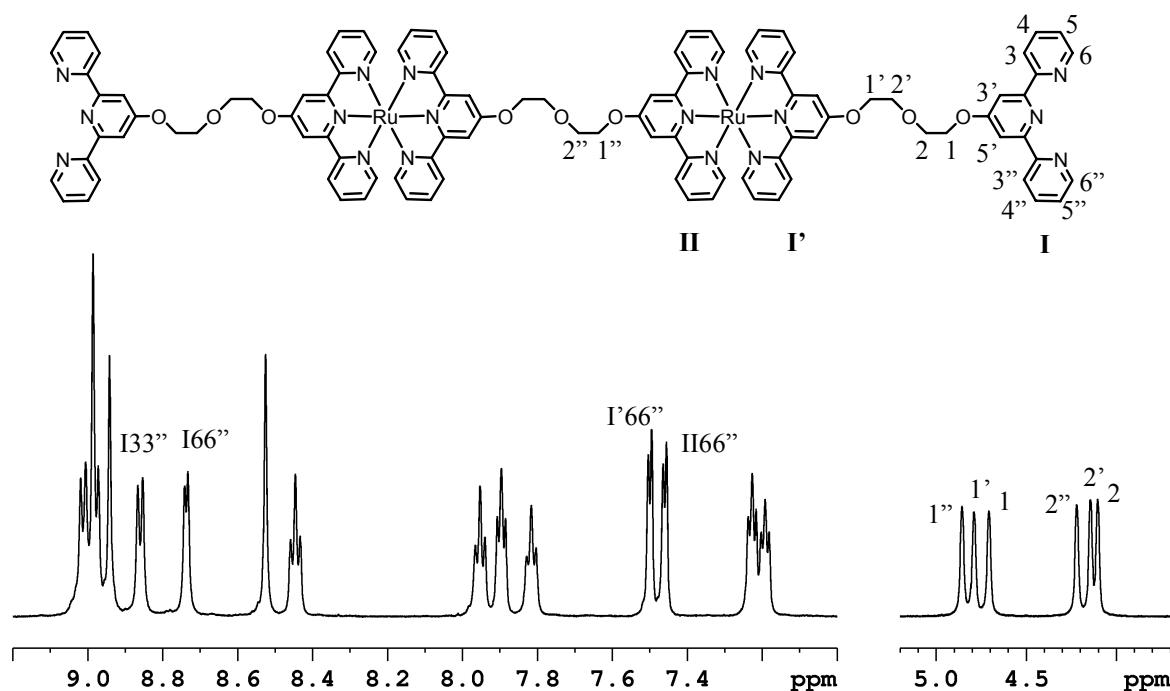


Figure 5.2 1D ¹H NMR spectrum of **2** in DMSO-*d*₆ at 293 K with some assignments, and a schematic representation of the cation of **2**. The numbering scheme given for terpyridine ligand I is also applicable to ligands I' and II.

5.3.2 Characterization of the paramagnetic trinuclear ruthenium complex **3**

The complex $[\text{Cl}_3\text{Ru}(\text{dtdeg})\text{Ru}(\text{dtdeg})\text{RuCl}_3]\text{Cl}_2$ (**3**) is a paramagnetic species, due to the presence of an unpaired electron in the t_{2g} orbital of the low-spin ruthenium(III) ions. Therefore, ^1H NMR resonances of the ruthenium(III) moieties are significantly broadened and shifted (Figure 5.3). Signals from the central diamagnetic ruthenium(II) moiety are broadened to some extent, but are observed in the normal diamagnetic envelop. In Chapter 2 of this thesis, a strategy for the characterization of paramagnetic trichlororuthenium(III)-terpyridine complexes by ^1H NMR spectroscopy has been presented using the complex $[(\text{tpy})\text{Ru}(\text{dtdeg})\text{RuCl}_3]^{2+}$ as a model compound. A similar strategy will be used for the characterization of **3** (and **4**).

The ^1H NMR spectrum of **3** has been acquired at 327 K. At this temperature the “paramagnetic” signals, *i.e.* the resonances of the paramagnetic ruthenium(III) moiety, do not overlap. The signal at 4.80 ppm has also been established as a “paramagnetic” signal, since it exhibits short longitudinal (T_1) and transverse (T_2) relaxation times (11 and 8 ms, respectively). Five resonances of similar intensity are observed in the aromatic region of the ^1H NMR spectrum for the terpyridine I' signals of the ruthenium(II) unit of **3**, which indicate the presence of two C_2 symmetry axes within the molecule. The resonances have been assigned by 2D COSY ^1H NMR experiments, using a relaxation delay of 20 ms (Figure 5.4).

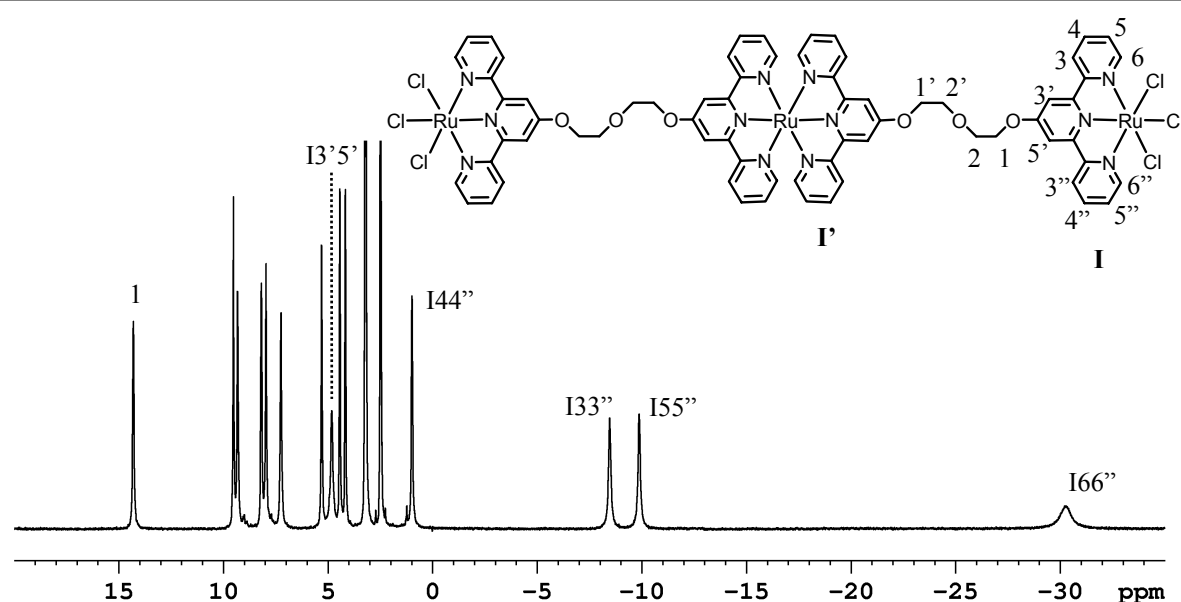


Figure 5.3 1D ^1H NMR spectrum of **3** in $\text{DMSO-}d_6$ at 327 K with the “paramagnetic” signals indicated, and molecular structure of the cation of **3**. The numbering scheme of I is also applicable to I'.

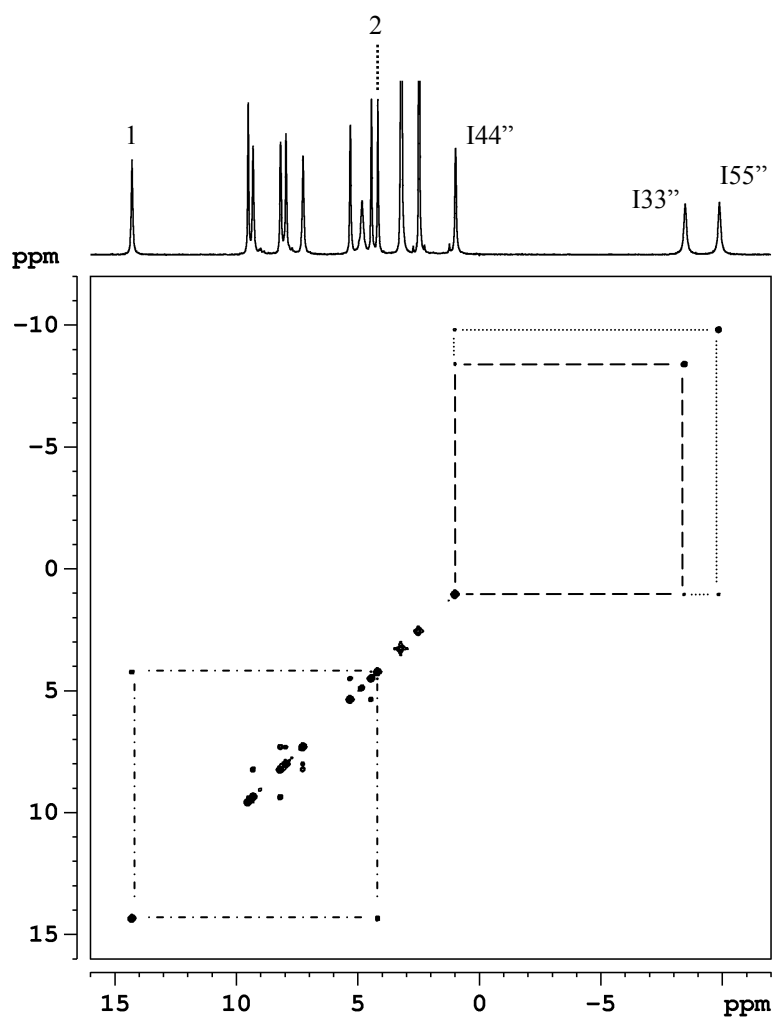


Figure 5.4 2D ^1H COSY NMR spectrum of **3** in $\text{DMSO-}d_6$ at 327 K with some cross peaks indicated, and some assignments given.

The I'33'' and I'66'' signal have been assigned by the characteristic upfield shift of the latter. The shift is due to deshielding of the aromatic rings. In analogy to **1**, the two resonances at 5.28 and 4.40 ppm have been ascribed to the diethylene protons 1' and 2', respectively.

In agreement with the double C_2 symmetry of the complex, five resonances have also been found for the protons of the paramagnetic ruthenium(III) units. They have partly been assigned by 2D COSY ^1H NMR spectroscopy (Figure 5.4). The signal at -30.25 ppm appears to be too broad to show cross peaks. In analogy with the complexes $[(\text{tpy})\text{Ru}(\text{dtdeg})\text{RuCl}_3]^{2+}$ (Chapter 2) and $[\text{Ru}(\text{tpy})\text{Cl}_3]$,^[15] the signal has been assigned to the I66'' protons. These are the protons closest to the paramagnetic ruthenium(III) moiety, and can therefore be expected to shift the most. The “paramagnetic” resonance at 0.96 ppm displays cross peaks to the signals at -8.52 and -9.91 ppm; hence, it has been attributed to the I44'' protons. The I33'' and I55'' protons cannot be assigned, yet. A two-spin system is shown by the resonances at 14.20

and 4.15 ppm, which assigns these signals to the diethylene protons 1 and 2. The resonance at 14.20 ppm has been ascribed to the linker protons 1, since they are closest to the paramagnetic center. 1D NOE difference experiments (Figure 5.5) complete the assignment of **3**.

Upon irradiation of the paramagnetic signal at 4.80 ppm, signal enhancements are displayed by the diethylene protons 1 at 14.20 ppm, and by the resonance at -8.52 ppm. As a result, the signal at 4.80 ppm has been assigned to the I3'5' protons. Consequently, the signal at -8.52 ppm can be ascribed to the I33'' protons. Irradiation of the largely shifted and broadened I66'' resonance at -30.25 ppm only results in a small NOE of the signal at -9.91 ppm.

The chemical shifts of all paramagnetic resonances have been monitored in the temperature range from 300 to 360 K. All signals appear to shift gradually to the diamagnetic region upon increasing the temperature. The observed chemical shifts have been plotted against reciprocal temperatures T^{-1} (Figure 5.6). For all resonances a linear decrease in the hyperfine shift is observed upon a stepwise decrease of $1/T$, which indicates Curie behavior. The intercepts, which are extrapolated at infinite temperature, differ only slightly from the diamagnetic values for most signals.

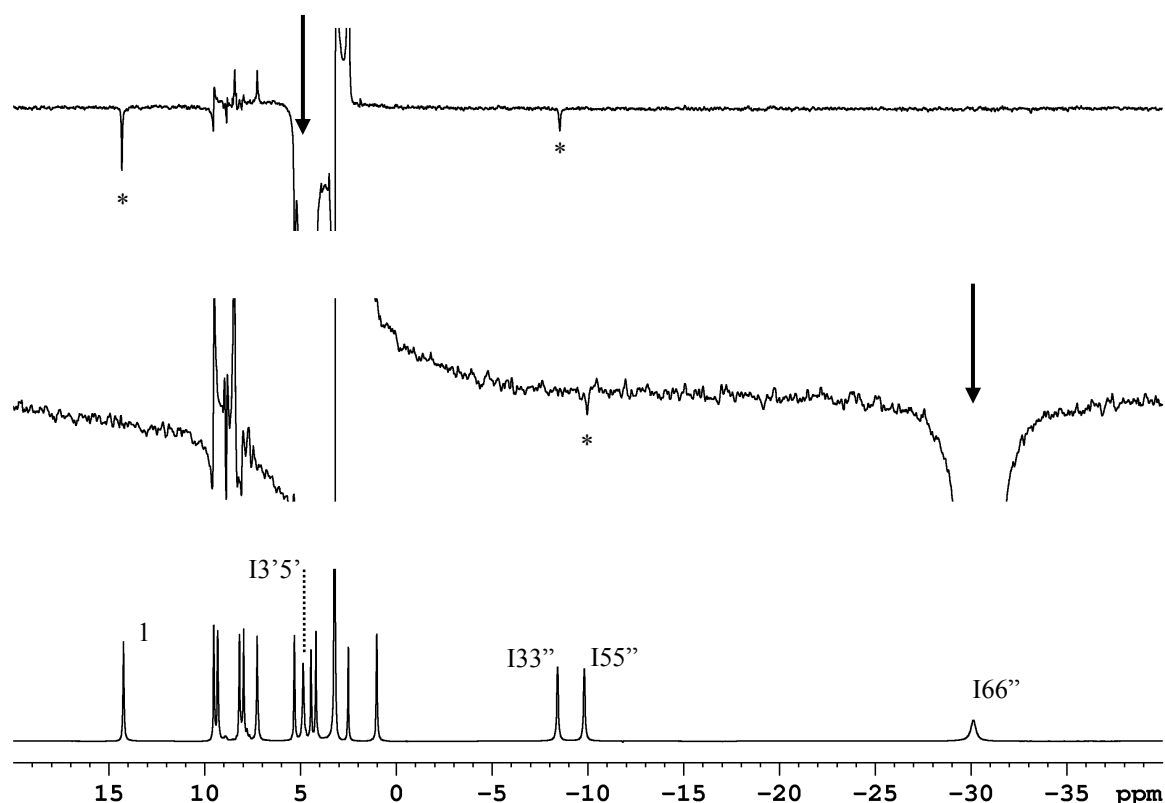


Figure 5.5 1D ^1H NOE difference NMR spectra (top and middle) and 1D ^1H NMR spectrum (bottom) of **3** in $\text{DMSO-}d_6$ at 327 K. Irradiated signals are indicated with an arrow. NOE's are indicated by an asterisk.

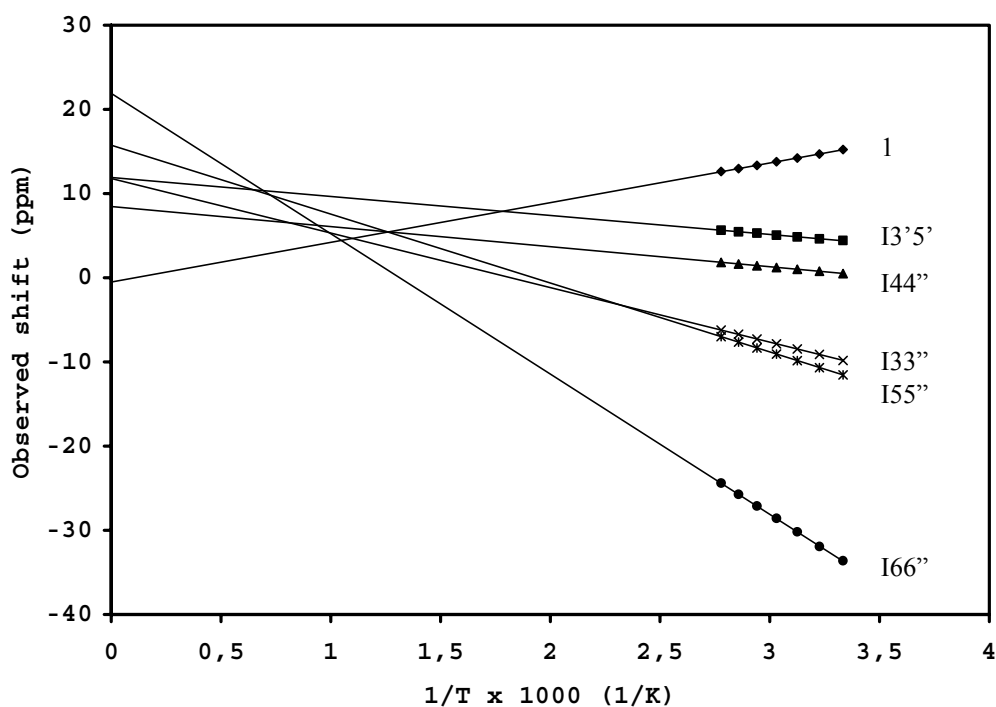


Figure 5.6 Plots of the chemical shifts *versus* $1/T$ for the “paramagnetic” signals of **3**.

Both dipolar and contact hyperfine interactions are likely to contribute to the hyperfine shift of complex **3**, as has been suggested for the analogues trichlororuthenium complex $[(\text{tpy})\text{Ru}(\text{dtdeg})\text{RuCl}_3]\text{Cl}_2$ (see Chapter 2 for more details).

5.3.3 Characterization of the paramagnetic tetranuclear ruthenium complex **4**

The complex $[\text{Cl}_3\text{Ru}(\text{dtdeg})\text{Ru}(\text{dtdeg})\text{Ru}(\text{dtdeg})\text{RuCl}_3]\text{Cl}_4$ (**4**) displays a spectrum similar to that of **3**. The “paramagnetic signals” of the ruthenium(III) moieties are observed outside the diamagnetic region, whereas the signals of the diamagnetic ruthenium(II) moieties are found within this region. The ^1H NMR spectrum of **4** in $\text{dms}\text{-}d_6$ at 315 K (overlap of “paramagnetic” signals is not observed at this temperature) is depicted in Figure 5.7.

Assignments have been done by 2D COSY NMR (data not shown), and 1D NOE difference experiments (Figure 5.8) in analogy to the characterization of **3**. The tetranuclear complex **4** contains two diamagnetic ruthenium(II) moieties, which are identical because of the presence of two C_2 symmetry axes. However, the two terpyridine ligands I' and II are inequivalent. Therefore, two sets of terpyridine signals are identified in the aromatic region of the COSY spectrum. Moreover, two two-spin systems are shown by the diethylene protons 1' and 2', and 1'' and 2'' in the region between 4 and 6 ppm.

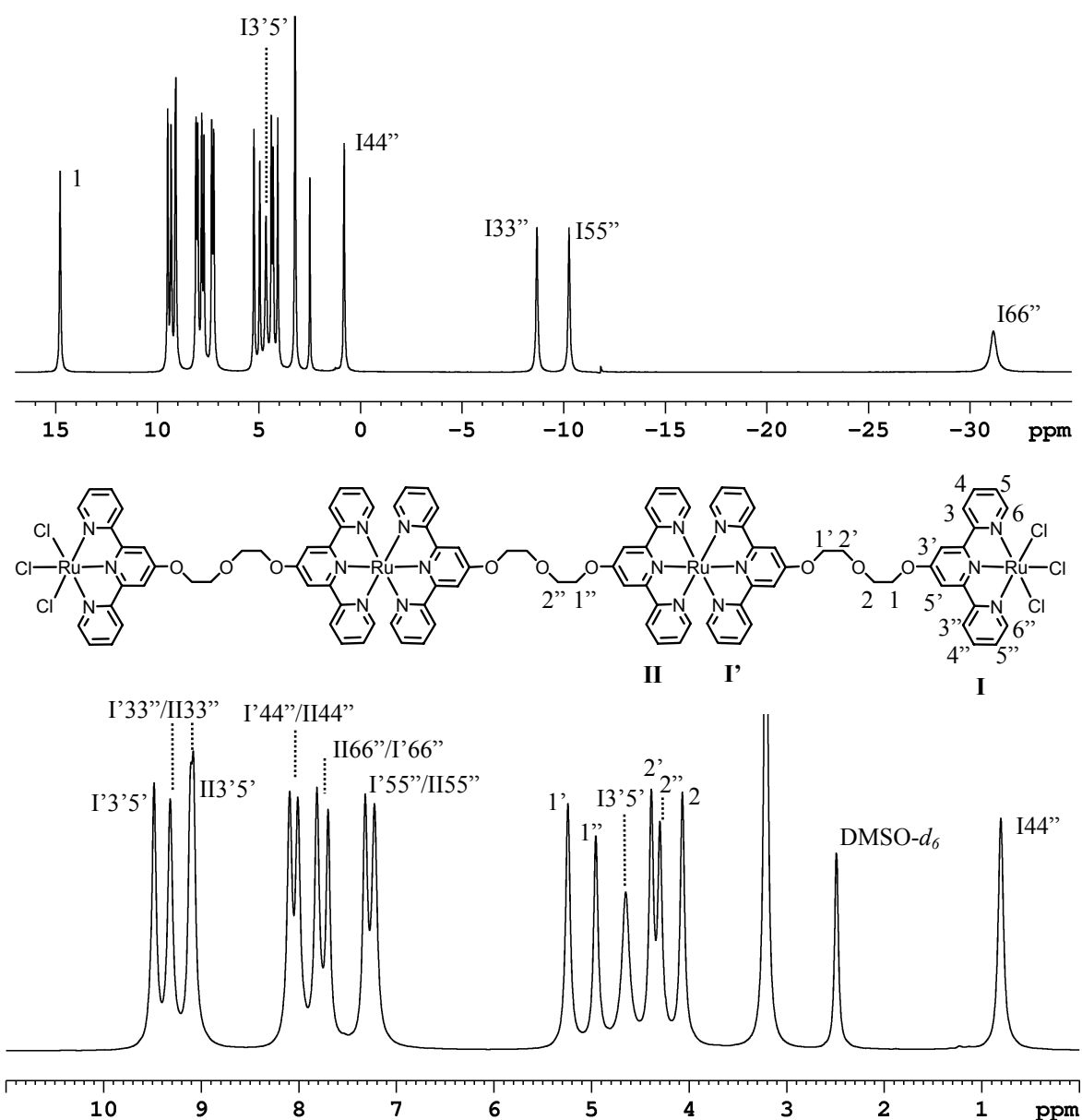


Figure 5.7 1D ^1H NMR spectra of **4** in $\text{DMSO-}d_6$ at 315 K with assignments, and molecular structure of the cation of **4**. The spectrum at the bottom is an enlargement of the diamagnetic region. The numbering scheme given for I is also applicable to I' and II. The terpyridine I' signals have not been distinguished from terpyridine II resonances.

The resonances at 5.52 and 4.66 have been assigned to the 1' and 2' protons, since these signals exhibit short T_1 values (77 and 115 ms, respectively) in comparison to the 1'' and 2'' resonances (137 and 158 ms, respectively). In 1D NOE difference experiments, I'3'5'–1' and II3'5'–1'' NOEs are observed (data not shown). However, I'3'5'–I'33'' and II3'5'–II33'' NOEs are not observed, probably because of partial overlap of the signals.

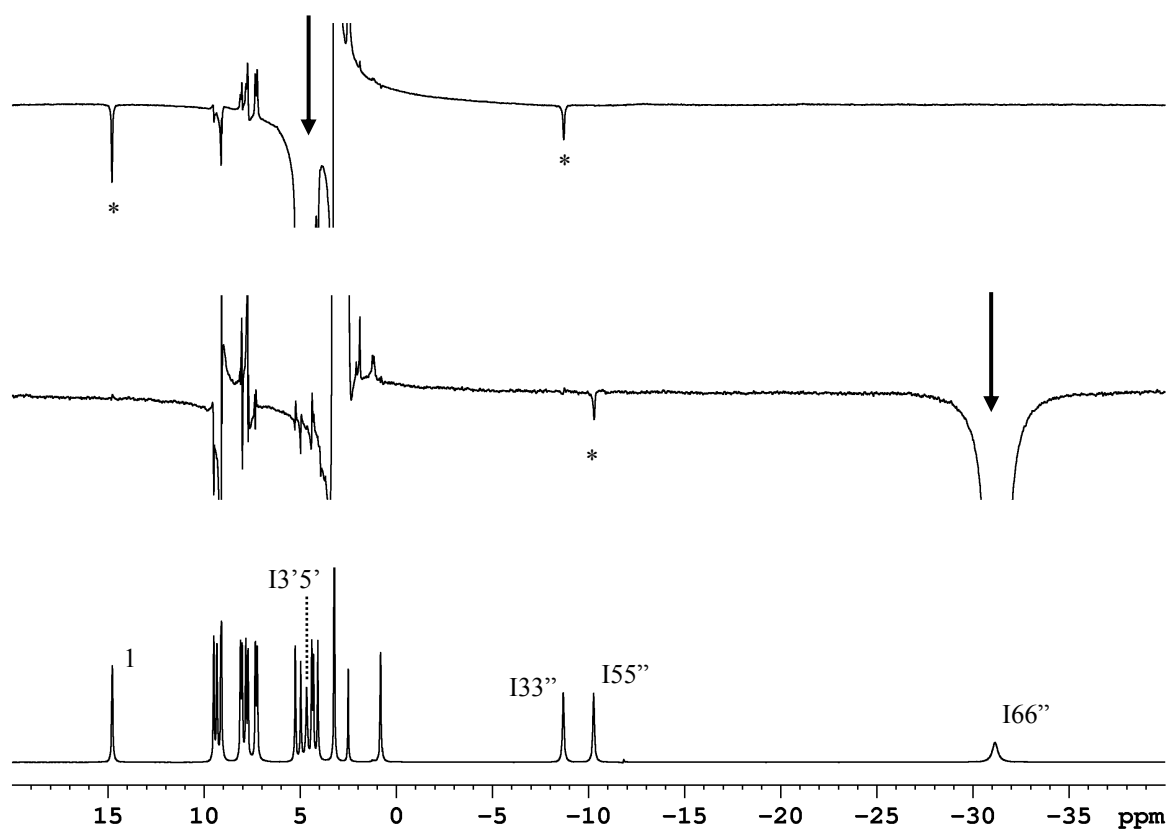


Figure 5.8 1D ^1H NOE difference NMR spectra (top and middle) and 1D ^1H NMR spectrum (bottom) of **4** in $\text{DMSO-}d_6$ at 315 K. Irradiated signals are indicated with an arrow. NOEs are indicated by an asterisk.

As a consequence, the two different terpyridine ligands I' and II cannot be distinguished. They can also not be distinguished by their T_1 values, since these are not clearly different for the two sets of terpyridine signals. The distance to the ruthenium(III) ion may vary due to internal movements of the flexible linker, thereby affecting the protons of the diamagnetic unit.

The “paramagnetic” signals of **4** show cross peaks comparable to those of **3** in the 2D COSY NMR spectrum. Therefore, these data are not shown. 1D NOE difference experiments are depicted in Figure 5.8. Similar to **3**, signal enhancements of the diethylene proton 1 and I33'' are seen upon irradiation of the “paramagnetic” signal at 4.93 ppm. Thereby, the latter can be attributed to the I3'5' protons. The I55'' resonance exhibits a NOE upon irradiation of the significantly broadened and shifted I66'' signal at -30.88 ppm. This confirms the assignment of the terpyridine I protons. Interestingly, the NOEs displayed by the different “paramagnetic” resonances are of considerable intensity. The large enhancement is, besides a high concentration, probably also due to the high molecular mass of the complex. The NOE

intensity for paramagnetic complexes is proportional to the rotational correlation time, which is significantly affected by a high molecular weight.^[18]

Hyperfine shifts have been observed over a temperature range from 300 to 360 K, and have been plotted against the reciprocal temperature T^{-1} (Figure 5.9). It can be concluded that all signals display Curie behavior, *i.e.* upon decreasing T^{-1} , a linear decrease in the hyperfine shift is observed for all resonances. The intercepts extrapolated at infinite temperature are close to the diamagnetic values for most signals.

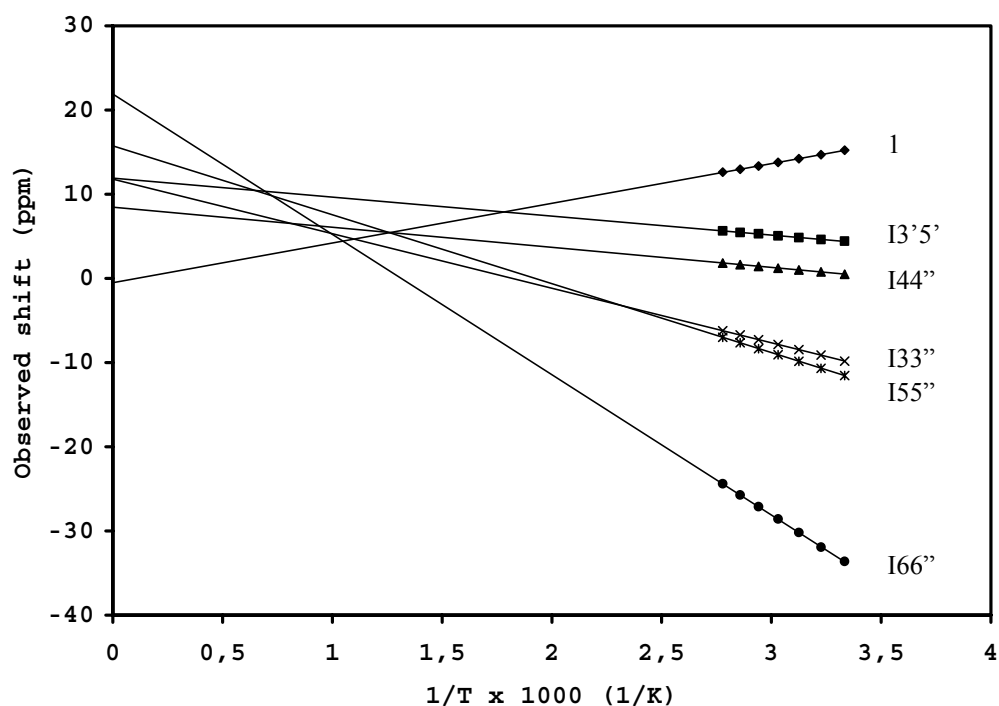


Figure 5.9 Plots of the chemical shifts *versus* $1/T$ for the “paramagnetic” signals of **4**.

5.3.4 Characterization of the polynuclear ruthenium platinum complexes **5** and **6**

The ruthenium(II)-platinum(II) complexes $[\text{ClPt}(\text{dtdeg})\text{Ru}(\text{dtdeg})\text{PtCl}]\text{Cl}_4$ (**5**) and $[\text{ClPt}(\text{dtdeg})\text{Ru}(\text{dtdeg})\text{Ru}(\text{dtdeg})\text{PtCl}]\text{Cl}_6$ (**6**) have been characterized by 1D and 2D ^1H NMR experiments, as well as with ^{195}Pt NMR spectroscopy (see experimental section). Their characterization is very similar to that of their precursors **1** and **2**, respectively. Both complexes are of C_2 symmetry, causing the appearance of four ethylene signals and two sets of terpyridine resonances in the ^1H NMR spectrum of **5** (Figure 5.10, top), and six ethylene signals and three sets of terpyridine resonances in the ^1H NMR spectrum of **6** (Figure 5.10, bottom).

The 33'' and 66'' signals have been assigned according to their specific J coupling constants of 9 and 5 Hz, respectively. The set of signals for terpyridine ligand I has been identified by the relatively downfield shift of the I66'' protons in comparison to the shift of the I'66'' and II66'' protons. The downfield shift of the I66'' protons is due to deshielding by the chloride ligand, which is coordinated to platinum. All expected cross peaks are observed in the 2D NOESY spectra of the complexes. The two terpyridine ligands I' and II of **6** have been distinguished by the 2-2' NOE, which indirectly indicates the I' signals via the 2'-1' COSY and I3'5'-1' NOE cross peaks.

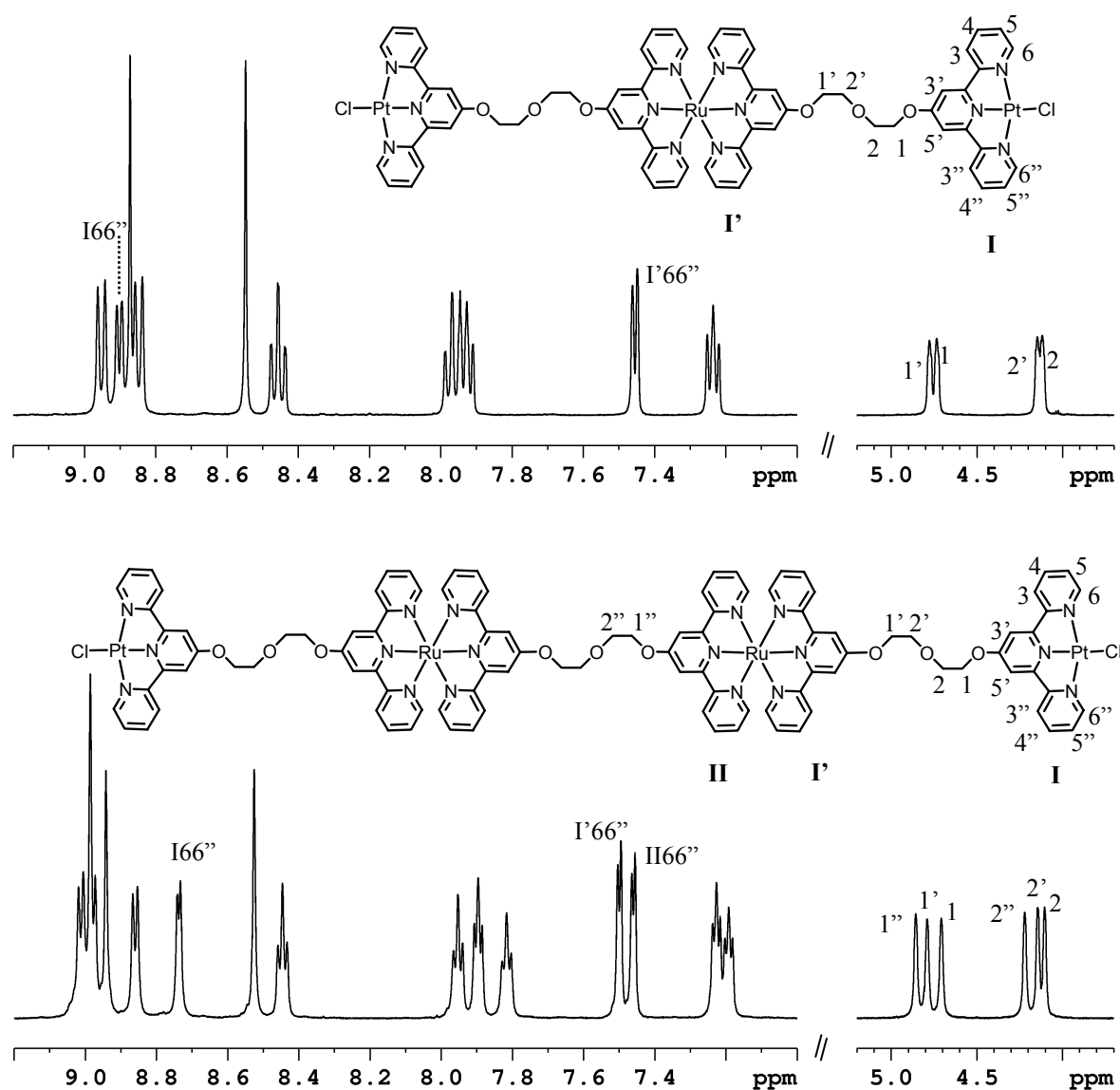


Figure 5.10 1D ^1H NMR spectra of **5** (top) and **6** (bottom) in $\text{DMSO-}d_6$ at 312 K and 298 K, respectively, with some assignments. The structures of the cations of **5** and **6** are also given. The numbering scheme of I is also applicable to I' and II.

5.3.5 Cytotoxicity tests

Cytotoxic activity of the tetranuclear complexes against A2780cis and A2780R cisplatin sensitive and resistant cell lines, respectively, is reported in Table 5.1. The IC₅₀ values have also been determined under the same conditions for the mononuclear derivatives [Ru(tpy)Cl₃] and [Pt(tpy)Cl]Cl, and cisplatin for comparison.

The complex [Cl₃Ru(dtdeg)Ru(dtdeg)Ru(dtdeg)RuCl₃]Cl₄ (**4**) displays activity against A2780cis cells with an IC₅₀ value of 8 μM. Moderate activity is displayed against A2780R cells. It shows higher activity than the mononuclear complex [Ru(tpy)Cl₃], which displays IC₅₀ values of 14 μM and 45 μM against A2780cis and A2780R cells, respectively. The complex [ClPt(dtdeg)Ru(dtdeg)Ru(dtdeg)PtCl]Cl₆ (**6**) shows moderate cytotoxicity against both cell lines. The trinuclear derivatives **3** and **5** inhibit cell growth of A2780cis cells for 50 % at a concentration of 20 μM. An IC₅₀ value could not be determined, since only one concentration showed an effect of 50 % of cell growth inhibition. Higher concentrations of **3** and **5** have not been tested, because of poor solubility in the used medium. The trinuclear complexes inhibit cell growth of A2780R cells for only 30 % at 20 μM.

Table 5.1 IC₅₀ values for the polynuclear complexes **3**, **4**, **5** and **6** calculated after 72 hours of treatment. IC₅₀ values given for **3** and **5** are only indicative.

Complex	IC ₅₀ (μM)						
	3	4	5	6	[Ru(tpy)Cl ₃]	[Pt(tpy)Cl]Cl	Cisplatin
A2780cis	~ 20	8	~ 20	15	14	1	1
A2780R	>> 20	20	>> 20	22	45	2	6

The complex [Ru(tpy)Cl₃] has been reported to display an IC₅₀ value of 7 μM against L1210cis cells.^[12] However, this result has not been reproduced by tests reported here. In fact, none of the ruthenium complexes described in this Chapter, including [Ru(tpy)Cl₃], considerably inhibits cell growth of L1210 cells. Of the ruthenium-platinum derivatives, only **6** shows moderate activity against the leukemia cell lines. It displays IC₅₀ values of 30 μM and 24 μM against L1210cis and L1210/2 cells, respectively.

In general, the trinuclear complexes also show no cytotoxic effect against Hs683 and U-373MG glioblastoma cells, HCT-15 and LoVo colorectal cancer cells, A549 lung cancer and MCF-7 breast cancer cells at the highest concentration tested (20 μM). At 50 μM, the tetranuclear complexes **4** and **6** show an average inhibition of cell growth of 55 % and 47 %, respectively. Complex **6** inhibits cell growth of Hs683, HCT-15 and MCF-7 cells for more than 50 %, but only at the highest concentration used, *i.e.* at 50 μM. Complex **4** inhibits 50 %

of cell growth of LoVo, HCT-15 and MCF-7 cells at concentrations between 10 and 30 μM , but the average inhibition of cell growth is approximately 40 % only. Therefore, IC₅₀ values have not been determined. At negligible DMSO concentrations, $[\text{Ru}(\text{tpy})\text{Cl}_3]$ shows an average inhibition of cell growth of 25 % at 50 μM against these cell lines. $[\text{Pt}(\text{tpy})\text{Cl}]\text{Cl}$ shows even higher activity than cisplatin against all cell lines tested. It displays IC₅₀ values that range between 1 and 5 μM .

The dinuclear derivatives $[(\text{tpy})\text{Ru}(\text{dtdeg})\text{RuCl}_3]\text{Cl}_2$ and $[(\text{tpy})\text{Ru}(\text{dtdeg})\text{PtCl}]\text{Cl}_3$, which have been presented in the previous Chapters, only show an average inhibition of cell growth of 55 % and 71 %, respectively, at 100 μM against Hs683, U-373MG, HCT-15, LoVo, A549 and MCF-7 cancer cells. Thus, of the polynuclear trichlororuthenium and platinum terpyridyl complexes the tetranuclear complexes show the highest inhibition of cell growth at similar concentrations.

The length of the linker may in part be of influence on the cytotoxicity of the polynuclear complexes. It has been reported that intercalation of platinum terpyridine complexes possibly requires a precise orientation of the preferred binding site.^[19] However, bisintercalation of dinuclear platinum terpyridine complexes has been implied to disrupt the DNA binding site.^[20] It has been suggested that the use of long linkers may allow both units to independently interact with the DNA. However, the cytotoxicity of **6**, which has been synthesized using an extremely long linker, is not as high as that of the mononuclear derivative $[\text{Pt}(\text{tpy})\text{Cl}]\text{Cl}$. The tetranuclear complex **4** exhibits appreciable cytotoxicity, but only against A2780cis cells. Thereby, **4** is more active than its mononuclear counterpart $[\text{Ru}(\text{tpy})\text{Cl}_3]$. However, it is not more active than cisplatin, which displays an IC₅₀ value of 1 μM against A2780cis cells.

5.3.6 Clotting of A2780cis cells.

Interestingly, clotting of A2780cis cells has been observed upon incubation with **4** (Figure 5.11). The cells seem to assemble on top of each other to form a kind of bundles, which remain attached to the bottom of the well during the tests. The effect is noticed after one day of incubation, and seems to be concentration dependent. It is already clearly seen at a concentration of 20 μM . At this particular concentration, almost no normally growing cells are observed (Figure 5.11). Within the clots some cells are still alive, as proven by the MTT assay, *i.e.* 35 % of cell growth is observed at 20 μM . An increase in concentration does not result in a significant increase in inhibition of cell growth. At 50 μM , 30 % of the cells are still alive. Higher concentrations have not been tested, due to poor solubility in the medium used.

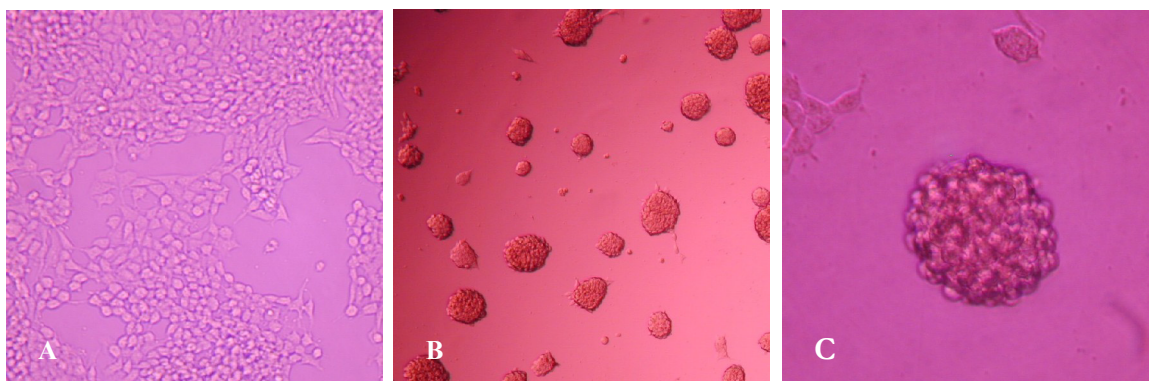


Figure 5.11 Analysis of cell growth of untreated A2780cis cells after 72 hours at 310 K (A), and of A2780cis cells after treatment with **4** for 72 hours at 310 K (B and C). Picture C represents an enlargement of one clot.

The cells return to their normal growth after plating treated cells into drug-free medium, which implies that **4** is not significantly taken up by the cells. Cell uptake experiments have not been performed to confirm this hypothesis, but the high positive charge (4+) of the complex is likely to affect internalization. The complex may remain on the negatively charged cell surface. A possible straightforward explanation for the clotting of the A2780cis cells is that electrostatic interactions between **4** and cell membranes join cells together. The trinuclear analogue **3**, which has a 2+ charge, shows the effect as well, albeit less significant. However, cells do not adhere together by incubation with the dinuclear complex $[(\text{tpy})\text{Ru}(\text{dtdeg})\text{RuCl}_3]\text{Cl}_2$, which is also 2+ charged. Moreover, the trinuclear and tetranuclear platinum analogues **5** and **6**, which display charges of 4+ and 6+, respectively, do not show the effect either. Therefore, the positive charge of the complexes cannot be the only factor causing this effect. The trichlororuthenium(III) moieties and the length of the linker seem to be of importance.

DNA is believed to be the ultimate target of many anticancer drugs,^[3] but the results imply that the activity of **4** may not be related to DNA binding. A target different from DNA has also been implied for the mononuclear complex NAMI-A.^[21] Its high activity *in vivo* against lung metastasis^[22] has been associated with inhibition of angiogenesis.^[8, 23] Further experiments have to be performed to elucidate the mechanism of action of complex **4**. Nevertheless, it is clear that the effect is only displayed by the tetranuclear complex **4**, and by its trinuclear derivative **3**, although to a lesser extent. The other complexes tested, including cisplatin, $[\text{Ru}(\text{tpy})\text{Cl}_3]$ and $[\text{Pt}(\text{tpy})\text{Cl}]\text{Cl}$, do not show the effect. Furthermore, the A2780R and the leukemia cells do not adhere together upon incubation with **4**. The Hs683, U-373MG,

HCT-15, LoVo, A549 and MCF-7 cancer cells have not specifically been observed for the appearance of the effect, but the low inhibition of cell growth suggests the absence of clotting cells. Thus, the effect appears to be specific for the particular structure of **4**, and is characteristic for the A2780cis cell line. The clotting of A2780cis cells may hamper migration and metastasis of these cancer cells, since the cells remain adhered to each other and do not dissociate from the clot.

5.4 Concluding remarks

The positively charged complexes $[(\text{dtdeg})\text{Ru}(\text{dtdeg})]\text{Cl}_2$ (**1**) and $[(\text{dtdeg})\text{Ru}(\text{dtdeg})\text{Ru}(\text{dtdeg})]\text{Cl}_4$ (**2**) have been synthesized and characterized. They have proven to be highly valuable for the simple construction of homo and heteropolynuclear complexes. They have been used for the syntheses of the new linear trinuclear and tetranuclear ruthenium(II)-ruthenium(III) complexes **3** and **4**, and that of the ruthenium(II)-platinum(II) analogues **5** and **6**, which have been presented in this Chapter. The paramagnetic complexes **3** and **4** have been characterized by ^1H NMR spectroscopy, including the use of 1D ^1H NOE difference experiments. Especially complex **4** displays strong NOE's even upon irradiation of signals which exhibit short T_1 values. The high molecular weight of **4** is probably of appreciable influence for the observed high intensity of the NOE's. The hyperfine shifts of the paramagnetic signals of **3** and **4** show Curie behavior. The shifts are approximately identical to those of the mononuclear and dinuclear derivatives $[\text{Ru}(\text{tpy})\text{Cl}_3]$ and $[(\text{tpy})\text{Ru}(\text{dtdeg})\text{RuCl}_3]\text{Cl}_2$. The ruthenium-platinum complexes have also been characterized by ^1H NMR spectroscopy.

Cytotoxicity tests reveal that the complexes do not show significant activity against a variety of cancer cell lines. Complex **6** exhibits moderate cytotoxicity against A2780 and L1210 cells. Complex **4** displays an IC_{50} value of 8 μM against A2780cis cells, and is moderately active against the cisplatin resistant cell line A2780R. An interesting effect has been observed upon analysis of cell growth of A2780cis cells. The cells adhere together and form clots upon incubation with **4**. The effect appears to be characteristic for the A2780cis cells and is specific for the particular structure of **4**.

Concluding, in addition to the dinuclear derivatives of NAMI-A^[8] and the trinuclear ruthenium complex ruthenium red^[24], this Chapter presents the first tetranuclear ruthenium complex, which shows biological activity against cancer cells. Considering the urgent need for targeted drugs, complex **4** may represent a true novelty. The clotting suggests that **4** may inhibit cell migration and metastasis. The relation between clotting and invasion inhibition needs to be studied in the future.

5.5 References

- [1] (a) Reedijk, J., *Proc. Natl. Acad. Sci. U. S. A.* **2003**, *100*, 3611-3616. (b) Wheate, N. J.; Collins, J. G., *Coord. Chem. Rev.* **2003**, *241*, 133-145.
- [2] Farrell, N.; Qu, Y.; Bierbach, U.; Valsecchi, M.; Menta, E., in *Cisplatin. Chemistry and Biochemistry of a Leading Anticancer Drug* (Ed.: Lippert, B.), Verlag Helvetica Chimica Acta, Zurich, Wiley-VCH, Weinheim, **1999**, 479-496.
- [3] Reedijk, J., *Chem. Rev.* **1999**, *99*, 2499-2510.
- [4] (a) Berners-Price, S. J.; Davies, M. S.; Cox, J. W.; Thomas, D. S.; Farrell, N., *Chem.-Eur. J.* **2003**, *9*, 713-725. (b) Cox, J. W.; Berners-Price, S.; Davies, M. S.; Qu, Y.; Farrell, N., *J. Am. Chem. Soc.* **2001**, *123*, 1316-1326.
- [5] Brabec, V.; Kašpárková, J., *Drug Resist. Update* **2002**, *5*, 147-161.
- [6] Qu, Y.; Scarsdale, N. J.; Tran, M. C.; Farrell, N. P., *J. Biol. Inorg. Chem.* **2003**, *8*, 19-28. (b) Hegmans, A.; Berners-Price, S. J.; Davies, M. S.; Thomas, D. S.; Humphreys, A. S.; Farrell, N., *J. Am. Chem. Soc.* **2004**, *126*, 2166-2180.
- [7] Lowe, G.; Droz, A. S.; Vilaivan, T.; Weaver, G. W.; Park, J. J.; Pratt, J. M.; Tweedale, L.; Kelland, L. R., *J. Med. Chem.* **1999**, *42*, 3167-3174.
- [8] Alessio, E.; Mestroni, G.; Bergamo, A.; Sava, G., *Metal Ions in Biological Systems* **2004**, *42*, 323-351.
- [9] (a) Clarke, M. J., *Coord. Chem. Rev.* **2003**, *236*, 209-233. (b) O'Reilly, F. M.; Kelly, J. M., *New J. Chem.* **1998**, *22*, 215-217. (b) Önfelt, B.; Lincoln, P.; Nordén, B., *J. Am. Chem. Soc.* **1999**, *121*, 10846-10847.
- [10] (a) Qu, Y.; Farrell, N., *Inorg. Chem.* **1995**, *34*, 3573-3576. (b) Milkevitch, M.; Storrie, H.; Brauns, E.; Brewer, K. J.; Shirley, B. W., *Inorg. Chem.* **1997**, *36*, 4534-4538. (b) Swavey, S.; Fang, Z. L.; Brewer, K. J., *Inorg. Chem.* **2002**, *41*, 2598-2607.
- [11] Van der Schilden, K.; Garcia, F.; Kooijman, H.; Spek, A. L.; Haasnoot, J. G.; Reedijk, J., *Angew. Chem.-Int. Edit.* **2004**, *43*, 5668-5670.
- [12] Nováková, O.; Kašpárková, J.; Vrána, O.; Van Vliet, P. M.; Reedijk, J.; Brabec, V., *Biochemistry* **1995**, *34*, 12369-12378.
- [13] Van Vliet, P. M.; Toekimin, S. M. S.; Haasnoot, J. G.; Reedijk, J.; Nováková, O.; Vrána, O.; Brabec, V., *Inorg. Chim. Acta* **1995**, *231*, 57-64.
- [14] (a) Jennette, K. W.; Lippard, S. J.; Vassiliades, G. A.; Bauer, W. R., *Proc. Natl. Acad. Sci. U. S. A.* **1974**, *71*, 3839-3843. (b) Howe-Grant, M.; Wu, K. C.; Bauer, W. R.; Lippard, S. J., *Biochemistry* **1976**, *15*, 4339-4346.
- [15] Velders, A. H., Ph.D. thesis, Leiden University (Leiden), **2000**.
- [16] (a) Dugad, L. B.; Lamar, G. N.; Banci, L.; Bertini, I., *Biochemistry* **1990**, *29*, 2263-2271. (b) Banci, L.; Bertini, I.; Luchinat, C.; Piccioli, M.; Scozzafava, A.; Turano, P., *Inorganic Chemistry* **1989**, *28*, 4650-4656.
- [17] (a) Tada, H.; Shiho, O.; Kuroshima, K.; Koyama, M.; Tsukamoto, K., *J. Immunol. Methods* **1986**, *93*, 157-165. (b) Mosmann, T., *J. Immunol. Methods* **1983**, *65*, 55-63. (b) Alley, M. C.; Scudiero, D. A.; Monks, A.; Hursey, M. L.; Czerwinski, M. J.; Fine, D. L.; Abbott, B. J.; Mayo, J. G.; Shoemaker, R. H.; Boyd, M. R., *Cancer Res.* **1988**, *48*, 589-601.
- [18] Bertini, I.; Luchinat, C., *NMR of paramagnetic substances, Vol. 150*, (Ed.: Lever, A. B. P.), Elsevier, Amsterdam, **1996**.
- [19] McFadyen, W. D.; Wakelin, L. P. G.; Roos, I. A. G.; Hillcoat, B. L., *Biochem. J.* **1986**, *238*, 757-763.
- [20] McFadyen, W. D.; Wakelin, L. P. G.; Roos, I. A. G.; Hillcoat, B. L., *Biochem. J.* **1987**, *242*, 177-183.

- [21] Zorzet, S.; Bergamo, A.; Cocchietto, M.; Sorc, A.; Gava, B.; Alessio, E.; Iengo, E.; Sava, G., *J. Pharmacol. Exp. Ther.* **2000**, *295*, 927-933.
- [22] Sava, G.; Zorzet, S.; Turrin, C.; Vita, F.; Soranzo, M.; Zabucchi, G.; Cocchietto, M.; Bergamo, A.; DiGiovine, S.; Pezzoni, G.; Sartor, L.; Garbisa, S., *Clin. Cancer Res.* **2003**, *9*, 1898-1905.
- [23] Vacca, A.; Bruno, M.; Boccarelli, A.; Coluccia, M.; Ribatti, D.; Bergamo, A.; Garbisa, S.; Sartor, L.; Sava, G., *Br. J. Cancer* **2002**, *86*, 993-998.
- [24] Anghileri, L. J.; Marchal, C.; Matrat, M.; Croneescanye, M. C.; Robert, J., *Neoplasma* **1986**, *33*, 603-608.

Chapter 6

Heteropolynuclear ruthenium(II)-platinum(II) complexes with short and semi-rigid linkers: synthesis, characterization and DNA-model base studies

Abstract – The paramagnetic ruthenium(III) complex $[\text{Ru}(\text{qpy})\text{Cl}_3]$ (**1**) (qpy = 4'-pyridyl-2,2':6',2''-terpyridine) has been characterized by ^1H NMR spectroscopy. The chemical shifts of the pendant pyridine protons demonstrate that spin delocalization partly occurs by a spin polarization mechanism. The water-soluble ruthenium(II) complexes $[(\text{tpy})\text{Ru}(\text{qpy})]\text{Cl}_2$ (**2**) and $[\text{Ru}(\text{qpy})_2]\text{Cl}_2$ (**3**) have been produced for the synthesis of the dinuclear and trinuclear ruthenium(II)-platinum(II) complexes $[(\text{tpy})\text{Ru}(\text{qpy})\text{Pt}(\text{en})\text{Cl}](\text{NO}_3)_3$ (**4**) and $[\text{Cl}(\text{en})\text{Pt}(\text{qpy})\text{Ru}(\text{qpy})\text{Pt}(\text{en})\text{Cl}](\text{NO}_3)_4$ (**5**), respectively (en = 1,2-ethylenediamine). The complexes have been characterized by different techniques. Electronic spectra show that coordination of platinum to the pendant pyridine of the qpy ligand lowers the energy level of the MLCT band of the ruthenium metal. It has been demonstrated that the polynuclear complexes do not hydrolyze in D_2O . In stead coordination to the DNA-model base 9-ethylguanine (9egua) occurs, as has been demonstrated for **4**. ^1H NMR data prove that the base coordinates to platinum via the N7, with its keto group directed towards the amine protons of the ethylene diamine ligand. The complexes do not show cytotoxicity against different cancer cell lines.

6.1 Introduction

Polynuclear platinum complexes have been developed as new anticancer drugs.^[1] The α,ω -diaminoalkane-linked polynuclear platinum complexes developed by Farrell *et al.* represent a very promising class of anticancer compounds.^[2] The long and flexible linker allows the formation of long-range adducts to the DNA, which is generally believed to be the target of platinum anticancer complexes.^[3] The formation of these specific adducts appears to be of importance for the high antitumor activity, which is displayed by the complexes.^[4] In contrast, dinuclear platinum complexes with short and rigid linkers, in which the platinum moieties are joined by pyrazole and a hydroxo group, have also been shown to exhibit high activity against different cancer cell lines.^[5] The two platinum centers have been found to be sufficiently close to mimic DNA binding of the antitumor drug cisplatin.^[6] However, they form the 1,2-intrastrand DNA adduct without major distortions of the DNA, which may avoid recognition and repair of the adduct.^[7]

Ruthenium compounds are also known for their antitumor activity,^[8] and some polynuclear complexes have been designed and studied as anticancer agents.^[9] Different heterocyclic bridging ligands have been used to link two ruthenium units, which resemble the antimetastatic complex NAMI-A.^[9] The complexes have been demonstrated to display antimetastatic activity *in vivo*, but not as profound as the mononuclear counterpart.^[10] A small variety of heterodinuclear ruthenium-platinum complexes have mainly been synthesized by the use of short bridging heterocyclic ligands.^[11] These compounds have been devised to photoreact with DNA. Light absorption of the ruthenium moiety, and subsequent energy transfer is thought to impart reactivity at the platinum unit, which can coordinate to DNA.

In this Chapter heteropolynuclear ruthenium-platinum complexes, for which the short and semi-rigid linking ligand^[12] 4'-pyridyl-2,2':6',2''-terpyridine (quaterpyridine or qpy) has been used, are described. The ligand qpy presents a tridentate coordination site, and can coordinate to a second metal via the fourth pyridine, which is appended at the 4' position of the terpyridine part. The syntheses of the mononuclear ruthenium complexes $[\text{Ru}(\text{qpy})\text{Cl}_3]$, $[\text{Ru}(\text{qpy})(\text{tpy})](\text{PF}_6)_2$, and $[\text{Ru}(\text{qpy})_2](\text{PF}_6)_2$ (tpy = 2,2':6',2''-terpyridine), in which qpy coordinates to ruthenium as a tridentate ligand, have already been reported elsewhere.^[13, 14] The non-coordinated pyridyl groups of the bis(quaterpyridine) ruthenium complex have been shown to react with a range of electrophiles.^[13] In this Chapter, the characterization of the paramagnetic ruthenium(III) complex $[\text{Ru}(\text{qpy})\text{Cl}_3]$ (**1**) is presented, as well as the syntheses of the water soluble ruthenium(II) complexes $[\text{Ru}(\text{qpy})(\text{tpy})]\text{Cl}_2$ (**2**), and $[\text{Ru}(\text{qpy})_2]\text{Cl}_2$ (**3**). The characterization of **2** and **3** will be discussed briefly.

The chloride salts **2** and **3** have been produced for the syntheses of the polynuclear complexes $[(\text{tpy})\text{Ru}(\text{qpy})\text{Pt}(\text{en})\text{Cl}](\text{NO}_3)_3$ and $[\text{Cl}(\text{en})\text{Pt}(\text{qpy})\text{Ru}(\text{qpy})\text{Pt}(\text{en})\text{Cl}](\text{NO}_3)_4$ ($\text{en} = 1,2$ -ethylenediamine) (**4** and **5**, respectively, Figure 6.1). These complexes consist of a bis(terpyridyl)-ruthenium(II) moiety, and one or two platinum-ethylenediamine centers, which coordinate to the fourth pyridine ligand of qpy. The ruthenium moiety can provide water solubility and electrostatic interactions with the DNA by its 2+ charge, as is known^[15] for the parental mononuclear complex $[\text{Ru}(\text{tpy})_2]^{2+}$. The ligand qpy may affect DNA binding affinity, due to its extended aromaticity. The platinum moieties can monofunctionally coordinate to the DNA by substitution of the relatively labile chloride ligand.

The dinuclear complex **4** has been reacted with the DNA-model base 9-ethylguanine (9egua) to study the DNA binding behavior of the platinum unit. The adduct $[(\text{tpy})\text{Ru}(\text{qpy})\text{Pt}(\text{en})(9\text{egua})](\text{PF}_6)_4$ (**6**) has been isolated, its characterization by ¹H NMR experiments is presented here as well. The complexes have been tested for cytotoxicity against different cancer cell lines.

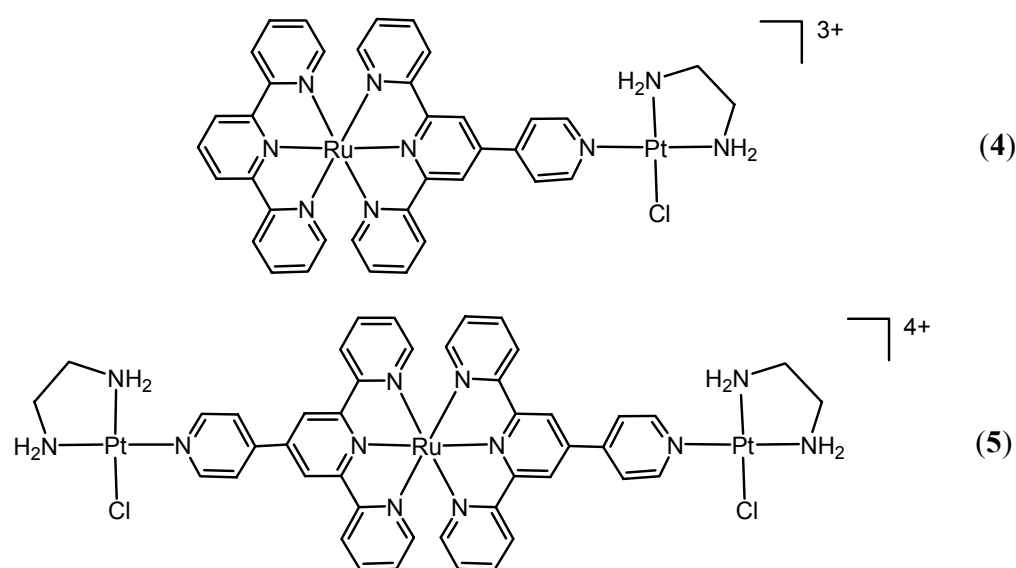


Figure 6.1 The polynuclear cationic ruthenium(II)-platinum(II) complexes **4** and **5**.

6.2 Experimental section

6.2.1 General methods and starting materials

Elemental analyses on C, H and N were performed on a Perkin Elmer series II CHNS/O Analyzer 2400. Electrospray mass spectra were recorded on a Finnigan TSQ-quantum

instrument with an electrospray interface (ESI). UV-VIS spectra were measured on a Cary 50 UV-VIS spectrometer version 3.00, from 200 to 800 nm. Hydrated $\text{RuCl}_3 \cdot x\text{H}_2\text{O}$ ($x \sim 3$) was used as received from Johnson & Matthey. The ligand tpy was obtained from Sigma, and $[\text{Pt}(\text{en})\text{Cl}_2]$ from Kreatech. The ligand qpy^[12] and the complex^[16] $[\text{Ru}(\text{tpy})\text{Cl}_3]$ were synthesized following known procedures. The preparation of the 0.1 M ruthenium(III) solution has been described elsewhere,^[17] and is reported in Chapter 2.

6.2.2 ¹H NMR measurements

NMR spectra were performed on a Bruker DPX 300, a DMX 600, and an AV 400 MHz spectrometer. Spectra were recorded in deuterated DMSO, acetone and water, and were calibrated on residual solvent peaks at δ 2.49, 2.06 and 4.75 ppm ($T = 298$ K), respectively. The 1D ¹H spectrum of the paramagnetic complex $[\text{Ru}(\text{qpy})\text{Cl}_3]$ (**1**) was obtained using a 100 ppm spectral width. Longitudinal relaxation times were measured by the standard inversion-recovery method, with 7 s relaxation delay and a spectral width of 100 ppm. Variable delays ranged from 50 μs to 3 s. Magnetization recovery was found to be exponential within experimental error. T_2 values were estimated from the peak half-widths. The COSY spectrum was obtained at 300 K by collecting 1024 $F_2 \times 1024 F_1$ data points with a relaxation delay of 20 ms.

6.2.3 Syntheses

$[\text{Ru}(\text{qpy})\text{Cl}_3]$, (1**):** The ligand qpy (200 mg; 0.645 mmol) was dissolved in 50 mL of MeOH by reflux. 0.1 M ruthenium(III) solution (6.5 mL; 0.65 mmol) was added drop wise to the solution. The mixture was refluxed for 1.5 hours, which resulted in precipitation of crude product. The mixture was filtered hot. Relatively pure complex precipitated from the filtrate at 253 K, and was obtained by filtration. Yield: 215 mg (65 %). ¹H NMR (300 MHz, DMSO, 298 K): $\delta = -8.61$ (s, 2H; 33''), -3.38 (s, 2H; 44''), -7.41 (s, 2H; 55''), -34.76 (s, 2H; 66''), 6.47 (s, 4H; 3'5'), 10.04 (s, 2H; 2''6''), 0.13 ppm (s, 2H; 3''5'').

$[\text{Ru}(\text{qpy})(\text{tpy})\text{Cl}_2]$, (2**):** An excess of AgBF_4 (120 mg; 0.616 mmol) was dissolved in 5 mL of acetone and filtered. $[\text{Ru}(\text{tpy})\text{Cl}_3]$ (20 mg; 0.045 mmol) was added to the filtrate and the mixture was refluxed in the dark for 16 hours. After filtration to remove precipitated AgCl , the filtrate was evaporated *in vacuo*, which resulted in a green oil (~ 0.5 mL). The ligand qpy (23 mg; 0.074 mmol) was added and the mixture was refluxed for 1.5 hours in 10 mL of DMF, which acted as the reducing agent. The red reaction mixture was filtered, and the filtrate was evaporated *in vacuo* until ~ 0.5 mL of a red oil resulted. To synthesize the

chloride salt of the product, 2 mL of a saturated LiCl solution in EtOH was added to the oil. The desired product was obtained by precipitation with a large amount of acetone (~ 100 mL). The product was partly purified by column chromatography on neutral alumina with CH₃CN/EtOH (v:v = 1:1). The orange fraction was precipitated with diethyl ether. The product was recrystallized from MeOH and diethyl ether. Yield: 24 mg (75 %). Elemental analysis (%) calculated for C₃₅H₂₅Cl₂N₇Ru: C 58.75, N 13.70, H 3.52. Found: C 58.13, N 13.46, H 3.87. ESI-MS: *m/z*: 322 [M²⁺]. ¹H NMR (300 MHz, DMSO, 298 K) (the qpy and tpy protons are denoted by I and II, respectively): δ = 9.14 (d, 2H; I33''), 8.08 (t, 2H; I44''), 7.29 (t, 2H; I55''), 7.45 (d, 2H; I66''), 9.60 (s, 2H; I3'5'), 8.98 (d, 2H; I2'''6'''), 8.45 (d, 2H; I3'''5'''), 8.85 (d, 2H; II33''), 8.02 (t, 2H; II44''), 7.25 (t, 2H; II55''), 7.52 (d, 2H; II66''), 9.11 (s, 2H; II3'5'), 8.55 ppm (t, 2H; II4'). UVVIS (H₂O): λ_{max} 484 (ε = 1.9 · 10⁴), 308 (ε = 5.1 · 10⁴), 272 nm (ε = 4.6 · 10⁴ M⁻¹ cm⁻¹).

[Ru(qpy)₂]Cl₂, (3): An excess of AgBF₄ (330 mg; 1.695 mmol) was dissolved in 20 mL of acetone and filtered. **1** (65 mg; 0.125 mmol) was added to the filtrate and the mixture was refluxed in the dark for 16 hours. After filtration and evaporation of the filtrate *in vacuo*, a green oil (~ 1 mL) resulted to which qpy (43 mg; 0.139 mmol) was added. The mixture was refluxed for 1.5 hours in 20 mL of DMF. The red reaction mixture was filtered, and the filtrate was evaporated *in vacuo* until an oil (~ 1 mL) resulted. 6 mL of a saturated LiCl solution in EtOH was added to the oil. The desired product was obtained by precipitation with a large amount of acetone (~ 350 mL). The product was purified by column chromatography on neutral alumina with acetone/EtOH/MeOH (v:v:v = 3:6:1). Red fractions were collected. Pure product was obtained by slow precipitation with diethyl ether. Yield: 43 mg (43 %). Elemental analysis (%) calculated for C₄₀H₂₈Cl₂N₈Ru: C 60.61, N 14.14, H 3.56. Found: C 59.91, N 13.84, H 3.82. ESI-MS: *m/z*: 361 [M²⁺]. ¹H NMR (300 MHz, DMSO, 298 K): δ = 8.99 (d, 4H; 33''), 8.09 (t, 4H; 44''), 7.28 (t, 4H; 55''), 7.56 (d, 4H; 66''), 9.61 (s, 4H; 3'5'), 9.13 (d, 4H; 2'''6'''), 8.44 ppm (d, 4H; 3'''5'''). UVVIS (H₂O): λ_{max} 490 (ε = 3.3 · 10⁴), 313 (ε = 5.8 · 10⁴), 274 (ε = 7.7 · 10⁴), 240 nm (ε = 4.5 · 10⁴ M⁻¹ cm⁻¹).

[(tpy)Ru(qpy)Pt(en)Cl](NO₃)₃, (4): An aqueous solution of AgNO₃ (14 mg in 0.55 mL) was added in five portions over 1 hour to a suspension of [Pt(en)Cl₂] (28 mg; 0.084 mmol) in 3 mL of H₂O at 310 K. Subsequently, the mixture was stirred for 2 hours at 310 K. After filtration, an aqueous solution of **2** (30 mg; 0.042 mmol) was added to the filtrate. The mixture was stirred at 363 K for 18 hours. The reaction mixture was concentrated *in vacuo* and coevaporated three times with EtOH/MeOH (v:v = 6:1) to remove the water. The residue was dissolved in MeOH. The product was precipitated by slow addition of diethyl ether. Yield: 28 mg (67 %). ESI-MS: *m/z*: 312 [M³⁺]. ¹H NMR (300 MHz, D₂O, 298 K): δ = 8.62 (d, 2H; I33''), 7.93 (t, 2H; I44''), 7.18 (t, 2H; I55''), 7.37 (d, 2H; I66''), 9.13 (s, 2H; I3'5'), 9.01

(d, 2H; I2''6''), 8.26 (d, 2H; I3''5''), 8.50 (d, 2H; II33''), 7.89 (t, 2H; II44''), 7.11 (t, 2H; II55''), 7.46 (d, 2H; II66''), 8.79 (s, 2H; II3'5'), 8.43 (t, 2H; II4'), 2.70 (s, 2H; b), 2.66 ppm (s, 2H; c). ^{195}Pt NMR (300 MHz, D_2O , 298 K): $\delta = -2517$ ppm. UVVIS (H_2O): λ_{max} 489 ($\epsilon = 2.0 \cdot 10^4$), 306 ($\epsilon = 4.7 \cdot 10^4$), 272 nm ($\epsilon = 4.2 \cdot 10^4 \text{ M}^{-1} \text{ cm}^{-1}$).

[Cl(en)Pt(qpy)Ru(qpy)Pt(en)Cl](NO₃)₄, (5): An aqueous solution of AgNO_3 (14 mg in 0.55 mL) was added in five portions over 1 hour to a suspension of $[\text{Pt}(\text{en})\text{Cl}_2]$ (28 mg; 0.084 mmol) in 3 mL of H_2O at 310 K. Subsequently, the mixture was stirred for 2 hours at 310 K. After filtration, an aqueous solution of **3** (18.2 mg; 0.023 mmol) was added to the filtrate. The mixture was stirred at 363 K for 18 hours. The reaction mixture was concentrated *in vacuo* and co-evaporated three times with EtOH/MeOH (v:v = 6:1) to remove the water. The residue was dissolved in MeOH. The product was precipitated by slow evaporation of the solution. Yield: 21 mg (63 %). Elemental analysis (%) calculated for $\text{C}_{44}\text{H}_{44}\text{Cl}_2\text{N}_{16}\text{O}_{12}\text{Pt}_2\text{Ru} \cdot 2.5\text{H}_2\text{O}$: C 33.11, N 14.04, H 3.09. Found: C 32.69, N 13.98, H 2.69. ^1H NMR (300 MHz, D_2O , 298 K): $\delta = 8.63$ (d, 4H; 33''), 7.94 (t, 4H; 44''), 7.17 (t, 4H; 55''), 7.42 (d, 4H; 66''), 9.14 (s, 4H; 3'5'), 9.02 (d, 4H; 2''6''), 8.26 ppm (d, 4H; 3''5''), 2.82 (s, 4H; b), 2.75 ppm (s, 4H; c). ^{195}Pt NMR (300 MHz, D_2O , 298 K): $\delta = -2518$ ppm. UVVIS (H_2O): λ_{max} 497 ($\epsilon = 2.7 \cdot 10^4$), 312 ($\epsilon = 3.6 \cdot 10^4$), 275 nm ($\epsilon = 4.7 \cdot 10^4 \text{ M}^{-1} \text{ cm}^{-1}$).

[(tpy)Ru(qpy)Pt(en)(9egua)](PF₆)₄, (6): A mixture of **4** (6 mg; 0.006 mmol) and 9egua (2 mg; 0.012 mmol) was stirred in 1.5 mL H_2O for 2 days at 310 K. A saturated NH_4PF_6 solution in H_2O was added until a precipitate was formed. The product was filtered off, and washed with a small amount of H_2O . Yield: 2 mg (20 %). ESI-MS (A mass spectrum was taken from a solution of an ^1H NMR experiment, in which $[(\text{tpy})\text{Ru}(\text{qpy})\text{Pt}(\text{en})(9\text{egua})]^{4+}$ was formed *in situ* from **4** and 9egua. Hence, the hydrochloric salt of the 9egua adduct has been found in the mass spectrum): m/z : 279 [$\text{M}^{4+} + \text{H}^+ + \text{Cl}^-$]. ^1H NMR (400 MHz, acetone, 294 K): $\delta = 8.93$ (d, 2H; I33''), 8.07 (t, 2H; I44''), 7.35 (t, 2H; I55''), 7.71 (d, 2H; I66''), 9.49 (s, 2H; I3'5'), 9.16 (d, 2H; I2''6''), 8.48 (d, 2H; I3''5''), 8.79 (d, 2H; II33''), 8.06 (t, 2H; II44''), 7.27 (t, 2H; II55''), 7.68 (d, 2H; II66''), 9.07 (s, 2H; II3'5'), 8.59 (t, 2H; II4'), 6.10 (s, 2H; a), 3.16 (s, 2H; b), 3.11 (s, 2H; c), 5.91 (s, 2H; d), 8.33 (s, 1H; H8), 6.62 (s, 1H; NH₂), 4.16 (q, 2H; CH₂), 1.41 ppm (t, 3H; CH₃).

6.2.4 Cytotoxicity tests

Cell cultures: A2780cis and A2780R cells (cisplatin sensitive and resistant human ovarian carcinoma, respectively) were maintained in Dulbecco's modified Eagle's Medium (DMEM: Gibco BRL™, Invitrogen Corporation, The Netherlands) supplemented with 10 % fetal calf serum (Perbio Science, Belgium), penicillin (100 units/mL: Duchefa Biochemie BV, The

Netherlands) and streptomycin (100 µg/mL: Duchefa Biochemie BV, The Netherlands) in a humidified 6 % CO₂, 94 % air atmosphere at 310 K. Cisplatin sensitive and resistant mouse leukemia L1210/0 and L1210/2 cells were grown (partly in suspension and partly adherent to the flasks) under the above mentioned conditions.

Cells were removed from the flasks by a 0.05 % trypsin solution. Cell viability was determined by the trypan blue exclusion test.

***In vitro* cytotoxicity evaluation:** Between 1000 and 5000 cells were seeded per well (depending on the cell type) onto 96-well plates (Corning Costar[®]) in 100 µl of complete medium with 5 to 10 % of FBS. Cells were treated 24 hours after sowing by addition of 100 µL of the complex in complete medium at the appropriate concentration. Cell growth was determined after 72 hours of incubation by the MTT assay, a colorimetric assay based on the ability of viable cells to reduce the soluble yellow 3-(4,5-dimethylthiazol-2-yl)-2,5-diphenyl-2H-tetrazolium bromide to blue formazan crystals by the mitochondria.^[18]

Final tested concentrations ranged between 10 µM and 100 µM and have been obtained by several dilutions with complete medium from stock solutions (2 mM) in sterile water. After 72 hours of incubation at 310 K, cells were incubated with 1 mg/mL MTT solution for 2 to 4 hour at 310 K. Subsequently, the medium was discarded and the formed crystals were dissolved in 100 µL DMSO per well. Optical density (OD) was measured at 590 nm with a Biorad 550 microplate reader. The OD is directly proportional to the number of living cells, which are compared to the control (untreated cells).

6.3 Results and discussion

6.3.1 Characterization of the mononuclear complexes 1, 2 and 3

The complex [Ru(qpy)Cl₃] (**1**) has been synthesized previously, but the complex was not characterized.^[13] Characterization of [Ru(Xtpy)Cl₃] complexes is often not performed, due to their insolubility in a wide variety of solvents.^[19] Complex **1** is indeed poorly soluble even in DMSO. Moreover, the paramagnetic ruthenium(III) ion of **1** hampers characterization of the complex by standard ¹H NMR techniques. Complex **1** has been characterized by ¹H NMR spectroscopy using a strategy similar to that described in Chapter 2 for the characterization of paramagnetic trichlororuthenium(III) terpyridine complexes. The 1D ¹H NMR spectrum of **1** in DMSO-*d*₆ is depicted in Figure 6.2. Signals have considerably shifted from the diamagnetic envelope from 0 to 12 ppm, because of the unpaired electron in the t_{2g} orbital of the low-spin d⁵ ruthenium(III) ion.

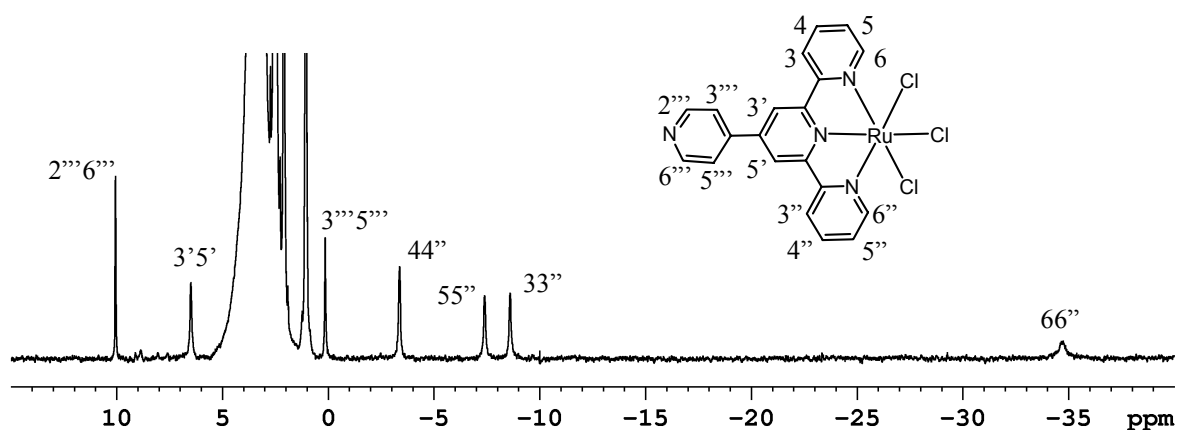


Figure 6.2 Schematic representation and ^1H NMR spectrum of **1** in $\text{DMSO-}d_6$ at 298 K with assignments.

Signals are also significantly broadened. In total, seven signals of identical intensity are observed in the region from 50 to -50 ppm, which agrees with C_2 symmetry of the complex. The 1D ^1H NMR spectrum of **1** shows minor amounts of impurities. In contrast, in the 1D ^1H NMR spectrum of its crude product (see experimental section) impurities are clearly observed in the diamagnetic region (data not shown). Complexes of the type $[\text{Ru}(\text{Xtpy})\text{Cl}_3]$ are often not purified, due to their poor solubility.^[19] However, for the synthesis of **2** the starting material, $[\text{Ru}(\text{qpy})\text{Cl}_3]$, should be as pure as possible. Therefore, characterization of **1** by ^1H NMR has been of significant use. Attempts to characterize **1** by different techniques have not been successful. The complex is most probably contaminated with ruthenium-oxo species, which are not observed in ^1H NMR.

The ^1H NMR resonances displayed by **1** have partly been assigned by a 2D COSY NMR experiment (Figure 6.3) using a relaxation delay of 20 ms. The signal at -34.76 ppm shows no crosspeaks, which is most probably due to its short longitudinal and transversal relaxation times T_1 (4.1 ms) and T_2 , respectively. Since the protons closest to the paramagnetic center are influenced the most, this signal has been assigned to the 66'' protons. The three-spin connectivity pattern in the upfield region of the spectrum assigns these signals to the 33'', 44'' and 55'' protons. The resonance at -3.38 ppm can be attributed to the 44'' protons, because it displays crosspeaks to both other signals. The signals at 10.04 and 0.13 ppm have been ascribed to the 2'''6''' and 3'''5''' protons, because of the COSY coupling. The resonance at 6.47 ppm has been assigned to the 3'5' protons, since it shows no crosspeaks.

1D NOE difference experiments, as described in the foregoing chapters, have been unsuccessful for **1**, due to its low solubility. However, the signals for the 2'''6''' and 3'''5''' protons have been assigned according to their T_1 values. The resonance at 10.04 exhibits a

longitudinal relaxation time of 378 ms, which is significantly larger than that displayed by the resonance at 0.13 ppm ($T_1 = 86.2$ ms). Therefore, the former has been ascribed to the protons furthest away from the paramagnetic center, *i.e.* the 2''6'' protons. The assignment is in agreement with that reported for the analogues complex [Ru(Phtpy)Cl₃], in which a phenyl group has been substituted at the 4' position of the terpyridine ligand.^[17] The T_1 values of the 33'' and 55'' signals do not differ greatly, which is probably due to the fact that the metal-proton distance for the 33'' protons (4.9 Å) is approximately similar to that for the 55'' protons (5.2 Å).^[20] However, from ¹H NMR studies of the complex^[17] [Ru(tpy)Cl₃] and its polynuclear derivatives (Chapters 2, 4 and 5), it has been found that the 33'' resonance displays a smaller T_1 value than the 55'' signal. The resonances at -7.41 and -8.61 ppm exhibit T_1 values of 33.5 and 25.2 ms, respectively. Consequently, the latter has been assigned to the 33'' protons. For [Ru(tpy)Cl₃], the most upfield shifted signal of the 33'' and 55'' resonances has also been assigned to the 33'' protons.

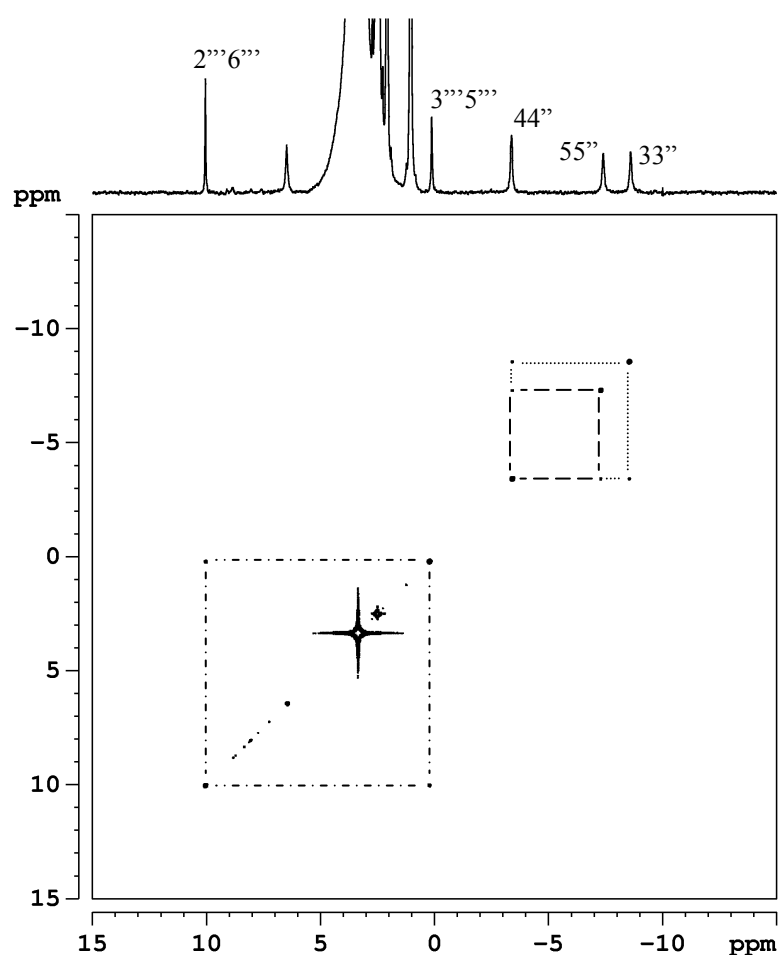


Figure 6.3 2D ¹H COSY NMR spectrum of **1** in DMSO-*d*₆ at 298 K with some assignments and crosspeaks indicated.

The observed chemical shifts have been plotted against $1/T$ (Figure 6.4). For all resonances a linear decrease in the hyperfine shift is observed upon a stepwise decrease of $1/T$, which indicates Curie behavior. The Curie law predicts zero magnetism at infinite temperatures. Thus, the observed shifts should approach the diamagnetic values. The intercepts extrapolated at $1/T = 0$ are close to the aromatic region, except for the 66'' signal. Deviation from Curie behavior will not be discussed, as it is not important for the discussion here. The decrease in shift is higher for the 33'' than for the 55'' protons. It confirms their assignment, as a similar behavior has also been observed for the analogous protons of $[\text{Ru}(\text{tpy})\text{Cl}_3]$ and its polynuclear derivatives (Chapters 2, 4 and 5).

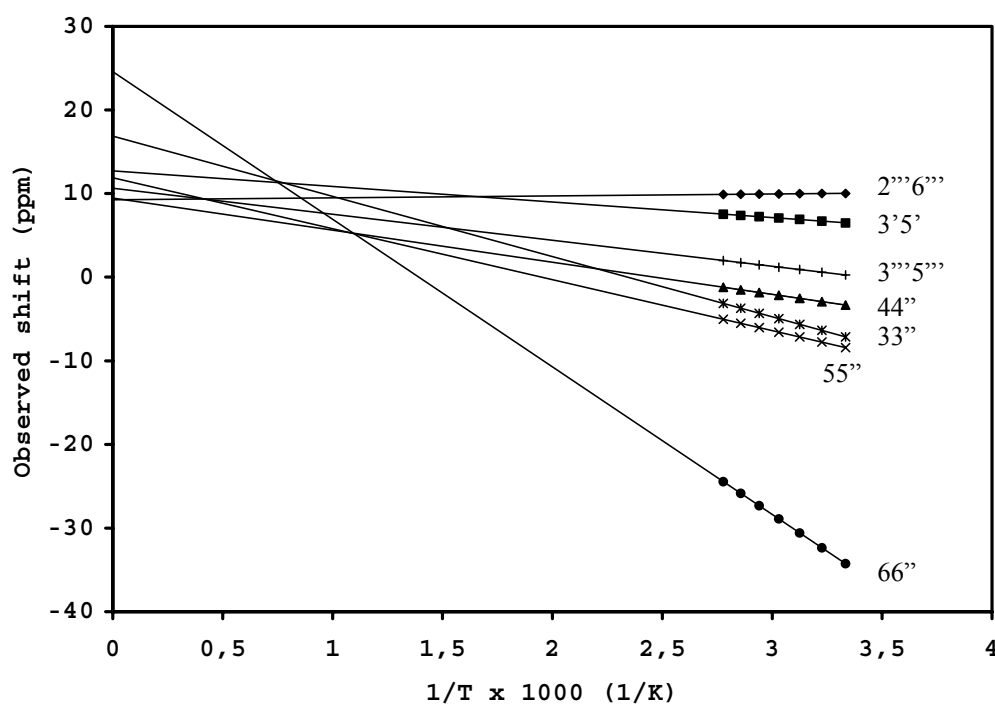


Figure 6.4 Plots of the chemical shifts *versus* $1/T$ for the signals of **1**.

The protons of the terpyridine part of **1** display a pattern of chemical shifts, which is similar to that of the corresponding protons of the mononuclear complex^[17] $[\text{Ru}(\text{tpy})\text{Cl}_3]$, and of the paramagnetic polynuclear derivatives (Chapters 2, 4 and 5). In addition, the chemical shifts of the protons of the 4'-pyridine are comparable to those of the phenyl ring protons of $[\text{Ru}(\text{phtpy})\text{Cl}_3]$ (phtpy = 4'-phenyl-2,2':6',2''-terpyridine).^[17] Therefore, it is likely that for the protons of **1** both contact (through bonds) and dipolar (through space) mechanisms contribute similarly to the hyperfine shift, *i.e.* the shift resulting from the interaction between the unpaired electron and the proton nucleus.

For $[\text{Ru}(\text{tpy})\text{Cl}_3]$, and the polynuclear ruthenium(III) terpyridine analogues, both contact (through chemical bonds) and dipolar (through space) interactions have been suggested to

contribute to the hyperfine shift (Chapter 2). A direct contact contribution to the chemical shift decreases rapidly as the number of chemical bonds between the metal and the resonating proton increases. Dipolar interactions decrease upon increasing metal-proton distances. The 33'', 44'', 55'' and 66'' protons of the trichlororuthenium(III) terpyridine complexes (including **1**) display hyperfine shifts, which agree with their metal-proton distances, as well as with the number of chemical bonds to the metal center. The protons closest to the unpaired electron (*i.e.* the 66'' protons) display the largest hyperfine shift, whereas the protons furthest away from the metal center (the 44'' protons) show a relatively small hyperfine shift.

A reversed pattern has been observed^[17] for the resonances of the central pyridine ring of [Ru(tpy)Cl₃]. The 3'5' protons, for which the metal proton distance is approximately similar to that of the 33'' and 55'' protons, displays a small upfield shift to 5.5 ppm. In contrast, the 4' proton, which is further away from the ruthenium(III) ion, exhibits a significant upfield shift (-23 ppm). It has been suggested that a spin polarization mechanism affects the chemical shifts of these protons in particular (Chapter 2). Spin polarization causes alternating upfield and downfield shifts in an aromatic system.^[21] Since the 3'5' resonance is not shifted downfield from the aromatic region, it is believed that spin polarization adds to a different mechanism. The sum does result in a positive shift of the 3'5' signal relative to the 33'' and 55'' resonances.

A small upfield shift is also observed for the 3'5' protons of **1** (Figure 6.2). Moreover, considering the metal-proton distance, a relatively large upfield shift is displayed by the 3'''5''' resonance (0.13 ppm). The 2'''6''' signal is shifted downfield with respect to its diamagnetic value (10.04 ppm). These shifts underline that the central pyridine ring of paramagnetic trichlororuthenium(III) terpyridine complexes is affected by a spin polarization mechanism. The conjugated π system of the quaterpyridine ligand clearly transfers unpaired spin density to the fourth pyridine through this mechanism. A different hyperfine interaction is probably also present in the pendant pyridine, since the absolute hyperfine shifts of the 3'''5''' and 2'''6''' protons are sensitive to the metal-proton distance.

The characterization of [Ru(qpy)(tpy)]Cl₂ (**2**), and [Ru(qpy)₂]Cl₂ (**3**) by ¹H NMR spectroscopy will not be discussed in detail, since the characterization of the hexafluorophosphate salts of the complex cations by 1D and 2D COSY ¹H NMR experiments has already been described.^[13, 14] However, the characterization by 2D NOESY experiments has not been reported earlier. The incomplete characterization is surprising. Whereas the 33'' and 66' signals can be distinguished by the difference in J values (5 and 9 Hz, respectively), the 2'''6''' and 3'''5''' resonances cannot. The most upfield shifted signal of the two doublets under consideration has been assigned to the 2'''6''' protons, to which the authors refer to as the ortho protons.^[13] However, here a NOE of the 3'5' qpy protons to the relatively upfield

shifted doublet at 8.45 ppm is clearly observed in the 2D NOESY spectra of **2** and **3** (data not shown). Hence, this doublet has been attributed to the 3'''5''' protons, whereas the doublet at approximately 9 ppm has been assigned to the 2'''6''' protons (*i.e.* the meta protons).

6.3.2 Characterization of the polynuclear complexes **4** and **5**

The complexes [(tpy)Ru(qpy)Pt(en)Cl](NO₃)₃ (**4**) and [Cl(en)Pt(qpy)Ru(qpy)Pt(en)Cl](NO₃)₄ (**5**) have been fully characterized by 1D (Figure 6.5) and 2D COSY and NOESY ¹H NMR, as well as ¹⁹⁵Pt NMR experiments (see experimental section). Complex **4** displays one set of signals in the aromatic region for the terpyridine ligand II, and one set of signals for the quaterpyridine ligand I.

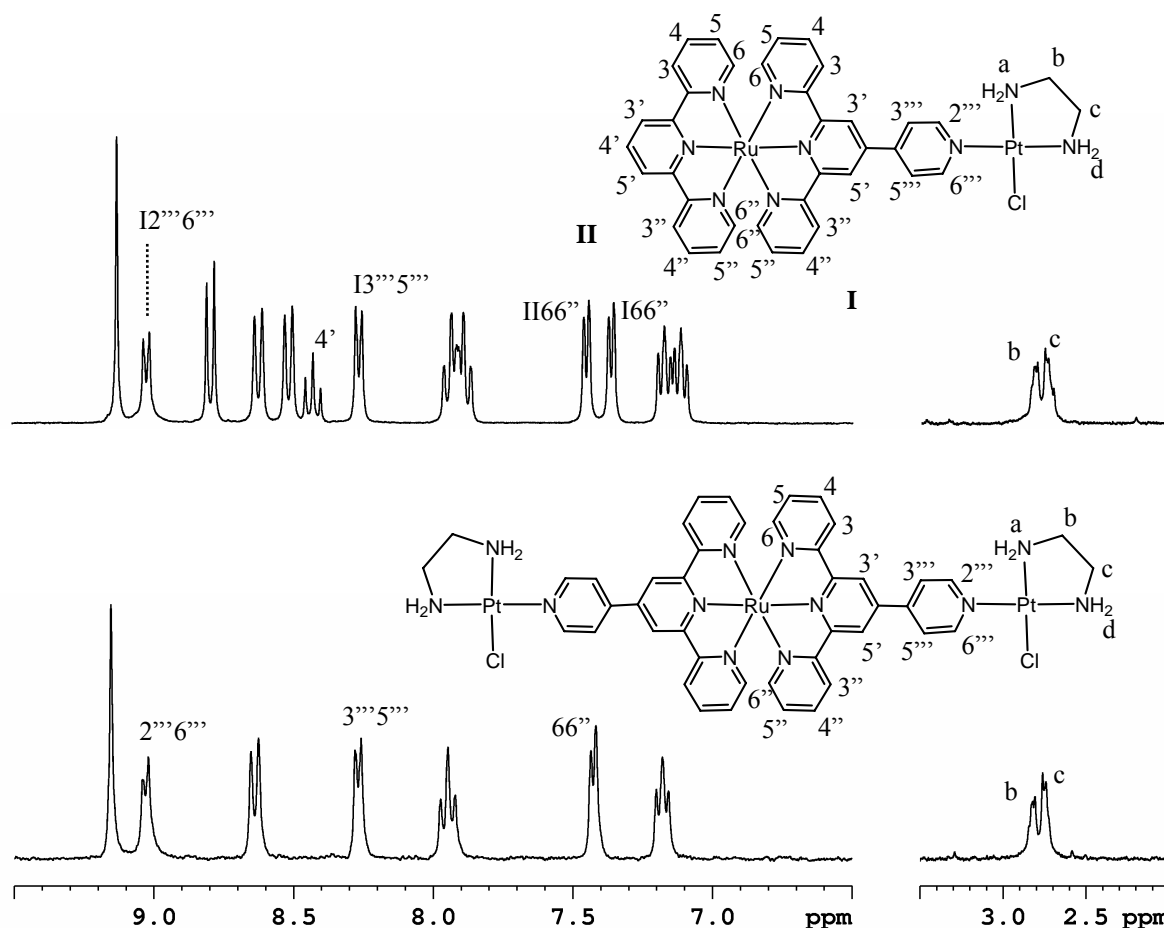


Figure 6.5 Schematic representation and 1D ¹H NMR spectra (300 MHz) of **4** (top) and **5** (bottom) in D₂O at 298 K, with some assignments. The numbering scheme for the qpy ligand I, tpy ligand II and the en protons of **4** are indicated. The numbering scheme for **5** is only partly given, because of the presence of C₂ symmetry.

The terpyridine signals have been identified by the signal for the 4' proton, which displays a relative intensity of one. The relative intensities of all other aromatic signals of **4** are two, which implies the presence of a C₂ symmetry axis. Complex **5** displays one set of signals in the aromatic region for the quaterpyridine signals, which agrees with C₂ symmetry. For both complexes the 66'' resonances have been distinguished from the 33'' resonances by the difference in J values, which are 5 and 9 Hz, respectively. A characteristic feature is the relative upfield shift of the 66'' protons of **4** and **5**, because of shielding by the other aromatic ligand. The chemical shifts of the 2'''6''' and 3'''5''' resonances of **4** have shifted downfield from the corresponding signals of the mononuclear derivative (0.24 and 0.28 ppm, respectively, in DMSO-*d*₆), which implies coordination of platinum to the quaterpyridine ligand. For **5** only the 3'''5''' resonance has shifted appreciably (0.16 ppm).

The complexes also display resonances for the protons a, b, c, and d of the ethylenediamine ligand coordinated to platinum. The resonances for the amine protons are not observed in D₂O, due to exchange with deuterated solvent. In DMSO-*d*₆, the amine signals a and d of **4** are seen at 6.66 and 5.89 ppm, respectively, at 298 K (data not shown). The corresponding resonances of **5** are observed at 6.25 and 5.90 ppm, respectively (data not shown). The resonances for the ethylene protons b and c overlap with residual solvent signal in DMSO-*d*₆. These signals are clearly observed between 2 and 3 ppm in D₂O (Figure 6.5). Their relative intensity indicates the formation of the polynuclear complexes **4** and **5**. The ¹⁹⁵Pt NMR shift for both **4** and **5** (~ -2517 ppm) in comparison to that of the starting complexes [Pt(en)Cl₂] and [Pt(en)(H₂O)Cl]⁺ (-2394 ppm and -2118, respectively, at 298 K in D₂O) proves coordination of the platinum center to the quaterpyridine ligand.

Electronic spectra were recorded in the range from 200 to 800 nm for aqueous solutions of **4** and **5**. Intense metal-to-ligand charge-transfer (MLCT) transitions are observed in the visible region (λ_{max} 489 (ε = 2.0 · 10⁴ M⁻¹ cm⁻¹) and λ_{max} 497 nm (ε = 2.7 · 10⁴ M⁻¹ cm⁻¹) for **4** and **5**, respectively). These MLCT transitions originate from charge-transfer from the ruthenium metal to the π* orbitals of the quaterpyridine ligand. The MLCT bands have shifted to lower energy in comparison with those of the mononuclear derivatives (λ_{max} 484 (ε = 1.9 · 10⁴ M⁻¹ cm⁻¹) and λ_{max} 490 (ε = 3.3 · 10⁴ M⁻¹ cm⁻¹) for **2** and **3**, respectively). These observations are consistent with coordination of the electron-withdrawing platinum unit to the free 4'-pyridine, which lowers the energy level of the empty π* orbitals of the quaterpyridine ligand.

6.3.3 Hydrolytic behavior

Hydrolysis of 0.1 mM solutions of **4** and **5** in D₂O at 310 K has been studied by ¹H NMR experiments. No changes in the 1D spectra were observed after several days, which implies

that the complexes do not hydrolyze. Even at 363 K, no significant hydrolysis was observed after a couple of days. Incubation with AgBF_4 for 2 days to remove the chloride ligand resulted in a slight downfield shift (~ 0.08 ppm) of the $3''5''$ signal for both **4** and **5**. A more significant shift was observed in ^{195}Pt NMR, *i.e.* from -2518 to -2327 ppm, which clearly proves substitution of the chloride ligand by D_2O .

The minimal change in chemical shift of the $3''5''$ ^1H NMR signal upon hydrolysis is surprising. A large difference in chemical shift (0.6 ppm) for the $3''5''$ signal has been observed (by others) upon protonation or methylation of the free pyridine of the $[\text{Ru}(\text{qpy})_2]^{2+}$ cation.^[13] For **4** and **5**, considerable changes in chemical shifts were also expected upon hydrolysis, because of the strong electron-withdrawing effect of the chloride ligand and the change of the total charge of the complex. The chloride ligand is possibly not substituted by a water molecule but by a hydroxide ion, which is electron withdrawing as well. Coordination of a hydroxide ion instead of water would result in a slightly acidic pH of the solution. Unfortunately, the pH has not been measured after hydrolysis. Electronic effects within the quaterpyridine ligand may be the reason why a change in chemical shift is observed for the $3''5''$ protons instead of a shift for the $2''6''$ protons, which are closer to the site where hydrolysis occurs.

For cisplatin, it is believed that hydrolysis occurs before coordination to DNA.^[22] It is not clear why **4** and **5** do not hydrolyze. Electronic effects within the extended aromatic system may also be of influence on the strength of the platinum-chloride coordination bond.

6.3.4 Coordination of the DNA-model base 9-ethylguanine to platinum

From the reaction of the dinuclear complex **4** with 9 egua , the monoadduct $[(\text{tpy})\text{Ru}(\text{qpy})\text{Pt}(\text{en})(9\text{egua})](\text{PF}_6)_4$ (**6**) has been isolated as the hexafluorophosphate salt. The hexafluorophosphate salt of the adduct is not soluble in water. Therefore, the 1D ^1H NMR spectrum of **6** has been acquired in acetone- d_6 , and is shown in Figure 6.6.

The adduct **6** displays similar symmetry as **4**, and the terpyridyl and quaterpyridyl ^1H NMR resonances have analogously been assigned (*vide supra*). The chemical shifts of the 9 egua protons of **6** in acetone- d_6 compared to those of the free DNA-model base indicate binding of 9 egua to the complex ($\delta = 1.41, 4.16, 6.62$ and 8.33 ppm *versus* $1.40, 4.06, 5.98$ and 7.60 ppm for $\text{CH}_3, \text{CH}_2, \text{NH}_2$ and H8 of **4** and **6**, respectively). The relative intensity of the 9 egua resonances indicates coordination of one base. The NH1 proton of 9 egua is not observed probably due to fast exchange with deuterated solvent. The large shift for the H8 resonance and the $I2''6''\text{--H8}$ NOE crosspeak present in the 2D NOESY spectrum of **6** (Figure 6.7) establish coordination of 9 egua by the N7 atom.

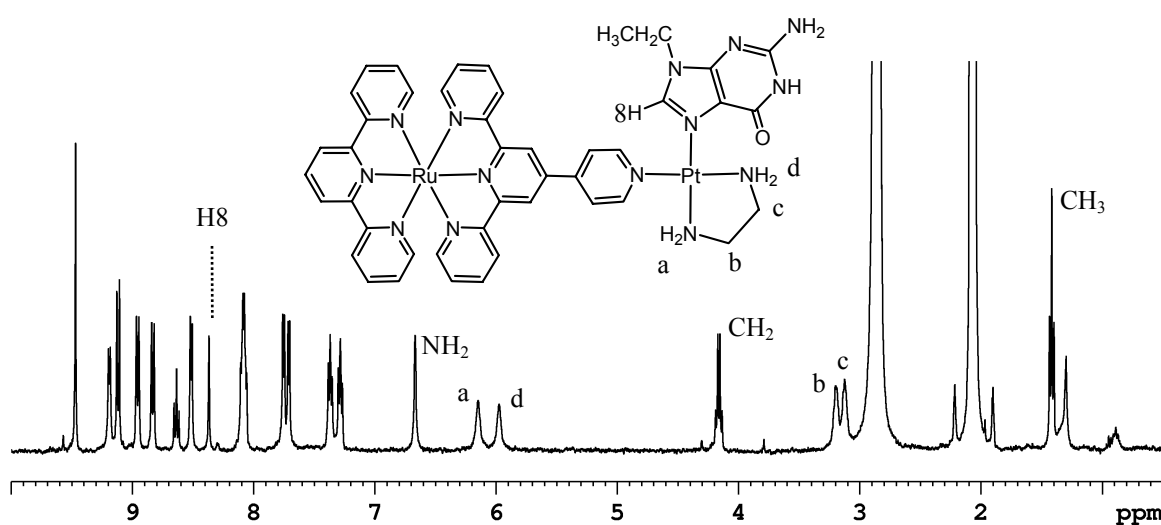


Figure 6.6 Schematic representation of **6** and its 1D ^1H NMR spectrum in acetone- d_6 at 294 K with some assignments.

The $^{12''6''}$ quaterpyridine signal displays a small upfield shift (0.06 ppm) upon coordination of **4** to 9egua, whereas the $^{13''5''}$ resonance shifts more appreciably (0.25 ppm). The C_2 symmetry displayed in the ^1H NMR spectrum of **6** suggests either a rigid structure of the adduct, or fast rotation of the coordinated DNA-model base. The conjugated π system of the quaterpyridine ligand probably prevents rotation within the ligand. The $^{12''6''}$ -H8 NOE crosspeak indicates that 9egua is directed with the H8 proton towards the quaterpyridine ligand. This orientation is most likely stabilized by H bonding between the keto group of the base and the NH_2 protons of the ethylene diamine ligand. Rotation around the platinum-pyridine coordination bond is theoretically possible, but the platinum-9egua unit may also be situated in the plane of symmetry of the molecule.

6.3.5 Cytotoxicity

The new complexes have been tested against human ovarian A2780 and mouse leukemia L1210 cisplatin sensitive and resistant cells. The mononuclear complex **2** and the dinuclear complex **4** do not display any toxicity against the A2780 cell lines at the tested concentrations (*i.e.* 100 μM), whereas the mononuclear bis(quaterpyridine)-ruthenium complex **3** inhibits 50 % of cell growth of A2780 cells at a similar concentration. The trinuclear complex **5** inhibits 50 % of cell growth of cisplatin sensitive A2780cis cells at a concentration of approximately 50 μM , and reaches 50 % of cell growth inhibition of cisplatin resistant A2780R cells at 100 μM . These results suggest that the quaterpyridine ligand affects the toxicity of these complexes, but coordination of platinum is of more importance. However, in

general the complexes do not display significant cytotoxicity. The complexes are not toxic against the leukemia cell lines either. Cytotoxicity has been reported^[23] for the mononuclear derivative $cis\text{-}[\text{Pt}(\text{NH}_3)_2(\text{pyridine})\text{Cl}]^+$, but $[\text{Pt}(\text{en})(\text{pyridine})\text{Cl}]^+$ did not show cytotoxicity.

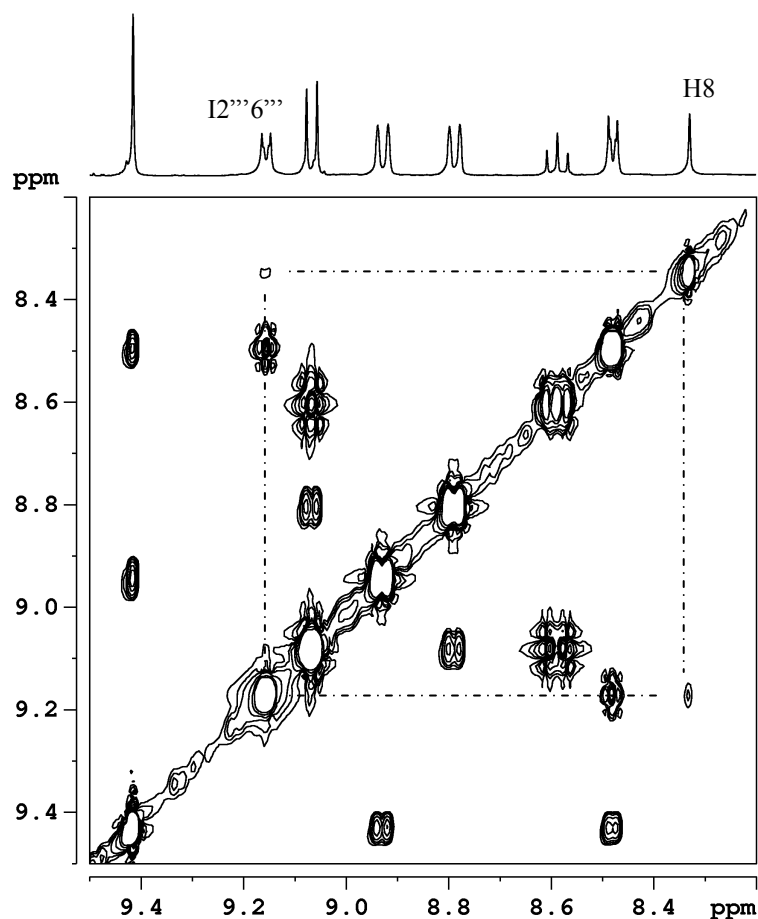


Figure 6.7 2D ^1H NOESY NMR spectrum of **6** in acetone- d_6 at 294 K with some assignments and the I2'''6'''-H8 crosspeak indicated.

6.4 Concluding remarks

The paramagnetic complex $[\text{Ru}(\text{qpy})\text{Cl}_3]$ (**1**) has been shown to display interesting ^1H NMR features, which have been studied by different ^1H NMR experiments. The alternating shifts of the central pyridine and the pendant pyridine protons stress that within these aromatic rings delocalization of spin density partly occurs by a spin polarization mechanism, as has been suggested for analogous paramagnetic trichlororuthenium complexes. The water soluble complexes $[(\text{tpy})\text{Ru}(\text{qpy})]\text{Cl}_2$ (**2**) and $[\text{Ru}(\text{qpy})_2]\text{Cl}_2$ (**3**) have been synthesized from $[\text{Ru}(\text{tpy})\text{Cl}_3]$ and **1**, respectively, for the assembly of the polynuclear ruthenium-platinum complexes $[(\text{tpy})\text{Ru}(\text{qpy})\text{Pt}(\text{en})\text{Cl}](\text{NO}_3)_3$ (**4**) and $[\text{Cl}(\text{en})\text{Pt}(\text{qpy})\text{Ru}(\text{qpy})\text{Pt}(\text{en})\text{Cl}](\text{NO}_3)_4$ (**5**).

It has been shown that the platinum ethylene diamine moiety of **4** does not hydrolyze at 310 K. Instead the platinum unit reacts with the DNA-model base 9-ethylguanine (9egua). It has been concluded that the base is coordinated to platinum via the N7 atom, and is pointing with the H8 proton towards the quaterpyridine ligand. This orientation is most probably stabilized by hydrogen bonding between the keto group of the base and the amine protons of the ethylene diamine ligand. Unfortunately, the complexes do not show significant cytotoxicity against a selection of cancer cell lines.

Electronic spectra have shown that coordination of platinum to the 4'-pyridine ligand lowers the energy level of the ruthenium-centered MLTC band. It would be of interest to study whether the platinum moiety is more reactive towards biomolecules by light excitation of the ruthenium moiety.

6.5 References

- [1] (a) Reedijk, J., *Proc. Natl. Acad. Sci. U. S. A.* **2003**, *100*, 3611-3616. (b) Wheate, N. J.; Collins, J. G., *Coord. Chem. Rev.* **2003**, *241*, 133-145.
- [2] Farrell, N.; Qu, Y.; Bierbach, U.; Valsecchi, M.; Menta, E., in *Cisplatin. Chemistry and Biochemistry of a Leading Anticancer Drug* (Ed.: Lippert, B.), Verlag Helvetica Chimica Acta, Zurich, Wiley-VCH, Weinheim, **1999**, 479-496.
- [3] Reedijk, J., *Chem. Rev.* **1999**, *99*, 2499-2510.
- [4] *Cisplatin. Chemistry and Biochemistry of a Leading Anticancer Drug* (Ed.: Lippert, B.), Verlag Helvetica Chimica Acta, Zurich, Wiley-VCH, Weinheim, **1999**.
- [5] (a) Komeda, S.; Lutz, M.; Spek, A. L.; Chikuma, M.; Reedijk, J., *Inorg. Chem.* **2000**, *39*, 4230-4236. (b) Komeda, S.; Lutz, M.; Spek, A. L.; Yamanaka, Y.; Sato, T.; Chikuma, M.; Reedijk, J., *J. Am. Chem. Soc.* **2002**, *124*, 4738-4746.
- [6] Komeda, S.; Ohishi, H.; Yamane, H.; Harikawa, M.; Sakaguchi, K.; Chikuma, M., *J. Chem. Soc.-Dalton Trans.* **1999**, 2959-2962.
- [7] Komeda, S., Ph.D. thesis, Leiden University (Leiden), **2002**.
- [8] Clarke, M. J., *Coord. Chem. Rev.* **2003**, *236*, 209-233.
- [9] Alessio, E.; Mestroni, G.; Bergamo, A.; Sava, G., *Metal Ions in Biological Systems* **2004**, *42*, 323-351.
- [10] Bergamo, A.; Stocco, G.; Casarsa, C.; Cocchietto, M.; Alessio, E.; Serli, B.; Zorzet, S.; Sava, G., *Int. J. Oncol.* **2004**, *24*, 373-379.
- [11] (a) Milkevitch, M.; Storrie, H.; Brauns, E.; Brewer, K. J.; Shirley, B. W., *Inorg. Chem.* **1997**, *36*, 4534-4538. (b) Swavey, S.; Fang, Z. L.; Brewer, K. J., *Inorg. Chem.* **2002**, *41*, 2598-2607.
- [12] Persaud, L.; Barbiero, G., *Can. J. Chem.-Rev. Can. Chim.* **1991**, *69*, 315-321.
- [13] Constable, E. C.; Cargill Thompson, A. M. W., *J. Chem. Soc.-Dalton Trans.* **1994**, 1409-1418.
- [14] Metcalfe, C.; Spey, S.; Adams, H.; Thomas, J. A., *J. Chem. Soc.-Dalton Trans.* **2002**, 4732-4739.
- [15] Kelly, J. M.; Tossi, A. B.; McConnell, D. J.; Ohuigin, C., *Nucleic Acids Res.* **1985**, *13*, 6017-6034.
- [16] Sullivan, B. P.; Calvert, J. M.; Meyer, T. J., *Inorg. Chem.* **1980**, *19*, 1404-1407.
- [17] Velders, A. H., Ph.D. thesis, Leiden University (Leiden), **2000**.
- [18] (a) Tada, H.; Shiho, O.; Kuroshima, K.; Koyama, M.; Tsukamoto, K., *J. Immunol. Methods* **1986**, *93*, 157-165. (b) Mosmann, T., *J. Immunol. Methods* **1983**, *65*, 55-63. (c) Alley, M. C.; Scudiero, D. A.;

- Monks, A.; Hursey, M. L.; Czerwinski, M. J.; Fine, D. L.; Abbott, B. J.; Mayo, J. G.; Shoemaker, R. H.; Boyd, M. R., *Cancer Res.* **1988**, *48*, 589-601.
- [19] (a) Constable, E. C., *Adv. Inorg. Chem. Radiochem.* **1986**, *30*, 69. (b) Constable, E. C.; Cargill Thompson, A. M. W.; Tocher, D. A.; Daniels, M. A. M., *New J. Chem.* **1992**, *16*, 855-867.
- [20] Laurent, F.; Plantalech, E.; Donnadiou, B.; Jimenez, A.; Hernandez, F.; Martinez-Ripoll, M.; Biner, M.; Llobet, A., *Polyhedron* **1999**, *18*, 3321-3331.
- [21] Bertini, I.; Luchinat, C., *NMR of paramagnetic substances, Coord. Chem. Rev. Vol. 150*, (Ed.: Lever, A. B. P.), Elsevier, Amsterdam, **1996**.
- [22] Reedijk, J., *Chem. Commun.* **1996**, 801-806.
- [23] Hollis, L. S.; Amundsen, A. R.; Stern, E. W., *J. Med. Chem.* **1989**, *32*, 128-136.

Chapter 7

Summary, general discussion and future prospects

7.1 Introduction

Cisplatin is successfully used in chemotherapy, but is effective only against a narrow range of tumors.^[1] The development of analogues has resulted in a few clinically useful complexes, most of which, however, are cross-resistant to cisplatin.^[2] Many cancers remain difficult to treat. Cisplatin derivatives probably lack activity against cancers, which are resistant to the parent drug, because they form a similar type of adducts to the DNA, the ultimate target of platinum drugs.^[3] Therefore, a variety of platinum complexes have been synthesized, which are structurally distinct from cisplatin, and as a result bind to DNA in a fundamentally different manner.^[4] A class of “non-classical” platinum compounds comprises polynuclear platinum complexes.^[5] It is believed that these complexes can overcome cisplatin resistance, because they are capable of specific interactions with biomolecules, which cannot be achieved by their mononuclear counterparts. Next to platinum, ruthenium is also used for the construction of anticancer agents.^[6] Because of the octahedral structure of ruthenium complexes, as opposed to the square-planar geometry of cisplatin, they interact differently with biological targets. The research described in this Thesis has been devoted to the design and development of polynuclear polypyridyl ruthenium and ruthenium-platinum complexes in search for new anticancer agents.

7.2 Summary and general discussion

Chapter 1 presents an introduction on the development of platinum and ruthenium anticancer complexes. The clinical success of cisplatin has been a tremendous impetus for the design of metal-based antitumor drugs. Its mechanism of action is therefore briefly discussed, as well as the toxic side effects of its clinical use and the cellular resistance to the drug. Cisplatin's side effects have led to the development of cisplatin analogues, whereas drug resistance has stimulated the construction of structurally different complexes. The main achievements in the development of mononuclear anticancer platinum and ruthenium complexes have been presented first. Of special interest are the polynuclear platinum compounds. An overview is given, and insight in their biological features is outlined. The last part of the introduction deals with the development of polynuclear ruthenium and polynuclear ruthenium-platinum DNA-binding complexes, the main topics of the research described in this Thesis.

In **Chapter 2** the synthesis of the dinuclear ruthenium(II)-ruthenium(III) complex $[(\text{tpy})\text{Ru}(\text{dtdeg})\text{RuCl}_3]\text{Cl}_2$, for which the long and flexible linker dtdeg has been used, is presented (dtdeg = bis[4'-(2,2':6',2''-terpyridyl)]-diethyleneglycolether, tpy = 2,2':6',2''-terpyridine). The development of the complex has been inspired by the antitumor-active mononuclear complex^[7] $[\text{Ru}(\text{tpy})\text{Cl}_3]$. The paramagnetic complex has been fully characterized in a straightforward manner by ¹H NMR experiments, which include the use of 1D ¹H NOE difference techniques. The complex represents a prototype of the various trichlororuthenium(III) terpyridyl complexes, which are described in this Thesis. For these complexes dipolar and contact interactions are suggested to contribute to the hyperfine shift and nuclear relaxation.

The dinuclear ruthenium(II) complexes $[\text{Cl}(\text{bpy})\text{Ru}(\text{dtdeg})\text{Ru}(\text{bpy})\text{Cl}]\text{Cl}_2$, $[(\text{tpy})\text{Ru}(\text{dtdeg})\text{Ru}(\text{bpy})\text{Cl}]\text{Cl}_3$, and $[(\text{tpy})\text{Ru}(\text{dtdeg})\text{Ru}(\text{tpy})]\text{Cl}_4$ are described in **Chapter 3** (bpy = 2,2'-bipyridine). The complexes consist of two metal moieties, of which at least one is capable of monofunctional coordination to biomolecules. The bifunctional complex $[\text{Cl}(\text{bpy})\text{Ru}(\text{dtdeg})\text{Ru}(\text{bpy})\text{Cl}]\text{Cl}_2$ has been studied for its hydrolysis, since it is generally believed that the chloride ligands of cisplatin are hydrolyzed before coordination to DNA.^[8] The complex has also been shown to coordinate to the DNA-model base 9-ethylguanine (9egua). Its monoadduct and bisadduct have been characterized by variable temperature ¹H NMR experiments. Free rotation of the base is hindered at room temperature. At 248 K 9egua is flipping between two enantiomeric rotamers. Despite the fact that the monofunctional metal moieties can coordinate to DNA, the complexes do not show cytotoxicity against different cancer cell lines. The complexes are taken up in the cell, but uptake is not related to cytotoxicity.

Variation of the metal may have an effect on the activity of the complexes against cancer cells. Therefore, the heterodinuclear ruthenium-platinum complex $[\text{Cl}_3\text{Ru}(\text{dtdeg})\text{PtCl}]\text{Cl}$, and its derivatives $[\text{Cl}(\text{bpy})\text{Ru}(\text{dtdeg})\text{PtCl}]\text{Cl}_2$ and $[(\text{tpy})\text{Ru}(\text{dtdeg})\text{PtCl}]\text{Cl}_3$, have been constructed, which is revealed in **Chapter 4**. The complexes vary in the structure of the ruthenium moiety. The platinum unit is derived from the cytotoxic^[9] mononuclear complex $[\text{Pt}(\text{tpy})\text{Cl}]\text{Cl}\cdot 2\text{H}_2\text{O}$. The crystal structure of $[(\text{tpy})\text{Ru}(\text{dtdeg})\text{PtCl}]\text{Cl}_3$ illustrates that the platinum moiety is capable of self-stacking interactions. DNA-model base studies show that the platinum moiety coordinates to a guanine derivative. The results imply that the platinum moiety is able to both intercalate and coordinate to the DNA, without being hindered by the dangling ruthenium moiety. The length of the linker can afford long-range DNA interactions of the dinuclear complexes. However, the complexes do not show cytotoxicity. Even complex $[\text{Cl}_3\text{Ru}(\text{dtdeg})\text{PtCl}]\text{Cl}$, in which two active units have been assembled, is deficient of any cytotoxicity.

To examine the influence of the nature and length of the linker on biological activity, the complexes $[(\text{dtdeg})\text{Ru}(\text{dtdeg})]\text{Cl}_2$ and $[(\text{dtdeg})\text{Ru}(\text{dtdeg})\text{Ru}(\text{dtdeg})]\text{Cl}_4$ have been developed. They have been produced to synthesize the trinuclear and tetranuclear ruthenium complexes $[\text{Cl}_3\text{Ru}(\text{dtdeg})\text{Ru}(\text{dtdeg})\text{RuCl}_3]\text{Cl}_2$ and $[\text{Cl}_3\text{Ru}(\text{dtdeg})\text{Ru}(\text{dtdeg})\text{Ru}(\text{dtdeg})\text{RuCl}_3]\text{Cl}_4$, and the trinuclear and tetranuclear ruthenium-platinum analogues $[\text{ClPt}(\text{dtdeg})\text{Ru}(\text{dtdeg})\text{PtCl}]\text{Cl}_4$ and $[\text{ClPt}(\text{dtdeg})\text{Ru}(\text{dtdeg})\text{Ru}(\text{dtdeg})\text{PtCl}]\text{Cl}_6$. The linkers most likely affect DNA affinity by electrostatic interactions. In general, the complexes show higher cytotoxicity than the dinuclear derivatives. The tetranuclear complex $[\text{Cl}_3\text{Ru}(\text{dtdeg})\text{Ru}(\text{dtdeg})\text{Ru}(\text{dtdeg})\text{RuCl}_3]\text{Cl}_4$ displays interesting biological features. Human ovarian cisplatin sensitive carcinoma (A2780cis) cells adhere together and form clots upon incubation with this complex. The effect is characteristic for these ovarian cancer cells in particular, and is specific for the structure of the tetranuclear ruthenium complex. These results are presented in **Chapter 5**.

In contrast to the long and flexible linker dtdeg, the short and semi-rigid bridging ligand 4'-pyridyl-2,2':6',2''-terpyridine (qpy) has been used for the development of the heteropolynuclear ruthenium-platinum complexes $[(\text{tpy})\text{Ru}(\text{qpy})\text{Pt}(\text{en})\text{Cl}](\text{NO}_3)_3$ and $[\text{Cl}(\text{en})\text{Pt}(\text{qpy})\text{Ru}(\text{qpy})\text{Pt}(\text{en})\text{Cl}](\text{NO}_3)_4$ (en = 1,2-ethylenediamine), which are described in **Chapter 6**. It has been demonstrated that the platinum moiety can coordinate to 9-ethylguanine. The adduct is most probably stabilized by a hydrogen bond between the amine protons of the en ligand and the keto group of the base. The complexes do not show cytotoxicity against a variety of cancer cell lines.

In conclusion, the research described in this Thesis has resulted in the synthesis of a class of polynuclear polypyridyl ruthenium and ruthenium-platinum complexes, for which the length of the linker appears to be of importance for biological activity. The work has led to the

development of a complex, *i.e.* $[\text{Cl}_3\text{Ru}(\text{dtdeg})\text{Ru}(\text{dtdeg})\text{Ru}(\text{dtdeg})\text{RuCl}_3]\text{Cl}_4$, which shows an interesting effect against human ovarian carcinoma cells. Considering the urgent need for highly selective drugs, this complex may represent a novelty. Significant activity against cisplatin-resistant cancer cells has, however, not been achieved. Variation of the metal, terminal ligands and the linker within this group of polynuclear polypyridyl complexes can provide promising agents, which may specifically be cytotoxic against drug-resistant carcinomas.

7.3 Future prospects

Several routes can be taken to improve the activity of the complexes presented in this Thesis. The results described in Chapter 3 have indicated that the dinuclear ruthenium complexes are taken up by cancer cells. Subsequently, it would be of interest to know whether the complexes reach the DNA inside the cell. DNA binding studies have shown that the complexes associate fast with the isolated duplex^[10] (data not shown), which is most likely due to electrostatic interactions. However, the DNA-model base studies described in Chapter 3 have shown flexible behavior of coordinated base, and even dissociation from ruthenium. DNA interactions can be enhanced by substitution of the terminal bipyridine ligand with a more extended aromatic ligand. Intercalation may then become feasible. Ongoing studies^[11] have already demonstrated increased cytotoxicity of the dppz (dppz = dipyrido-[3,2-*a*:2',3'-*c*]-phenazine) derivative of complex $[\text{Cl}(\text{bpy})\text{Ru}(\text{dtdeg})\text{Ru}(\text{bpy})\text{Cl}]\text{Cl}_2$ (Figure 7.1). Extended aromatic ligands may also render the ruthenium complexes fluorescent.

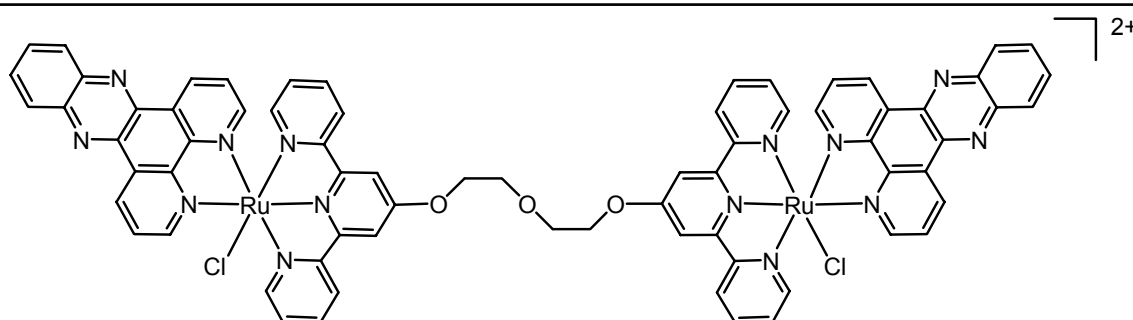


Figure 7.1 The cationic dinuclear dppz complex $[\text{Cl}(\text{dppz})\text{Ru}(\text{dtdeg})\text{Ru}(\text{dppz})\text{Cl}]^{2+}$.

For the dinuclear ruthenium-platinum complexes, with which Chapter 4 deals, self-stacking interactions of the platinum terpyridine moieties have been observed. It would be of interest to study the intercalation of the platinum moiety into DNA. Replacement of the platinum bound chloride ligand, with for example 4-picoline (Figure 7.2) may result in increased DNA binding, as is observed for the parent mononuclear complex.^[12]

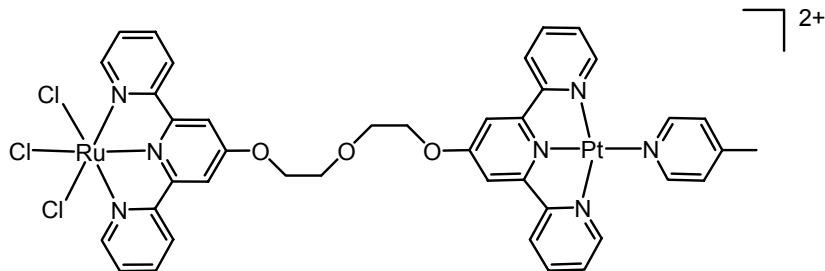


Figure 7.2 The 2+ charged dinuclear 4-picoline ruthenium(III)-platinum(II) complex $[\text{Cl}_3\text{Ru}(\text{dtdeg})\text{Pt}(4\text{-picoline})]^{2+}$.

This strategy is especially attractive to apply to the water-insoluble complex $[\text{Cl}_3\text{Ru}(\text{dtdeg})\text{PtCl}]\text{Cl}$, in which two active mononuclear complexes are joined. The 2+ charge of the resulting platinum moiety most likely yields increased water solubility and DNA affinity, which may affect cytotoxicity. Introduction of thiolate ligands on the platinum-terpyridine moiety represents a different approach. Interaction with DNA and the selenoenzyme thioredoxin reductase has been reported for thiolate platinum-terpyridine complexes.^[13] It would also be interesting to use gold instead of platinum as the second metal, since gold(III) complexes represent another class of anticancer agents.^[14] Gold-terpyridine complexes have already been reported to display significant cytotoxicity against cisplatin-sensitive and -resistant human ovarian carcinoma cells.^[15]

The tetranuclear complex $[\text{Cl}_3\text{Ru}(\text{dtdeg})\text{Ru}(\text{dtdeg})\text{Ru}(\text{dtdeg})\text{RuCl}_3]\text{Cl}_4$ presented in Chapter 5, has already been shown to induce clotting of human ovarian cancer cells. The effect indicates that the complex may inhibit cell migration and metastasis. The relation between clotting and invasion inhibition is currently under study. To better understand the effect of the nature and length of the linker in more detail, it would be of interest to synthesize the spermidine and spermine derivatives of these complexes (Figure 7.3). Spermidine and spermine are known to play essential roles in normal cell growth and differentiation.^[16] They have already been used for the construction of polynuclear platinum complexes, which show promising anticancer activity.^[17] In addition to electrostatic interactions, the polyamines can also hydrogen bond to the DNA, which may tune the biological properties of the polynuclear complexes. Variation of the metal and terminal ligands, as has been suggested for the dinuclear ruthenium and ruthenium-platinum complexes, can be extended to these trinuclear and tetranuclear complexes.

To enhance cytotoxicity of the short-linked quaterpyridine complexes presented in Chapter 6, the number of labile chloride ligands on the platinum moieties may be varied. The synthesis of the *cis* and *trans* dichloro species, in analogy to cisplatin and transplatin, is of relevance.

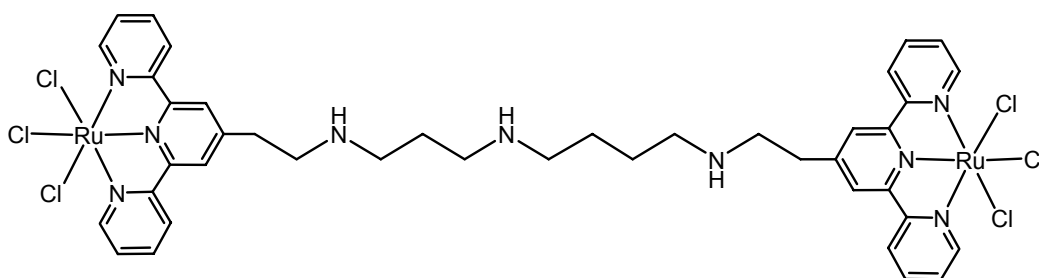


Figure 7.3 The spermidine analogue of the dinuclear cationic ruthenium(III) complex $[\text{Cl}_3\text{Ru}(\text{dtdeg})\text{Ru}(\text{dtdeg})\text{RuCl}_3]^{2+}$. The spermidine linker will be protonated at physiological pH, which will result in a 3+ total charge for the complex.

Attempts to vary the ruthenium unit of the dinuclear complex $[(\text{tpy})\text{Ru}(\text{qpy})\text{Pt}(\text{en})\text{Cl}](\text{NO}_3)_3$ have already been performed, but were unsuccessful so far. The poor solubility of the trichlororuthenium(III) quaterpyridine complex represented a major problem for the synthesis of polynuclear ruthenium(III)-platinum(II) derivatives. Preliminary results have indicated that synthesis of the bipyridine complex $[\text{Cl}(\text{bpy})\text{Ru}(\text{qpy})\text{Pt}(\text{en})\text{Cl}](\text{NO}_3)_3$ is possible, but hydrolysis of the ruthenium moiety occurs. Substitution of the chloride ligand can provide a solution to this problem. The ligand can be chosen in a way to generate electron transfer from the ruthenium unit to the platinum moiety upon light excitation of the former, which may lead to increased reactivity of the latter towards biomolecules. A different strategy can be employed, in which platinum coordinates to the terpyridine part of the quaterpyridine ligand, and ruthenium to the fourth pyridine. It would for example be attractive to construct polynuclear ruthenium-platinum complexes, which resemble Keppler-type complexes with exception of the charge (Figure 7.4).^[18] The Keppler-type complexes are of general formula $(\text{HL})[\text{RuCl}_4\text{L}_2]$ (where L is imidazole or indazole).

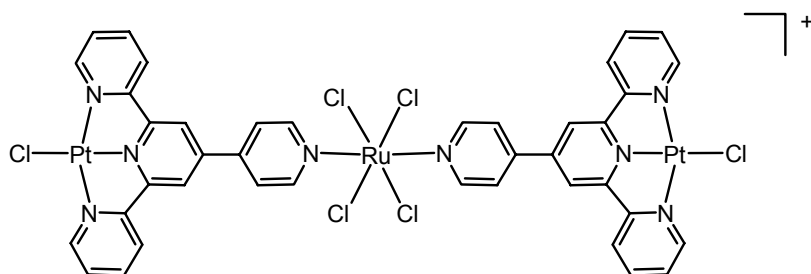


Figure 7.4 A trinuclear ruthenium(III)-platinum(II) quaterpyridine complex, in which the ruthenium moiety resembles the promising anticancer agent $(\text{Hind})[\text{RuCl}_4(\text{ind})_2]$ (KP1019, ind = indazole).

Clearly, the above suggested variations of the metal, terminal ligands, or linker can provide a wealth of polynuclear polypyridyl complexes, which may display interesting biological features.

7.4 References

- [1] *Cisplatin. Chemistry and Biochemistry of a Leading Anticancer Drug* (Ed.: Lippert, B.), Verlag Helvetica Chimica Acta, Zurich, Wiley-VCH, Weinheim, **1999**.
- [2] Jakupec, M. A.; Galanski, M.; Keppler, B. K., *Rev. Physiol. Biochem. Pharmacol.* **2003**, *146*, 1-53.
- [3] Reedijk, J., *Chem. Rev.* **1999**, *99*, 2499-2510.
- [4] (a) Wong, E.; Giandomenico, C. M., *Chem. Rev.* **1999**, *99*, 2451-2466. (b) Reedijk, J., *Proc. Natl. Acad. Sci. U. S. A.* **2003**, *100*, 3611-3616.
- [5] Wheate, N. J.; Collins, J. G., *Coord. Chem. Rev.* **2003**, *241*, 133-145.
- [6] Clarke, M. J., *Coord. Chem. Rev.* **2003**, *236*, 209-233.
- [7] Nováková, O.; Kašpárková, J.; Vrána, O.; Van Vliet, P. M.; Reedijk, J.; Brabec, V., *Biochemistry* **1995**, *34*, 12369-12378.
- [8] Reedijk, J., *Chem. Commun.* **1996**, 801-806.
- [9] Lowe, G.; Droz, A. S.; Vilaivan, T.; Weaver, G. W.; Park, J. J.; Pratt, J. M.; Tweedale, L.; Kelland, L. R., *J. Med. Chem.* **1999**, *42*, 3167-3174.
- [10] Nováková, O. and Brabec, V., *personal communication* **2004**.
- [11] Roy, S., *personal communication* **2005**.
- [12] McCoubrey, A.; Latham, H. C.; Cook, P. R.; Rodger, A.; Lowe, G., *FEBS Lett.* **1996**, *380*, 73-78.
- [13] Becker, K.; Herold-Mende, C.; Park, J. J.; Lowe, G.; Schirmer, R. H., *J. Med. Chem.* **2001**, *44*, 2784-2792.
- [14] Sadler, P. J.; Sue, R. E., *Metal based drugs* **1994**, *1*, 107-144.
- [15] Messori, L.; Abbate, F.; Marcon, G.; Orioli, P.; Fontani, M.; Mini, E.; Mazzei, T.; Carotti, S.; O'Connell, T.; Zanello, P., *J. Med. Chem.* **2000**, *43*, 3541-3548.
- [16] (a) Tabor, C. W.; Tabor, H., *Annu. Rev. Biochem.* **1984**, *53*, 749-790. (b) Pegg, A. E., *Biochem. J.* **1986**, *234*, 249-262. (c) Pegg, A. E., *Cancer Res.* **1988**, *48*, 759-774.
- [17] Rauter, H.; DiDomenico, R.; Menta, E.; Oliva, A.; Qu, Y.; Farrell, N., *Inorg. Chem.* **1997**, *36*, 3919-3927.
- [18] Galanski, M.; Arion, V. B.; Jakupec, M. A.; Keppler, B. K., *Curr. Pharm. Design* **2003**, *9*, 2078-2089.

Samenvatting

Ontwerp en ontwikkeling van polynucleaire ruthenium-complexen en ruthenium-platinacomplexen

Op zoek naar nieuwe medicijnen tegen kanker

Het antikankermedicijn cisplatina wordt succesvol gebruikt in chemotherapie maar is slechts actief tegen een klein aantal tumoren. Alhoewel de ontwikkeling van analoga wel heeft geresulteerd in een aantal klinisch waardevolle verbindingen, zijn veel vormen van kanker nog steeds moeilijk te behandelen. De meeste cisplatinaderivaten zijn alleen werkzaam tegen tumoren waartegen cisplatina ook actief is. Waarschijnlijk komt dit omdat ze soortgelijke adducten vormen met DNA, het doelwit van antikanker-platinamedicijnen. Daarom zijn platinacomplexen ontwikkeld die structureel niet gerelateerd zijn aan cisplatina en die op een fundamenteel verschillende wijze aan DNA binden. Polynucleaire platinacomplexen zijn een voorbeeld van een groep niet-klasseke platinaverbindingen. In vergelijking met mononucleaire complexen zijn deze verbindingen in staat tot unieke interacties met biomoleculen waardoor cisplatinaresistentie overwonnen kan worden. Naast platina wordt ruthenium ook gebruikt voor het ontwikkelen van antikankergeneesmiddelen. In tegenstelling tot de vlakvierkante geometrie van cisplatina hebben veel rutheniumcomplexen een octaëdrische structuur. Door deze structuur kunnen rutheniumverbindingen een andere werking hebben op cellulaire componenten. Het onderzoek dat in dit proefschrift is beschreven heeft zich gericht op de ontwikkeling van polynucleaire rutheniumcomplexen en ruthenium-platinacomplexen met als doel nieuwe medicijnen tegen kanker te ontdekken.

Hoofdstuk 1 is een algemene inleiding waarin de ontwikkeling van antikanker-platinacomplexen en -rutheniumverbindingen samengevat is. Het klinische succes van cisplatina is van enorme invloed geweest op het ontwerp van metaalgebaseerde antikankermedicijnen. Daarom wordt het mechanisme van cisplatina, de toxische bijeffecten en de cellulaire resistentie tegen het medicijn kort besproken. De toxische bijeffecten van het

medicijn hebben geresulteerd in de synthese van cisplatinaderivaten. Cisplatinaresistentie van verschillende kankers heeft geleid tot de constructie van complexen die structureel niet gerelateerd zijn aan cisplatina. De belangrijkste resultaten die behaald zijn in de ontwikkeling van mononucleaire platina- en rutheniumcomplexen worden gepresenteerd. Polynucleaire platinacomplexen zijn van speciale interesse geweest voor het onderzoek dat in dit proefschrift is beschreven. Een overzicht van deze groep van verbindingen wordt gegeven en biologische eigenschappen worden belicht. Omdat het in dit proefschrift gepresenteerde onderzoek zich heeft gericht op de synthese en evaluatie van polynucleaire rutheniumcomplexen en polynucleaire ruthenium-platinacomplexen worden deze twee klassen van verbindingen ook besproken.

In **Hoofdstuk 2** wordt de synthese van het dinucleaire ruthenium(II)-ruthenium(III)complex $[(\text{tpy})\text{Ru}(\text{dtdeg})\text{RuCl}_3]\text{Cl}_2$ beschreven waarvoor de lange en flexibele linker dtdeg is gebruikt (dtdeg = bis[4'-(2,2':6',2''-terpyridyl)]-diethyleenglycolether, tpy = 2,2':6',2''-terpyridine). De ontwikkeling van het complex is gebaseerd op het antitumor-active mononucleaire complex $[\text{Ru}(\text{tpy})\text{Cl}_3]$. In tegenstelling tot $[\text{Ru}(\text{tpy})\text{Cl}_3]$ is $[(\text{tpy})\text{Ru}(\text{dtdeg})\text{RuCl}_3]\text{Cl}_2$ in water oplosbaar. Het paramagnetische dinucleaire complex wordt volledig gekarakteriseerd met behulp van ^1H NMR, waaronder 1D ^1H NOE difference experimenten. Het complex is een prototype voor de verschillende trichlororuthenium(III)complexen die in dit proefschrift zijn beschreven. Waarschijnlijk beïnvloeden dipolaire- en contactinteracties de hyperfine shift en nucleaire relaxatie van de verschillende protonen van deze verbindingen.

De dinucleaire ruthenium(II)complexen $[\text{Cl}(\text{bpy})\text{Ru}(\text{dtdeg})\text{Ru}(\text{bpy})\text{Cl}]\text{Cl}_2$, $[(\text{tpy})\text{Ru}(\text{dtdeg})\text{Ru}(\text{bpy})\text{Cl}]\text{Cl}_3$, en $[(\text{tpy})\text{Ru}(\text{dtdeg})\text{Ru}(\text{tpy})]\text{Cl}_4$ zijn behandeld in **Hoofdstuk 3** (bpy = 2,2'-bipyridine). Het eerste complex bestaat uit twee metaaleenheden, die elk in staat zijn om monofunctioneel te coördineren aan biomoleculen. De laatste twee complexen bestaan uit tenminste één substitutie-inerte rutheniumeenheid. Omdat men aanneemt dat de chlorideliganden van cisplatina hydrolyseren vóór coördinatie aan DNA is de hydrolyse van het bifunctionele complex $[\text{Cl}(\text{bpy})\text{Ru}(\text{dtdeg})\text{Ru}(\text{bpy})\text{Cl}]\text{Cl}_2$ bestudeerd. Het complex coördineert aan de DNA-modelbase 9-ethylguanine (9egua). Zowel het monoadduct als het bisadduct zijn gekarakteriseerd met behulp van ^1H NMR experimenten bij verschillende temperaturen. De base wordt gehinderd in vrije rotatie bij kamertemperatuur. Bij 248 K flipt 9egua tussen twee enantiomere rotameren. Ondanks het feit dat de monofunctionele metaalunits aan DNA kunnen coördineren zijn de complexen niet cytotoxisch. De complexen worden door de cel opgenomen maar de opname is duidelijk niet gecorreleerd aan cytotoxiciteit.

Variatie van het metaal kan van invloed zijn op de cytotoxiciteit. Daarom zijn het heterodinucleaire ruthenium(III)-platina(II)complex $[\text{Cl}_3\text{Ru}(\text{dtdeg})\text{PtCl}]\text{Cl}$ en de

ruthenium(II)derivaten $[\text{Cl}(\text{bpy})\text{Ru}(\text{dtdeg})\text{PtCl}]\text{Cl}_2$ en $[(\text{tpy})\text{Ru}(\text{dtdeg})\text{PtCl}]\text{Cl}_3$ gesynthetiseerd. De synthese en karakterisering van de complexen zijn beschreven in **Hoofdstuk 4**. De complexen variëren in de structuur van de rutheniumeenheid. De platina-unit is afgeleid van het cytotoxische mononucleaire complex $[\text{Pt}(\text{tpy})\text{Cl}]\text{Cl}$. In de kristalstructuur van $[(\text{tpy})\text{Ru}(\text{dtdeg})\text{PtCl}]\text{Cl}_3$ zijn self-stacking interacties van de platina-eenheden te zien. DNA-modelbase studies geven aan dat het platinadeel kan coördineren aan een guaninederivaat. De resultaten impliceren dat de platina-eenheid zowel kan intercaleren als coördineren aan DNA zonder dat het daarbij gehinderd wordt door de verbonden rutheniumeenheid. De complexen kunnen mogelijk over een lange afstand aan DNA binden door de lengte van de flexibele linker (14.5 Å). Helaas is gebleken dat de complexen niet actief zijn tegen verschillende kankercellijnen. Zelfs het complex $[\text{Cl}_3\text{Ru}(\text{dtdeg})\text{PtCl}]\text{Cl}$, waarin twee active eenheden zijn verbonden, is niet cytotoxisch.

De ruthenium(II)complexen $[(\text{dtdeg})\text{Ru}(\text{dtdeg})]\text{Cl}_2$ en $[(\text{dtdeg})\text{Ru}(\text{dtdeg})\text{Ru}(\text{dtdeg})]\text{Cl}_4$ zijn ontwikkeld om de invloed van de lading en de lengte van de linker op de cytotoxiciteit van de polynucleaire complexen te bestuderen. Uitgaande van deze verbindingen zijn de trinucleaire en tetranucleaire ruthenium(II)-ruthenium(III)complexen $[\text{Cl}_3\text{Ru}(\text{dtdeg})\text{Ru}(\text{dtdeg})\text{RuCl}_3]\text{Cl}_2$ en $[\text{Cl}_3\text{Ru}(\text{dtdeg})\text{Ru}(\text{dtdeg})\text{Ru}(\text{dtdeg})\text{RuCl}_3]\text{Cl}_4$ gesynthetiseerd, evenals de trinucleaire en tetranucleaire ruthenium(II)-platina(II) analoga $[\text{ClPt}(\text{dtdeg})\text{Ru}(\text{dtdeg})\text{PtCl}]\text{Cl}_4$ en $[\text{ClPt}(\text{dtdeg})\text{Ru}(\text{dtdeg})\text{Ru}(\text{dtdeg})\text{PtCl}]\text{Cl}_6$. De positieve lading van de linkers beïnvloedt hoogst waarschijnlijk DNA-affiniteit door elektrostatische interacties. In het algemeen zijn de complexen actiever dan de dinucleaire derivaten tegen verschillende kankercellijnen. Het tetranucleaire complex $[\text{Cl}_3\text{Ru}(\text{dtdeg})\text{Ru}(\text{dtdeg})\text{Ru}(\text{dtdeg})\text{RuCl}_3]\text{Cl}_4$ heeft een karakteristieke uitwerking op de groei van menselijke ovarium-kankercellen die gevoelig zijn voor cisplatina (A2780cis). Deze cellen klonteren samen als ze geïncubeerd worden met het tetranucleaire complex en overleven voor slechts 35 % bij een concentratie van 20 μM van $[\text{Cl}_3\text{Ru}(\text{dtdeg})\text{Ru}(\text{dtdeg})\text{Ru}(\text{dtdeg})\text{RuCl}_3]\text{Cl}_4$. Het effect is karakteristiek voor deze ovarium-kankercellen en is specifiek voor de structuur van het tetranucleaire rutheniumcomplex. Deze resultaten worden gepresenteerd in **Hoofdstuk 5**.

In tegenstelling tot de lange en flexibele linker dtdeg, is de korte en semistarre linker 4'-pyridyl-2,2':6',2''-terpyridine (qpy) gebruikt voor de ontwikkeling van de heteropolynucleaire ruthenium(II)-platina(II)complexen $[(\text{tpy})\text{Ru}(\text{qpy})\text{Pt}(\text{en})\text{Cl}](\text{NO}_3)_3$ en $[\text{Cl}(\text{en})\text{Pt}(\text{qpy})\text{Ru}(\text{qpy})\text{Pt}(\text{en})\text{Cl}](\text{NO}_3)_4$ (en = 1,2-ethyleendiamine). De synthese en karakterisering van deze complexen is beschreven in **Hoofdstuk 6**. Het is bewezen dat de platina-eenheid kan coördineren aan 9-ethylguanine. Het adduct wordt waarschijnlijk gestabiliseerd door een waterstofbinding tussen de amineprotonen van het

ethyleendiamineligand en de ketongroep van de base. De complexen zijn niet cytotoxisch voor verschillende kankercellijnen.

In **Hoofdstuk 7** wordt een samenvatting gegeven van het in dit proefschrift beschreven onderzoek en wordt vooruitgeblikt op mogelijke uitbreidingen op de gepresenteerde polynucleaire complexen.

Samenvattend vormen de ontwikkelde polynucleaire rutheniumcomplexen en ruthenium-platinacomplexen die in dit proefschrift zijn beschreven een waardevolle uitbreiding op het bestaande repertoire van potentiële anorganische antikankerverbindingen. Het onderzoek heeft geleid tot de synthese van een klasse van verbindingen waarvoor de lengte en misschien ook de lading van de linker van belang zijn voor biologische activiteit. Resultaten wijzen uit dat speciaal het tetranucleaire complex $[\text{Cl}_3\text{Ru}(\text{dtdeg})\text{Ru}(\text{dtdeg})\text{Ru}(\text{dtdeg})\text{RuCl}_3]\text{Cl}_4$ interessante biologische eigenschappen bezit. Omdat er grote behoefte is aan selectieve geneesmiddelen vertegenwoordigt dit complex misschien een belangrijk nieuw antikankermedicijn. Helaas zijn de complexen niet actief tegen cisplatinaresistente kankercellen. Variatie van het metaal, de terminale liganden en de linker van deze groep van polynucleaire polypyridylcomplexen kan leiden tot specifieke cytotoxiciteit tegen cisplatinaresistente kankers.

Curriculum vitae

Karlijn van der Schilden was born in Haarlem on May 27th, 1974. After her secondary education at the Ashram College in Alphen aan den Rijn, she commenced her academic studies in chemistry in September 1994 at Leiden University. From February 1998 to November 1999, undergraduate research was performed in the Coordination and Bioinorganic Chemistry group of Prof. Dr. J. Reedijk, which resulted in the master thesis “Ruthenium(II) bis(2-phenylazopyridine) complexes and the binding of β -[Ru(azpy)₂(NO₃)₂] to 9-ethylguanine”. As part of a summer research program she joined the group of Prof. Dr. K. A. Bruns of Southwestern University, Georgetown, Texas USA, from May 1998 to August 1998. In November 1999 she obtained her doctorandus (Master of Science) degree.

She was affiliated with Leiden University as a Ph.D. student from July 2000 to April 2005 under supervision of Dr. J. G. Haasnoot and Prof. Dr. J. Reedijk to perform the research described in this thesis. During her Ph.D. she supervised one bachelor and four master students for their bachelor and master thesis, respectively. In April 2004 she visited the group of Prof. V. Brabec at the Institute of Biophysics with financial support of COST D20.

She was awarded a bursary for a postgraduate researcher to attend the COST D8 final workshop in Dublin, Ireland (2001). Parts of the research described in this thesis have been presented at several national and international meetings, including the 10th International Conference on Bioinorganic Chemistry (ICBIC-10) and the COST D20 meeting in Florence, Italy (2001), the 35th International Conference on Coordination Chemistry (ICCC-35) and the COST D20 meeting in Heidelberg, Germany (2002), the COST D20 meeting in Brno, Czech Republic (2002), the BIOMAC symposium in Leiden, The Netherlands (2002), the COST midterm evaluation meeting in Trieste, Italy (2003), and the 9th International Symposium on Platinum Coordination Compounds in Cancer Chemotherapy in New York, USA (2003).

Since September 2005 she is working at the University of Zurich as a post-doctoral fellow in the group of Prof. Dr. R. Alberto. Research is conducted, aimed at the development of polynuclear rhenium complexes, which catalyze the production of dihydrogen.

List of publications

Unusual coordination of the rare neutral imine tautomer of 9-methyladenine chelating in the N6,N7-mode to ruthenium(II) complexes

Hotze, A. C. G.; Broekhuizen, M. E. T.; Velders, A. H.; Van der Schilden, K.; Haasnoot, J. G.; Reedijk, J., *Eur. J. Inorg. Chem.* **2002**, 369-376.

The hydrolysis of the anti-cancer ruthenium complex NAMI-A affects its DNA binding and antimetastatic activity: an NMR evaluation

Bacac, M.; Hotze, A. C. G.; Van der Schilden, K.; Haasnoot, J. G.; Pacor, S.; Alessio, E.; Sava, G.; Reedijk, J., *J. Inorg. Biochem.* **2004**, 98, 402-412.

Dichlorobis(2-phenylazopyridine)ruthenium(II) complexes: characterisation, spectroscopic and structural properties of four isomers

Velders, A. H.; Van der Schilden, K.; Hotze, A. C. G.; Reedijk, J.; Kooijman, H.; Spek, A. L., *Dalton Trans.* **2004**, 448-455.

A highly flexible dinuclear ruthenium(II)-platinum(II) complex: crystal structure and binding to 9-ethylguanine

Van der Schilden, K.; Garcia, F.; Kooijman, H.; Spek, A. L.; Haasnoot, J. G.; Reedijk, J., *Angew. Chem. Int. Ed.* **2004**, 43, 5668-5670.

Proton NMR spectroscopy and magnetic properties of a solution-stable dicopper(II) complex bearing a single μ -hydroxo bridge

Koval, I. A.; Van der Schilden, K.; Schuitema, A. M.; Gamez, P.; Belle, C.; Pierre, J.-L.; Lüken, M.; Krebs, B.; Roubeau, O.; Reedijk, J., *Inorg. Chem.* **2005**, 44, 4372-4382.

Dinuclear ruthenium(II) complexes with long and flexible linkers: rotational behavior of coordinated 9-ethylguanine

Van der Schilden, K. et al., *Manuscript in preparation*.

Paramagnetic polynuclear ruthenium(II)-ruthenium(III) complexes: synthesis and ^1H NMR studies

Van der Schilden, K. et al., *Manuscript in preparation*.

Polynuclear ruthenium and platinum complexes as potential anticancer agents

Van der Schilden, K. et al., *Manuscript in preparation*.

Heteropolynuclear ruthenium(II)-platinum(II) complexes with short and semi-rigid linkers: synthesis, characterization and DNA-model base studies

Van der Schilden, K. et al., *Manuscript in preparation*.

Nawoord

Dit proefschrift had ik niet kunnen schrijven zonder al mijn lieve familie, vrienden en vriendinnetjes. Het is mooi om een dankwoord aan jullie te wijden, maar ik zou jullie allemaal veel liever een dikke zoen willen geven! Allereerst wil ik mijn ouders noemen. Jullie onvoorwaardelijke steun hebben mij tot dit punt gebracht. Mijn zusje en broers zijn minstens even belangrijk geweest. Door de liefde en onstuimigheden in onze familie realiseer ik mij wat echt belangrijk is.

Veel mensen hebben bijgedragen aan het in dit proefschrift beschreven onderzoek. Vooral stagestudenten hebben een groot aandeel gehad. Ik vond de samenwerking met jullie erg leuk en heb er veel van geleerd. Ik ben heel dankbaar voor jullie inzet en enthousiasme. Loes, jij was de eerste en onder andere daarom speciaal. Jouw enorme doorzettingsvermogen en precisie hebben uiteindelijk geleid tot mooie en interessante resultaten. Fedora, your laugh has contributed to a very nice atmosphere in the ruthenium group, and your beautiful crystals have resulted in one of the highlights in this Thesis. Michiel en Victor, jullie hebben gezwoegd op een nieuw project. Dat was niet gemakkelijk, maar heeft toch mooie complexen opgeleverd. Jolanda, jij hebt als mijn laatste student veel puntjes op de “i” gezet en hopelijk doe je in Triëste nog meer mooie ontdekkingen!?

The collaboration with Olga Nováková and Prof. V. Brabec have inspired me at the lab. I have enjoyed the stay in Brno, and the discussions at the Institute of Biophysics as well as in the pub. I have appreciated the collaboration with Alberta Bergamo and Prof. G. Sava from the University of Trieste. Unfortunately the dinuclear complexes did not show interesting features. Hopefully, the trinuclear and tetranuclear complexes will provide nice results!

De hulp en gezellige praat van Fons Lefeber en Kees Erkelens bij de NMR zijn onmisbaar geweest. Kees, ik ben blij dat je zo je best hebt gedaan voor mijn “vervelende” paramagnetische complexen. Jos van Brussel stond altijd voor mij klaar met een nieuwe kolom. Hopelijk hoor ik je nog eens op de saxofoon spelen. Het was heel fijn dat Jopie Erkelens de synthese van chloorterpyridine heeft uitgevoerd toen dit ligand wat te duur werd om steeds te bestellen. Bij Bertil Hofte kon ik terecht voor het meten van massaspectra bij hoge resolutie. Hans den Dulk is zeer behulpzaam geweest bij het uitvoeren van

cytotoxiciteitstesten in Leiden. I would like to thank J. Dewelle and R. Kiss for the cytotoxicity tests, which were performed at the University of Brussels. Ik ben Dr. Huub Kooijman en Prof. A. L. Spek van de Universiteit Utrecht zeer erkentelijk voor het oplossen van de kristalstructuur. Yvonne Snellenberg, Ingrid Bekooy en Marianne Kooistra van het secretariaat zorgden voor een soepele ondersteuning van de dagelijkse gang van zaken en Gé van Albada, John van Dijk en de ama's voor technische hulp.

Ik vond het aio-bestaan in het CBAC geweldig dankzij de mooie chemie en de leuke mensen waarvan ik er een aantal speciaal wil noemen. Aldrikus, jij hebt mij de liefde voor de rutheniumchemie bijgebracht. Dankjewel! Bovendien heb jij de eerste stappen van dit onderzoek gezet. Anna, jij was mijn "zusje" op het lab en daar ben ik heel erg dankbaar voor. We hebben veel gedeeld, stress maar ook lol, zoals vandaag! Marciemarc, eigenlijk hoorde jij ook bij de rutheniumfamilie, te meer omdat ik een soort van hybride ben. Met jullie drietjes waren de CBAC-aangelegenheden en zeker de congresjes een ware belevenis. Marina, you have been a ruthenium sister for a while, which was a nice period. Anja, Remy en Michiel, het lab was erg gezellig met jullie "naast" mijn zuurkast en de stiltekamer was gelukkig niet zo stil met de jongens(!). Daarnaast wil ik ook Olivier ("knulletje"), Guillem, Annemarieke, Christophe and Manu (without you guys I would have been like Maradona by now), Steven en Elena ("guapisima") noemen. Ariadna, Eva and Sudeshna, it was nice to share some ruthenium chemistry with you.

Zonder vrienden buiten het lab was de tijd op het lab minder "luchtig" geweest dan het was. Met "de meisjes", mijn "scheikundevriendjes", Fleur, de meiden van Supernova, Bas en Frankje, en de Oppenheimboys was het mooi vertoeven als aio in Leiden. Jullie vriendschap is van onschatbare waarde. I have also appreciated the nice time with the people from "Bergerland" during the writing in Zurich.

Tenslotte Jeroen, zonder jou zijn de wolken niet zo roze. "Danck voor u sachte kuskens en voor als". Voor jou wil ik nog duizendmiljoen keer heten...

Karlijn